Title: Quantum criticality and black holes

Date: Apr 23, 2008 02:00 PM

URL: http://pirsa.org/08040006

Abstract: I will describe antiferromagnets and superconductors near quantum phase transitions. There is a remarkable analogy between their dynamics and the holographic description of Hawking radiation from black holes. I will show how insights from this analogy have shed light on experiments on the cuprate high temperature superconductors.

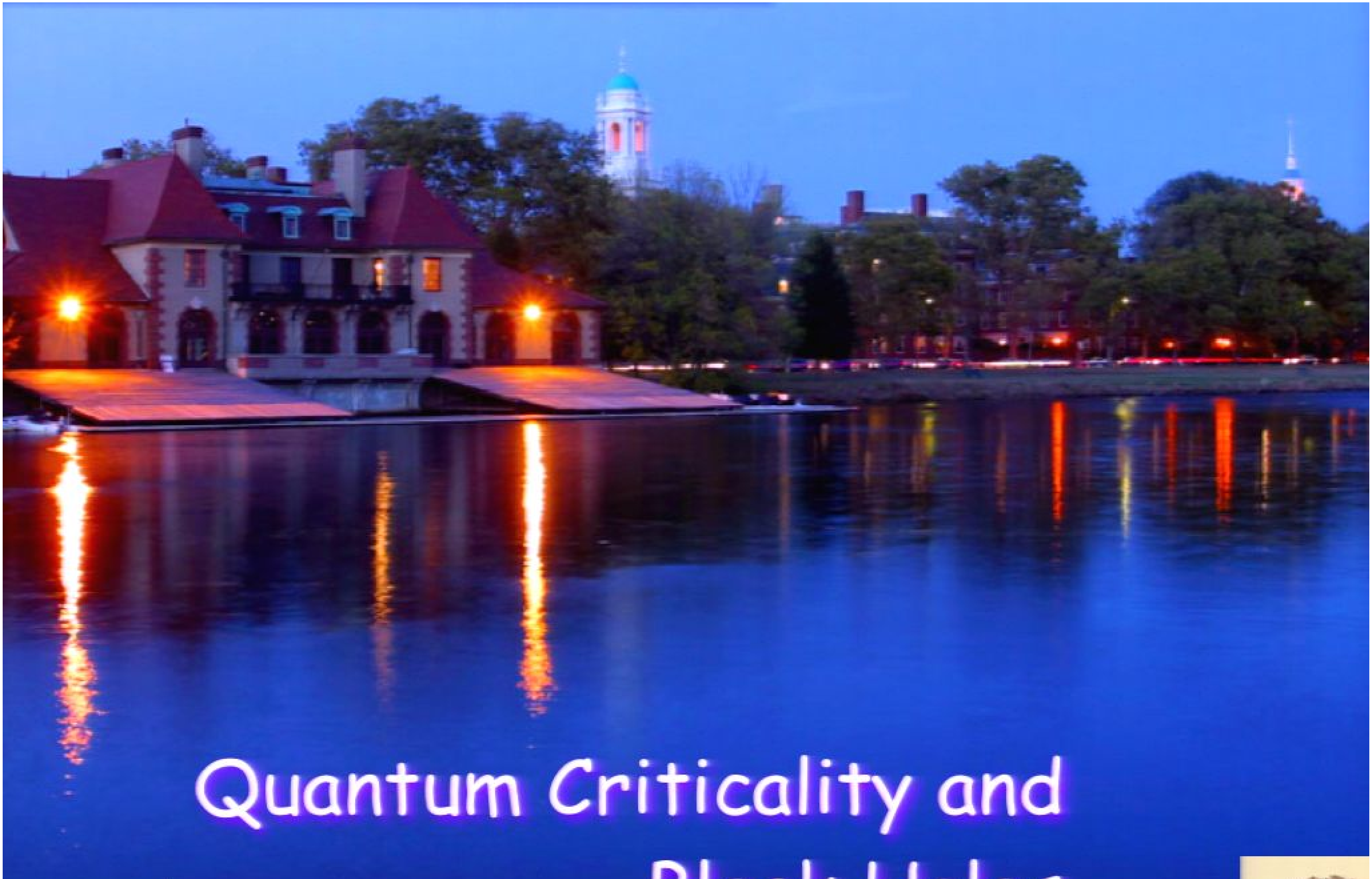

Quantum Criticality and Black Holes

Talk online: sachdev.physics.harvard.edu

Particle theorists

Sean Hartnoll, KITP
Christopher Herzog, Princeton
Pavel Kovtun, Victoria
Dam Son, Washington

Condensed matter theorists

Markus Mueller, Harvard
Subir Sachdev, Harvard

Quantum Entanglement

Hydrogen atom:

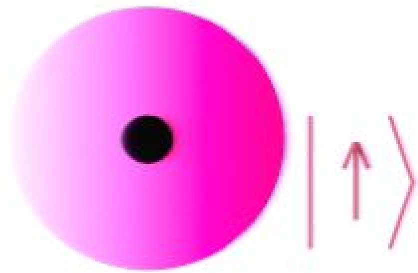

Hydrogen molecule:

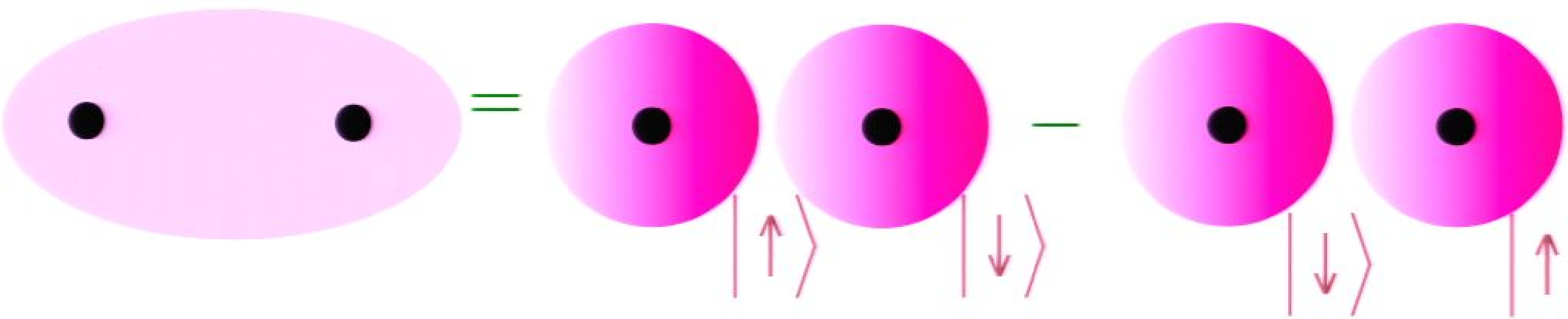

$$= \frac{1}{\sqrt{2}} \left(|\uparrow\downarrow\rangle - |\downarrow\uparrow\rangle \right)$$

Superposition of two electron states leads to non-local correlations between spins

Quantum Phase Transition

Change in the nature of entanglement in a macroscopic quantum system.

Quantum Phase Transition

Change in the nature of entanglement in a macroscopic quantum system.

Familiar phase transitions, such as water boiling to steam, also involve macroscopic changes, but in thermal motion

Quantum Criticality

The complex and non-local entanglement at the critical point between two quantum phases

Outline

1. Entanglement of spins

   Experiments on antiferromagnetic insulators

2. Black Hole Thermodynamics

   Connections to quantum criticality

3. Nernst effect in the cuprate superconductors

   Quantum criticality and dyonic black holes

4. Quantum criticality in graphene

   Hydrodynamic cyclotron resonance and Nernst effect

Outline

1. Entanglement of spins
   Experiments on antiferromagnetic insulators

2. Black Hole Thermodynamics
   Connections to quantum criticality

3. Nernst effect in the cuprate superconductors
   Quantum criticality and dyonic black holes

4. Quantum criticality in graphene
   Hydrodynamic cyclotron resonance and Nernst effect

The cuprate superconductors

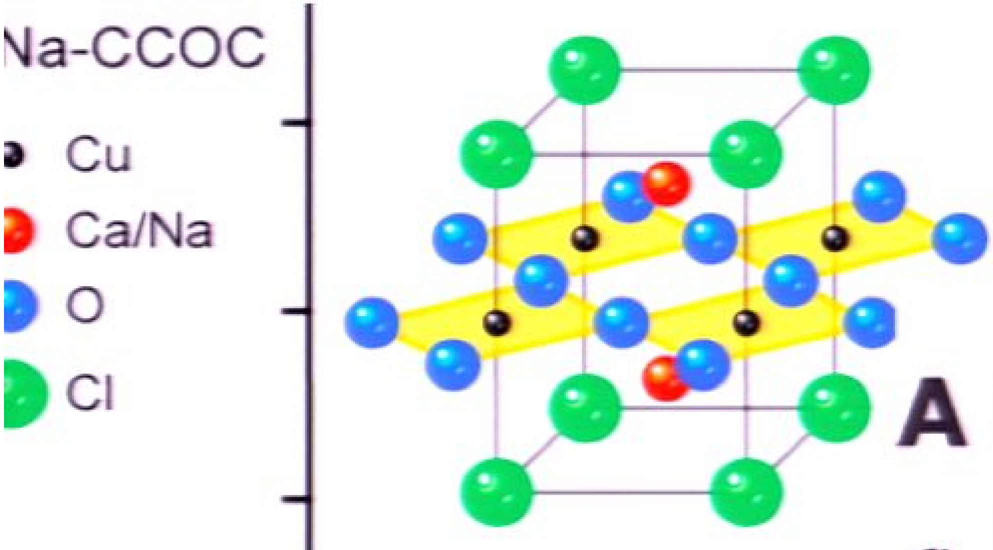

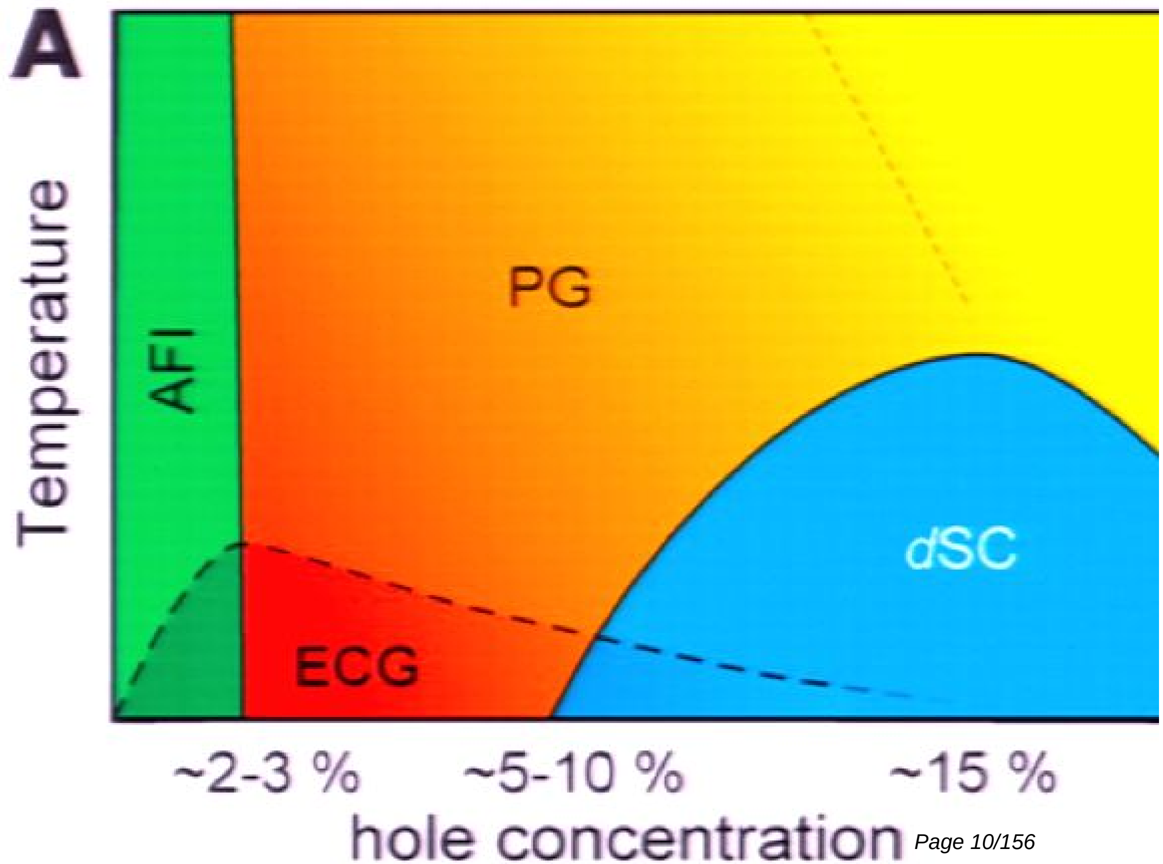

Antiferromagnetic (Neel) order in the insulator

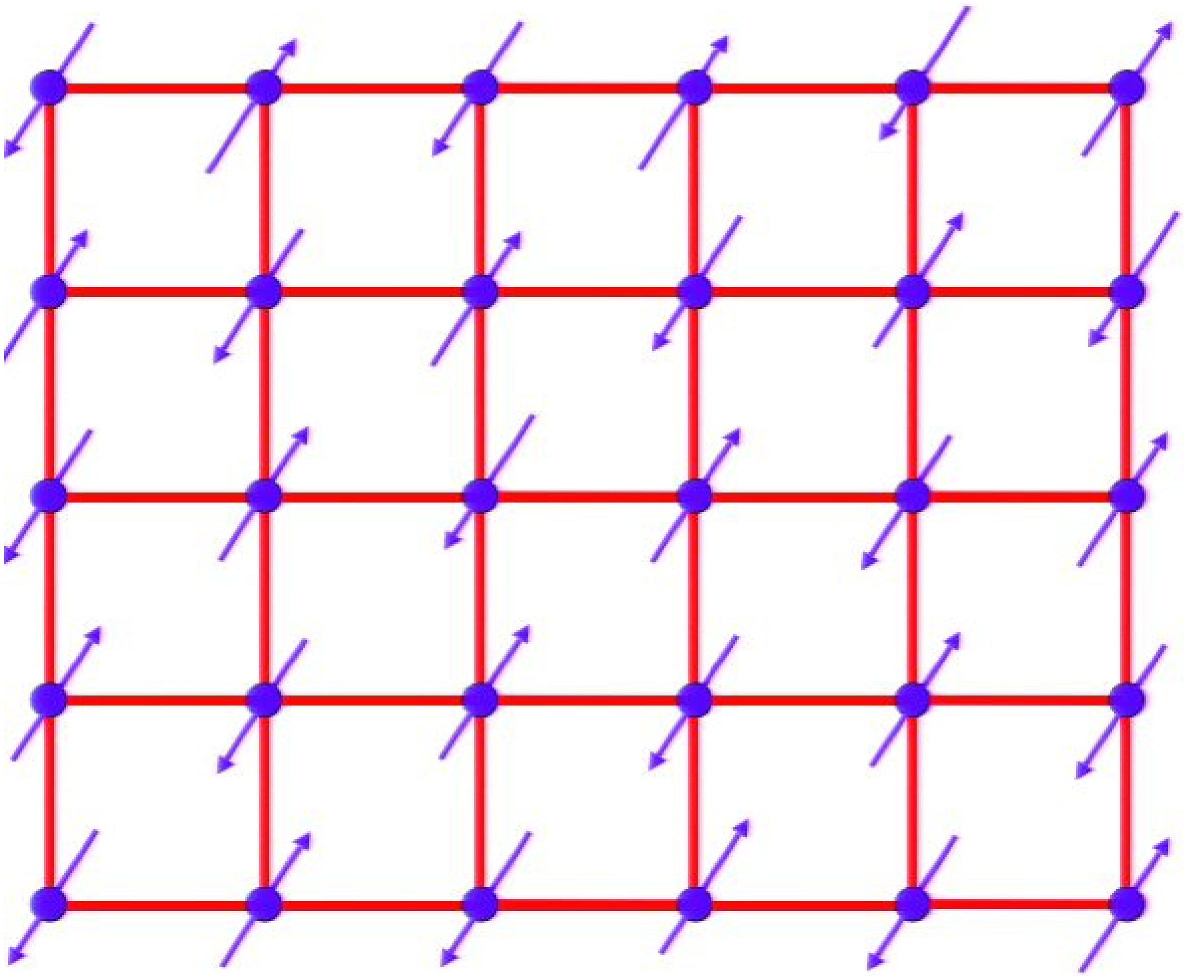

Antiferromagnetic (Neel) order in the insulator

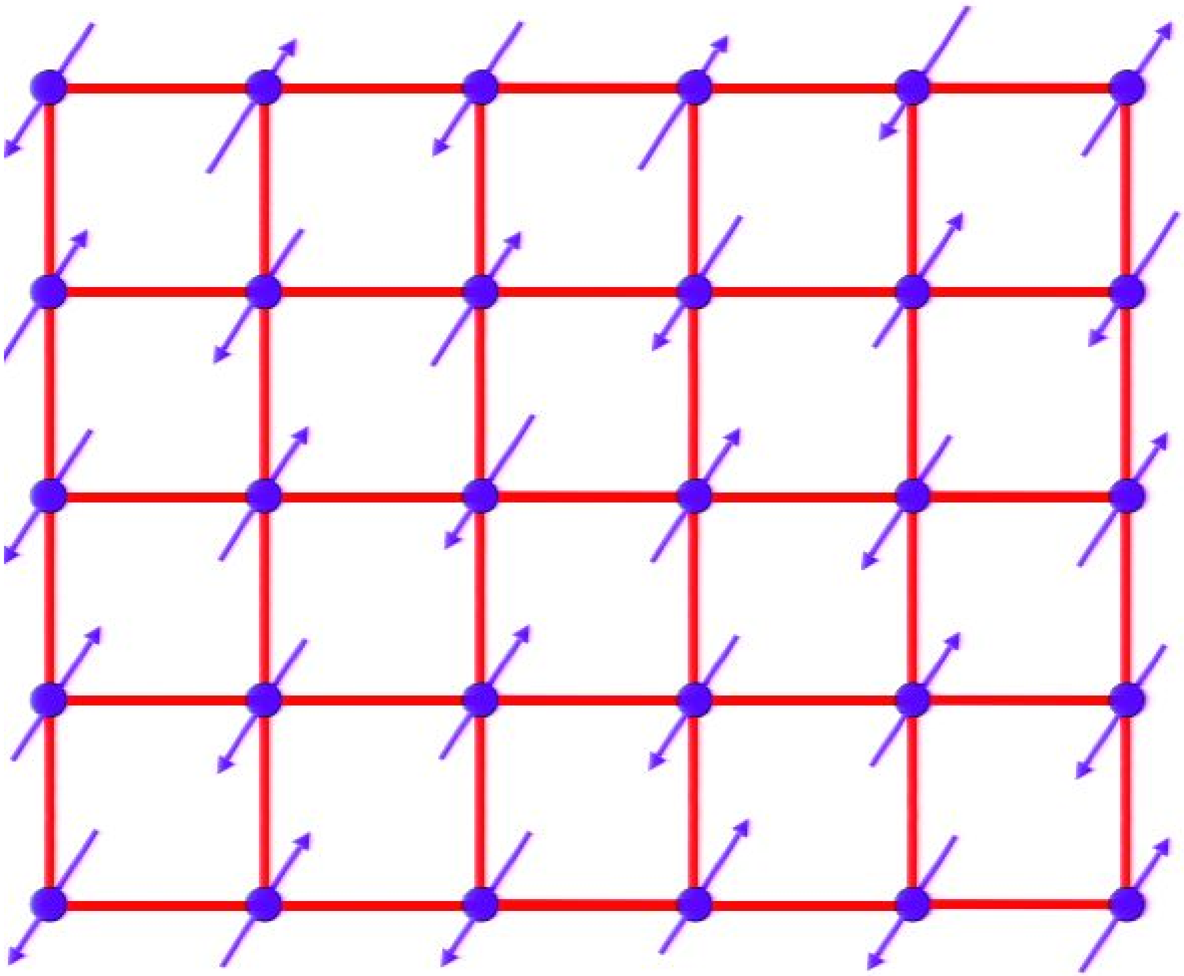

No entanglement of spins

Antiferromagnetic (Neel) order in the insulator

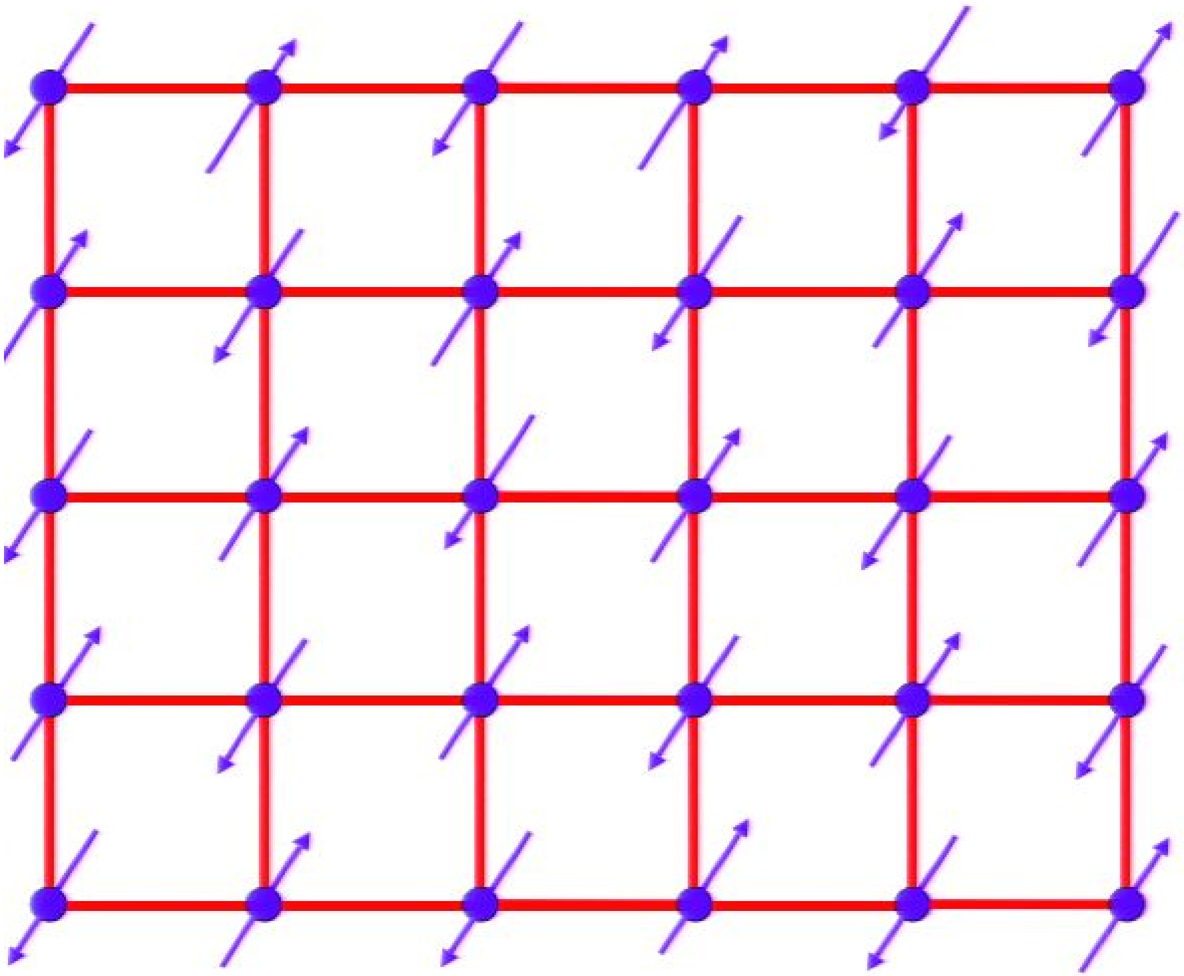

Excitations: 2 spin waves (Goldstone modes)

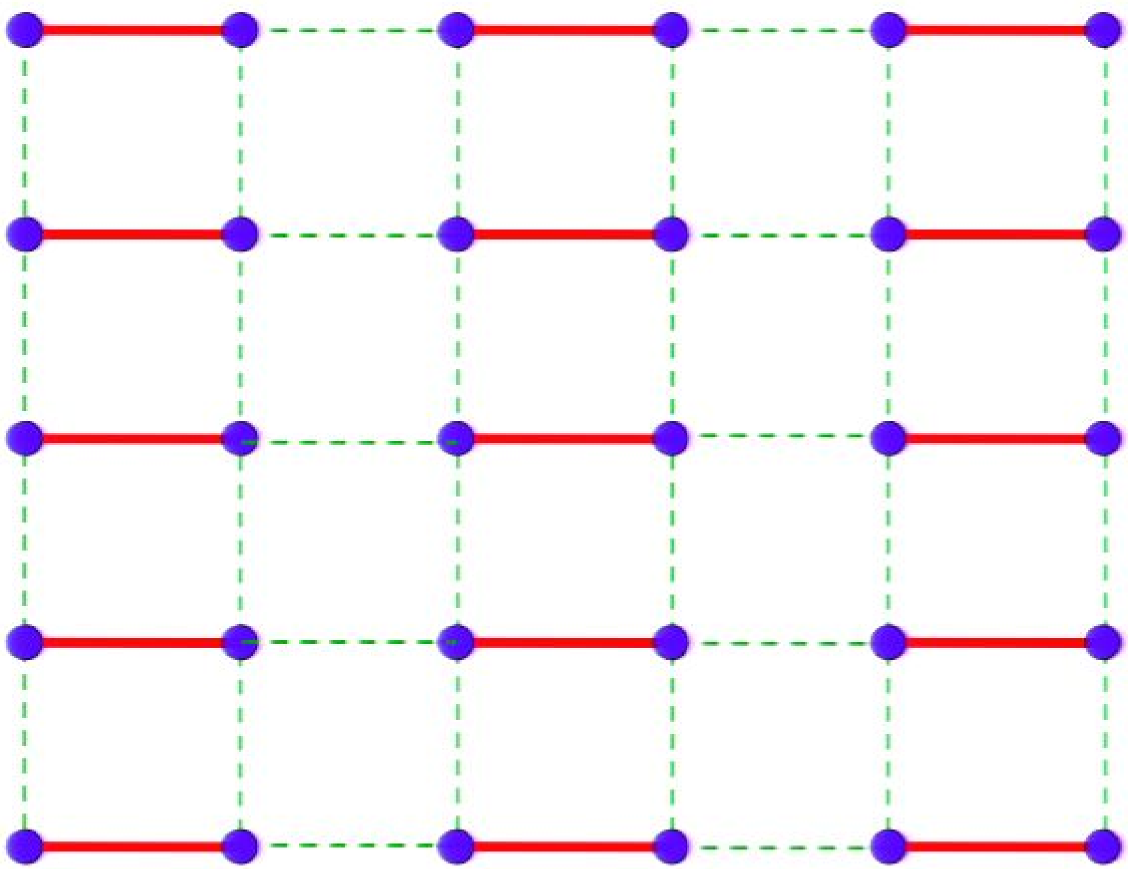

Weaken some bonds to induce spin entanglement in a new quantum phase

Antiferromagnetic (Neel) order in the insulator

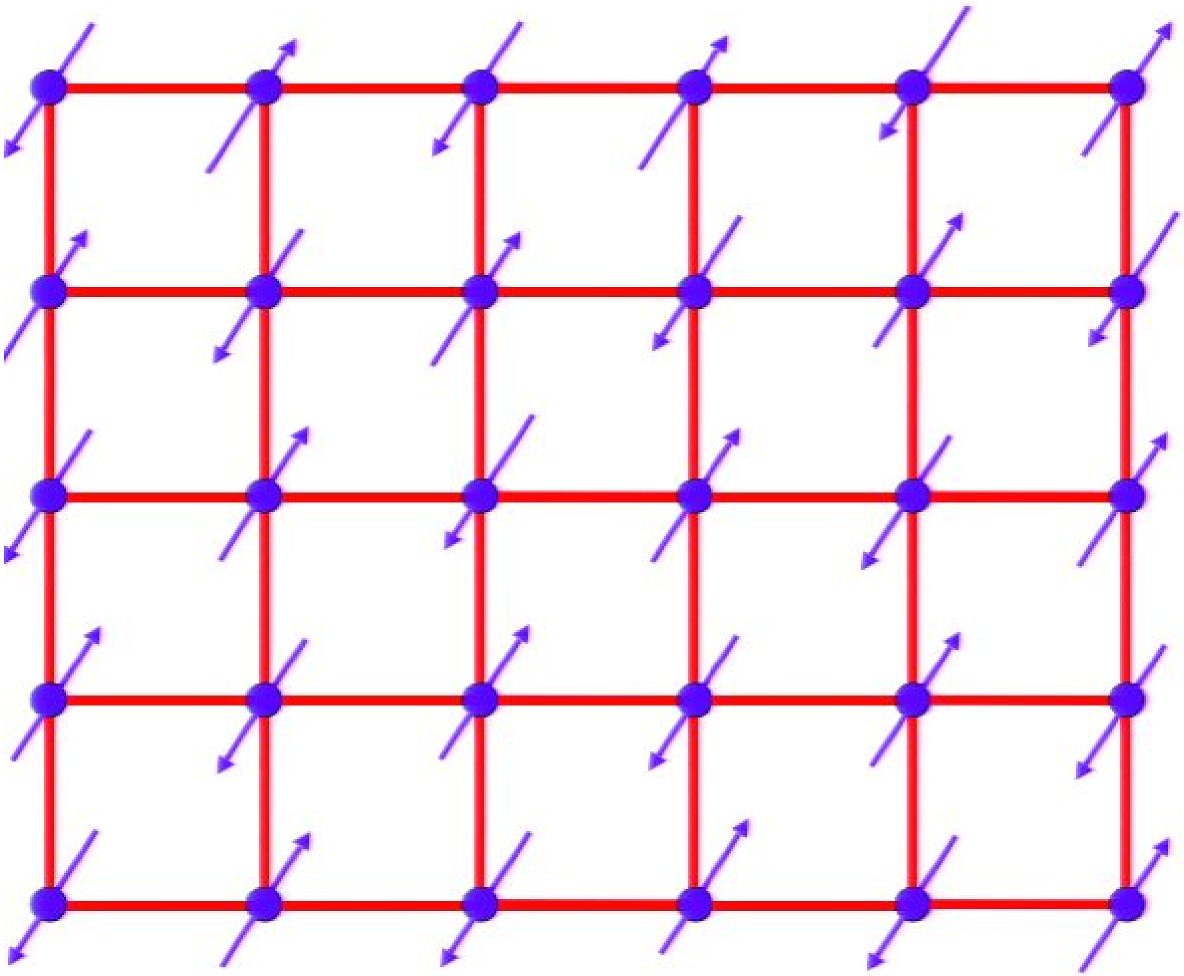

Excitations: 2 spin waves (Goldstone modes)

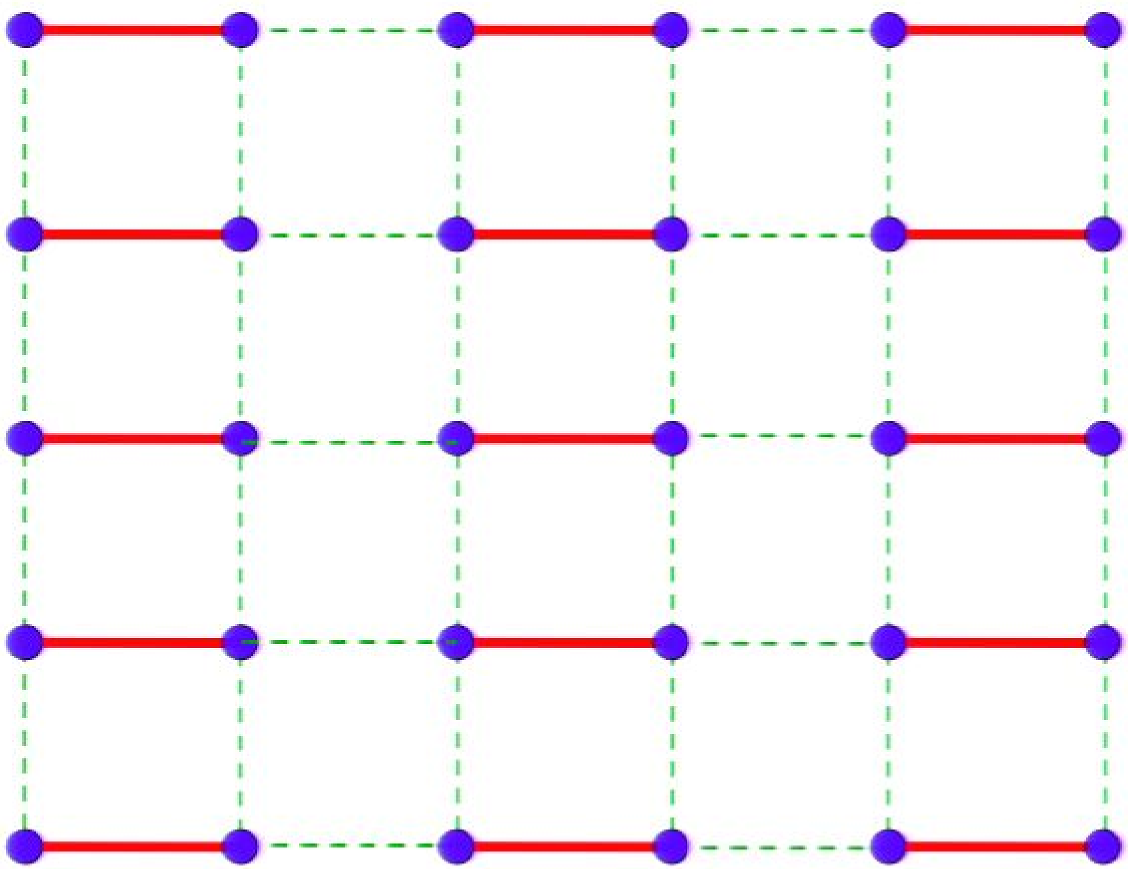

Weaken some bonds to induce spin entanglement in a new quantum phase

Antiferromagnetic (Neel) order in the insulator

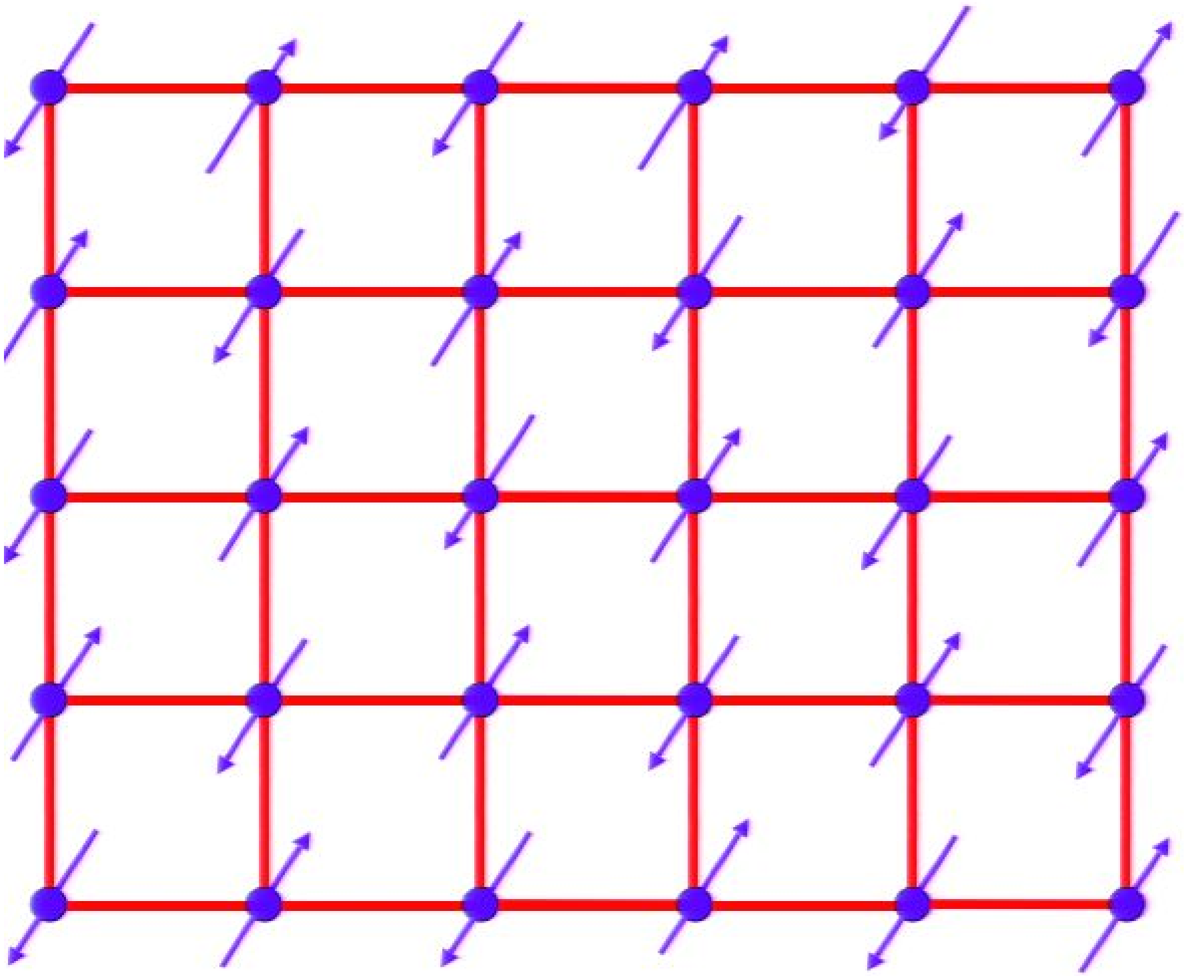

Excitations: 2 spin waves (Goldstone modes)

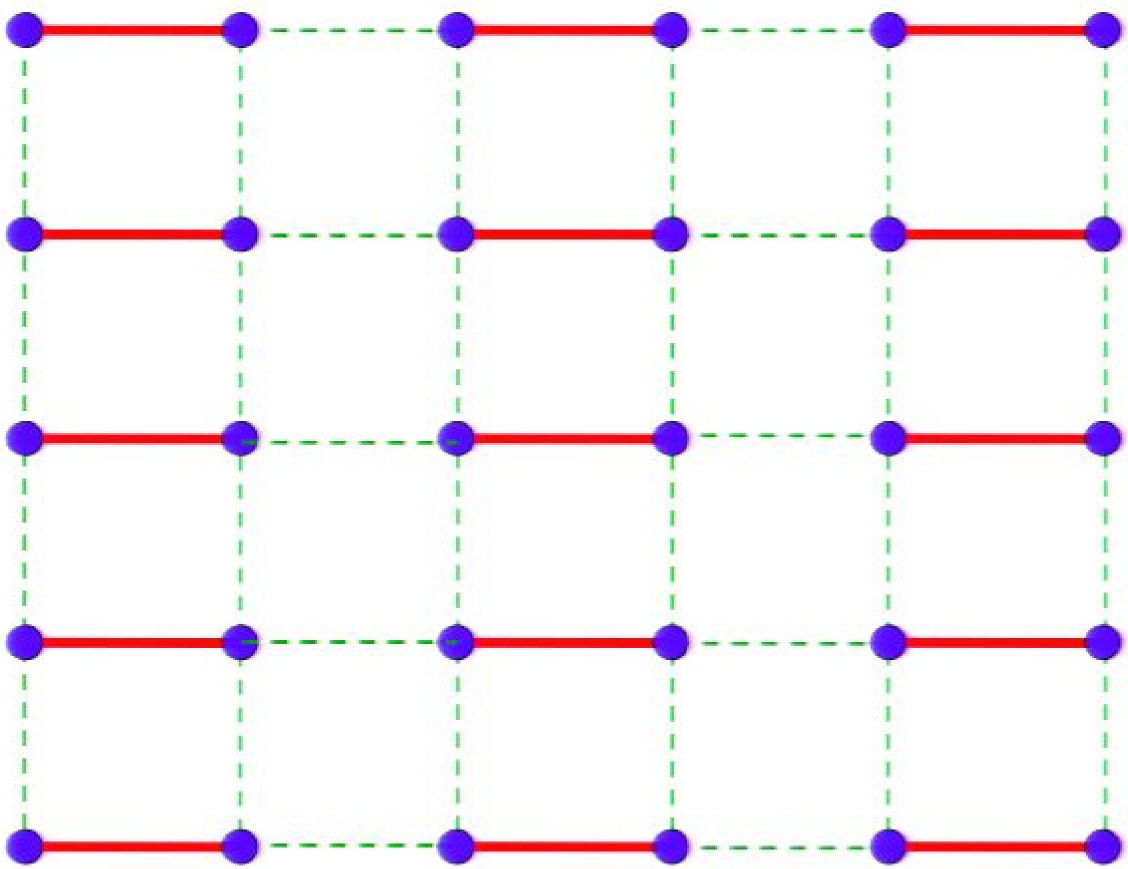

Weaken some bonds to induce spin entanglement in a new quantum phase

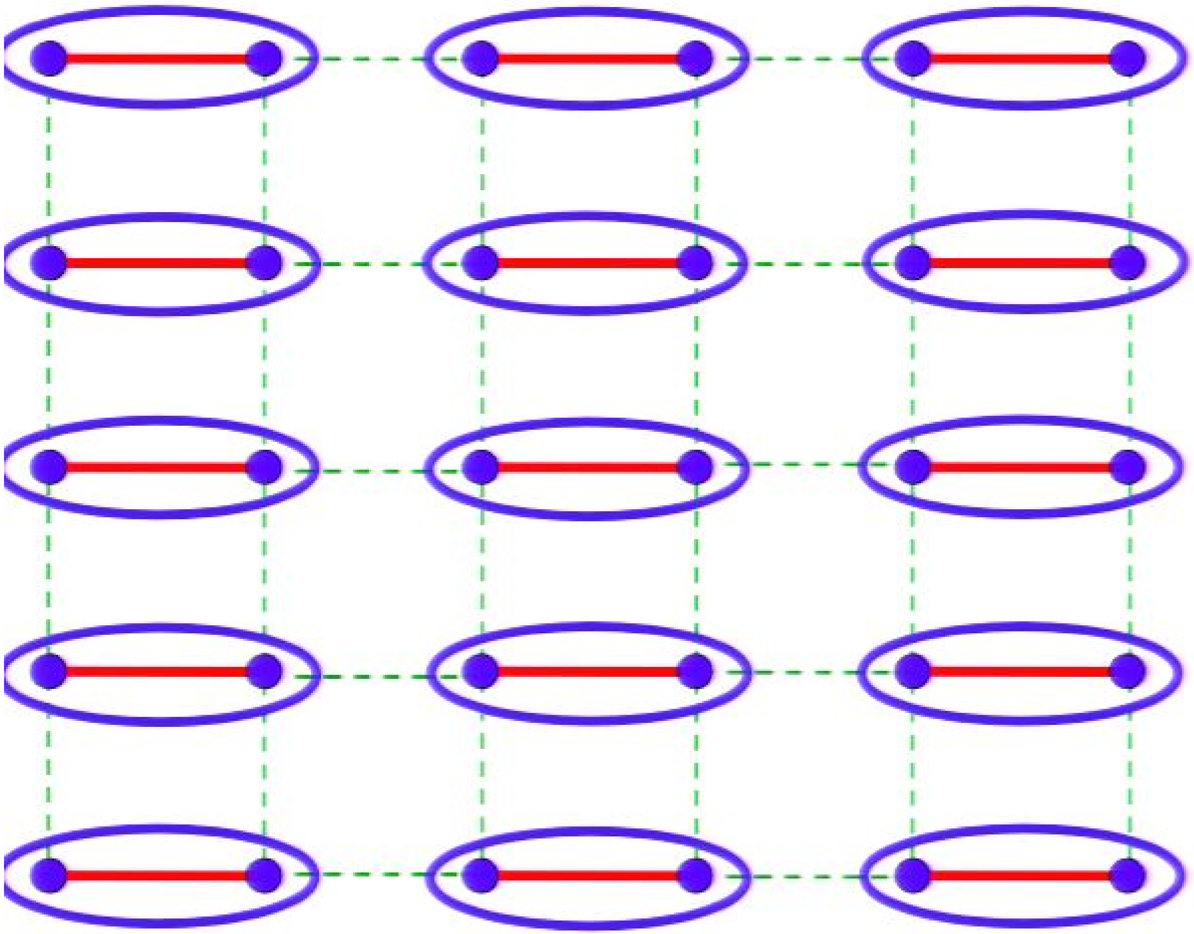

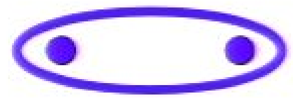

$$= \frac{1}{\sqrt{2}}\left(\left|\uparrow\downarrow\right\rangle - \left|\downarrow\uparrow\right\rangle\right)$$

Ground state is a product of pairs
of entangled spins.

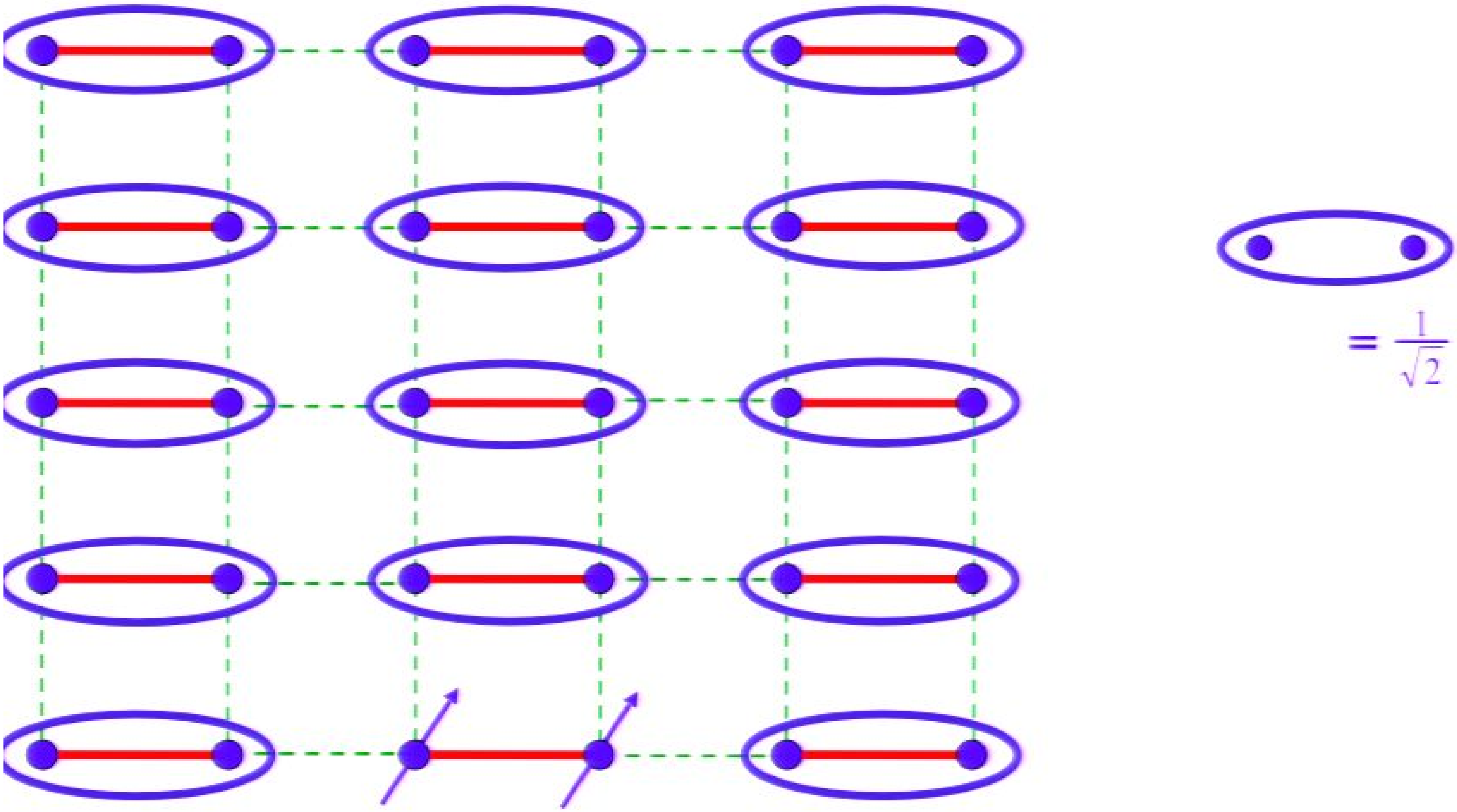

$$= \frac{1}{\sqrt{2}}\left(\left|\uparrow\downarrow\right\rangle - \left|\downarrow\uparrow\right\rangle\right)$$

Excitations: 3 $S=1$ triplons

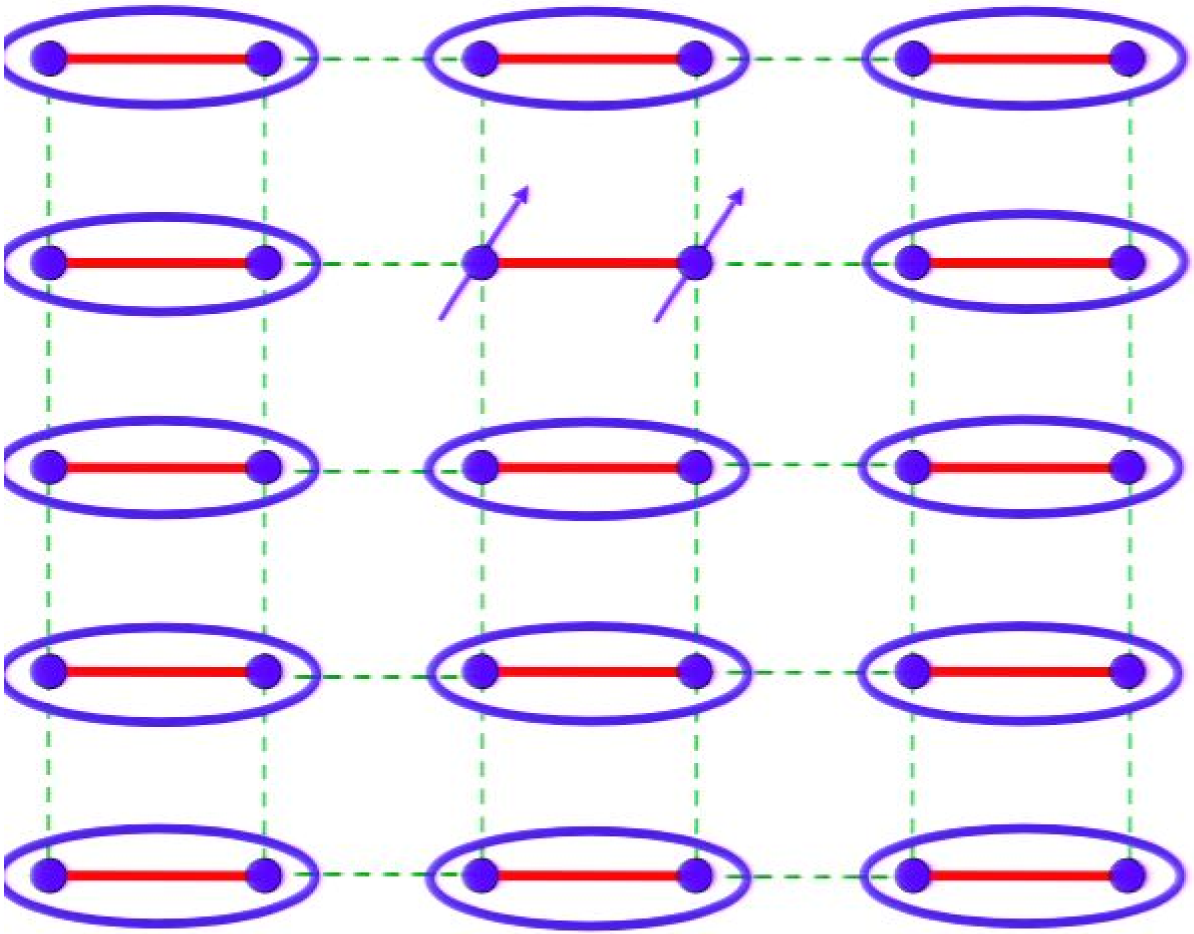

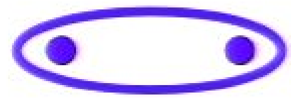

$$= \frac{1}{\sqrt{2}}\left(\left|\uparrow\downarrow\right\rangle - \left|\downarrow\uparrow\right\rangle\right)$$

Excitations: 3 $S=1$ triplons

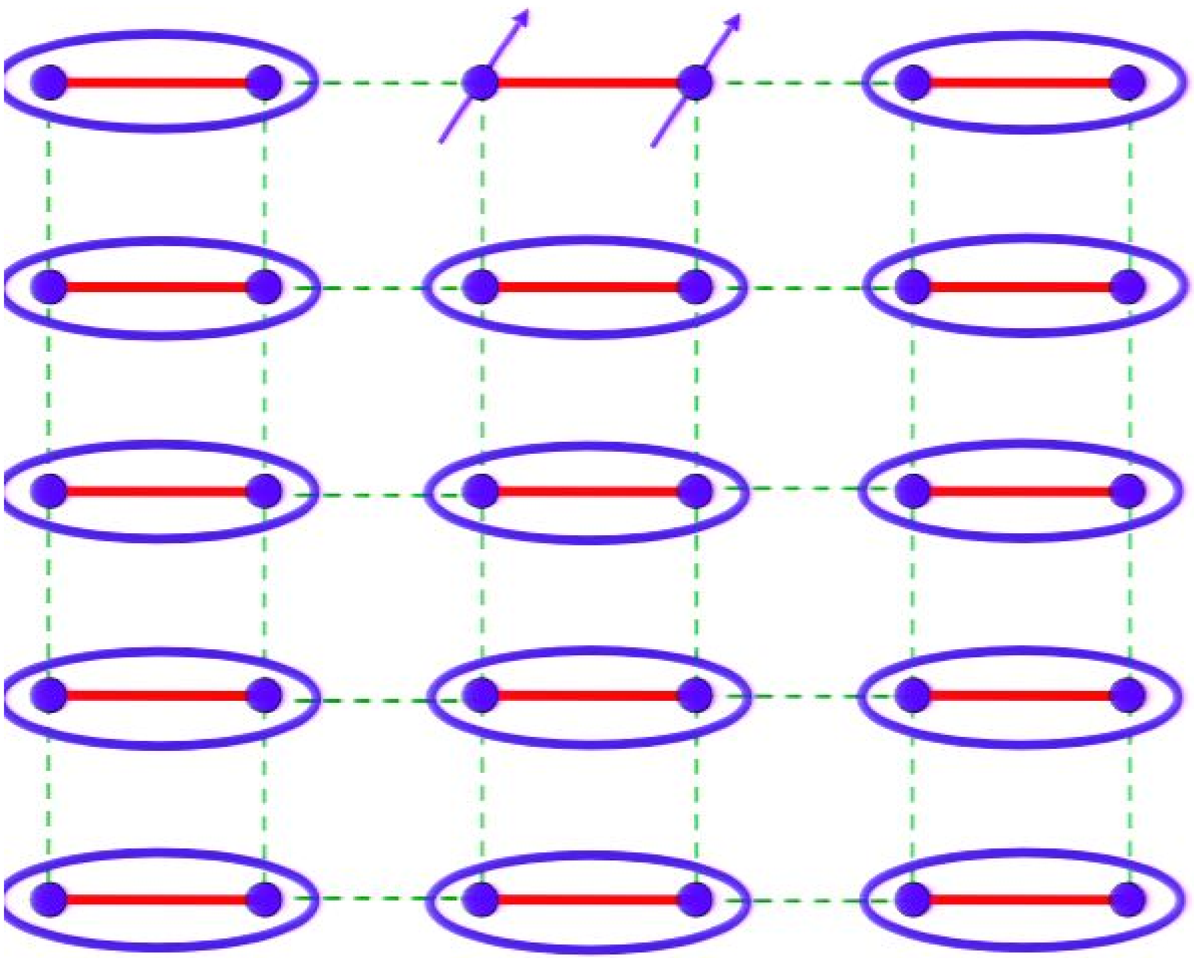

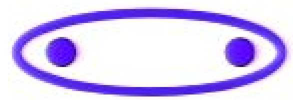

$= \frac{1}{\sqrt{2}} \left(\left| \uparrow \downarrow \right\rangle - \left| \downarrow \uparrow \right\rangle \right)$

Excitations: 3 *S*=*1* triplons

Phase diagram as a function of the ratio of exchange interactions, λ

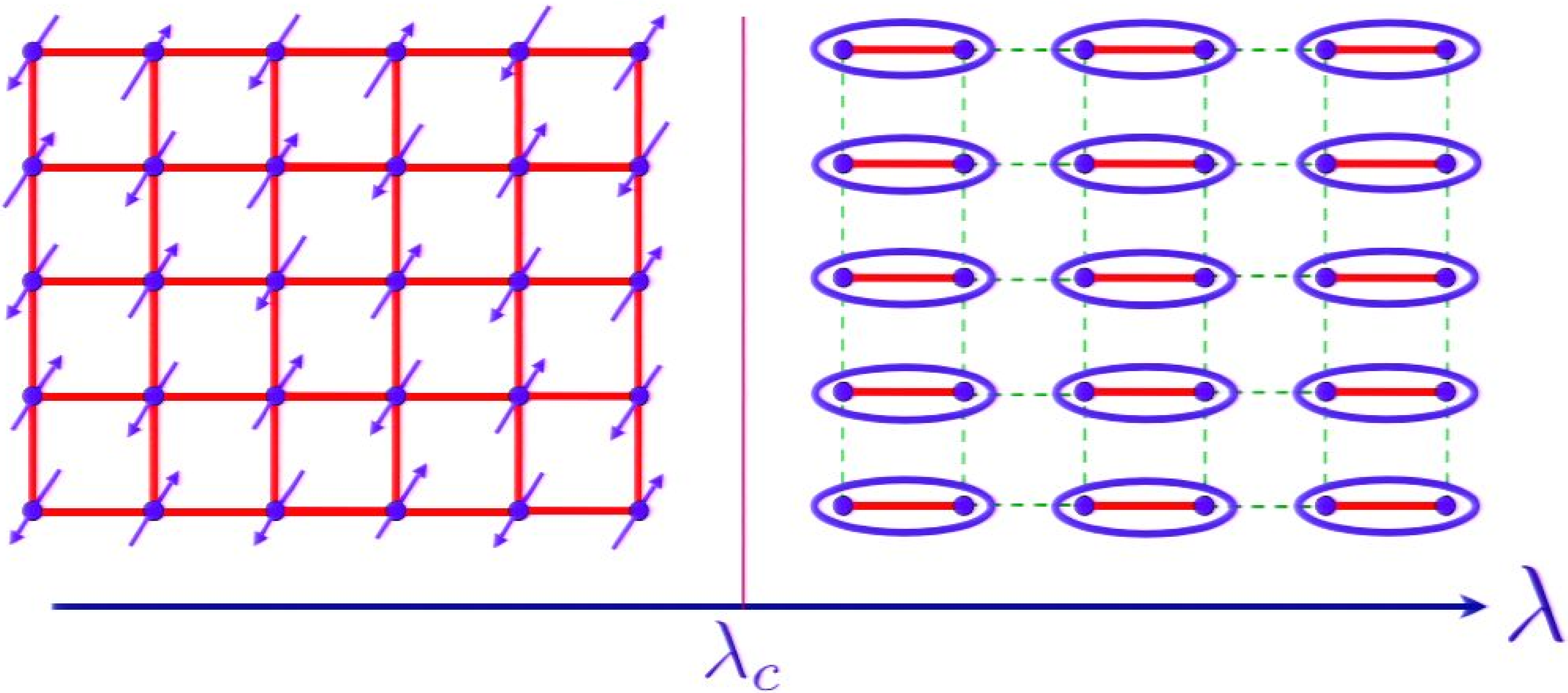

Phase diagram as a function of the ratio of exchange interactions, λ

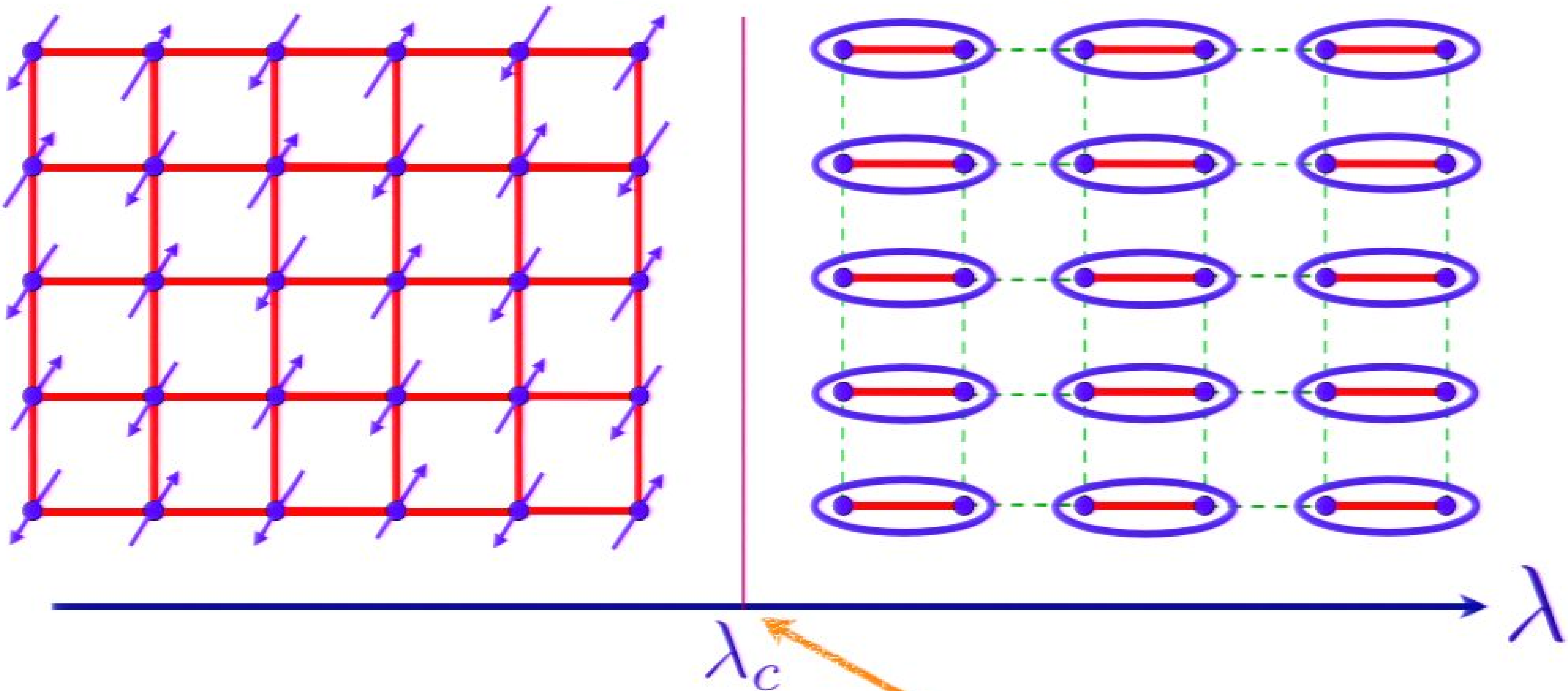

Quantum critical point with non-local entanglement in spin wavefunction

$TlCuCl_3$

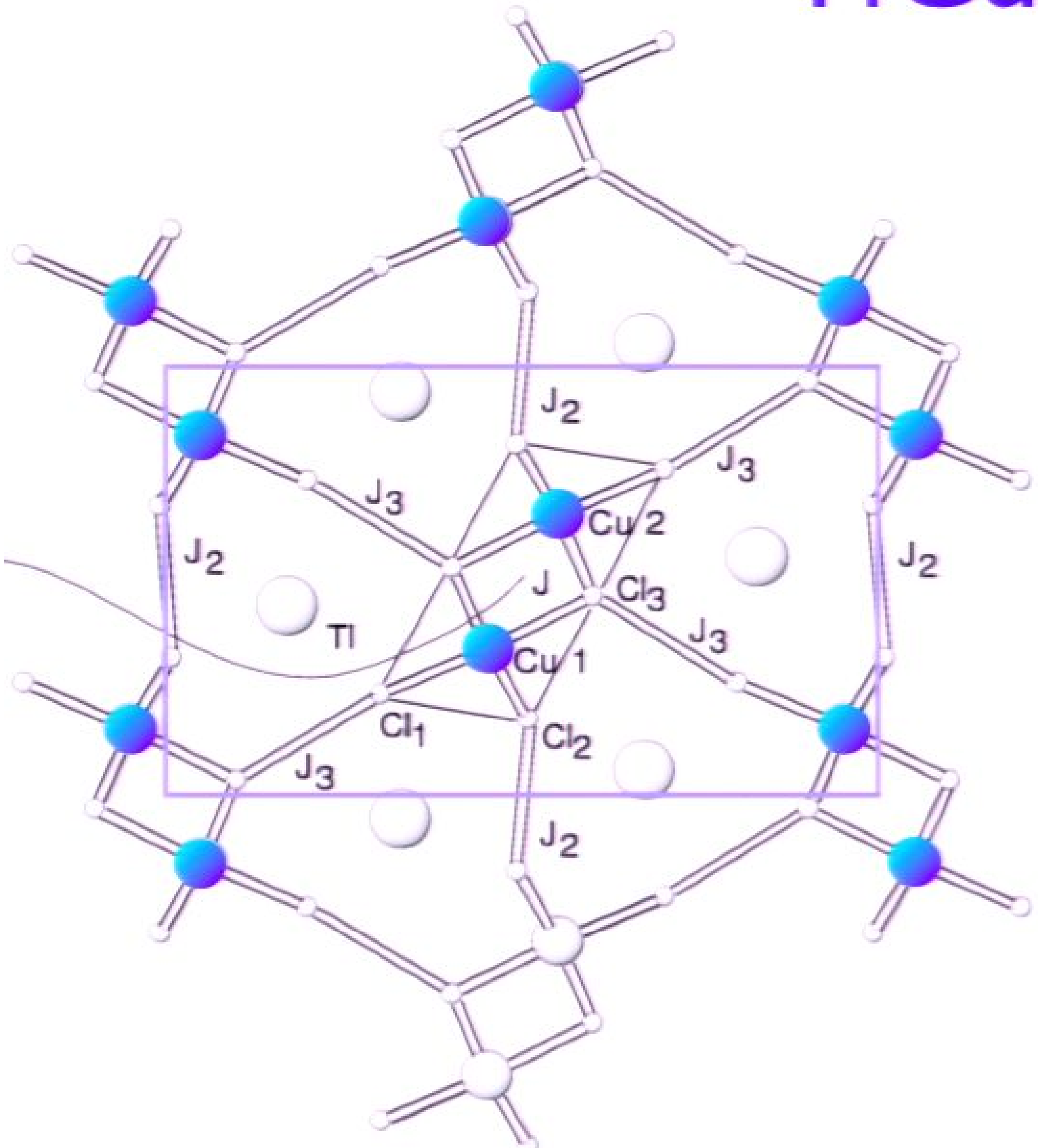

J2
J3
J3
Cu 2
J2
J
Cl3
J2
Tl
J3
Cu 1
Cl1
Cl2
J3
J2

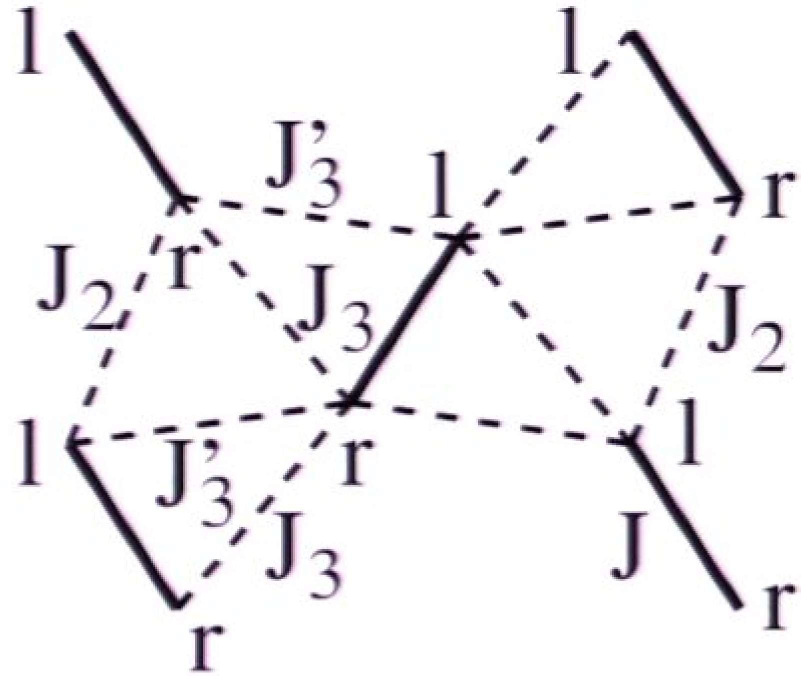

l
J'3
l
l
r
r
J2
J3
J2
l
r
l
J'3
J3
J
r
r

Phase diagram as a function of the ratio of exchange interactions, λ

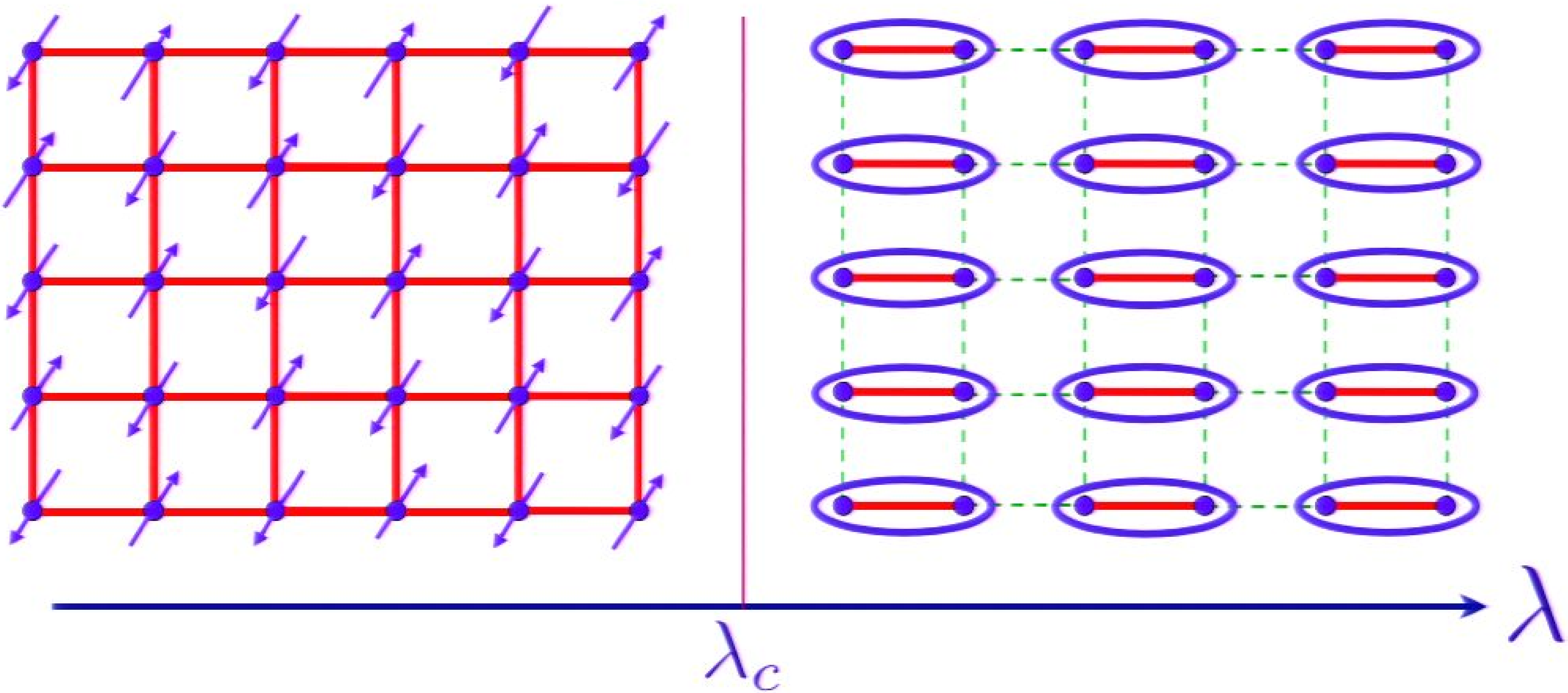

Phase diagram as a function of the ratio of exchange interactions, λ

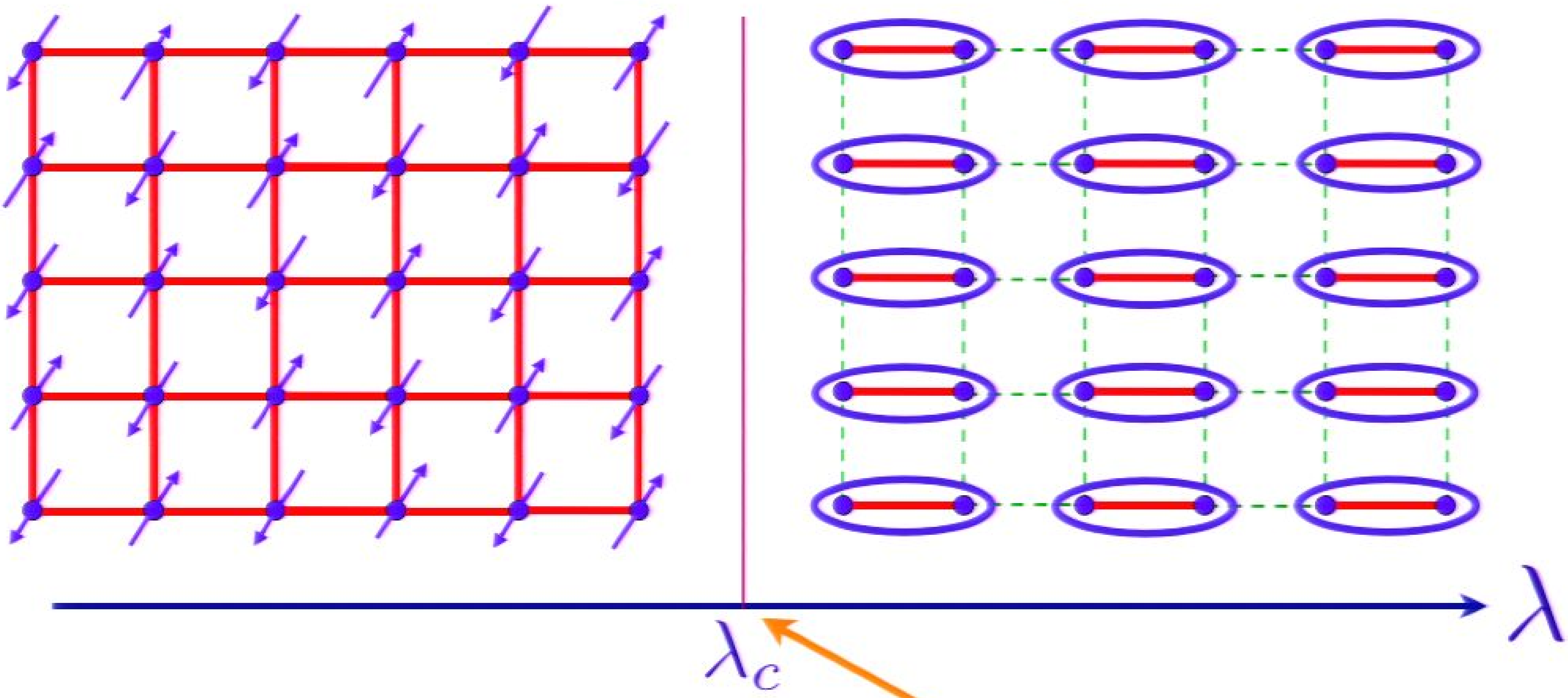

Quantum critical point with non-local entanglement in spin wavefunction

$TlCuCl_3$

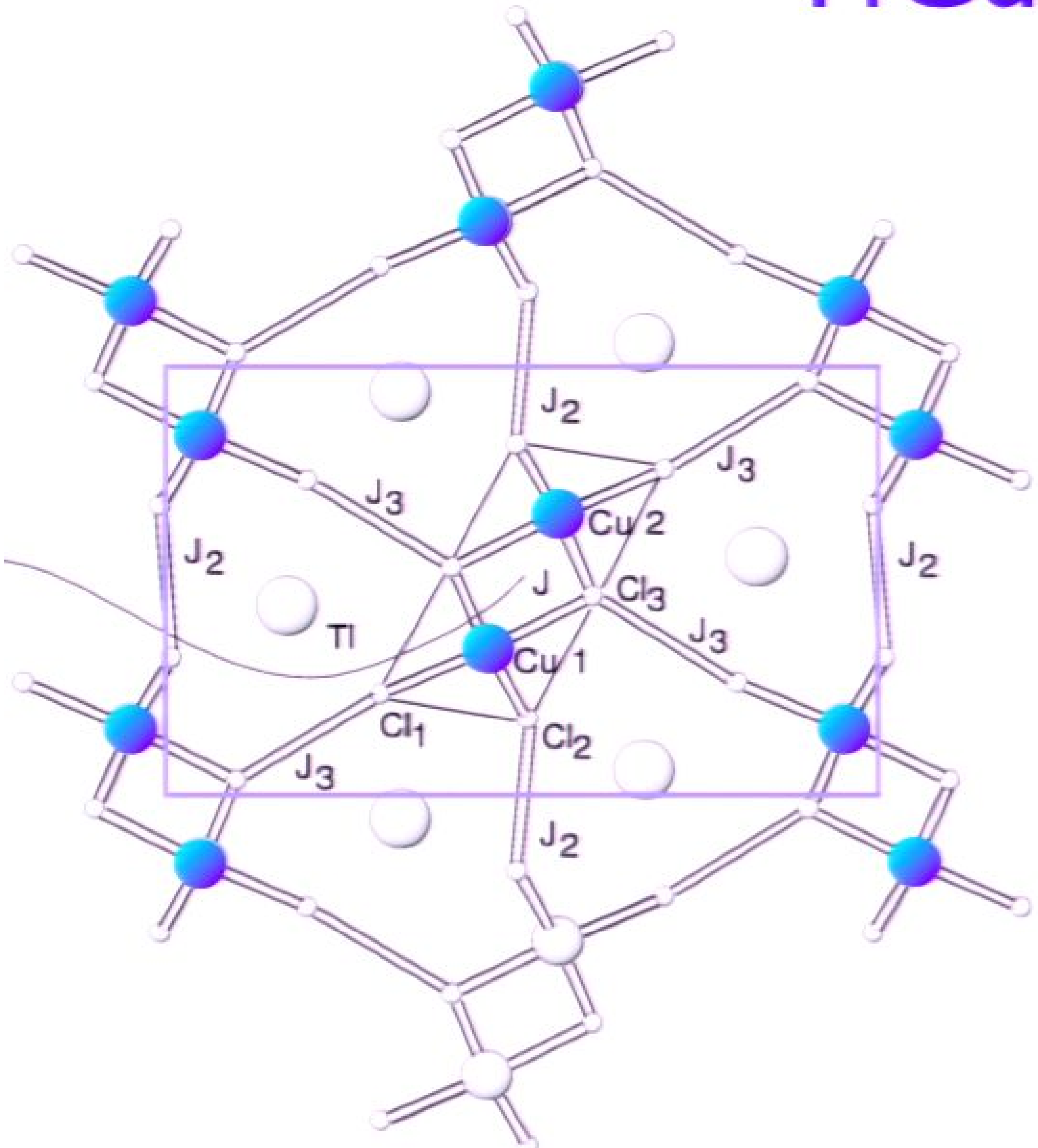

J2
J3
Cu 2
J2
J
Cl3
J2
Tl
J3
Cu 1
Cl1
Cl2
J3
J2

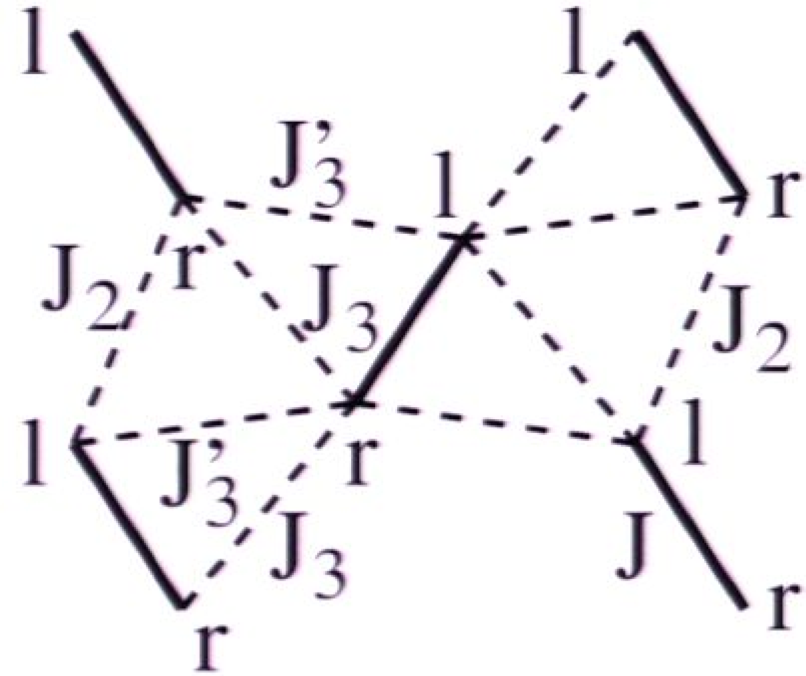

l
J'3
l
l
r
r
J2
J3
J2
l
r
l
J'3
J3
J
r
r

Phase diagram as a function of the ratio of exchange interactions, λ

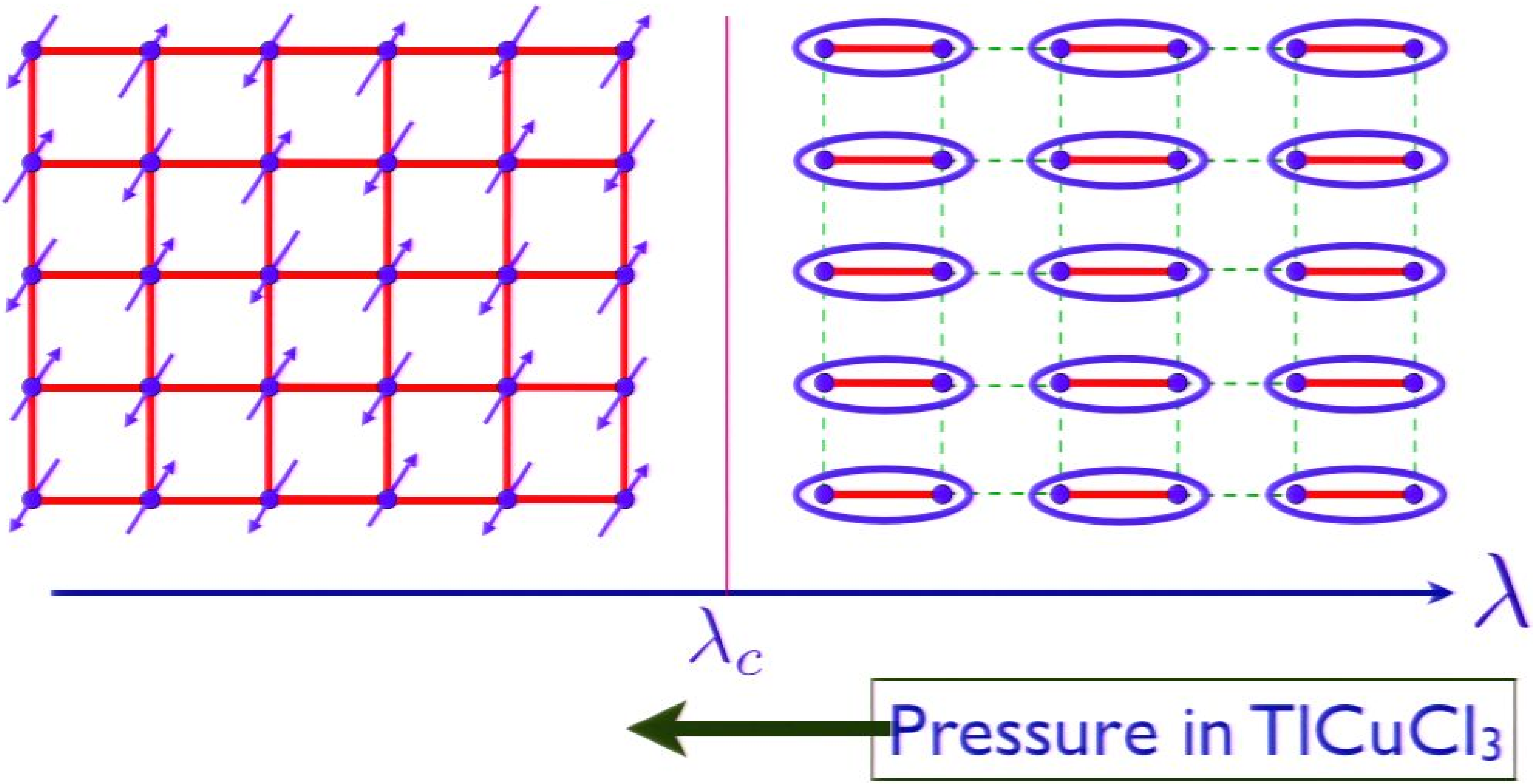

Phase diagram as a function of the ratio of exchange interactions, λ

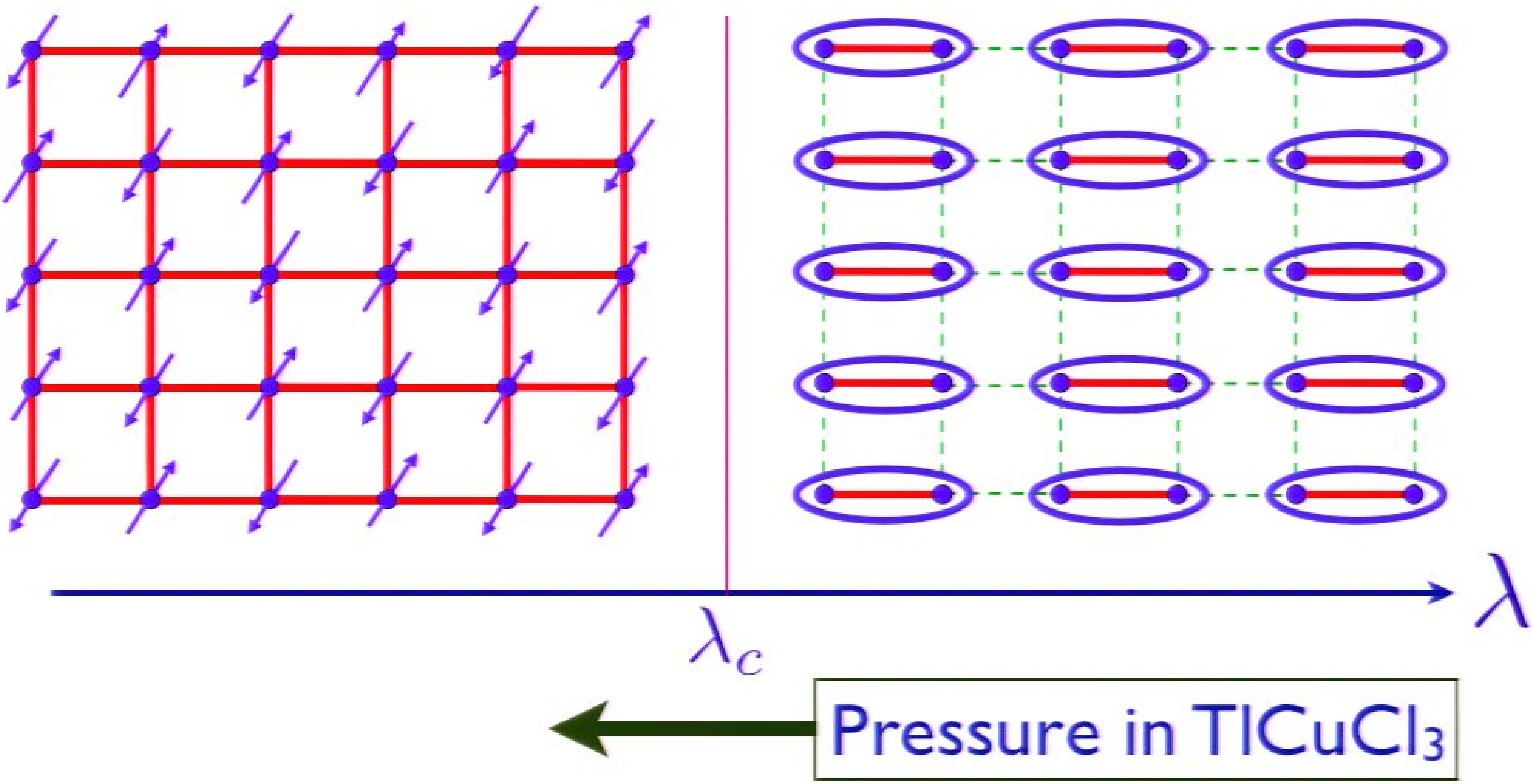

$TlCuCl_3$ at ambient pressure

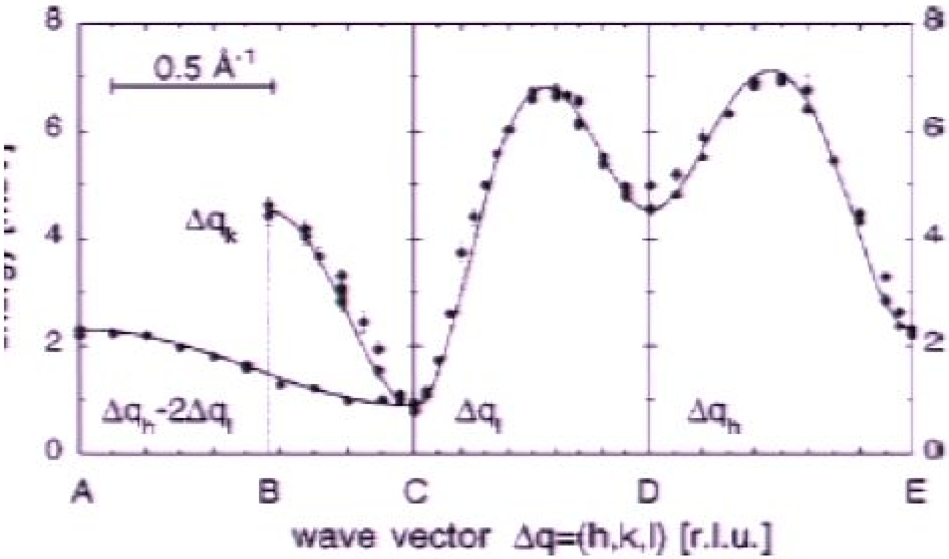

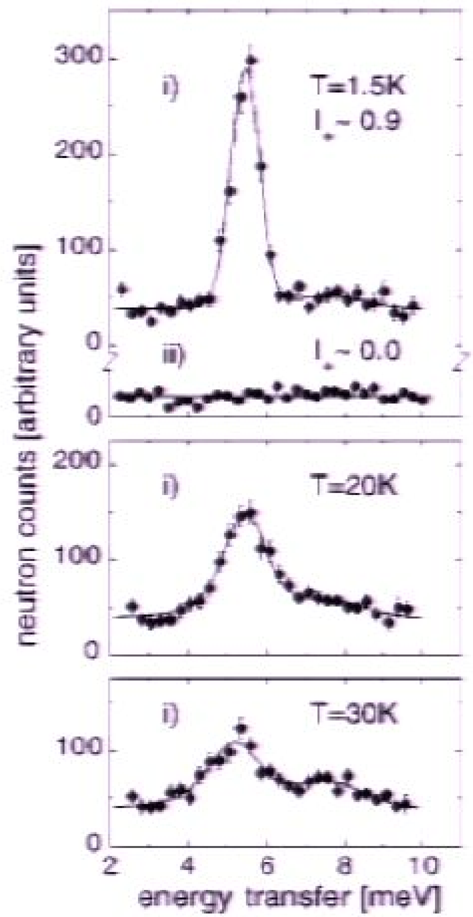

FIG. 1. Measured neutron profiles in the a^*c^* plane of $TlCuCl_3$ for $i=(1.35,0,0)$, $ii=(0,0,3.15)$ [r.l.u]. The spectrum at $T=1.5$ K

N. Cavadini, G. Heigold, W. Henggeler, A. Furrer, H.-U. Güdel, K. Krämer and H. Mutka, *Phys. Rev.* B 63 172414 (2001).

$TlCuCl_3$ at ambient pressure

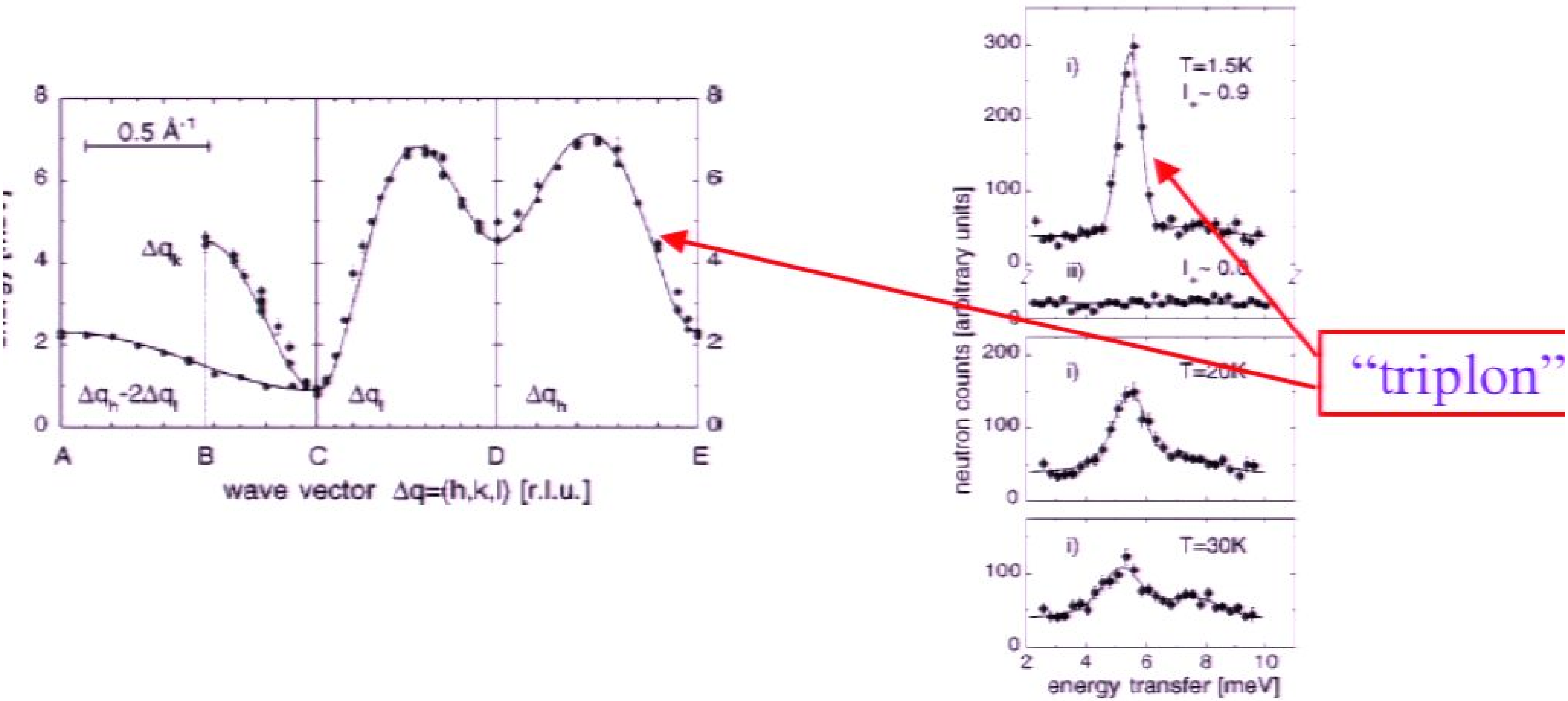

FIG. 1. Measured neutron profiles in the a^*c^* plane of $TlCuCl_3$ for $i=(1.35,0,0)$, $ii=(0,0,3.15)$ [r.l.u]. The spectrum at $T=1.5$ K

N. Cavadini, G. Heigold, W. Henggeler, A. Furrer, H.-U. Güdel, K. Krämer and H. Mutka, *Phys. Rev.* B 63 172414 (2001).

$TlCuCl_3$ with varying pressure

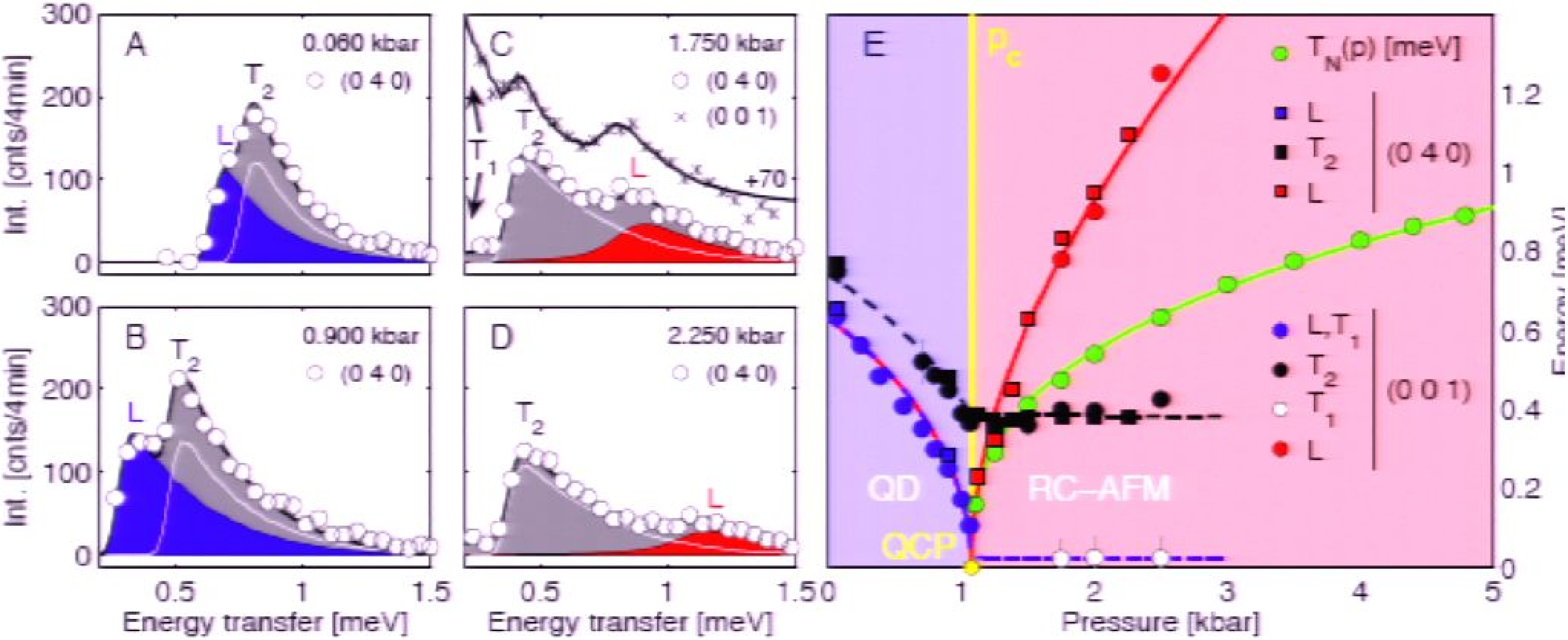

Observation of 3 → 2 low energy modes, emergence of new longitudinal mode in Néel phase, and vanishing of Néel temperature at the quantum critical point

Christian Ruegg, Bruce Normand, Masashige Matsumoto, Albert Furrer, Desmond McMorrow, Karl Kramer, Hans–Ulrich Gudel, Severian Gvasaliya, Hannu Mutka, and Martin Boehm, arXiv:0803.372

$TlCuCl_3$ at ambient pressure

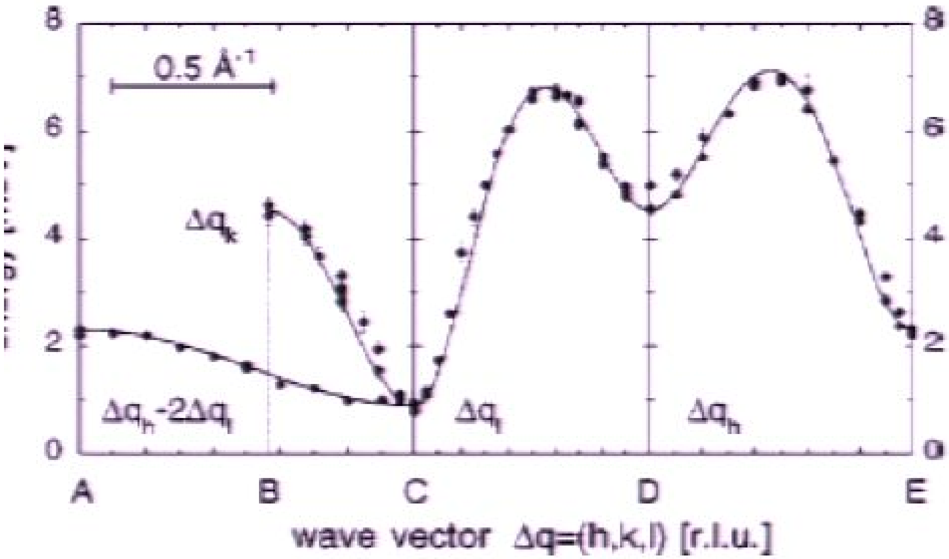

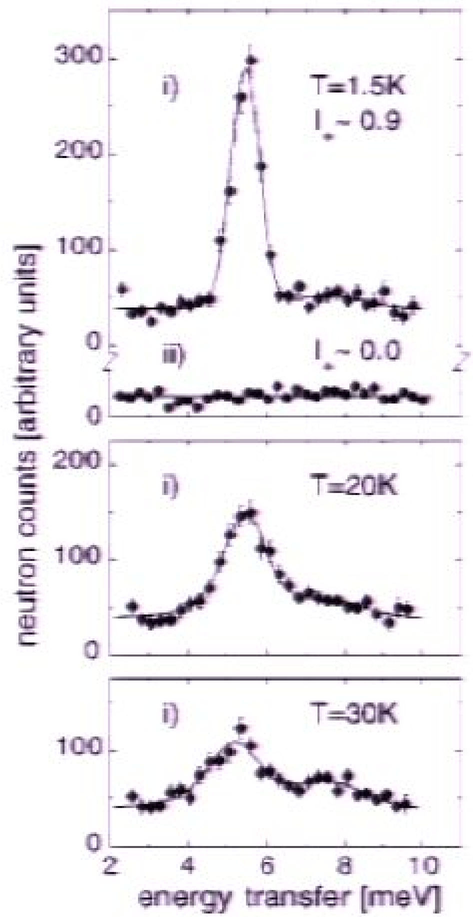

FIG. 1. Measured neutron profiles in the a^*c^* plane of $TlCuCl_3$ for $i=(1.35,0,0)$, $ii=(0,0,3.15)$ [r.l.u]. The spectrum at $T=1.5$ K

N. Cavadini, G. Heigold, W. Henggeler, A. Furrer, H.-U. Güdel, K. Krämer and H. Mutka, *Phys. Rev.* B 63 172414 (2001).

Phase diagram as a function of the ratio of exchange interactions, λ

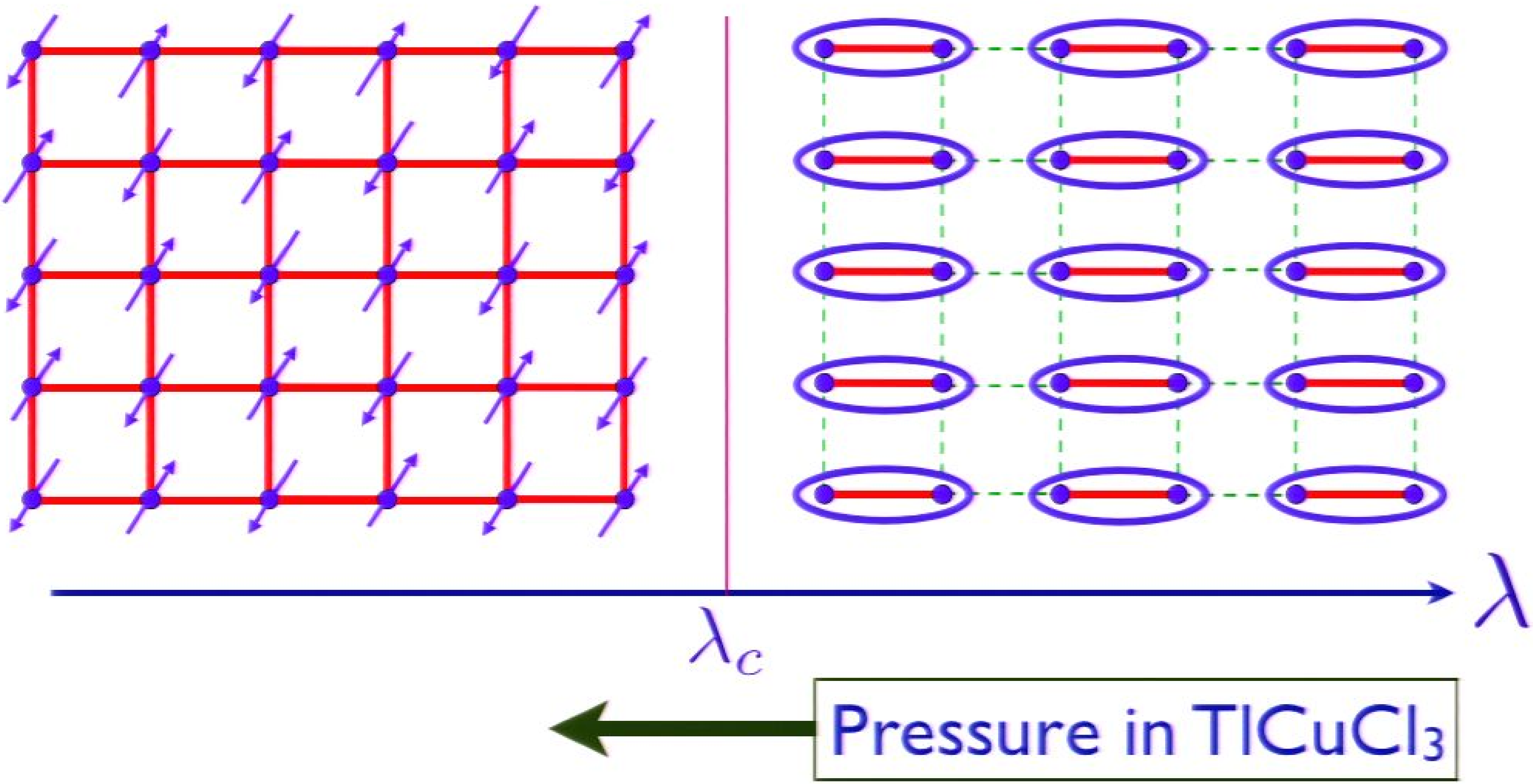

$TlCuCl_3$ at ambient pressure

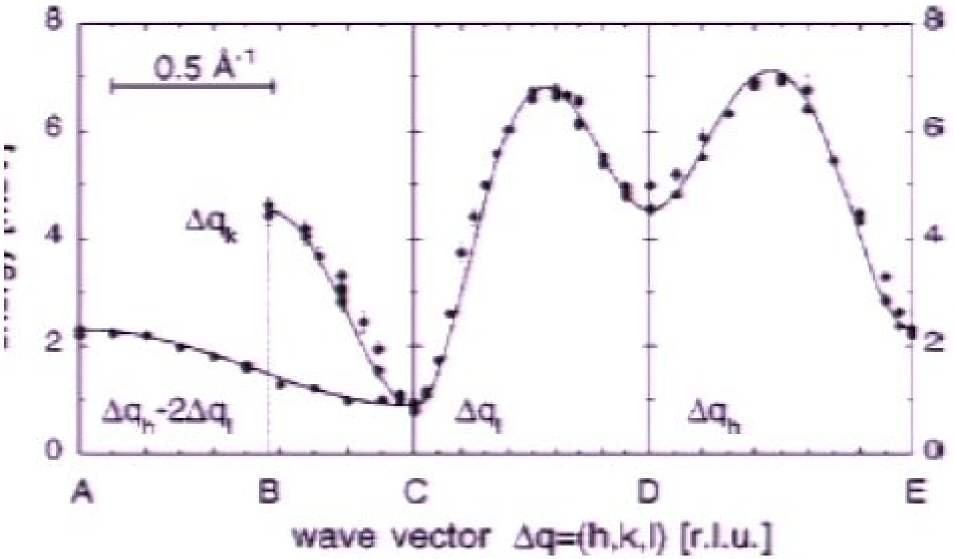

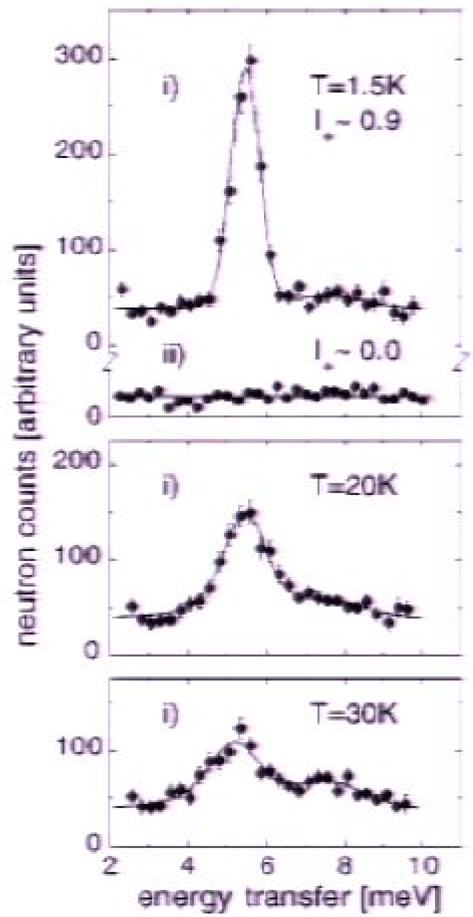

FIG. 1. Measured neutron profiles in the a^*c^* plane of $TlCuCl_3$ for $i=(1.35,0,0)$, $ii=(0,0,3.15)$ [r.l.u]. The spectrum at $T=1.5$ K

N. Cavadini, G. Heigold, W. Henggeler, A. Furrer, H.-U. Güdel, K. Krämer and H. Mutka, *Phys. Rev.* B 63 172414 (2001).

$TlCuCl_3$ with varying pressure

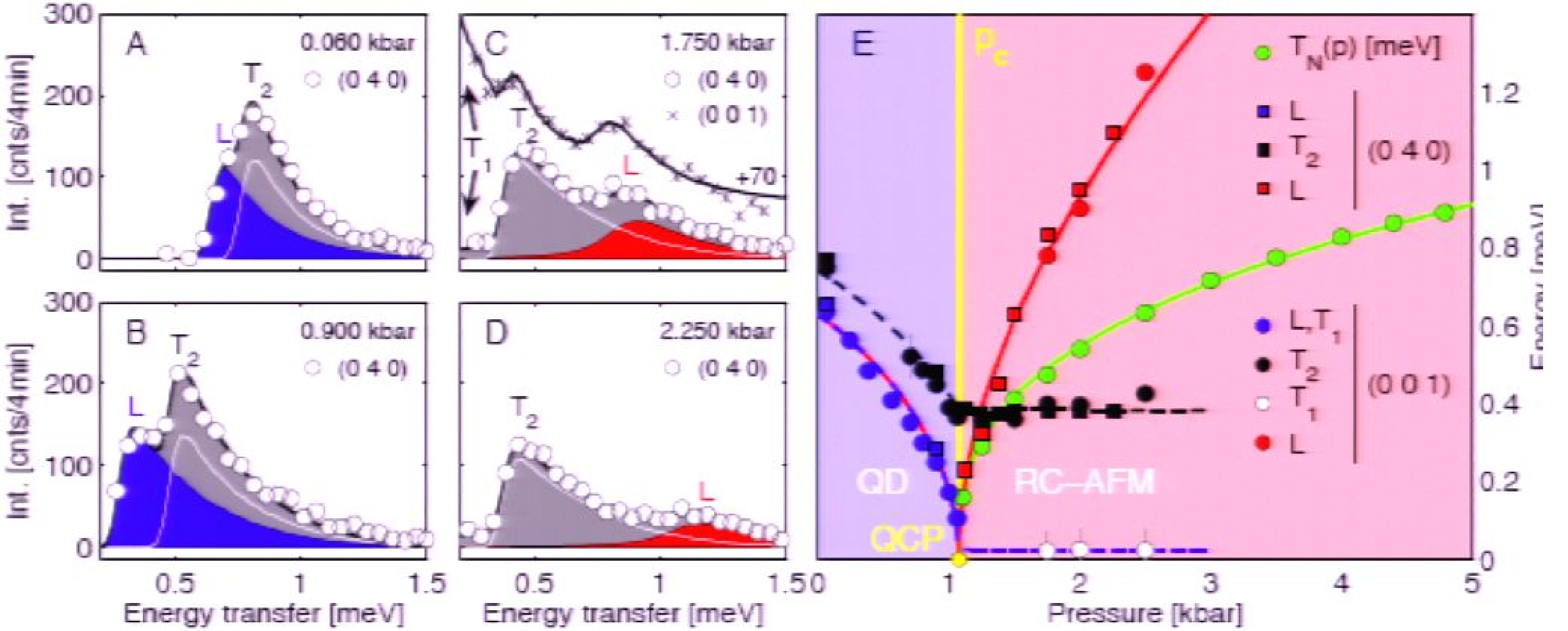

Observation of 3 → 2 low energy modes, emergence of new longitudinal mode in Néel phase, and vanishing of Néel temperature at the quantum critical point

Christian Ruegg, Bruce Normand, Masashige Matsumoto, Albert Furrer, Desmond McMorrow, Karl Kramer, Hans-Ulrich Gudel, Severian Gvasaliya, Hannu Mutka, and Martin Boehm, arXiv:0803.372

$TlCuCl_3$ at ambient pressure

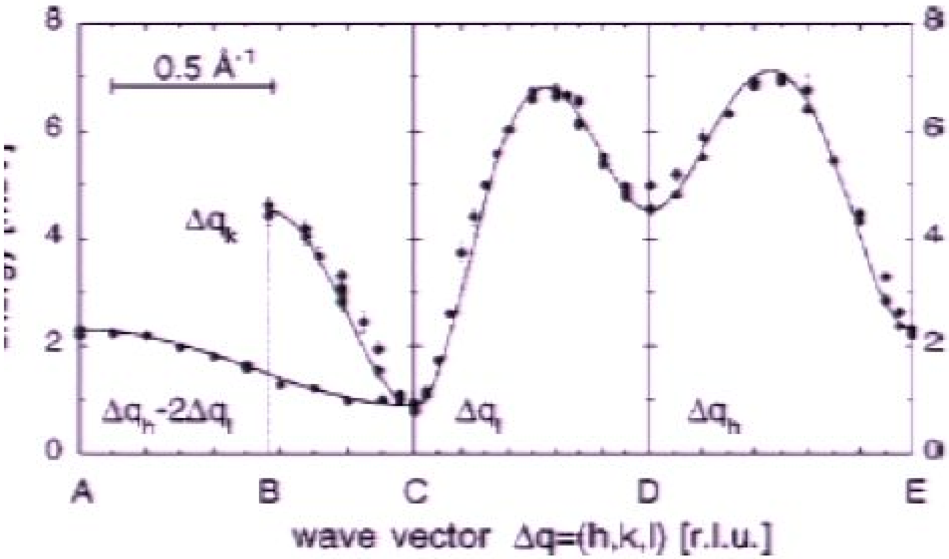

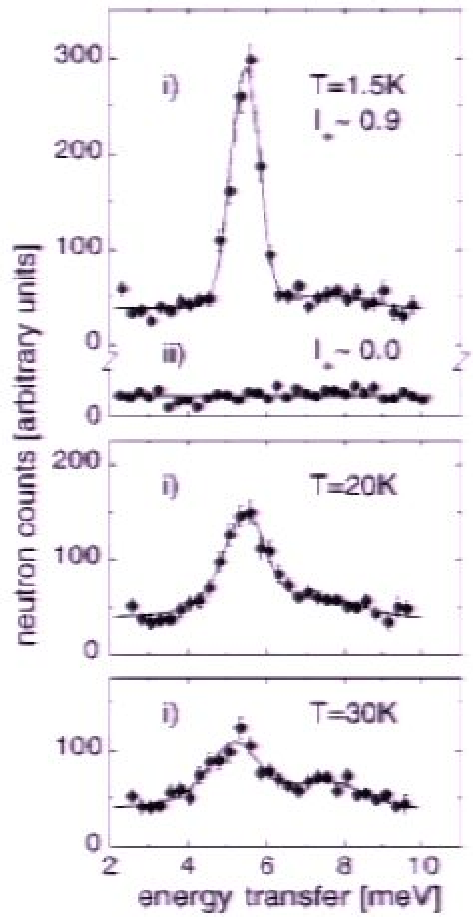

FIG. 1. Measured neutron profiles in the a^*c^* plane of $TlCuCl_3$ for $i=(1.35,0,0)$, $ii=(0,0,3.15)$ [r.l.u]. The spectrum at $T=1.5$ K

N. Cavadini, G. Heigold, W. Henggeler, A. Furrer, H.-U. Güdel, K. Krämer and H. Mutka, *Phys. Rev.* B 63 172414 (2001).

$TlCuCl_3$ at ambient pressure

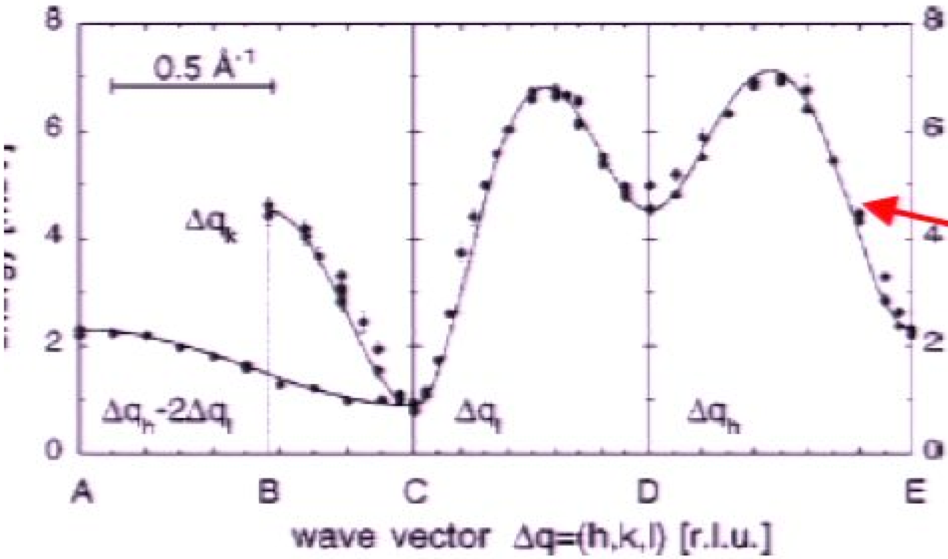

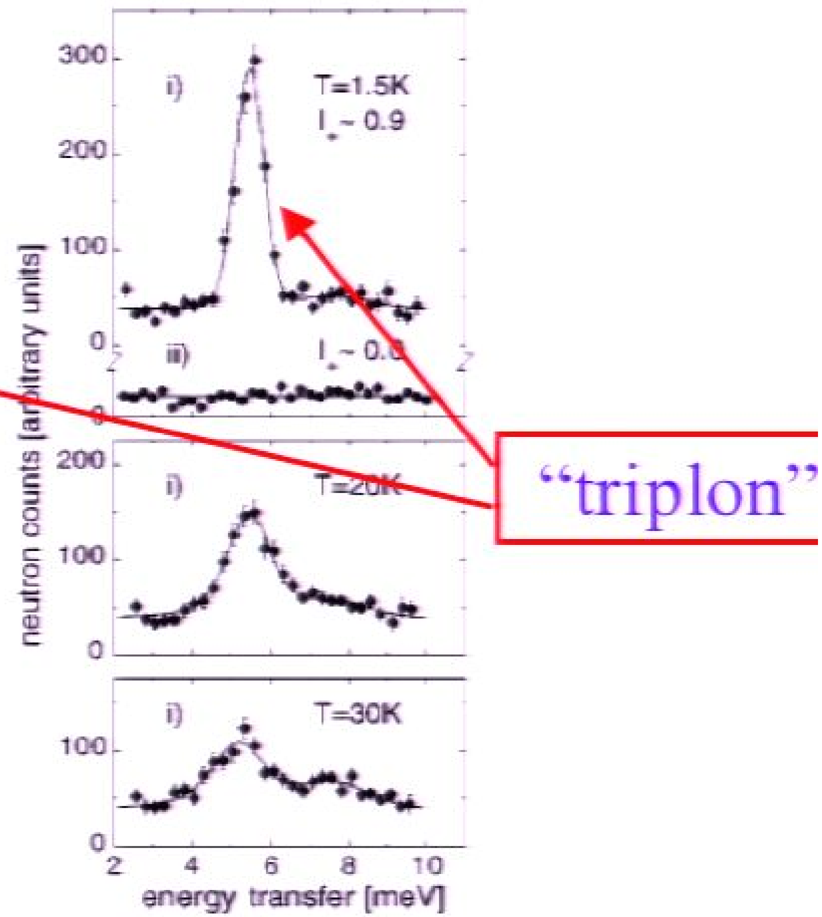

FIG. 1. Measured neutron profiles in the a^*c^* plane of $TlCuCl_3$ for $i=(1.35,0,0)$, $ii=(0,0,3.15)$ [r.l.u]. The spectrum at $T=1.5$ K

N. Cavadini, G. Heigold, W. Henggeler, A. Furrer, H.-U. Güdel, K. Krämer and H. Mutka, *Phys. Rev.* B 63 172414 (2001).

TlCuCl$_3$ with varying pressure

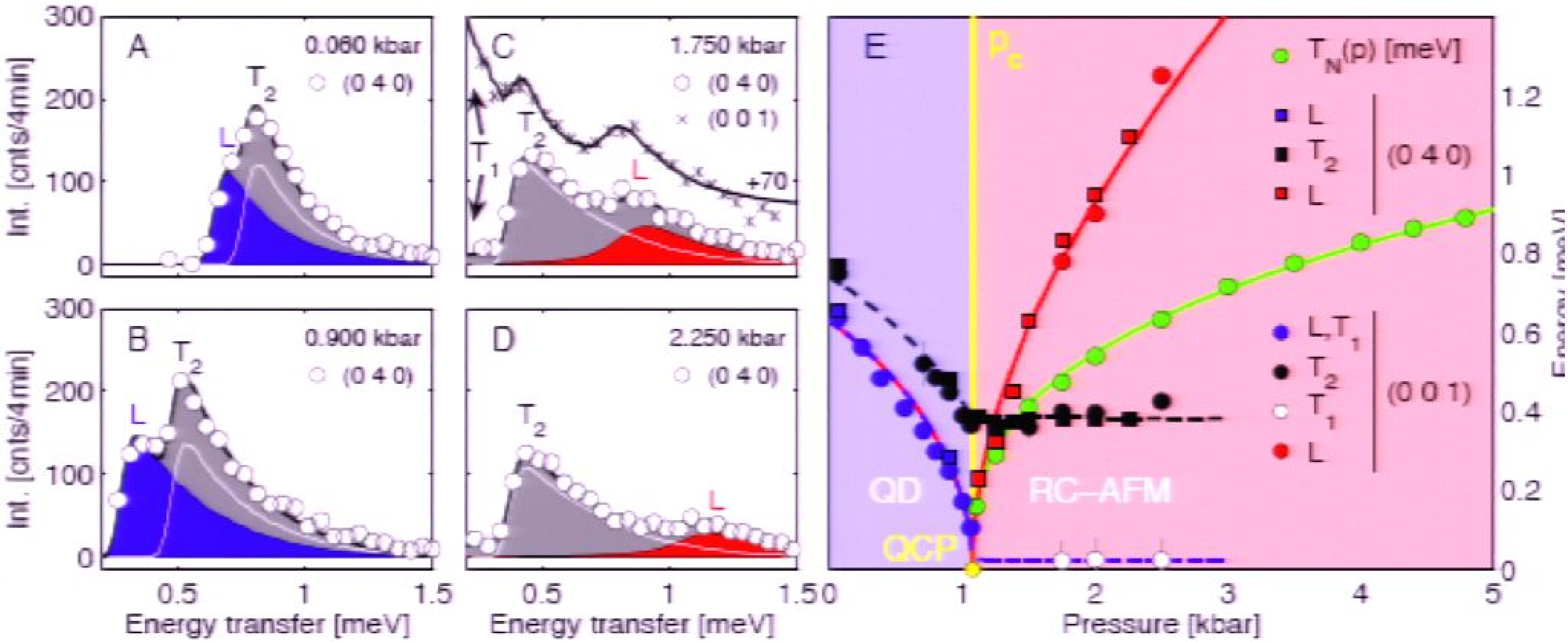

Observation of 3 → 2 low energy modes, emergence of new longitudinal mode in Néel phase, and vanishing of Néel temperature at the quantum critical point

Christian Ruegg, Bruce Normand, Masashige Matsumoto, Albert Furrer, Desmond McMorrow, Karl Kramer, Hans–Ulrich Gudel, Severian Gvasaliya, Hannu Mutka, and Martin Boehm, arXiv:0803.372

Quantum phase transition with full square lattice symmetry

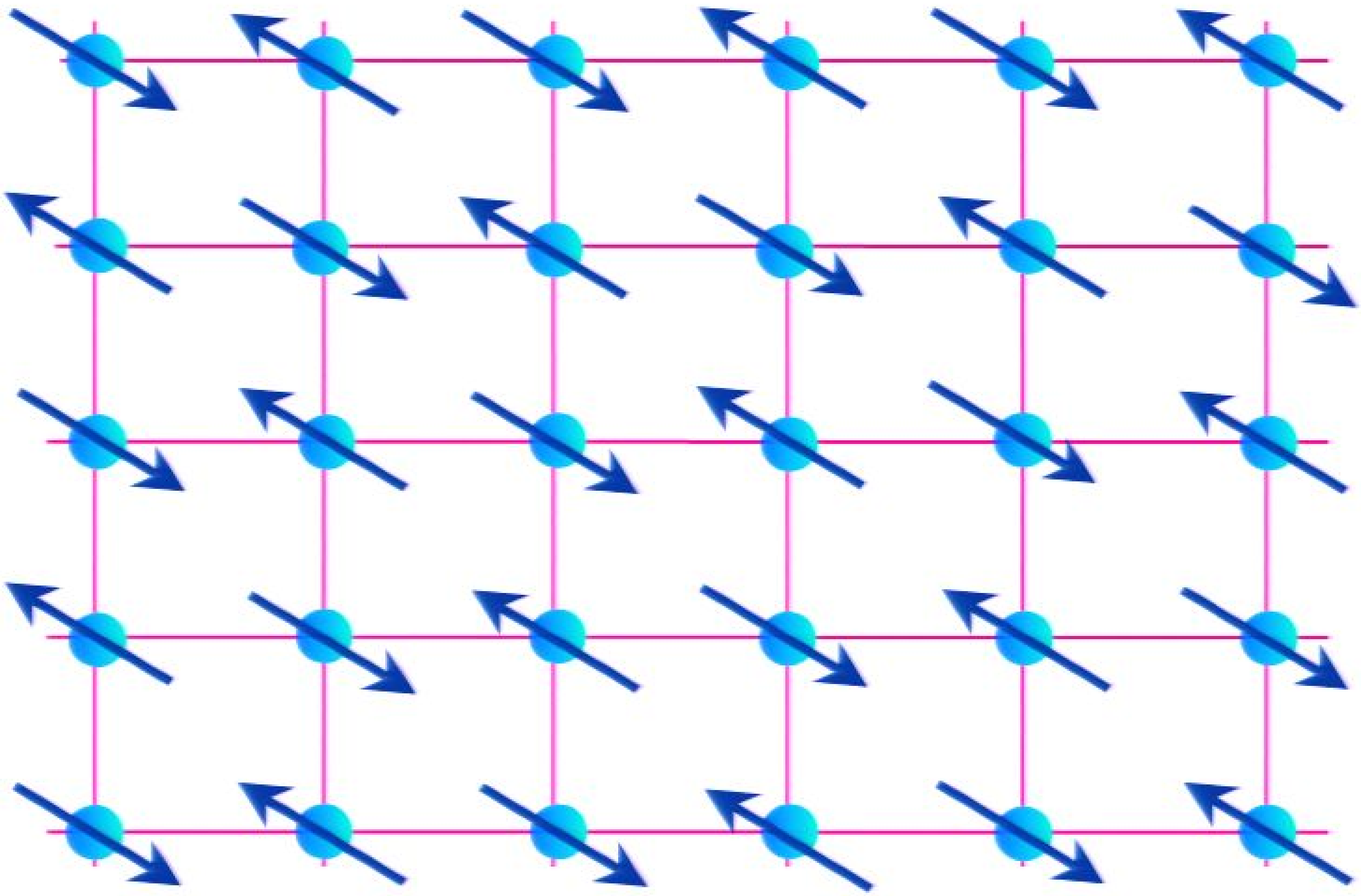

$$H = J \sum_{\langle ij \rangle} \vec{S}_i \cdot \vec{S}_j \quad ; \quad \vec{S}_i \Rightarrow \text{ spin operator with } S = 1/2$$

TlCuCl$_3$ at ambient pressure

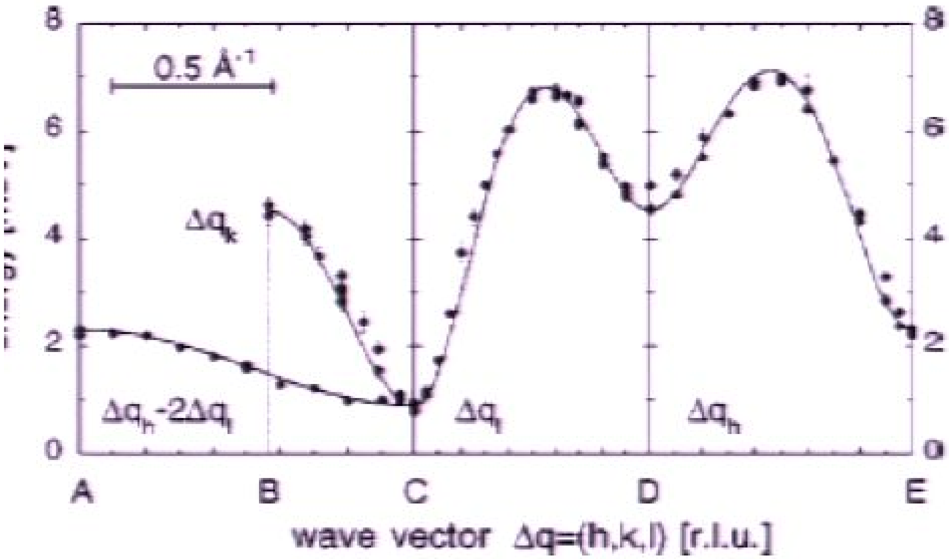

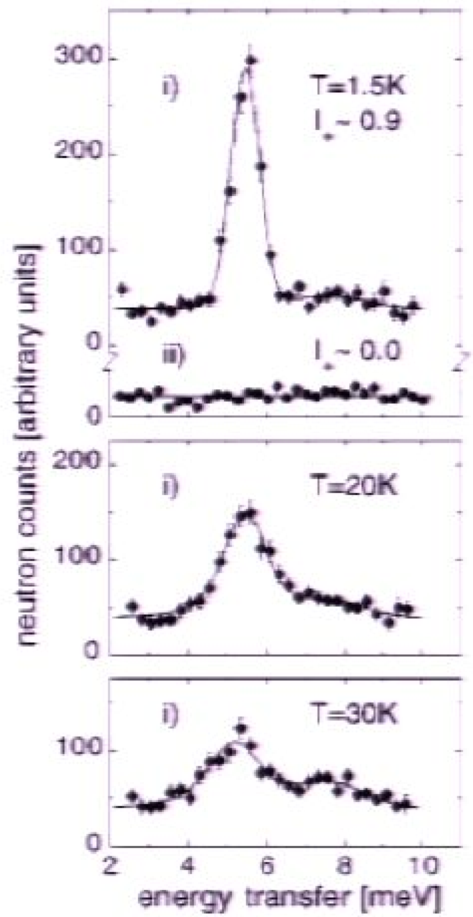

FIG. 1. Measured neutron profiles in the a^*c^* plane of TlCuCl$_3$ for $i=(1.35,0,0)$, $ii=(0,0,3.15)$ [r.l.u]. The spectrum at $T=1.5$ K

N. Cavadini, G. Heigold, W. Henggeler, A. Furrer, H.-U. Güdel, K. Krämer and H. Mutka, *Phys. Rev.* B 63 172414 (2001).

Phase diagram as a function of the ratio of exchange interactions, λ

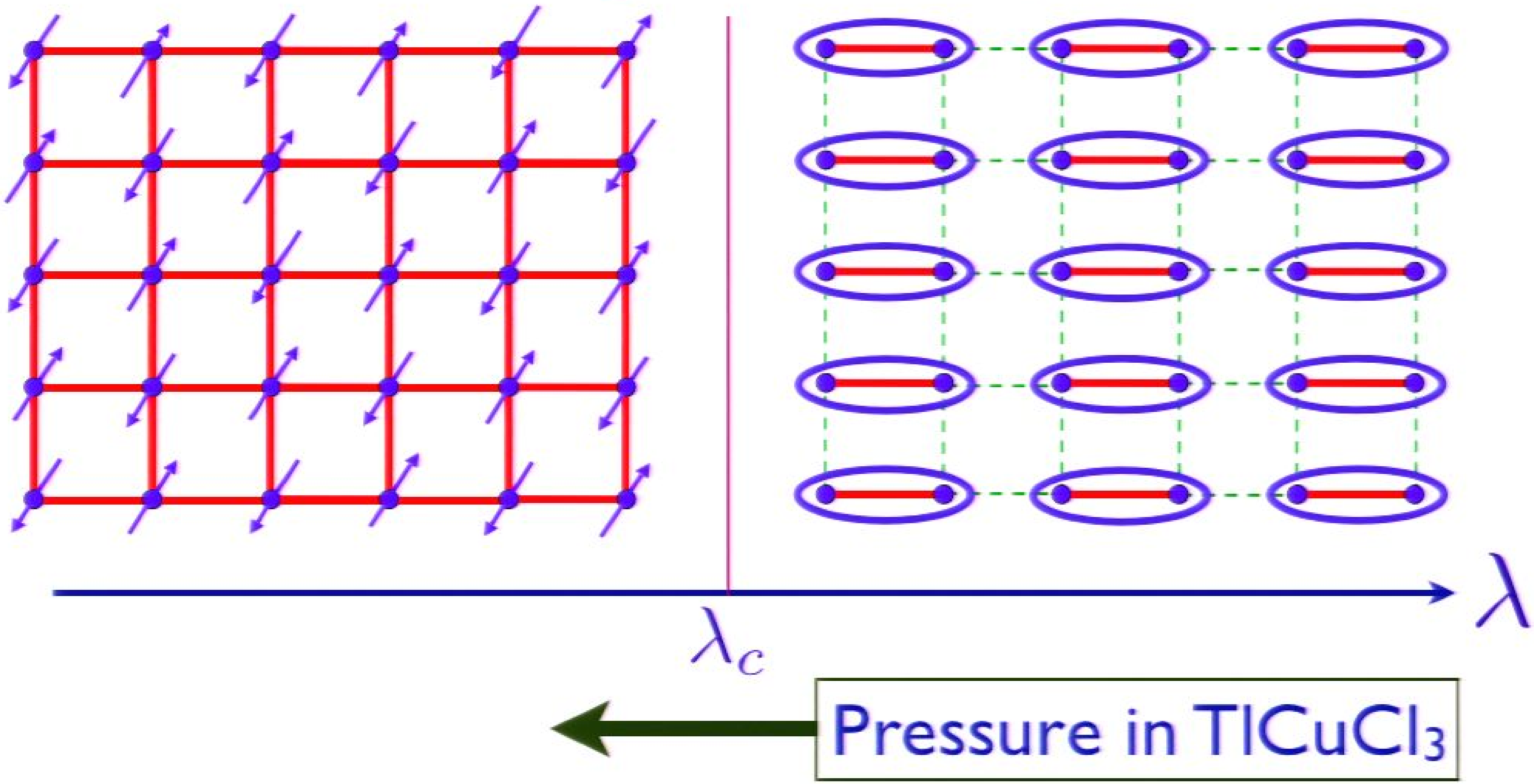

$TlCuCl_3$ at ambient pressure

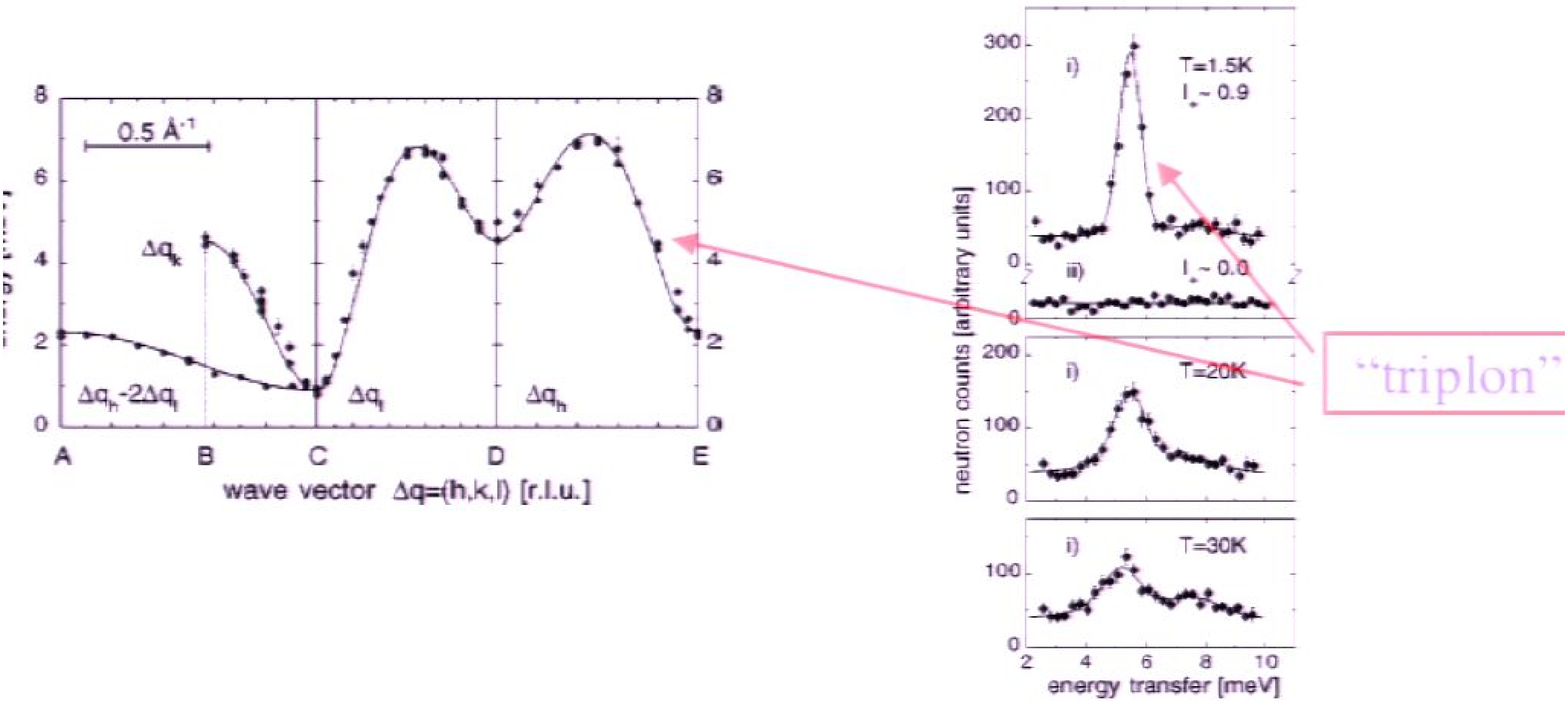

FIG. 1. Measured neutron profiles in the a^*c^* plane of $TlCuCl_3$ for $i=(1.35,0,0)$, $ii=(0,0,3.15)$ [r.l.u]. The spectrum at $T=1.5$ K

N. Cavadini, G. Heigold, W. Henggeler, A. Furrer, H.-U. Güdel, K. Krämer and H. Mutka, *Phys. Rev.* B 63 172414 (2001).

Quantum phase transition with full square lattice symmetry

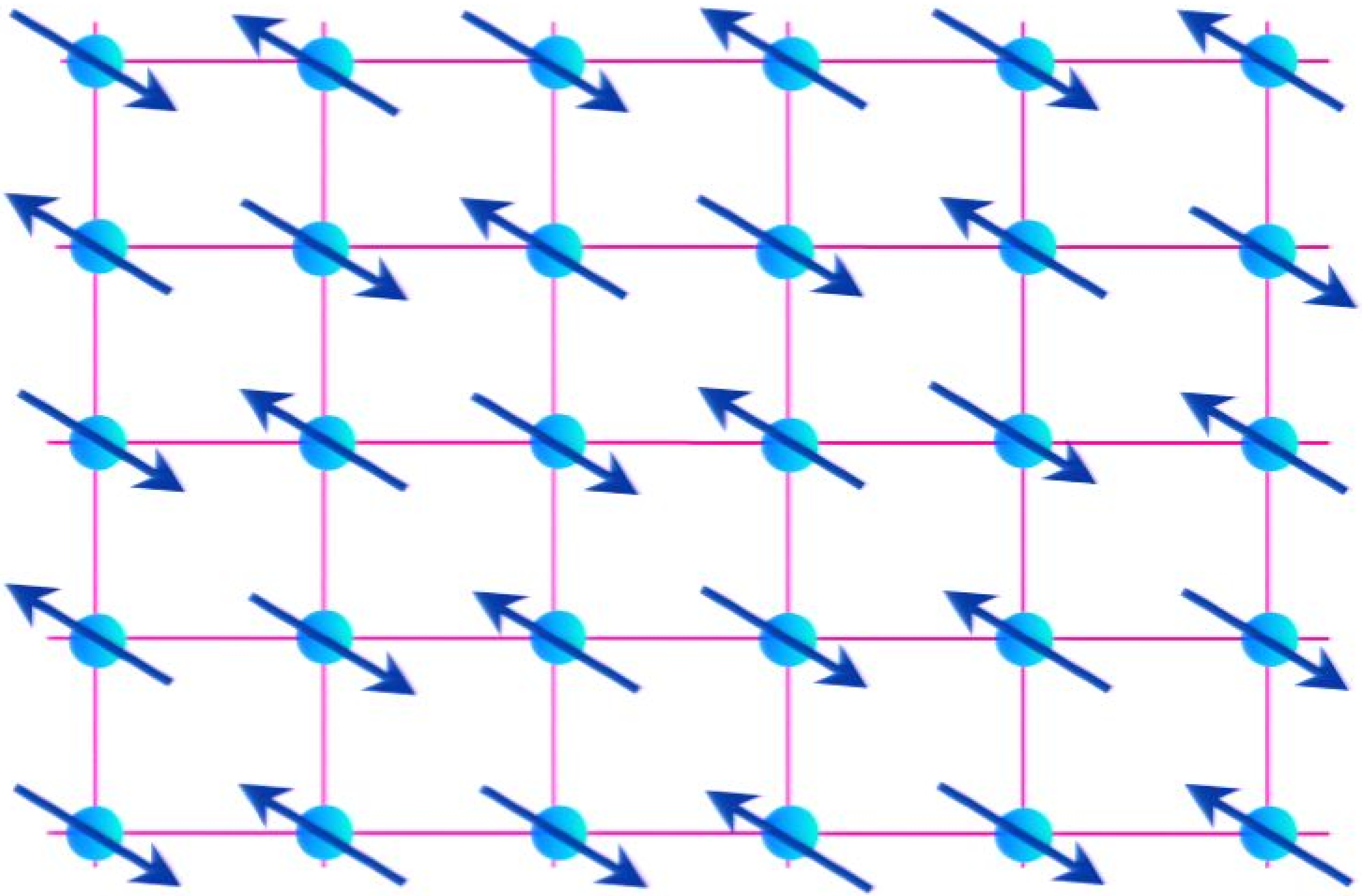

$$H = J \sum_{\langle ij \rangle} \vec{S}_i \cdot \vec{S}_j \;\; ; \;\; \vec{S}_i \;\Rightarrow\; \text{spin operator with } S = 1/2$$

Quantum phase transition with full square lattice symmetry

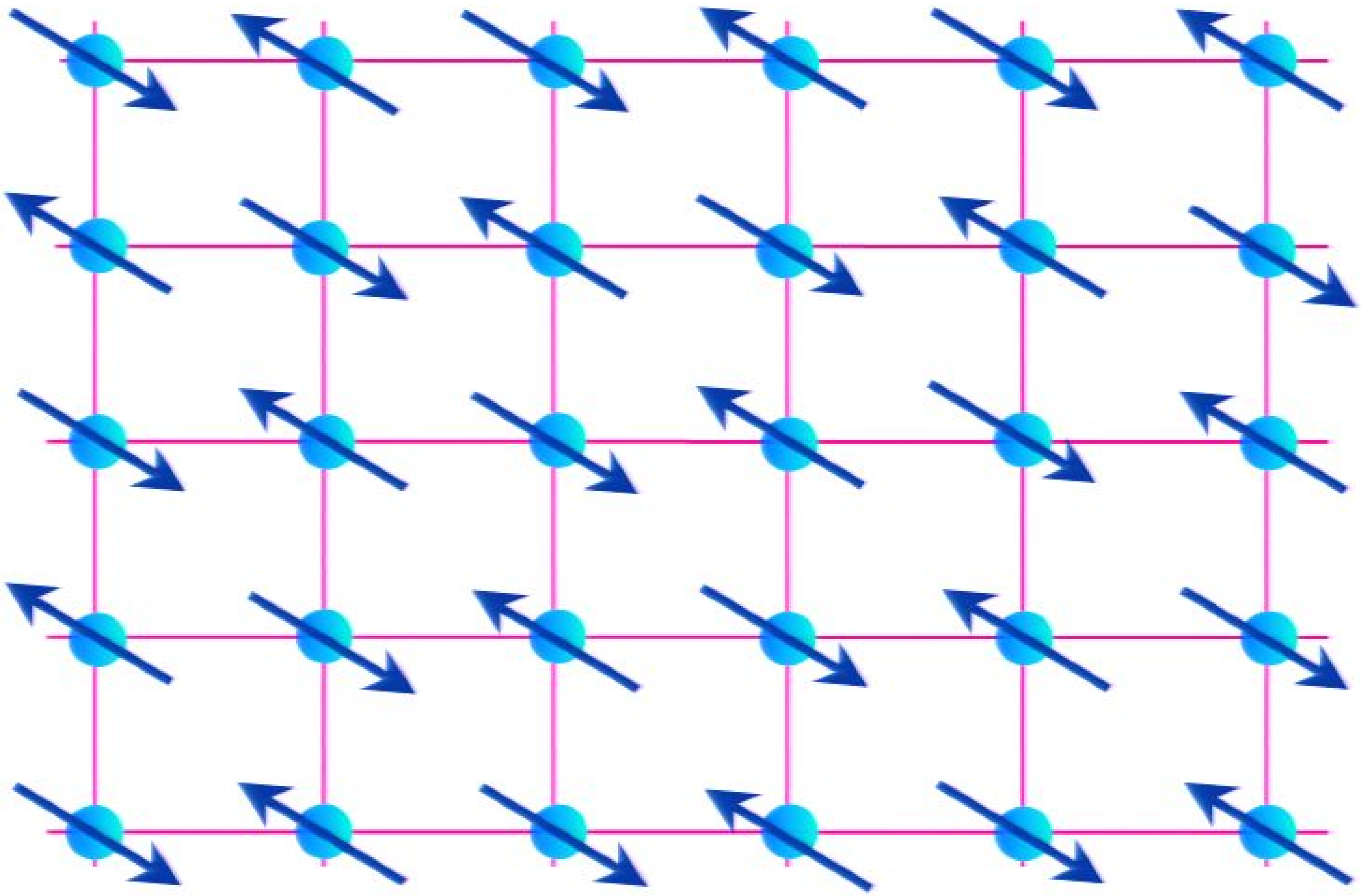

$$H = J \sum_{\langle ij \rangle} \vec{S}_i \cdot \vec{S}_j \quad ; \quad \vec{S}_i \Rightarrow \text{ spin operator with } S = 1/2$$

Quantum phase transition with full square lattice symmetry

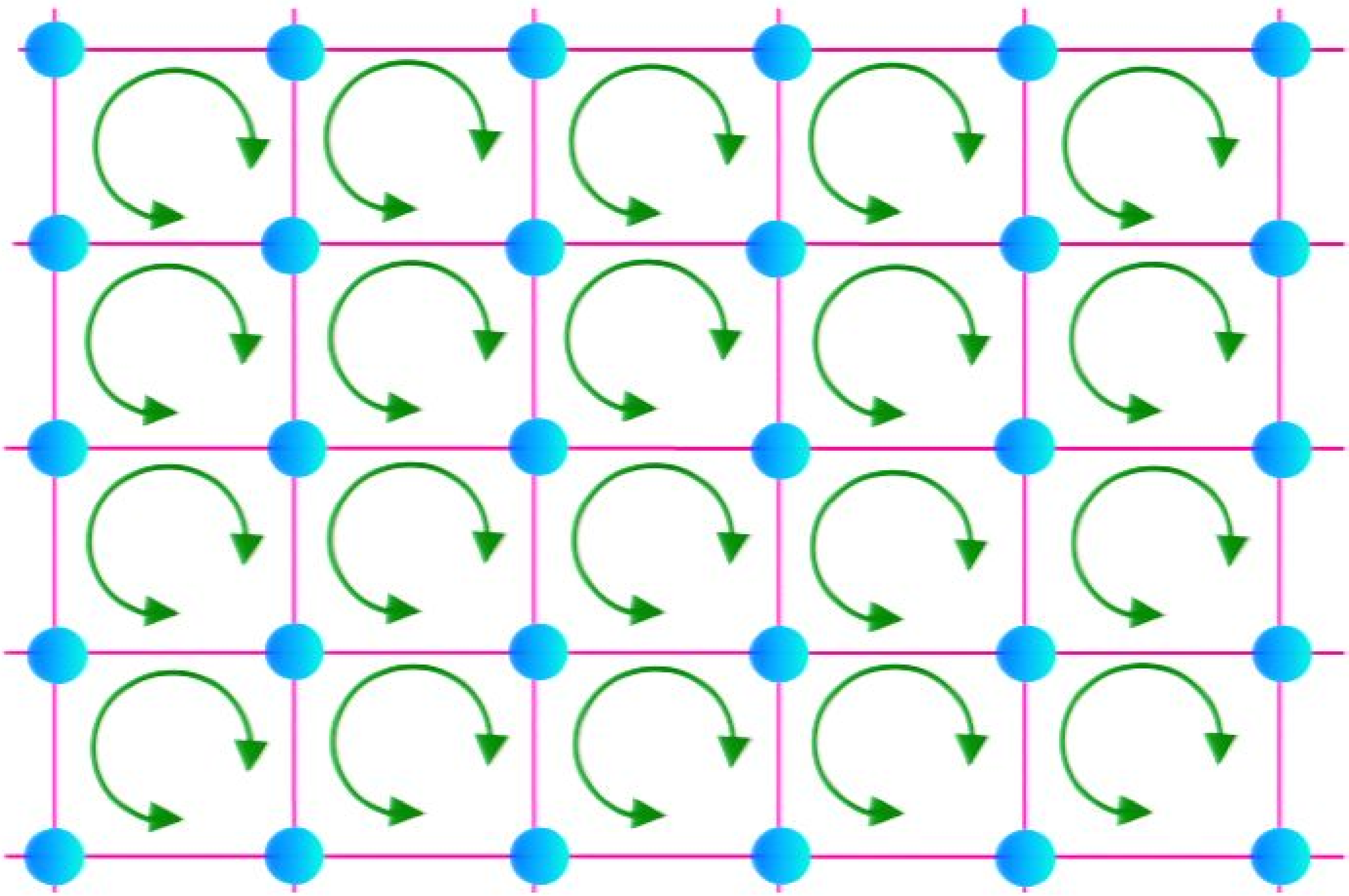

$$H = J \sum_{\langle ij \rangle} \vec{S}_i \cdot \vec{S}_j + K \sum_{\square} \text{four spin exchange}$$

A. W. Sandvik, *Phys. Rev. Lett.* **98**, 227202 (2007)

Quantum phase transition with full square lattice symmetry

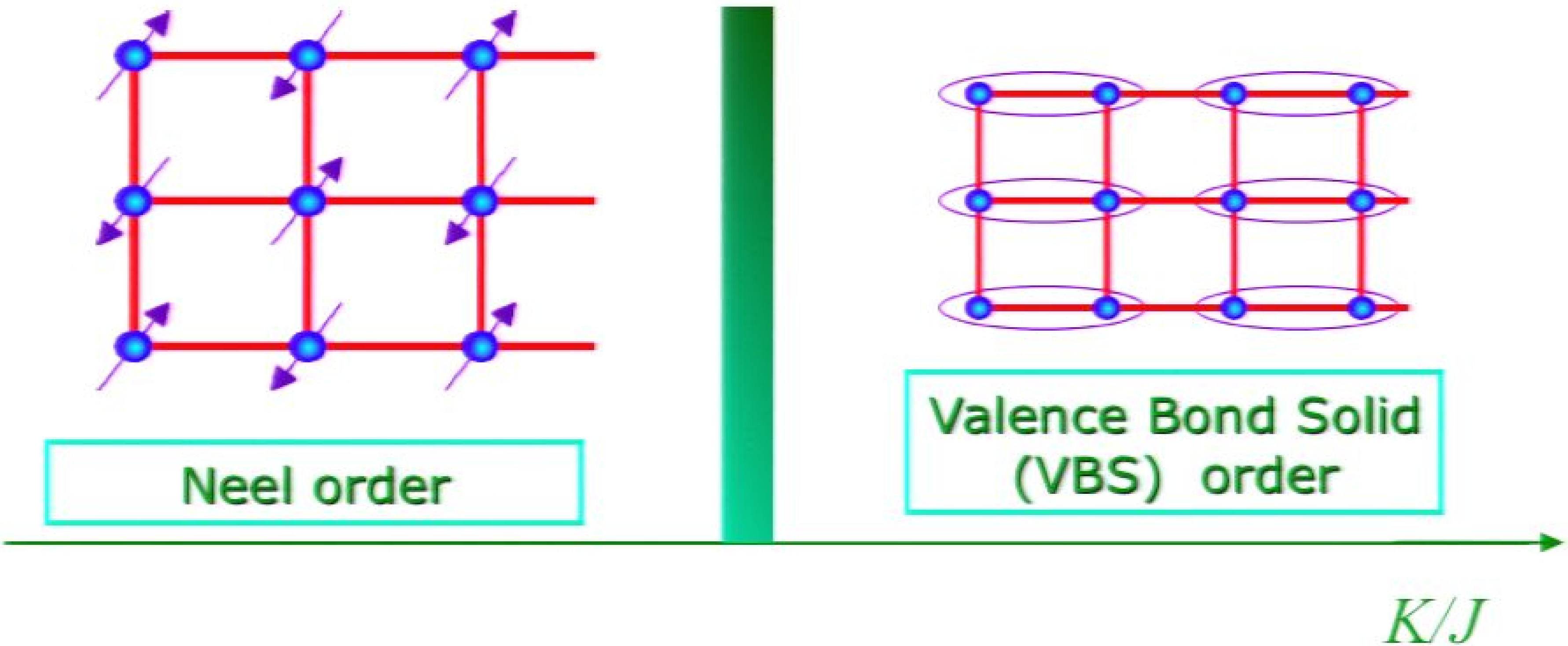

$$H = J \sum_{\langle ij \rangle} \vec{S}_i \cdot \vec{S}_j + K \sum_{\Box} \text{four spin exchange}$$

A. W. Sandvik, *Phys. Rev. Lett.* **98**, 227202 (2007)
N. Read and S. Sachdev, *Phys. Rev. Lett.* **62**, 1694 (1989)

Why should we care about the entanglement at an isolated critical point in the parameter space ?

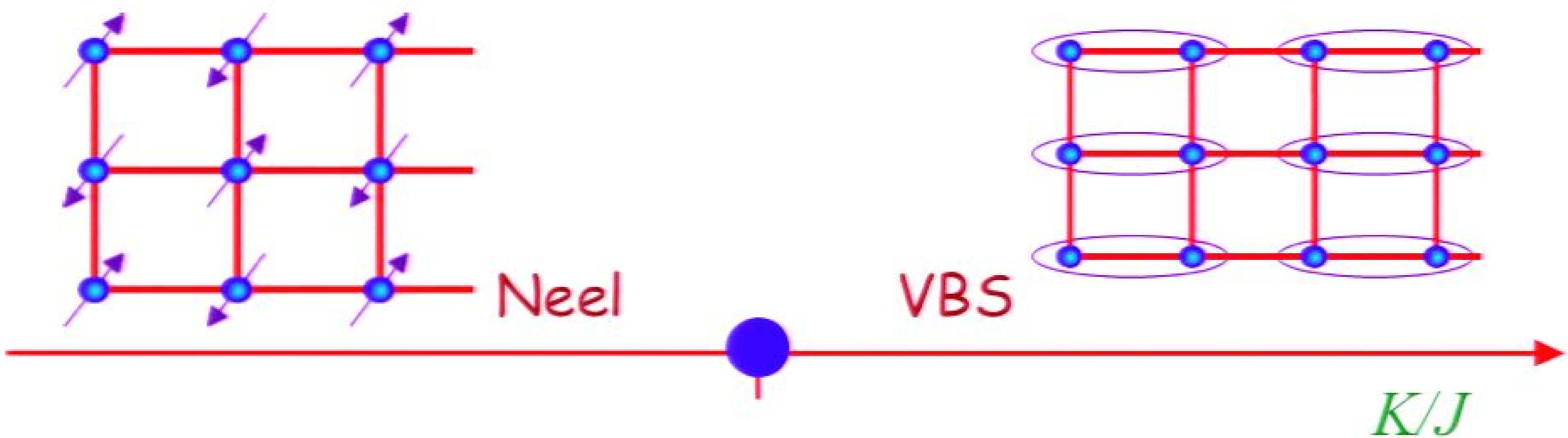

Neel
VBS
K/J

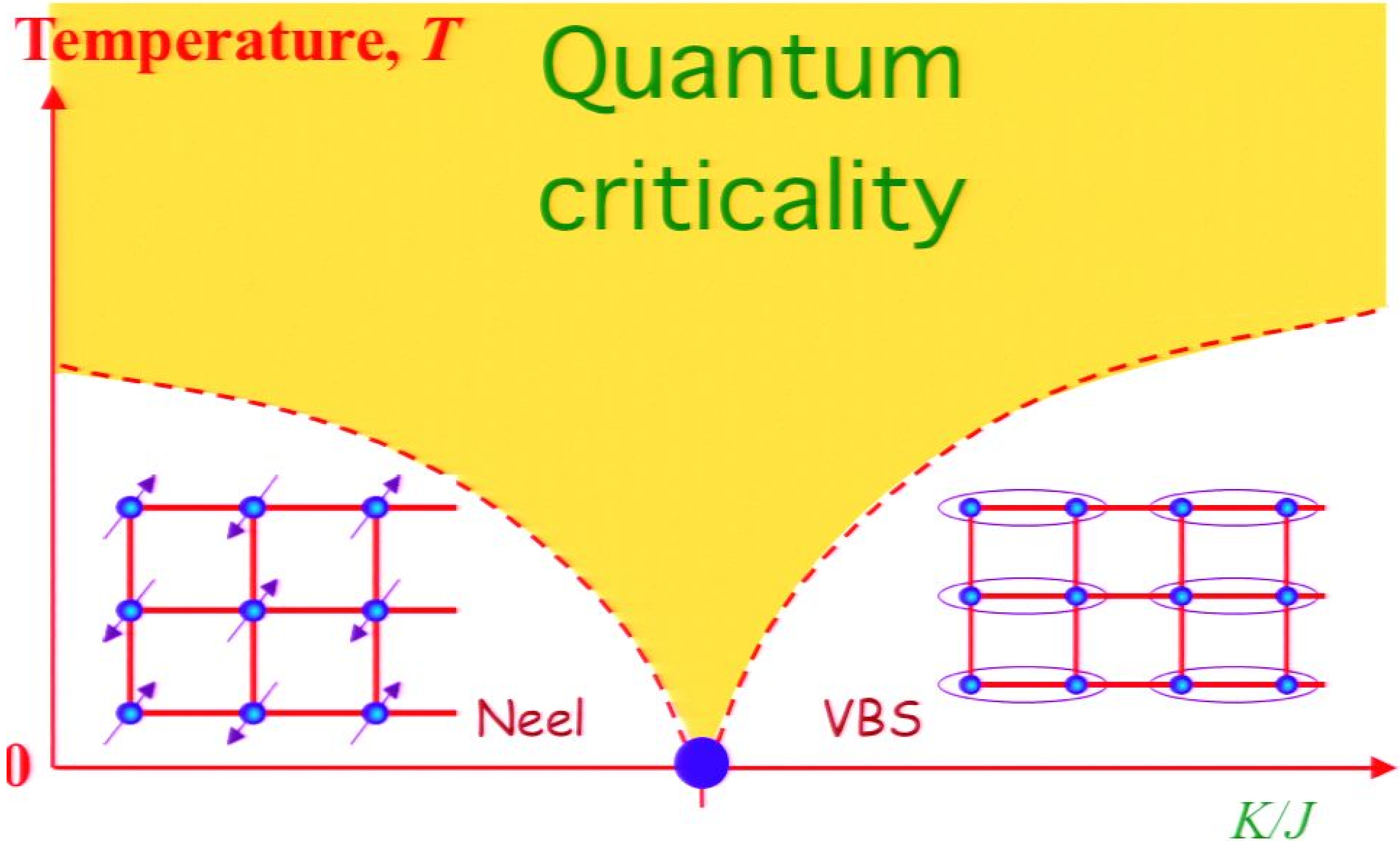

Temperature, T
Quantum
criticality
Neel
VBS
0
K/J

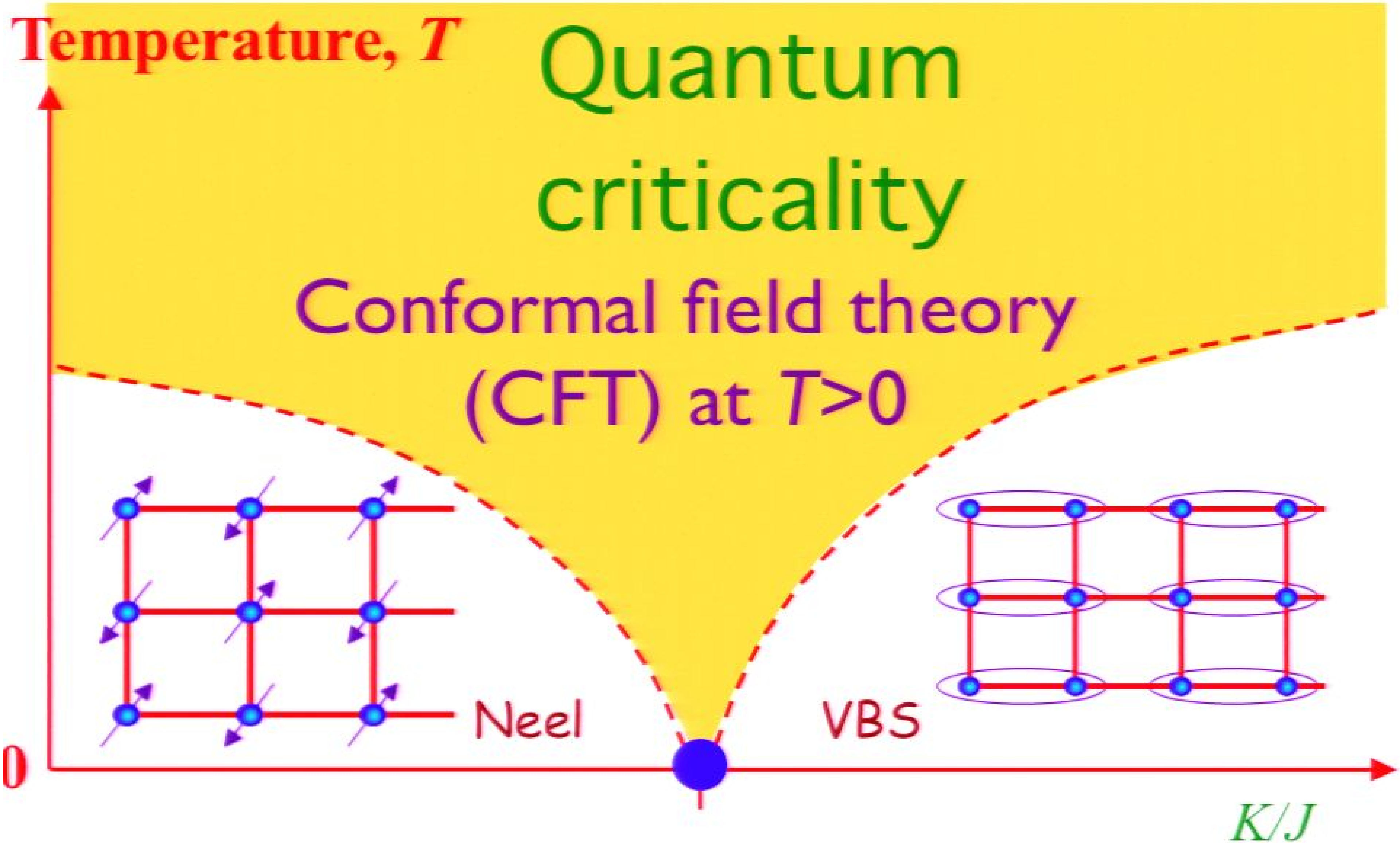
Temperature, T
Quantum criticality
Conformal field theory (CFT) at $T>0$
Neel
VBS
0
K/J

Outline

1. Entanglement of spins
   Experiments on antiferromagnetic insulators

2. Black Hole Thermodynamics
   Connections to quantum criticality

3. Nernst effect in the cuprate superconductors
   Quantum criticality and dyonic black holes

4. Quantum criticality in graphene
   Hydrodynamic cyclotron resonance and Nernst effect

Outline

1. Entanglement of spins

   Experiments on antiferromagnetic insulators

2. Black Hole Thermodynamics

   Connections to quantum criticality

3. Nernst effect in the cuprate superconductors

   Quantum criticality and dyonic black holes

4. Quantum criticality in graphene

   Hydrodynamic cyclotron resonance and Nernst effect

Black Holes

Objects so massive that light is gravitationally bound to them.

Black Holes

Objects so massive that light is gravitationally bound to them.

The region inside the black hole horizon is causally disconnected from the rest of the universe.

$$\text{Horizon radius } R = \frac{2GM}{c^2}$$

Black Hole Thermodynamics

Bekenstein and Hawking discovered astonishing connections between the Einstein theory of black holes and the laws of thermodynamics

Black Hole Thermodynamics

Bekenstein and Hawking discovered astonishing connections between the Einstein theory of black holes and the laws of thermodynamics

Entropy of a black hole $S = \dfrac{k_B A}{4\ell_P^2}$
where A is the area of the horizon, and
$\ell_P = \sqrt{\dfrac{G\hbar}{c^3}}$ is the Planck length.

Black Hole Thermodynamics

Bekenstein and Hawking discovered astonishing connections between the Einstein theory of black holes and the laws of thermodynamics

Entropy of a black hole $S = \frac{k_B A}{4\ell_P^2}$ where A is the area of the horizon, and $\ell_P = \sqrt{\frac{G\hbar}{c^3}}$ is the Planck length.

The Second Law: $dA \geq 0$

Black Hole Thermodynamics

Bekenstein and Hawking discovered astonishing connections between the Einstein theory of black holes and the laws of thermodynamics

$$\text{Horizon temperature: } 4\pi k_B T = \frac{\hbar^2}{2M\ell_P^2}$$

AdS/CFT correspondence

The quantum theory of a black hole in a 3+1-dimensional negatively curved AdS universe is holographically represented by a CFT (the theory of a quantum critical point) in 2+1 dimensions

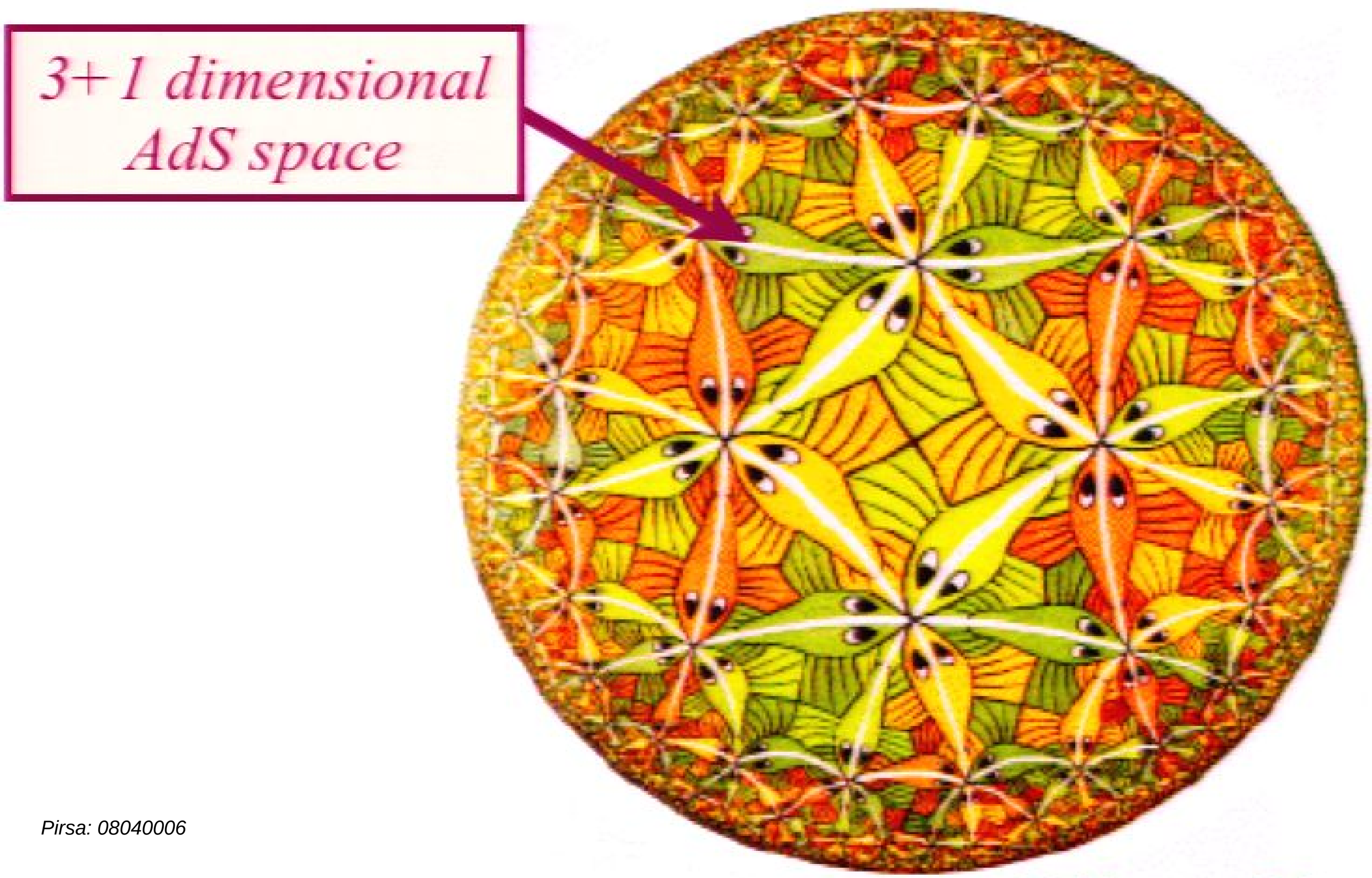

Maldacena, Gubser, Klebanov, Polyakov, Witt

AdS/CFT correspondence

The quantum theory of a black hole in a 3+1-dimensional negatively curved AdS universe is holographically represented by a CFT (the theory of a quantum critical point) in 2+1 dimensions

3+1 dimensional AdS space

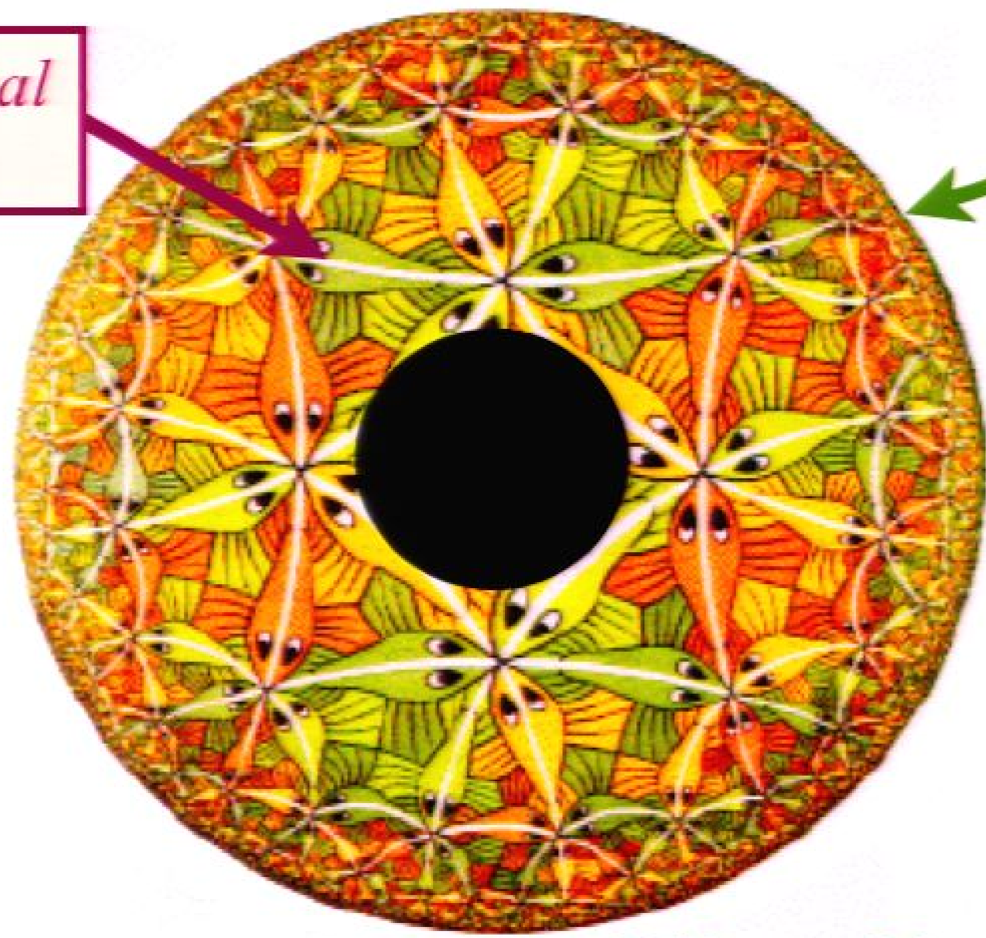

A 2+1 dimensional system at its quantum critical point

Maldacena, Gubser, Klebanov, Polyakov, Witte

AdS/CFT correspondence

The quantum theory of a black hole in a 3+1-dimensional negatively curved AdS universe is holographically represented by a CFT (the theory of a quantum critical point) in 2+1 dimensions

3+1 dimensional AdS space

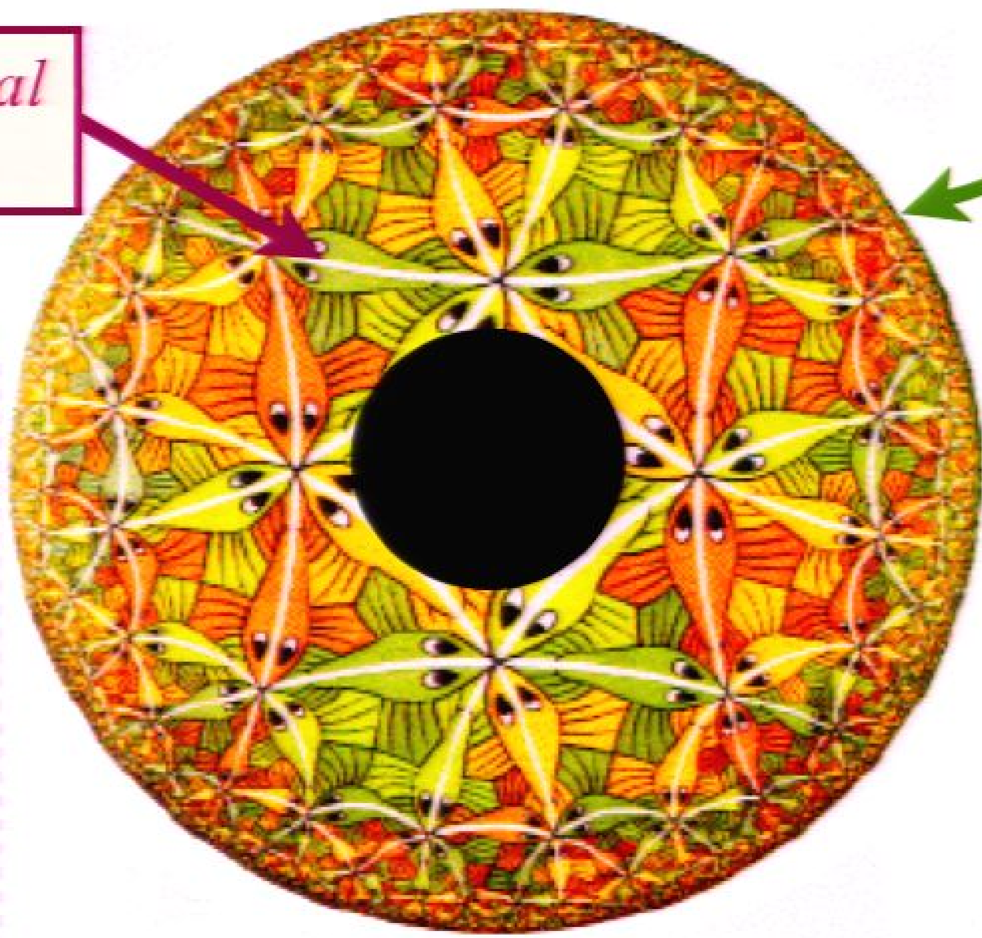

Quantum criticality in 2+1 dimensions

Black hole temperature = temperature of quantum criticality

AdS/CFT correspondence

The quantum theory of a black hole in a 3+1-dimensional negatively curved AdS universe is holographically represented by a CFT (the theory of a quantum critical point) in 2+1 dimensions

3+1 dimensional AdS space

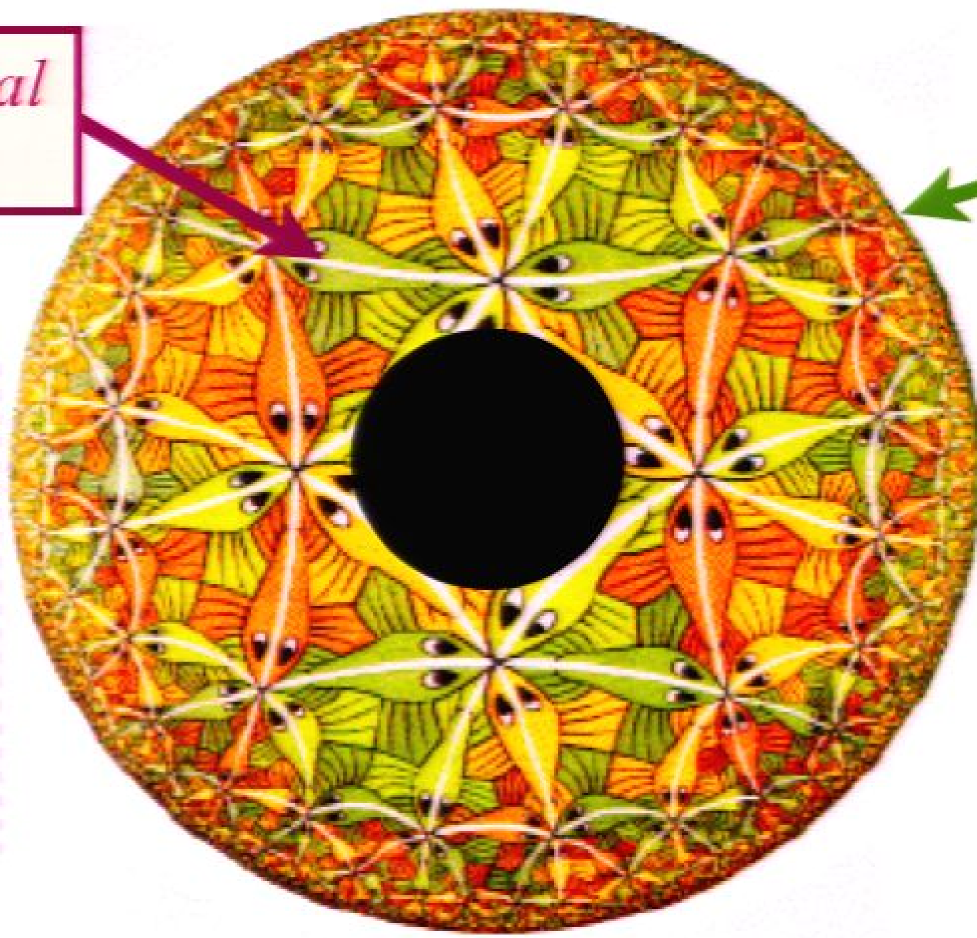

Quantum criticality in 2+1 dimensions

Black hole entropy = entropy of quantum criticality

AdS/CFT correspondence

The quantum theory of a black hole in a 3+1-dimensional negatively curved AdS universe is holographically represented by a CFT (the theory of a quantum critical point) in 2+1 dimensions

3+1 dimensional AdS space

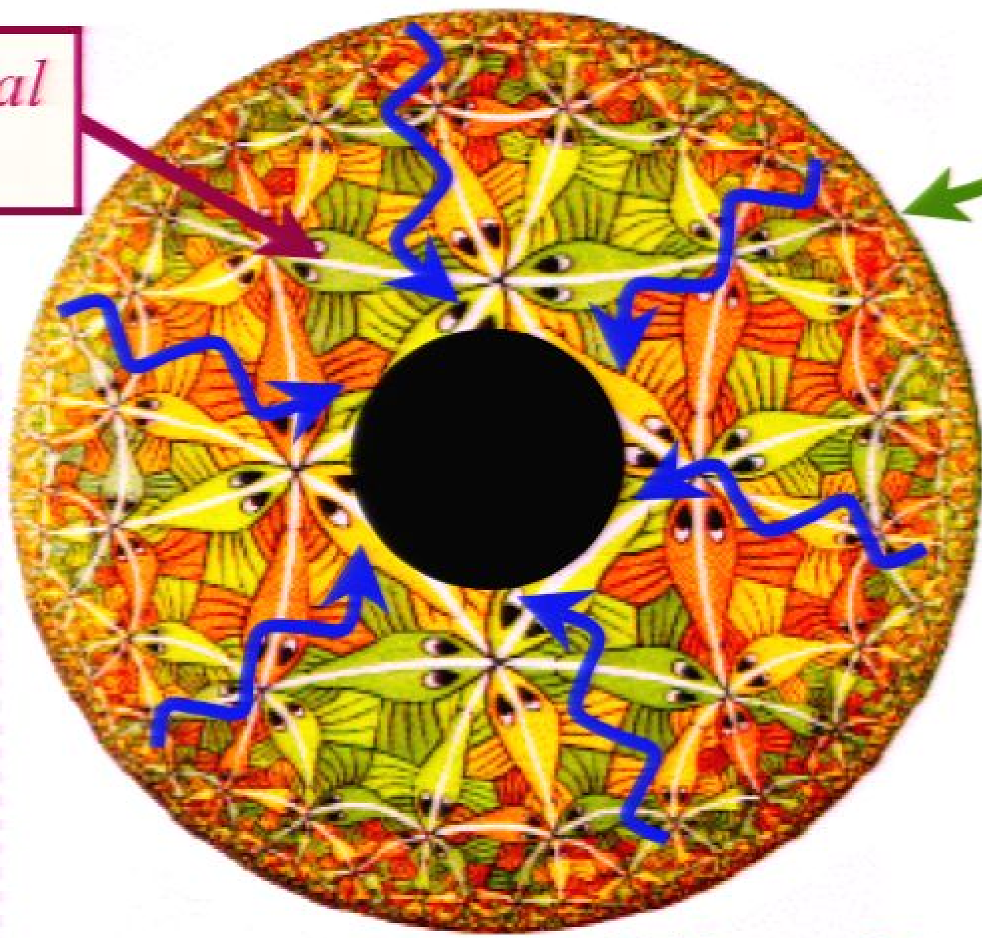

Quantum criticality in 2+1 dimensions

Quantum critical dynamics = waves in curved space

Maldacena, Gubser, Klebanov, Polyakov, Witte

AdS/CFT correspondence

The quantum theory of a black hole in a 3+1-dimensional negatively curved AdS universe is holographically represented by a CFT (the theory of a quantum critical point) in 2+1 dimensions

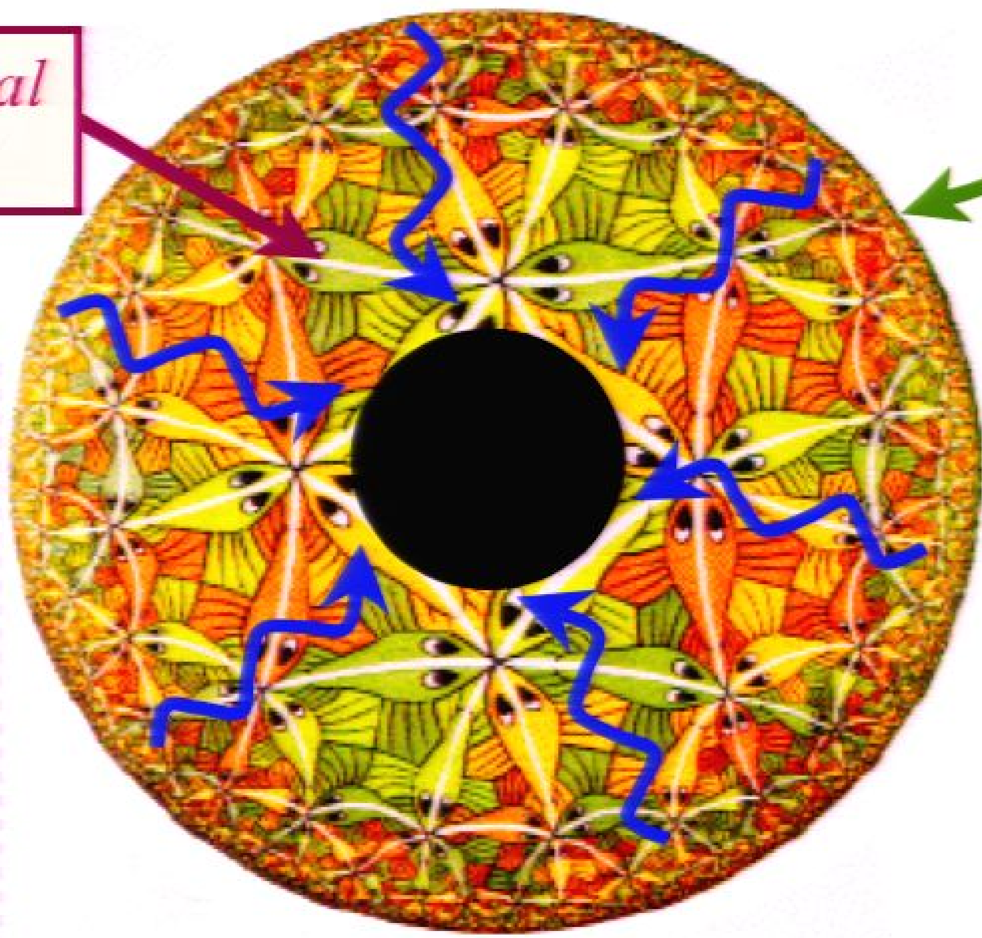

Friction of quantum criticality = waves falling into black hole

Son

Outline

1. Entanglement of spins
   Experiments on antiferromagnetic insulators

2. Black Hole Thermodynamics
   Connections to quantum criticality

3. Nernst effect in the cuprate superconductors
   Quantum criticality and dyonic black holes

4. Quantum criticality in graphene
   Hydrodynamic cyclotron resonance and Nernst effect

Black Holes

Objects so massive that light is gravitationally bound to them.

The region inside the black hole horizon is causally disconnected from the rest of the universe.

$$\text{Horizon radius } R = \frac{2GM}{c^2}$$

Quantum phase transition with full square lattice symmetry

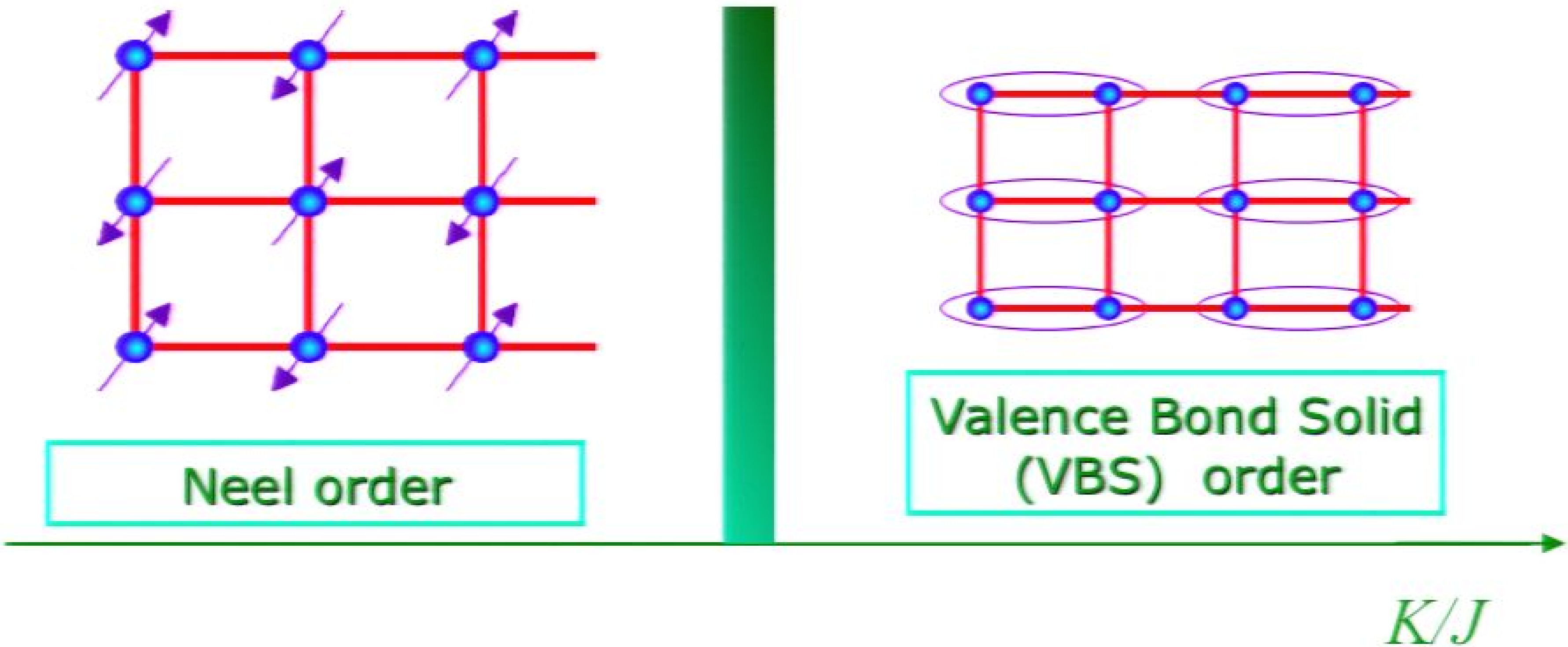

$$H = J \sum_{\langle ij \rangle} \vec{S}_i \cdot \vec{S}_j + K \sum_{\square} \text{four spin exchange}$$

A. W. Sandvik, *Phys. Rev. Lett.* **98**, 227202 (2007)
N. Read and S. Sachdev, *Phys. Rev. Lett.* **62**, 1694 (1989)

Quantum phase transition with full square lattice symmetry

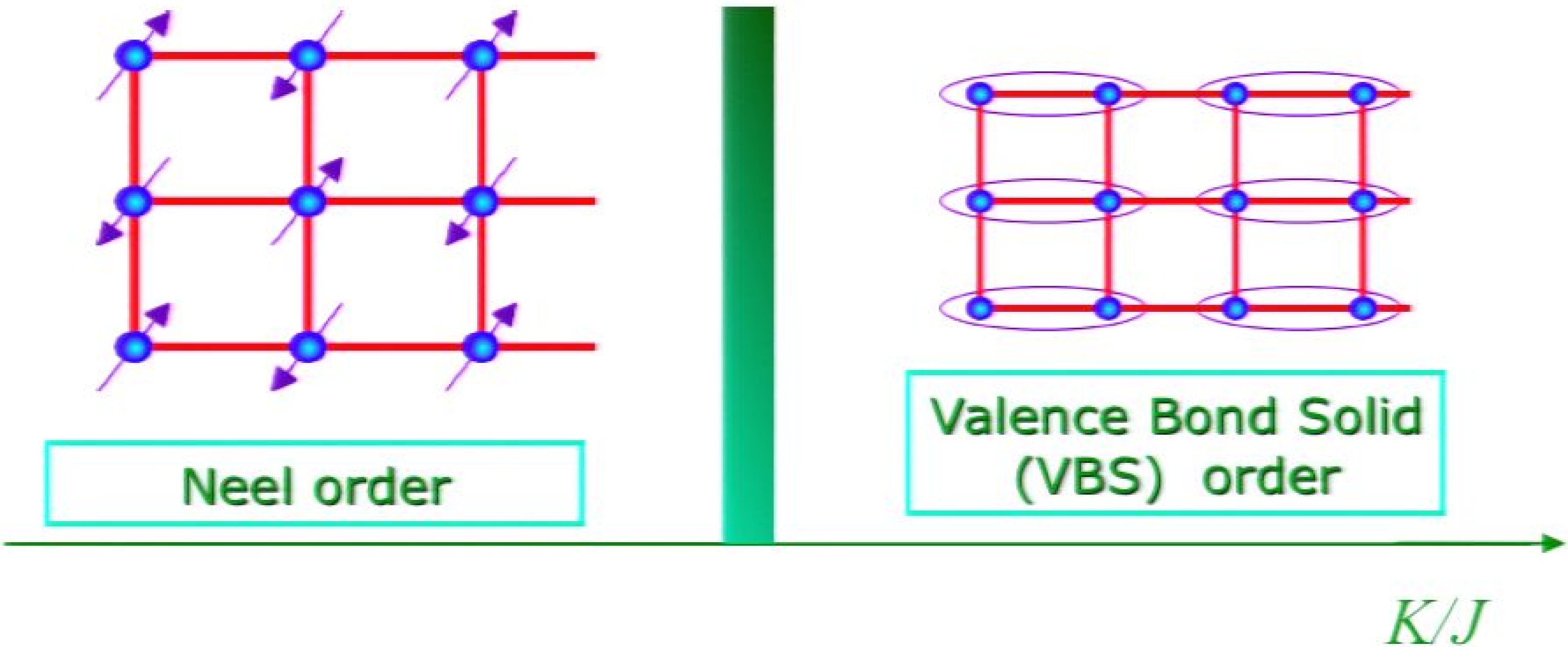

$$H = J \sum_{\langle ij \rangle} \vec{S}_i \cdot \vec{S}_j + K \sum_{\square} \text{four spin exchange}$$

A. W. Sandvik, *Phys. Rev. Lett.* **98**, 227202 (2007)
N. Read and S. Sachdev, *Phys. Rev. Lett.* **62**, 1694 (1989)

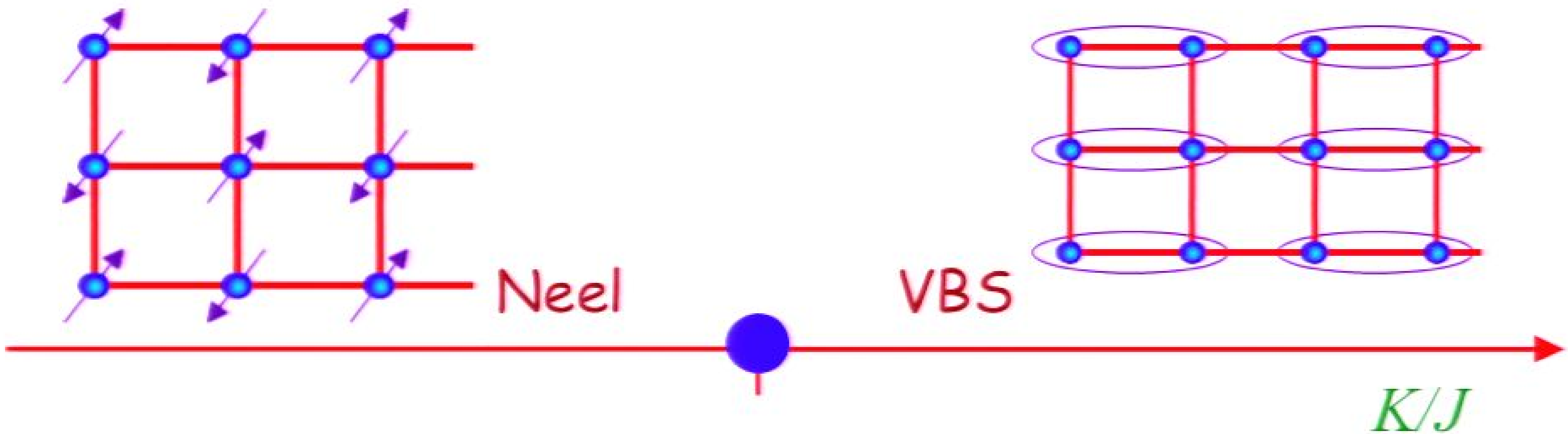
Neel
VBS
K/J

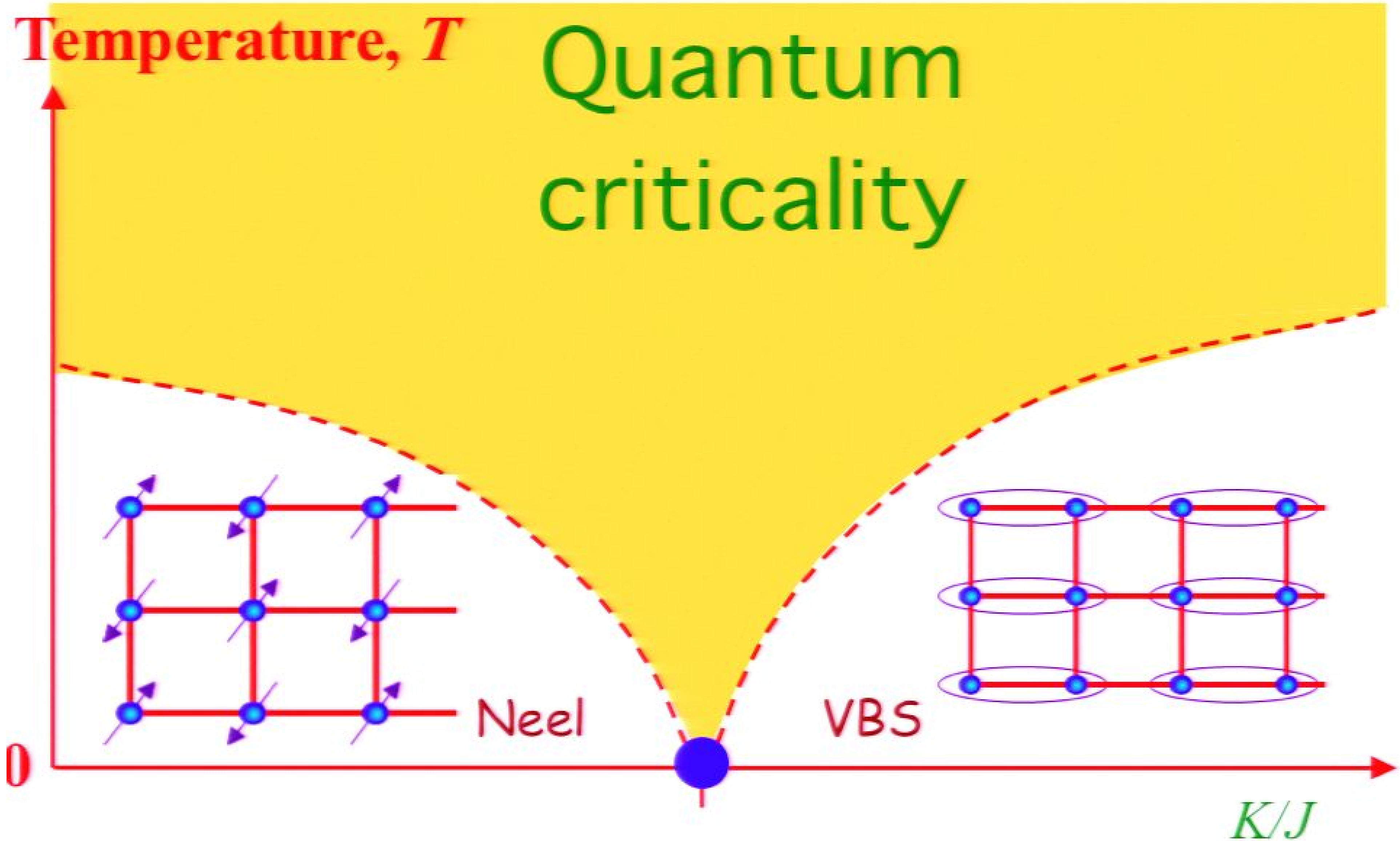
Temperature, T
Quantum
criticality
Neel
VBS
0
K/J

Outline

1. Entanglement of spins
   Experiments on antiferromagnetic insulators

2. Black Hole Thermodynamics
   Connections to quantum criticality

3. Nernst effect in the cuprate superconductors
   Quantum criticality and dyonic black holes

4. Quantum criticality in graphene
   Hydrodynamic cyclotron resonance and Nernst effect

Black Hole Thermodynamics

Bekenstein and Hawking discovered astonishing connections between the Einstein theory of black holes and the laws of thermodynamics

Entropy of a black hole $S = \dfrac{k_B A}{4\ell_P^2}$

where A is the area of the horizon, and

$\ell_P = \sqrt{\dfrac{G\hbar}{c^3}}$ is the Planck length.

The Second Law: $dA \geq 0$

Black Hole Thermodynamics

Bekenstein and Hawking discovered astonishing connections between the Einstein theory of black holes and the laws of thermodynamics

$$\text{Horizon temperature: } 4\pi k_B T = \frac{\hbar^2}{2M\ell_P^2}$$

AdS/CFT correspondence

The quantum theory of a black hole in a 3+1-dimensional negatively curved AdS universe is holographically represented by a CFT (the theory of a quantum critical point) in 2+1 dimensions

3+1 dimensional AdS space

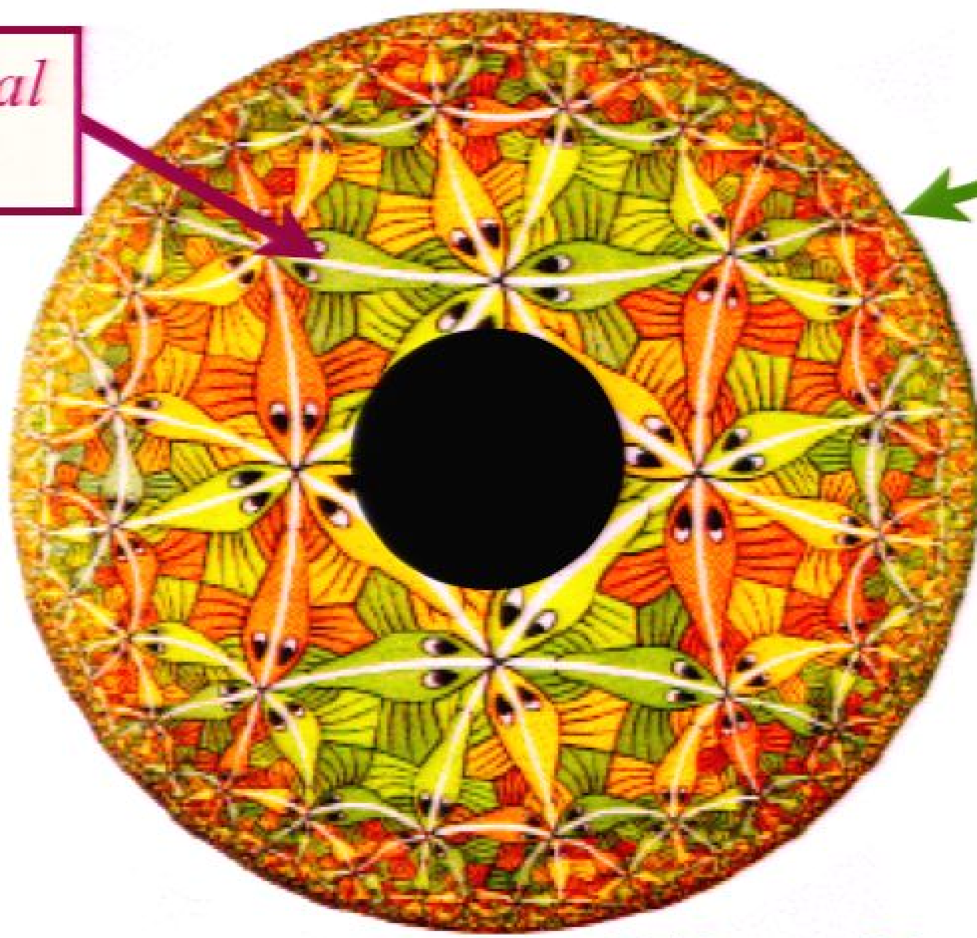

A 2+1 dimensional system at its quantum critical point

Maldacena, Gubser, Klebanov, Polyakov, Witte

AdS/CFT correspondence

The quantum theory of a black hole in a 3+1-dimensional negatively curved AdS universe is holographically represented by a CFT (the theory of a quantum critical point) in 2+1 dimensions

3+1 dimensional AdS space

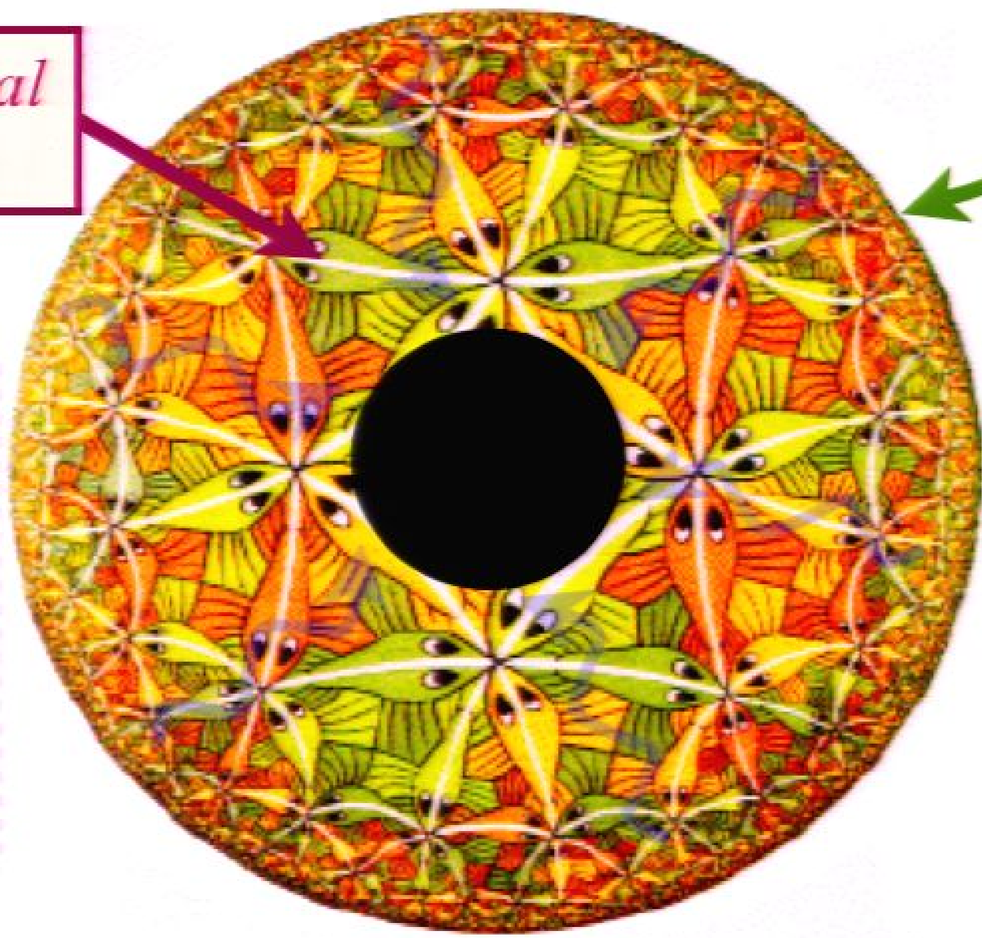

Quantum criticality in 2+1 dimensions

Black hole entropy = entropy of quantum criticality

AdS/CFT correspondence

The quantum theory of a black hole in a 3+1-dimensional negatively curved AdS universe is holographically represented by a CFT (the theory of a quantum critical point) in 2+1 dimensions

3+1 dimensional AdS space

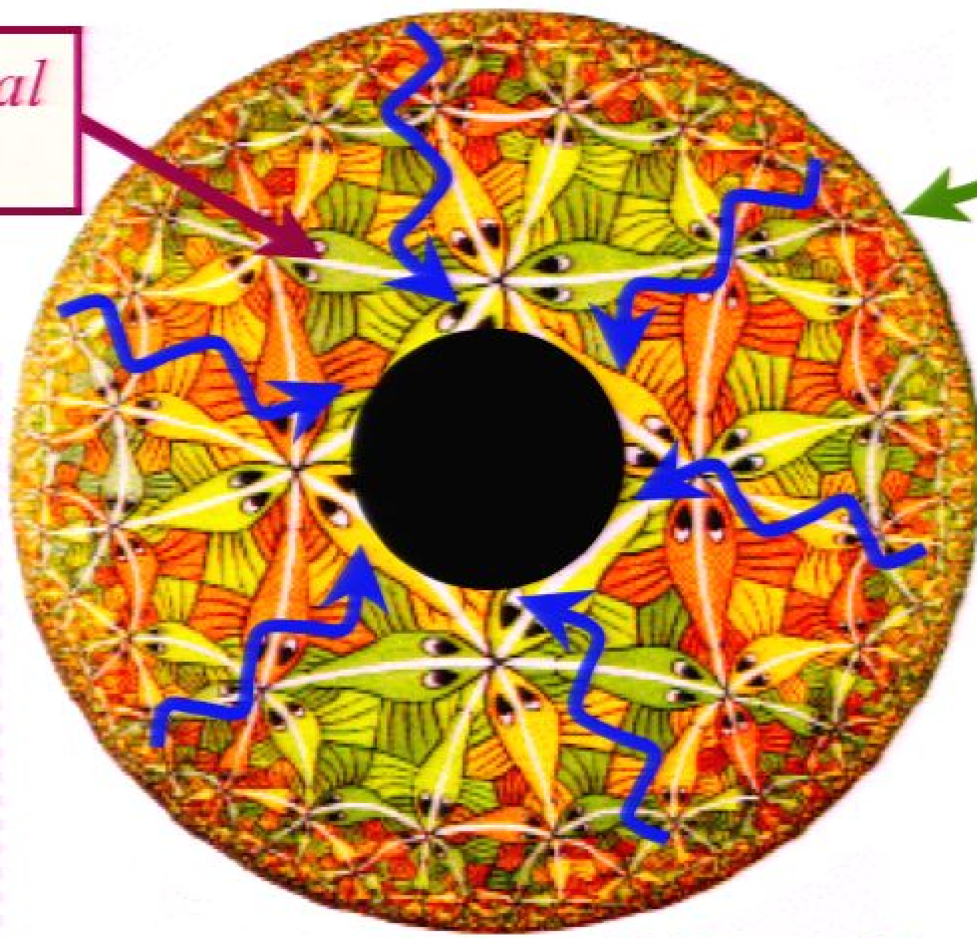

Quantum criticality in 2+1 dimensions

Quantum critical dynamics = waves in curved space

Outline

1. Entanglement of spins
   Experiments on antiferromagnetic insulators

2. Black Hole Thermodynamics
   Connections to quantum criticality

3. Nernst effect in the cuprate superconductors
   Quantum criticality and dyonic black holes

4. Quantum criticality in graphene
   Hydrodynamic cyclotron resonance and Nernst effect

Outline

1. Entanglement of spins
   Experiments on antiferromagnetic insulators

2. Black Hole Thermodynamics
   Connections to quantum criticality

3. Nernst effect in the cuprate superconductors
   Quantum criticality and dyonic black holes

4. Quantum criticality in graphene
   Hydrodynamic cyclotron resonance and Nernst effect

Dope the antiferomagnets with charge carriers of density x by applying a chemical potential μ

$Ca_{1.90}Na_{0.10}CuO_2Cl_2$

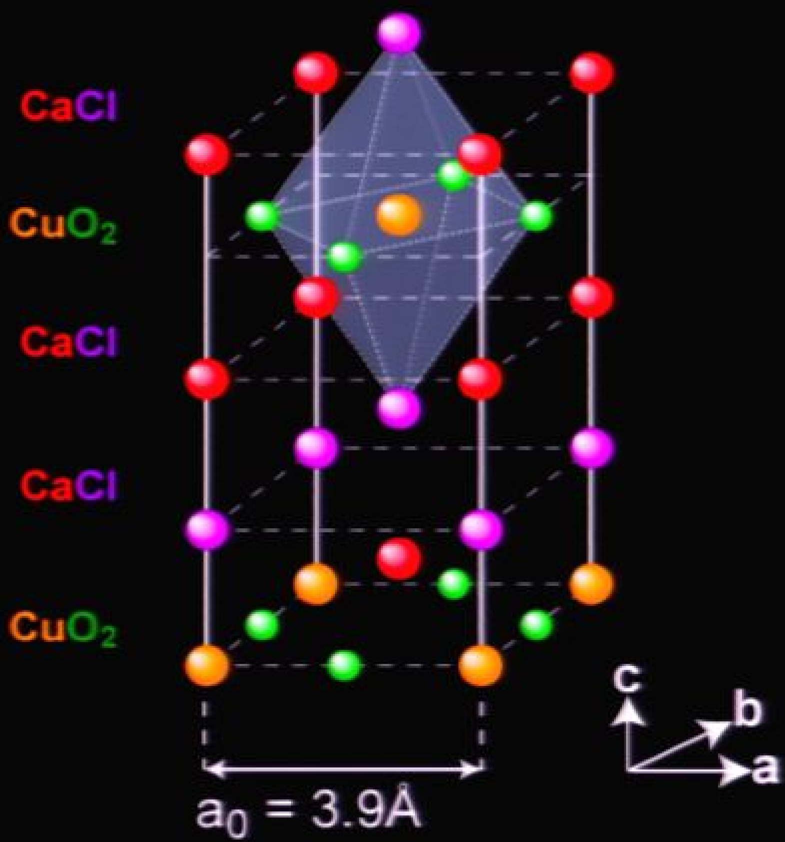

$Bi_{2.2}Sr_{1.8}Ca_{0.8}Dy_{0.2}Cu_2O_y$

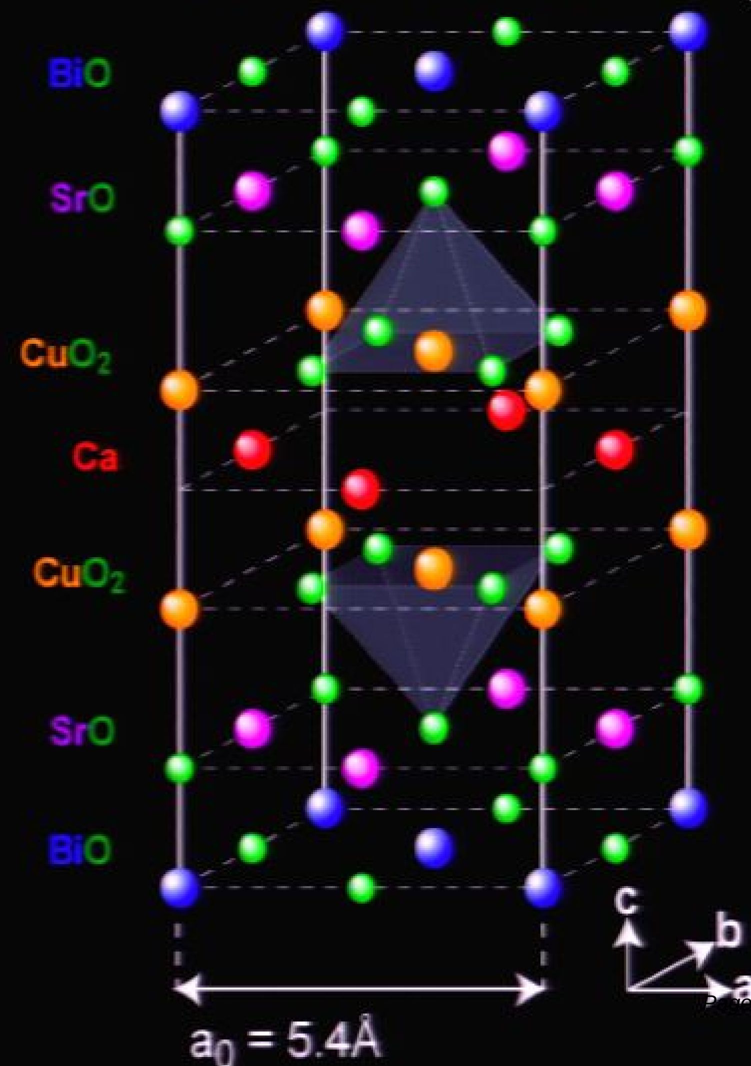

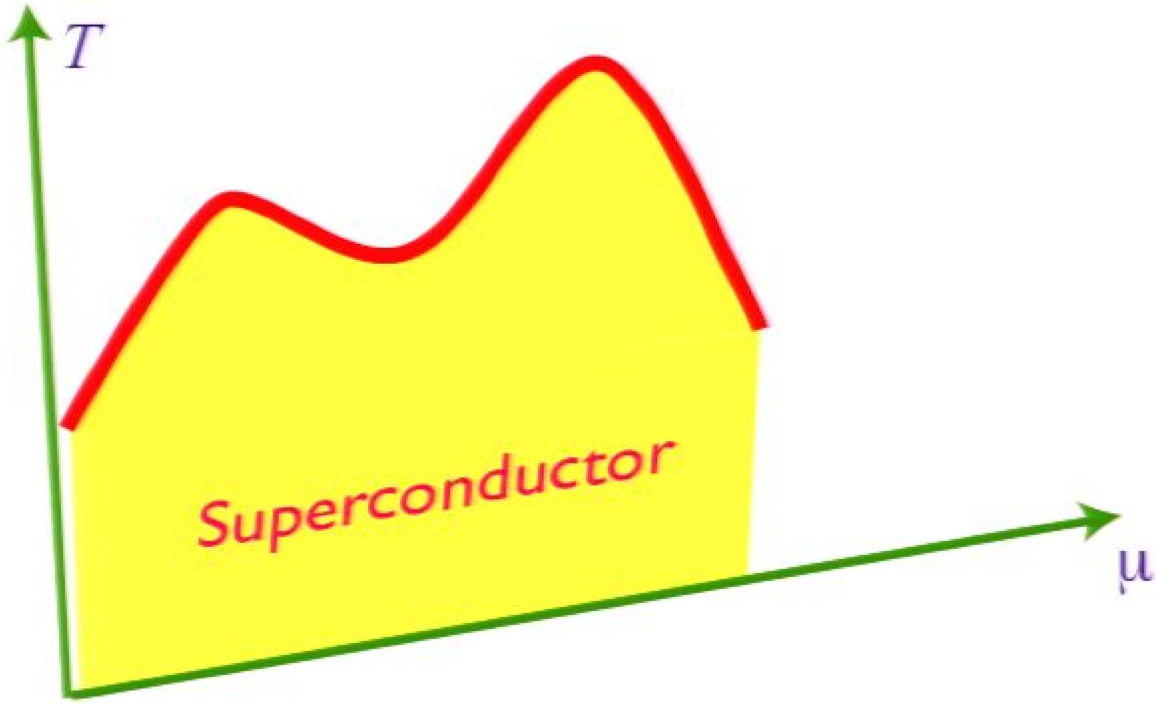
T
Superconductor
μ

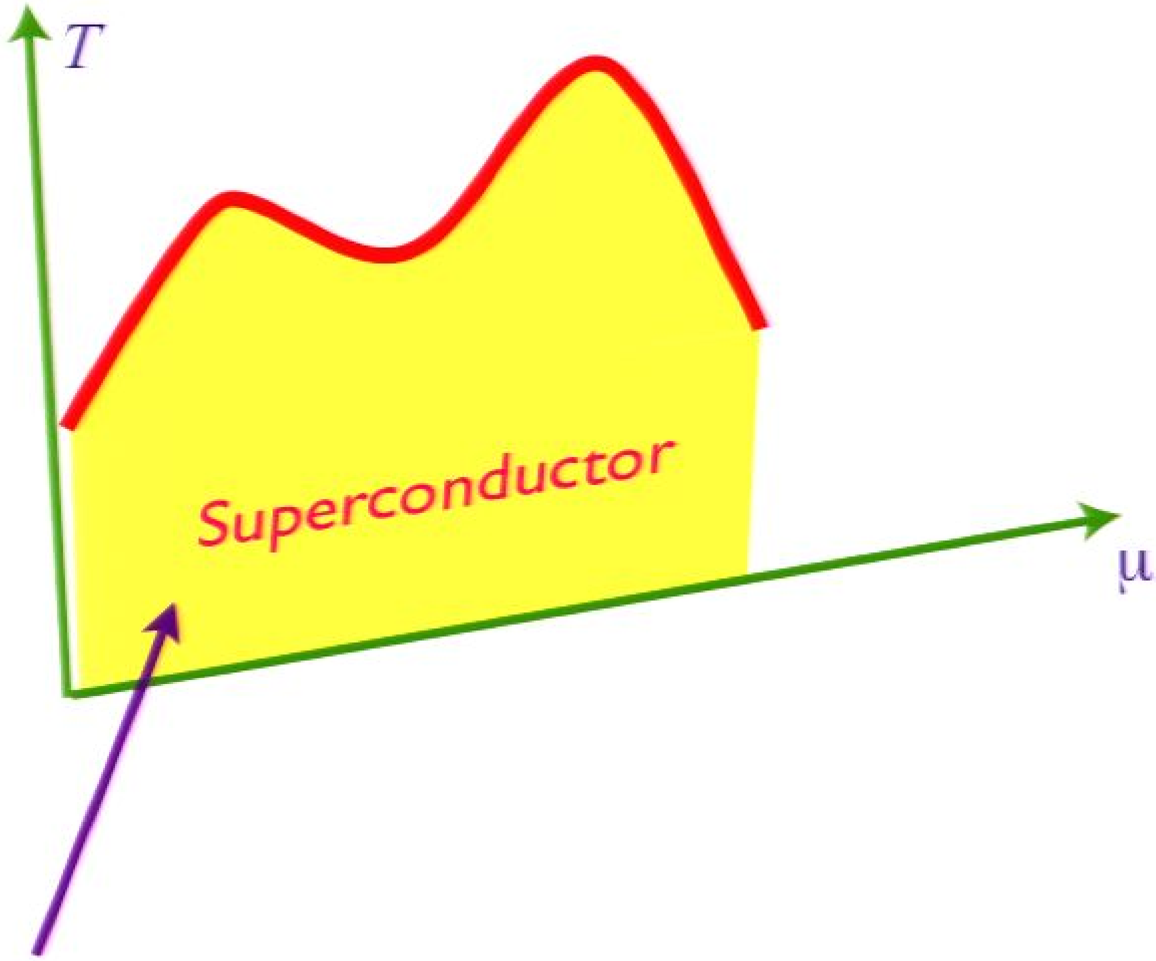

Scanning tunnelling microscopy

STM studies of the underdoped superconductor

$Ca_{1.90}Na_{0.10}CuO_2Cl_2$

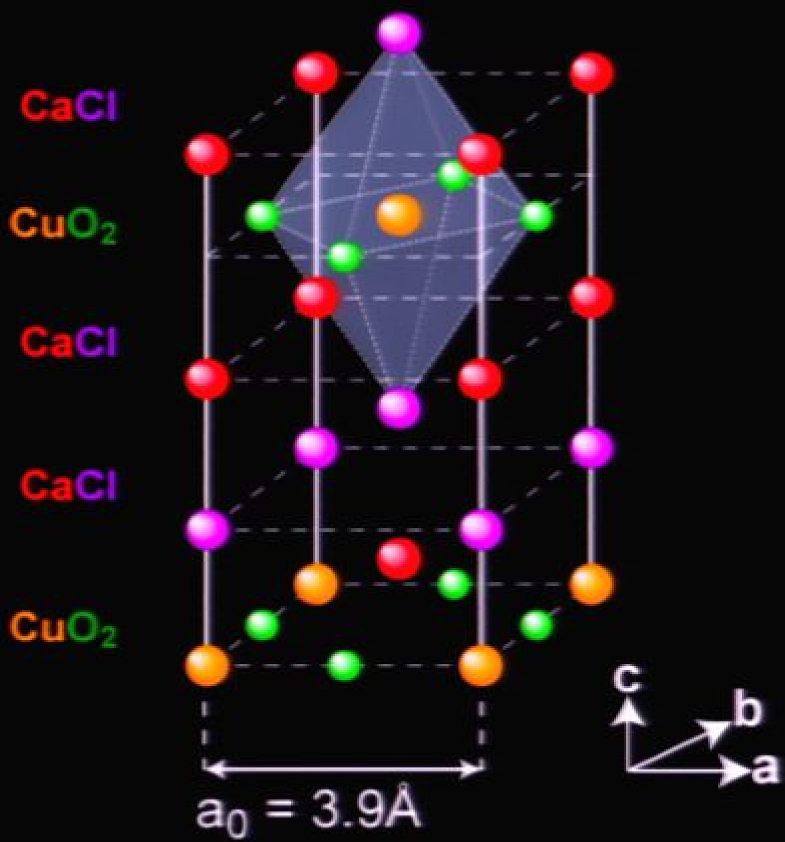

$Bi_{2.2}Sr_{1.8}Ca_{0.8}Dy_{0.2}Cu_2O_y$

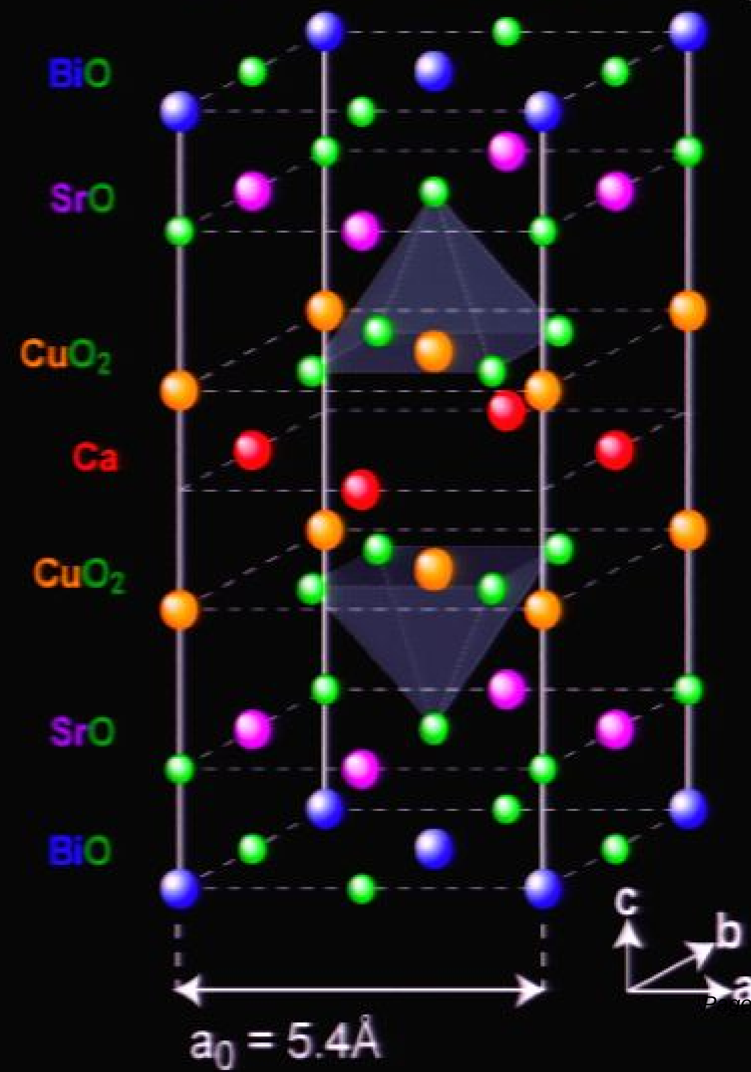

Topograph

$Ca_{1.90}Na_{0.10}CuO_2Cl_2$

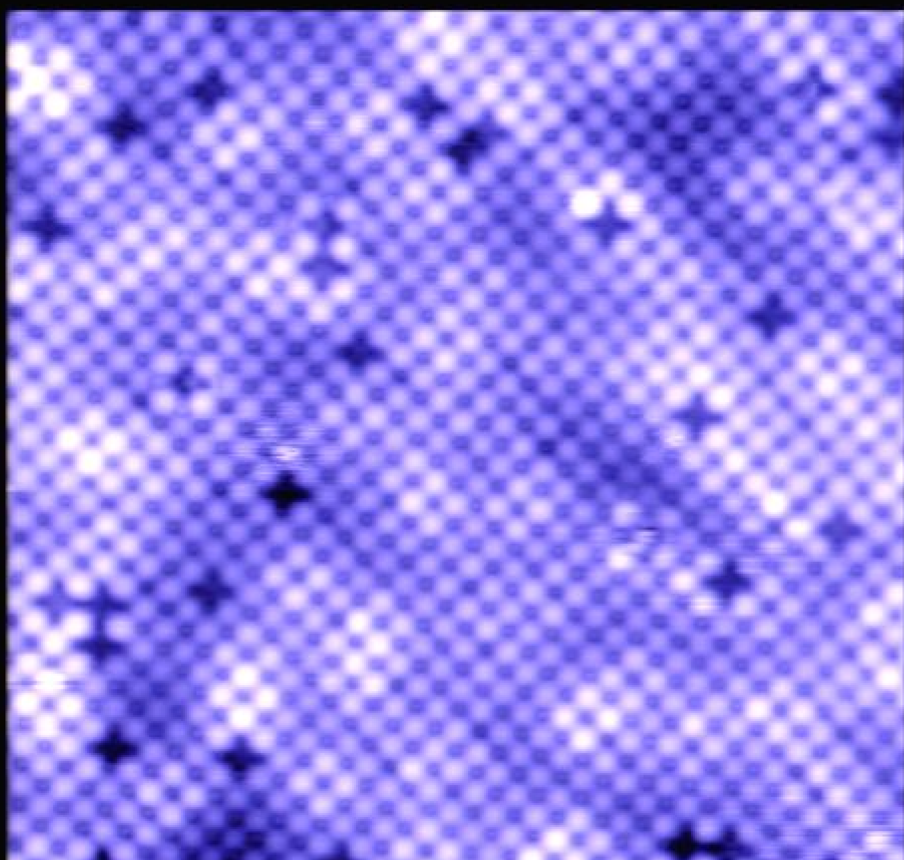

$Bi_{2.2}Sr_{1.8}Ca_{0.8}Dy_{0.2}Cu_2O_y$

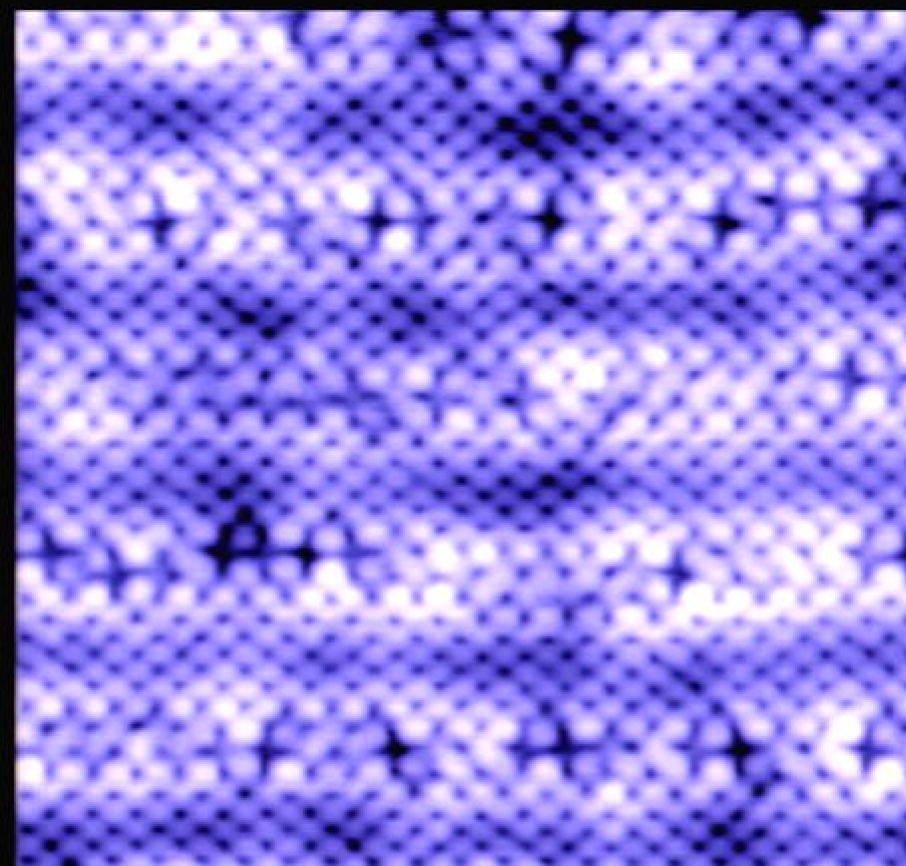

Y. Kohsaka et al. Science 315, 1380 (2007

dI/dV Spectra

$Ca_{1.90}Na_{0.10}CuO_2Cl_2$

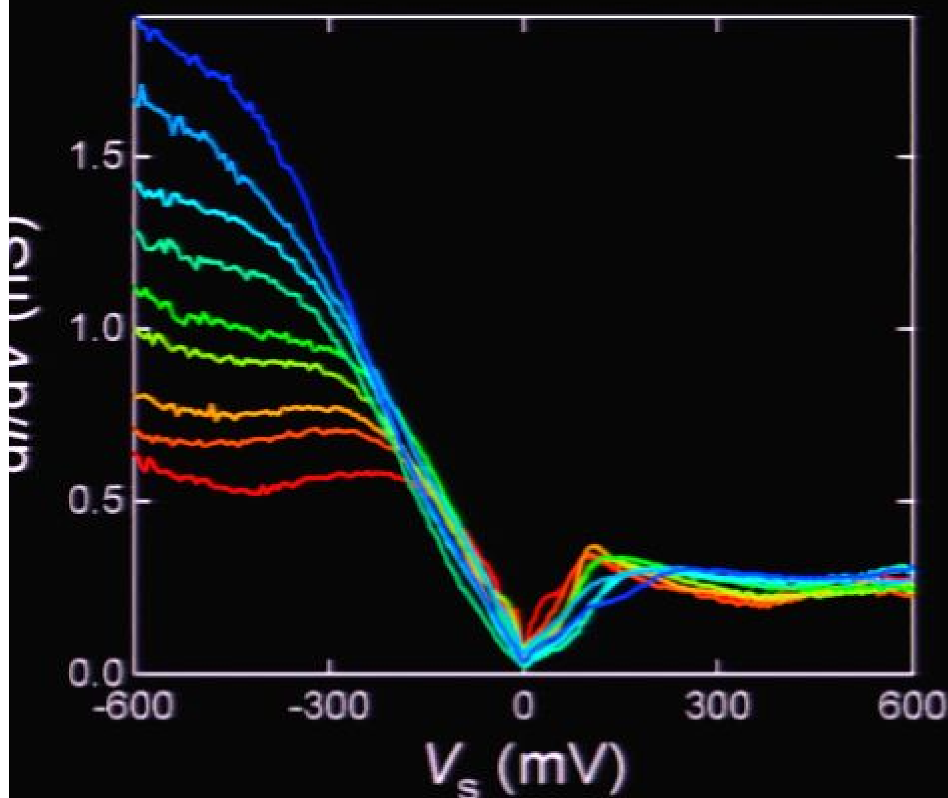

$Bi_{2.2}Sr_{1.8}Ca_{0.8}Dy_{0.2}Cu_2O_y$

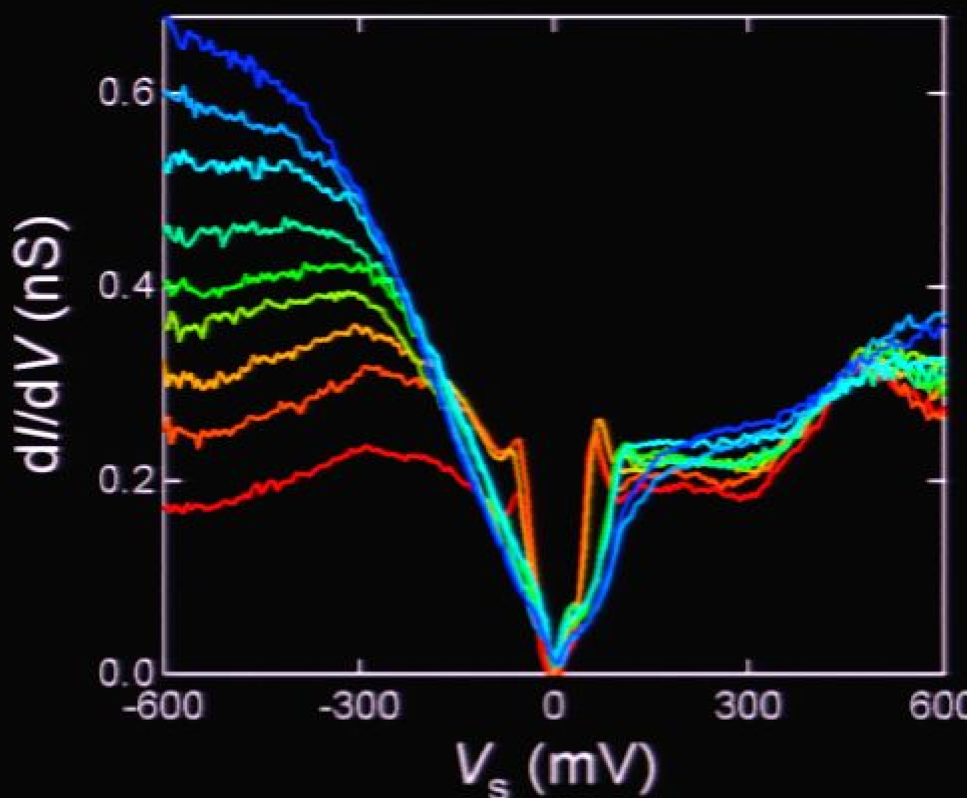

Intense Tunneling-Asymmetry (TA)
variation are highly similar

Y. Kohsaka et al., Science 315, 1380 (2007

Topograph

$Ca_{1.90}Na_{0.10}CuO_2Cl_2$

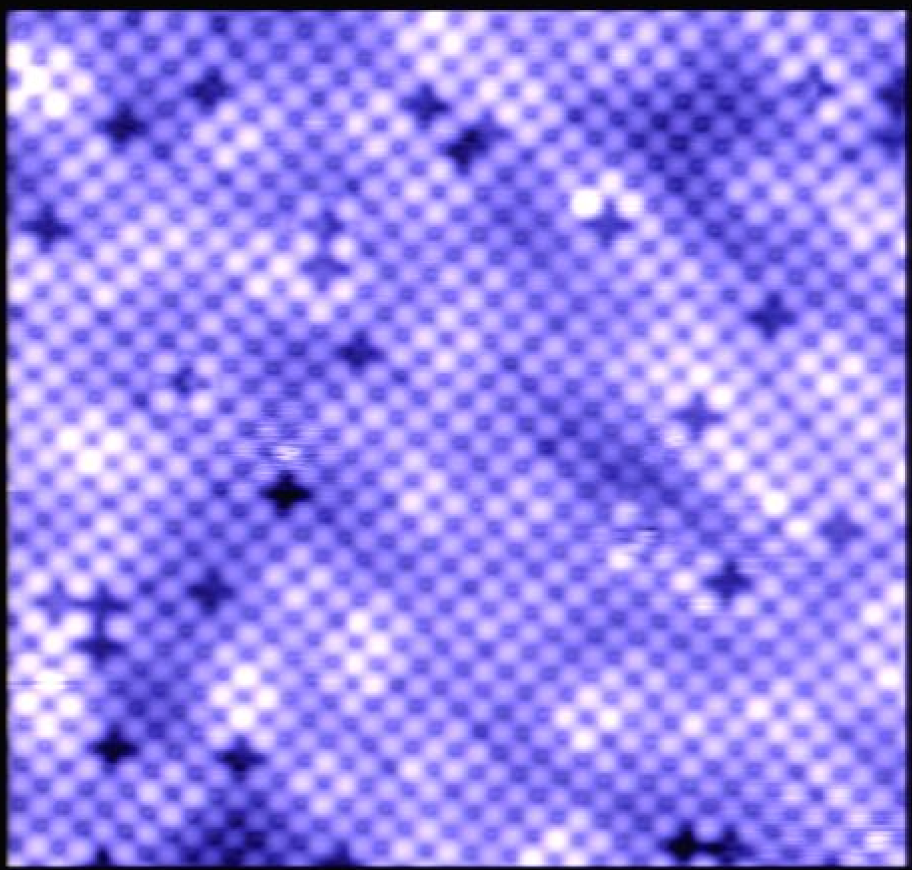

$Bi_{2.2}Sr_{1.8}Ca_{0.8}Dy_{0.2}Cu_2O_y$

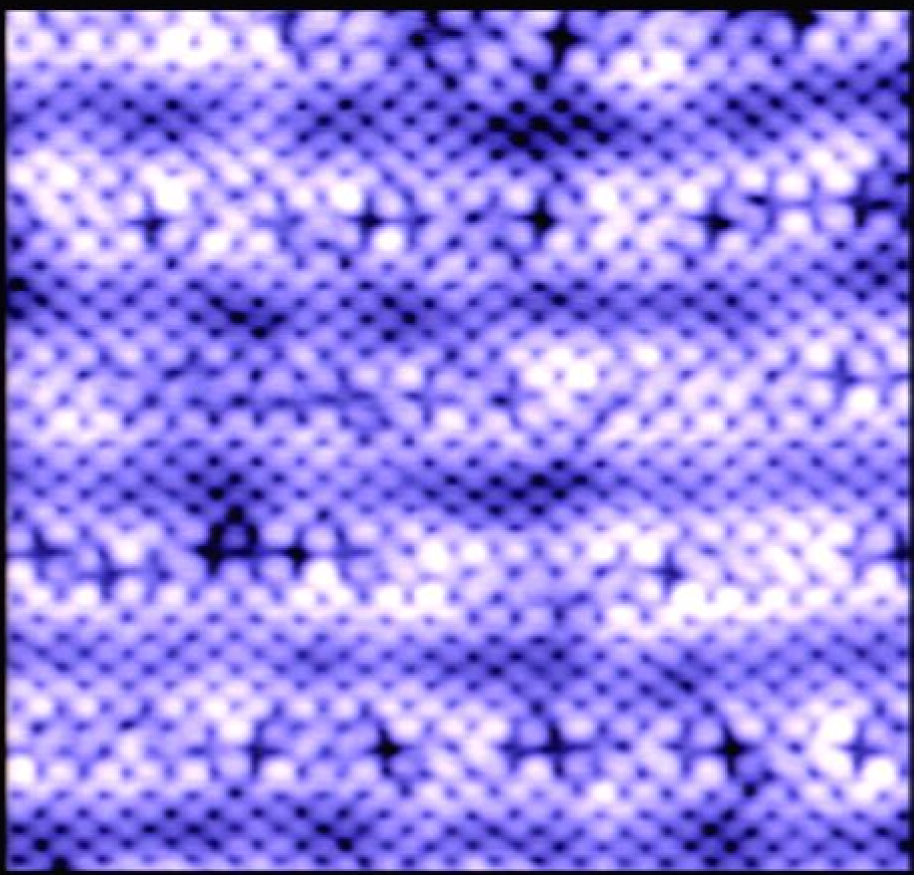

Y. Kohsaka et al., Science 315, 1380 (2007

dI/dV Spectra

$Ca_{1.90}Na_{0.10}CuO_2Cl_2$ $Bi_{2.2}Sr_{1.8}Ca_{0.8}Dy_{0.2}Cu_2O_y$

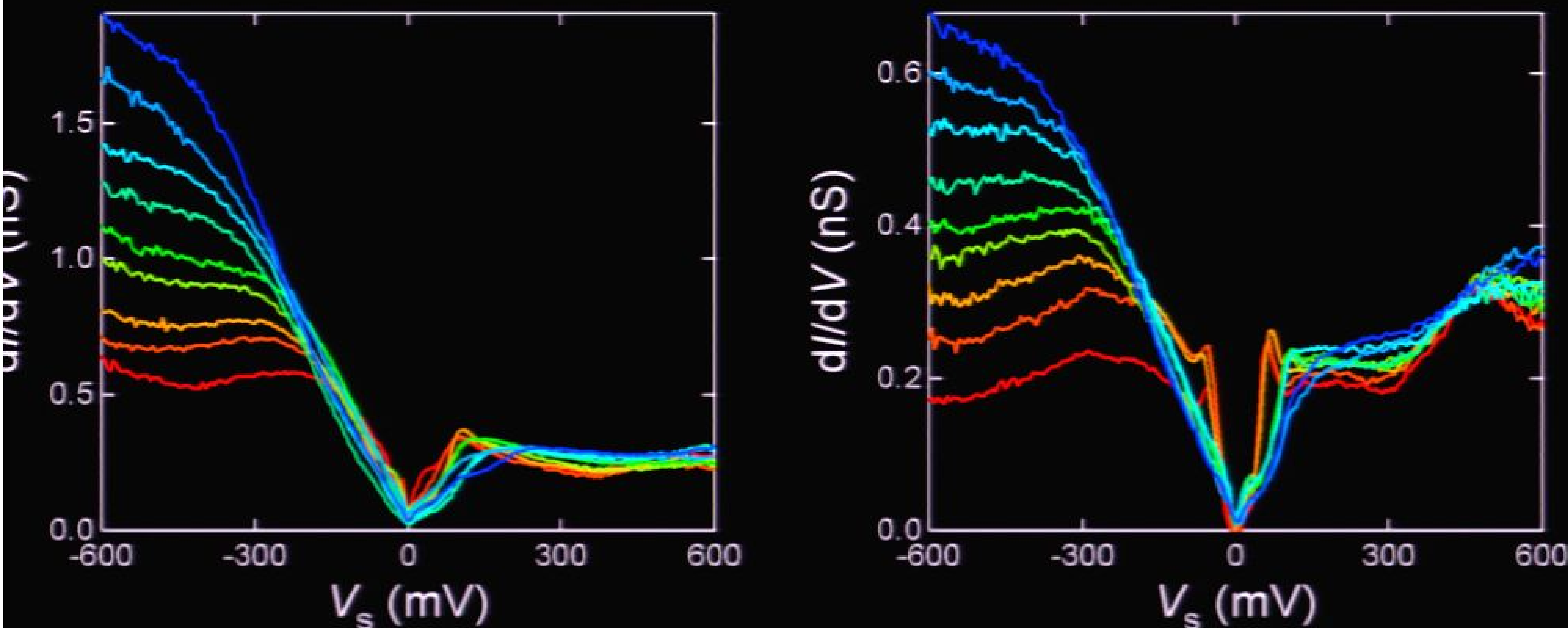

Intense Tunneling-Asymmetry (TA)
variation are highly similar

Y. Kohsaka et al., Science 315, 1380 (2007

Topograph

$Ca_{1.90}Na_{0.10}CuO_2Cl_2$

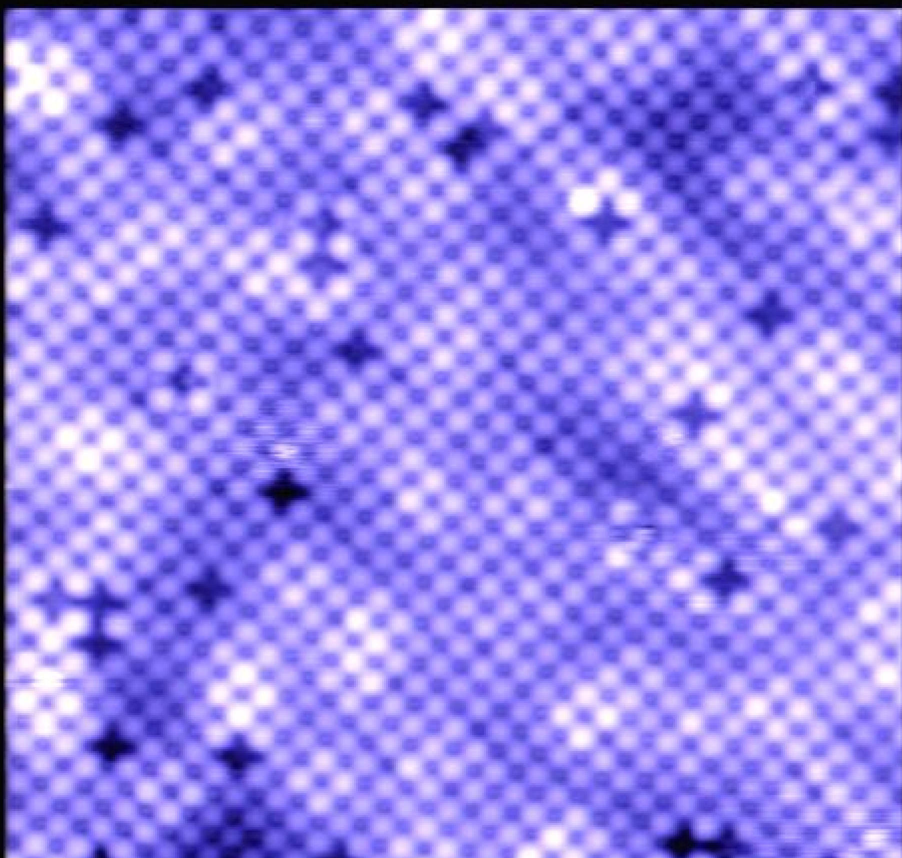

$Bi_{2.2}Sr_{1.8}Ca_{0.8}Dy_{0.2}Cu_2O_y$

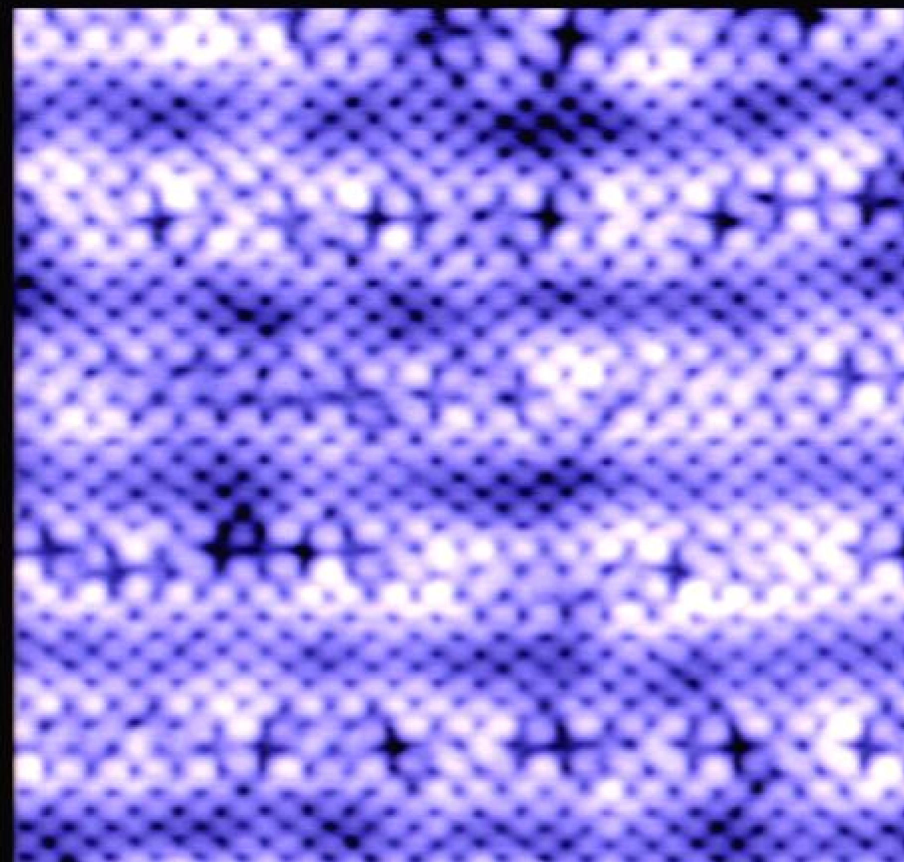

Y. Kohsaka et al., Science 315, 1380 (2007

dI/dV Spectra

$Ca_{1.90}Na_{0.10}CuO_2Cl_2$ $Bi_{2.2}Sr_{1.8}Ca_{0.8}Dy_{0.2}Cu_2O_y$

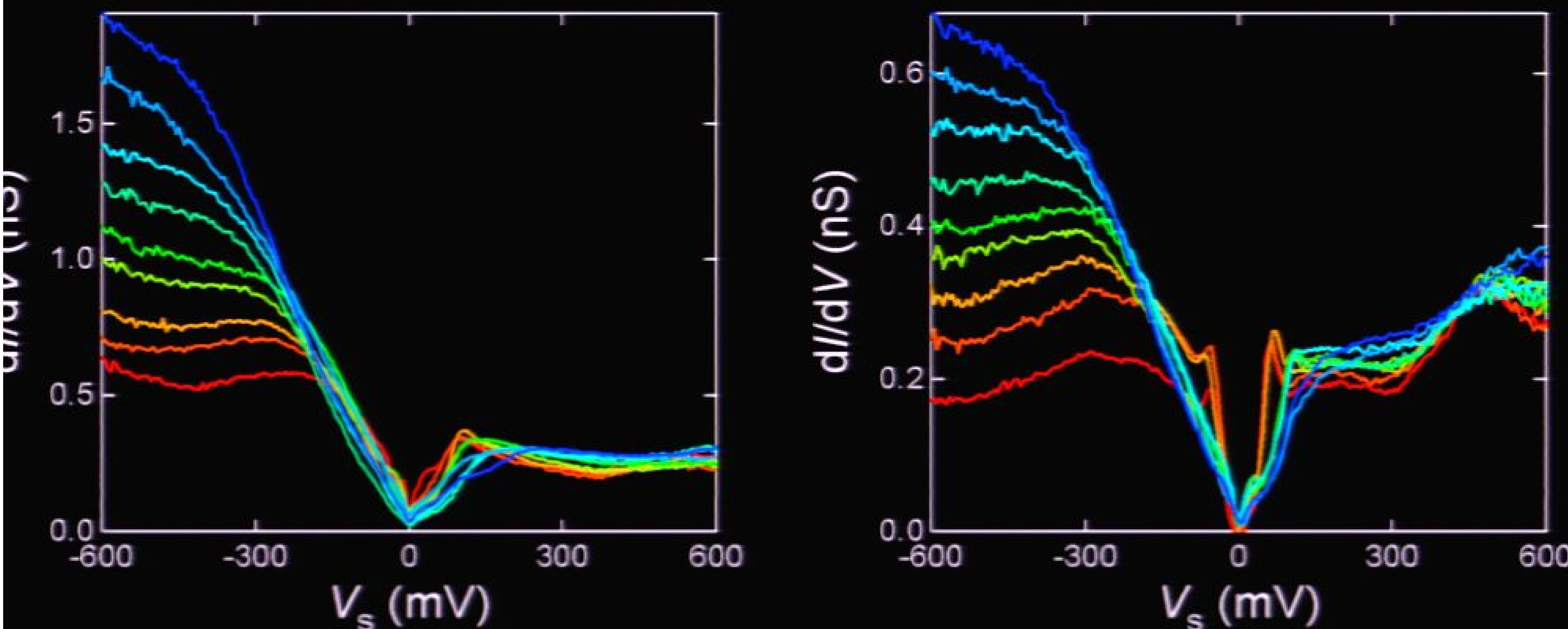

Intense Tunneling-Asymmetry (TA)
variation are highly similar

Y. Kohsaka et al., Science 315, 1380 (2007

Topograph

$Ca_{1.90}Na_{0.10}CuO_2Cl_2$

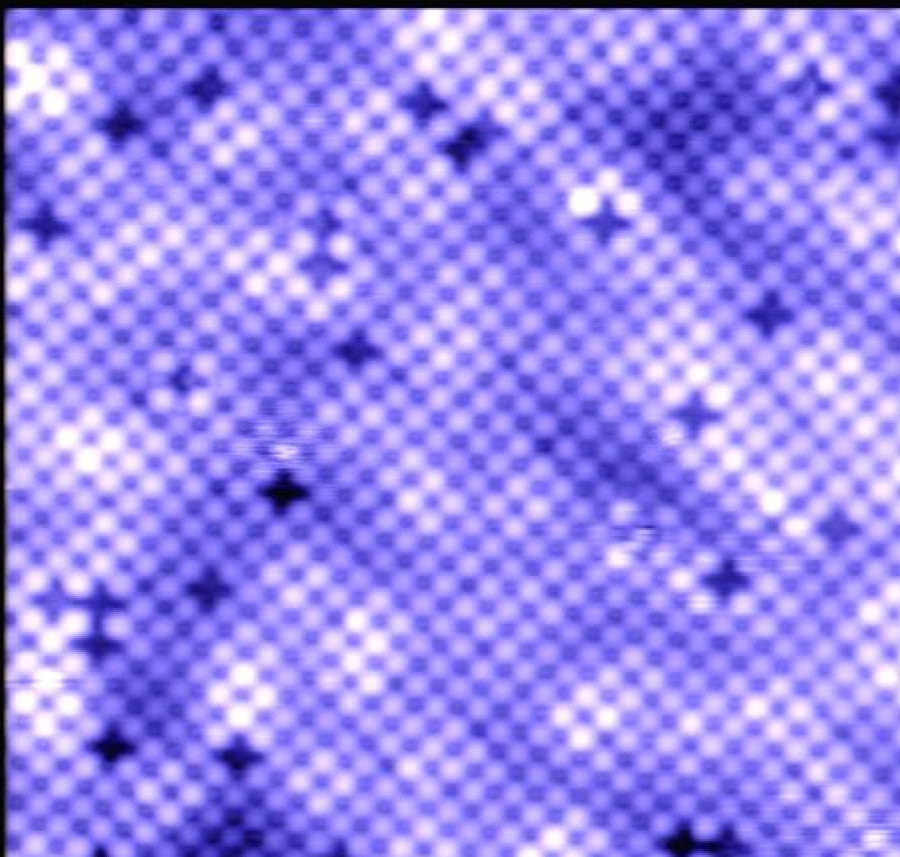

$Bi_{2.2}Sr_{1.8}Ca_{0.8}Dy_{0.2}Cu_2O_y$

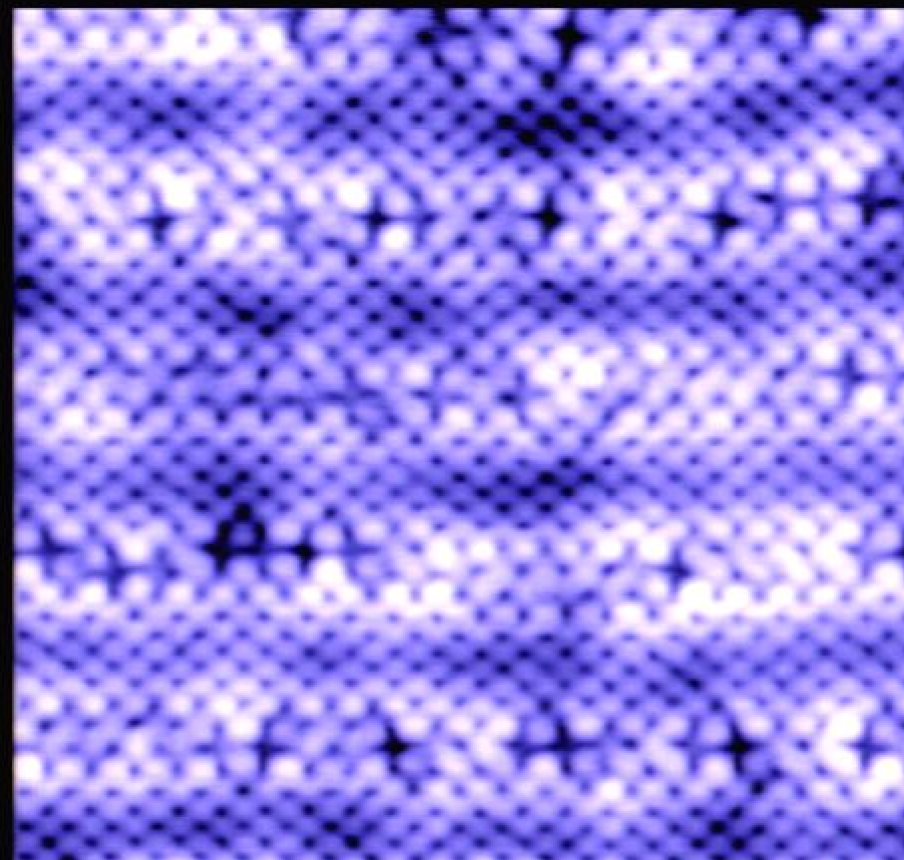

Y. Kohsaka et al. Science 315, 1380 (2007

Tunneling Asymmetry (TA)-map at E=150meV

$Ca_{1.90}Na_{0.10}CuO_2Cl_2$

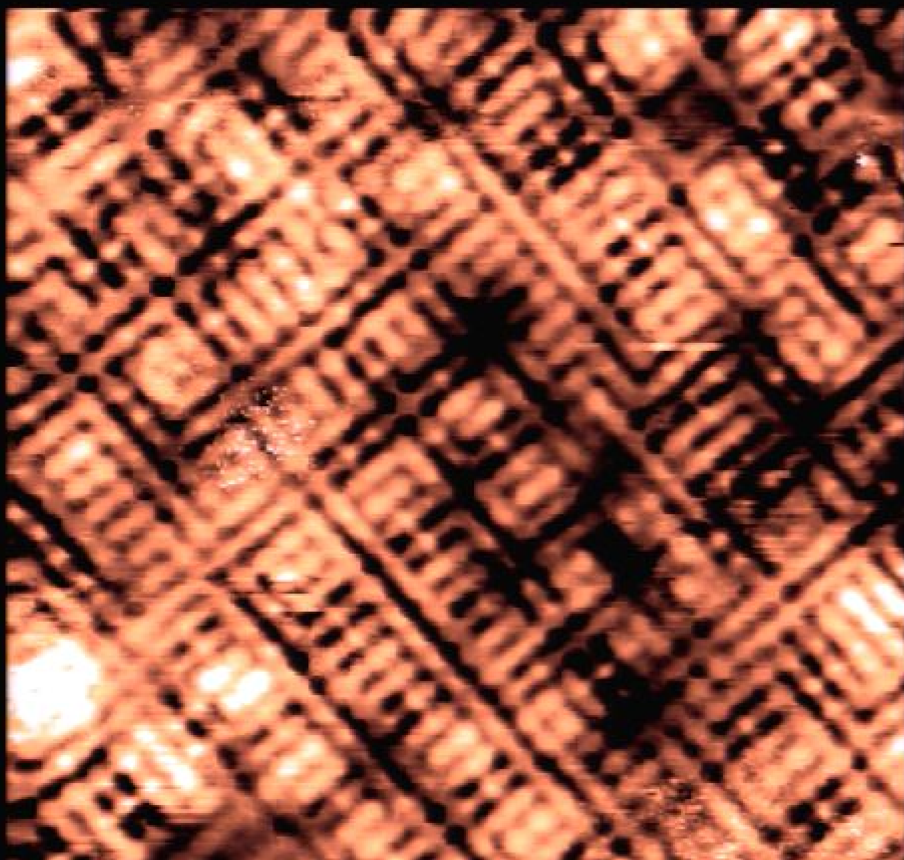

$Bi_{2.2}Sr_{1.8}Ca_{0.8}Dy_{0.2}Cu_2O_y$

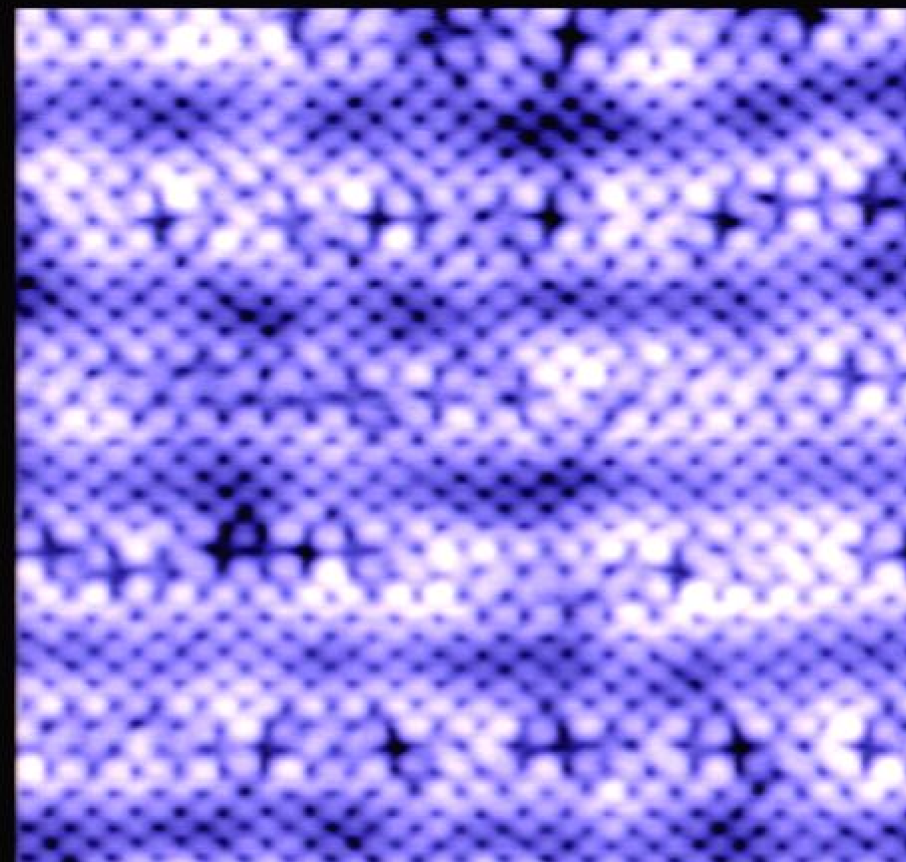

Y. Kohsaka et al., Science 315, 1380 (2007

Tunneling Asymmetry (TA)-map at E=150meV

$Ca_{1.90}Na_{0.10}CuO_2Cl_2$

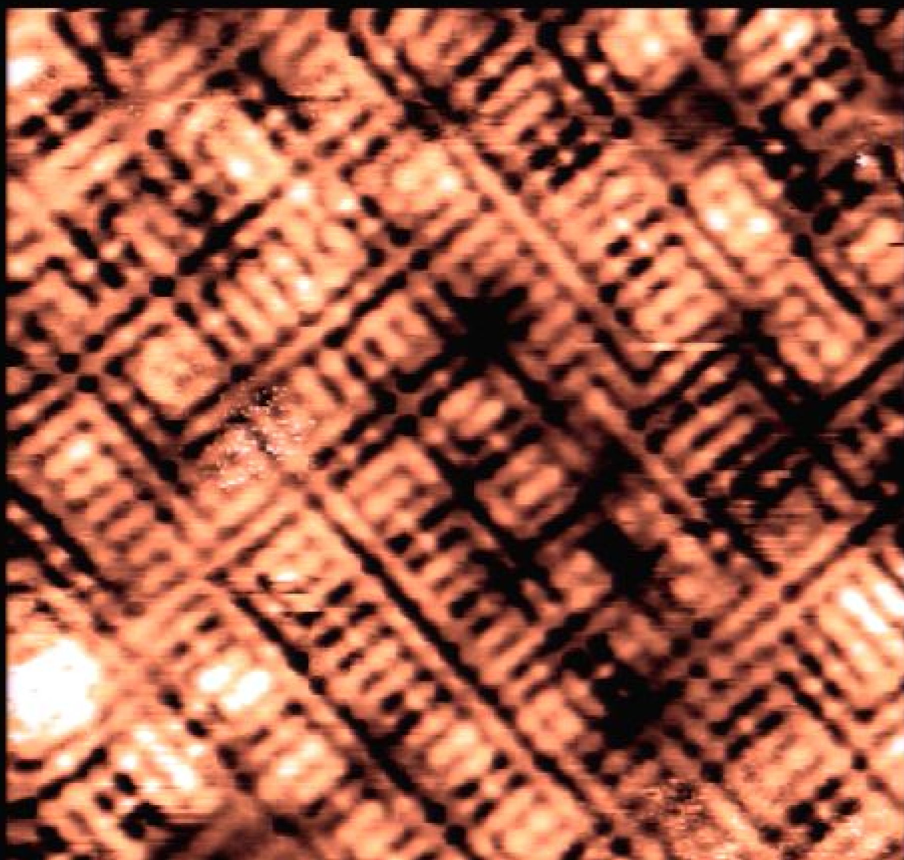

$Bi_{2.2}Sr_{1.8}Ca_{0.8}Dy_{0.2}Cu_2O_y$

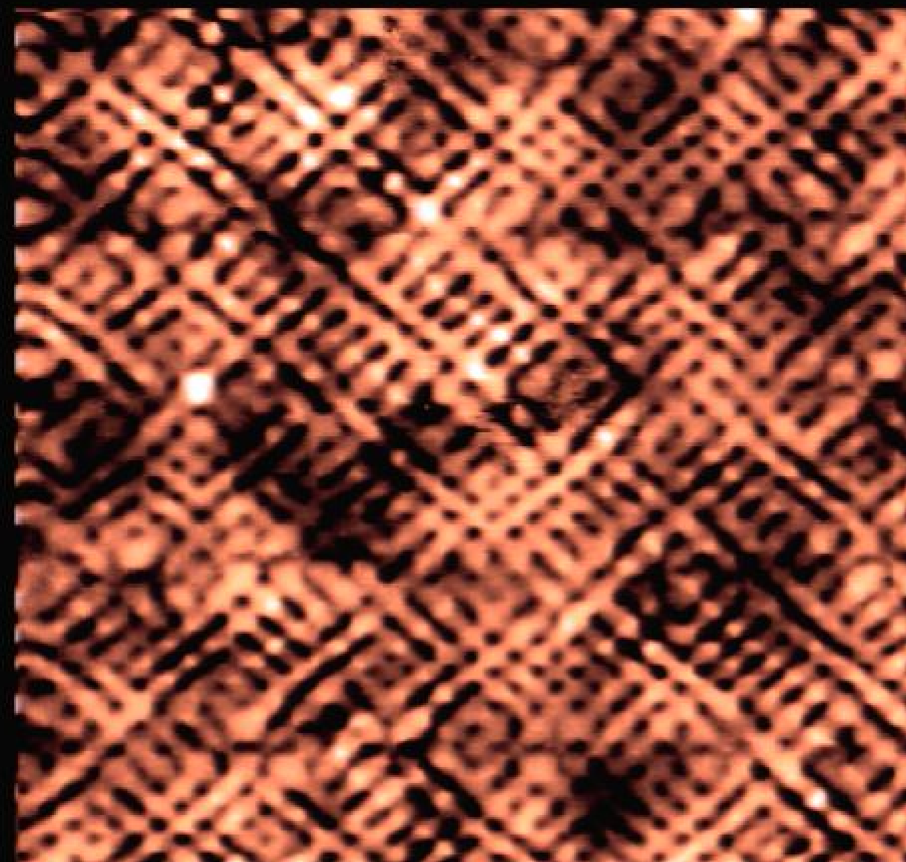

Y. Kohsaka et al., Science 315, 1380 (2007

Tunneling Asymmetry (TA)-map at E=150meV

$Ca_{1.90}Na_{0.10}CuO_2Cl_2$

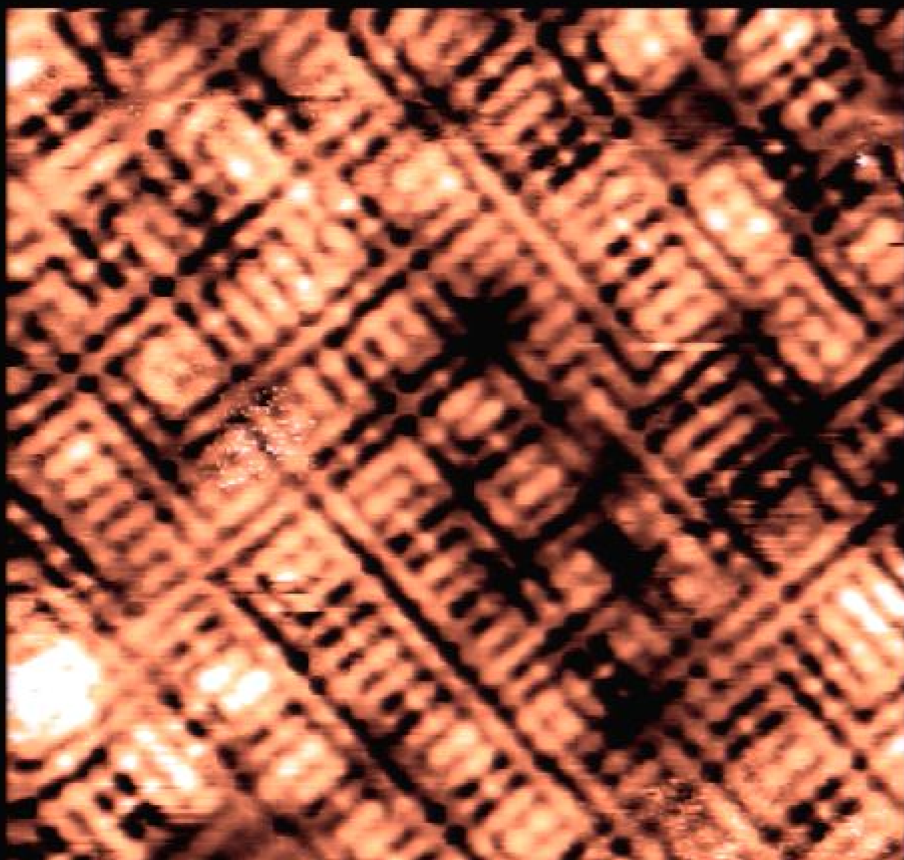

$Bi_{2.2}Sr_{1.8}Ca_{0.8}Dy_{0.2}Cu_2O_y$

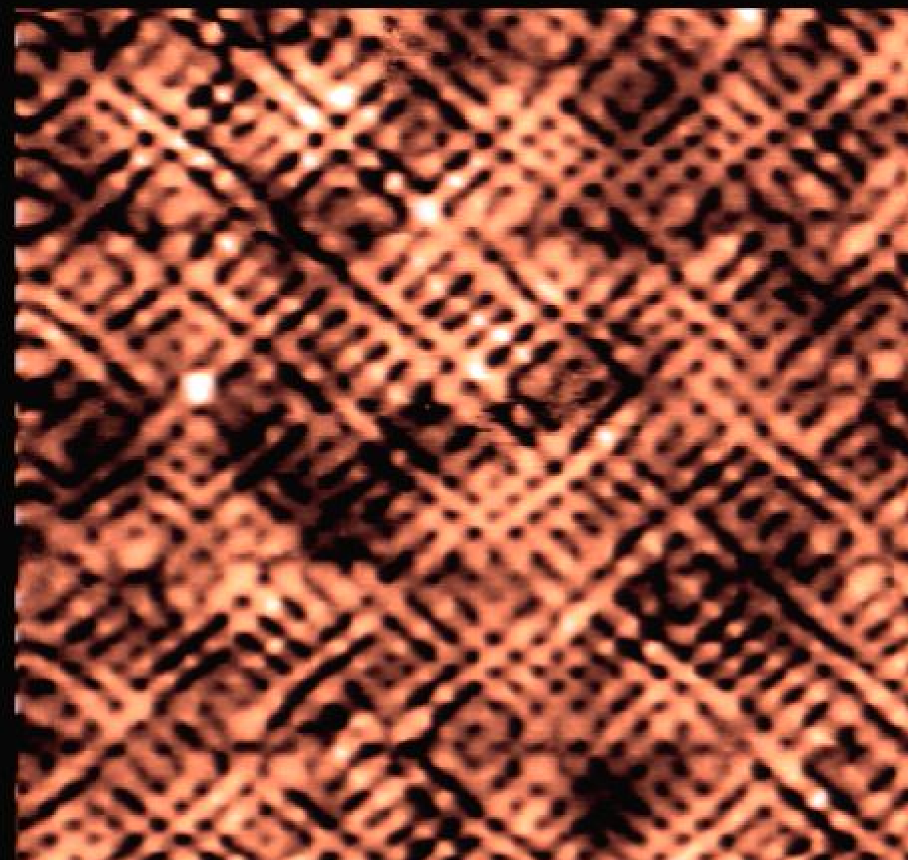

Indistinguishable bond-centered TA contrast

with disperse $4a_0$-wide nanodomains

Y. Kohsaka et al., Science 315, 1380 (2007

TA Contrast is at oxygen site (Cu-O-Cu bond-centered)

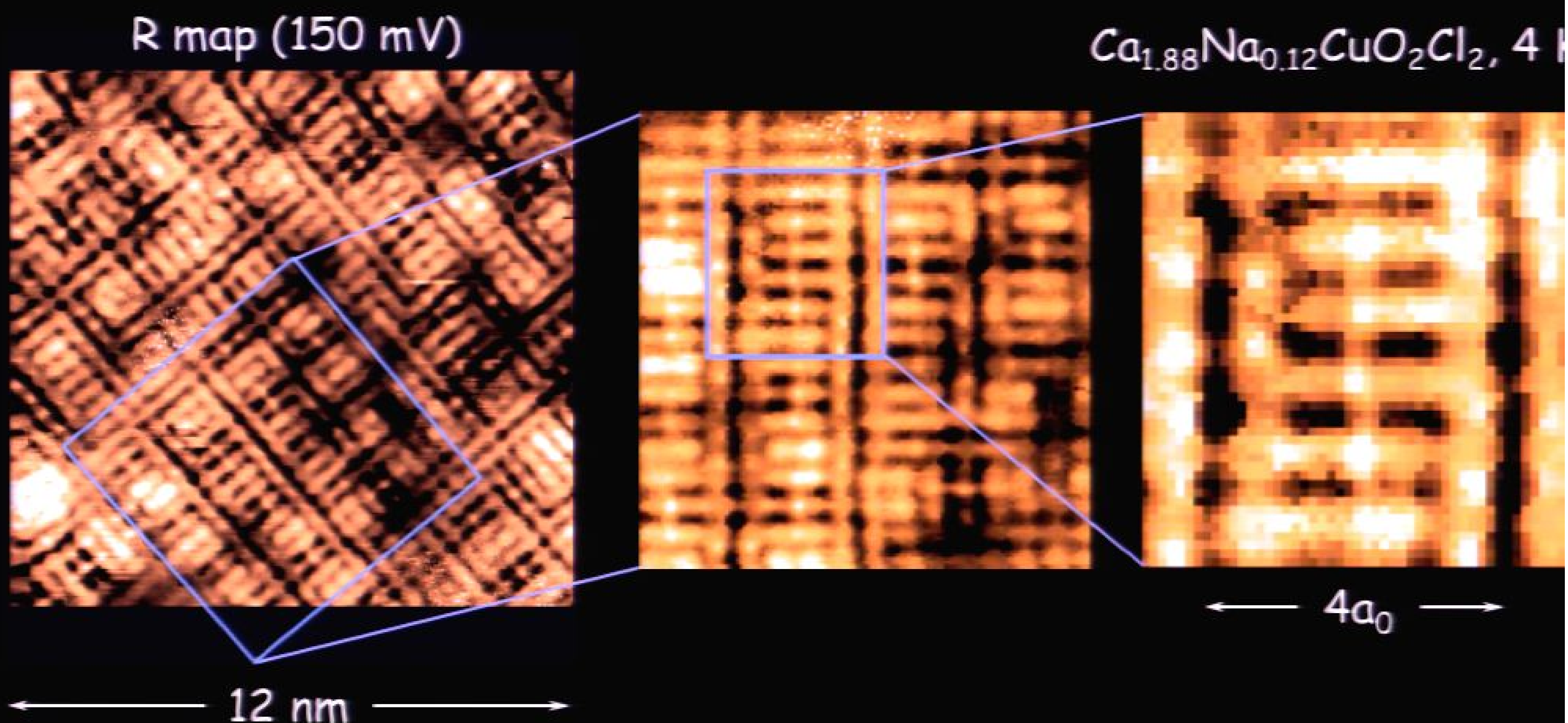

Y. Kohsaka et al., Science 315, 1380 (2007

TA Contrast is at oxygen site (Cu-O-Cu bond-centered)

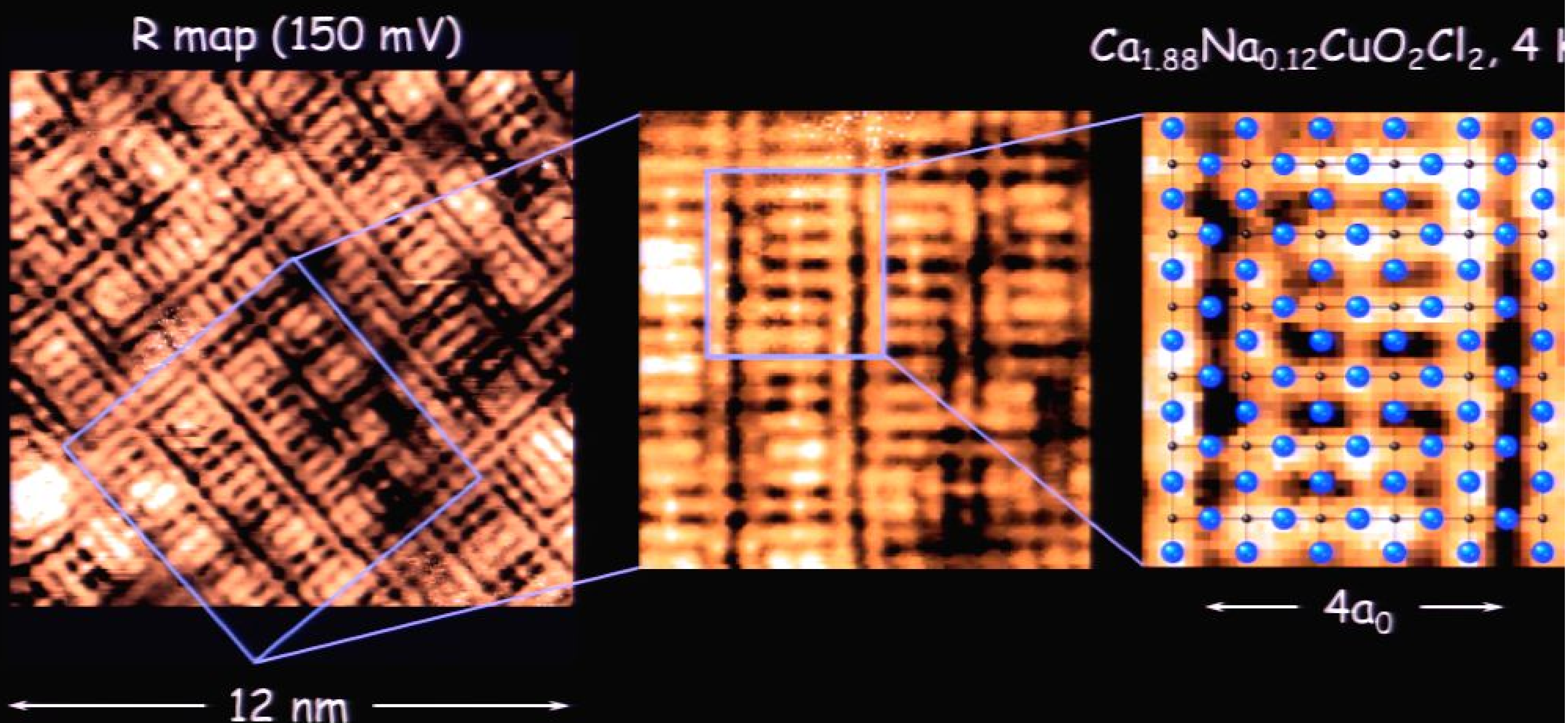

Y. Kohsaka et al., Science 315, 1380 (2007

TA Contrast is at oxygen site (Cu-O-Cu bond-centered)

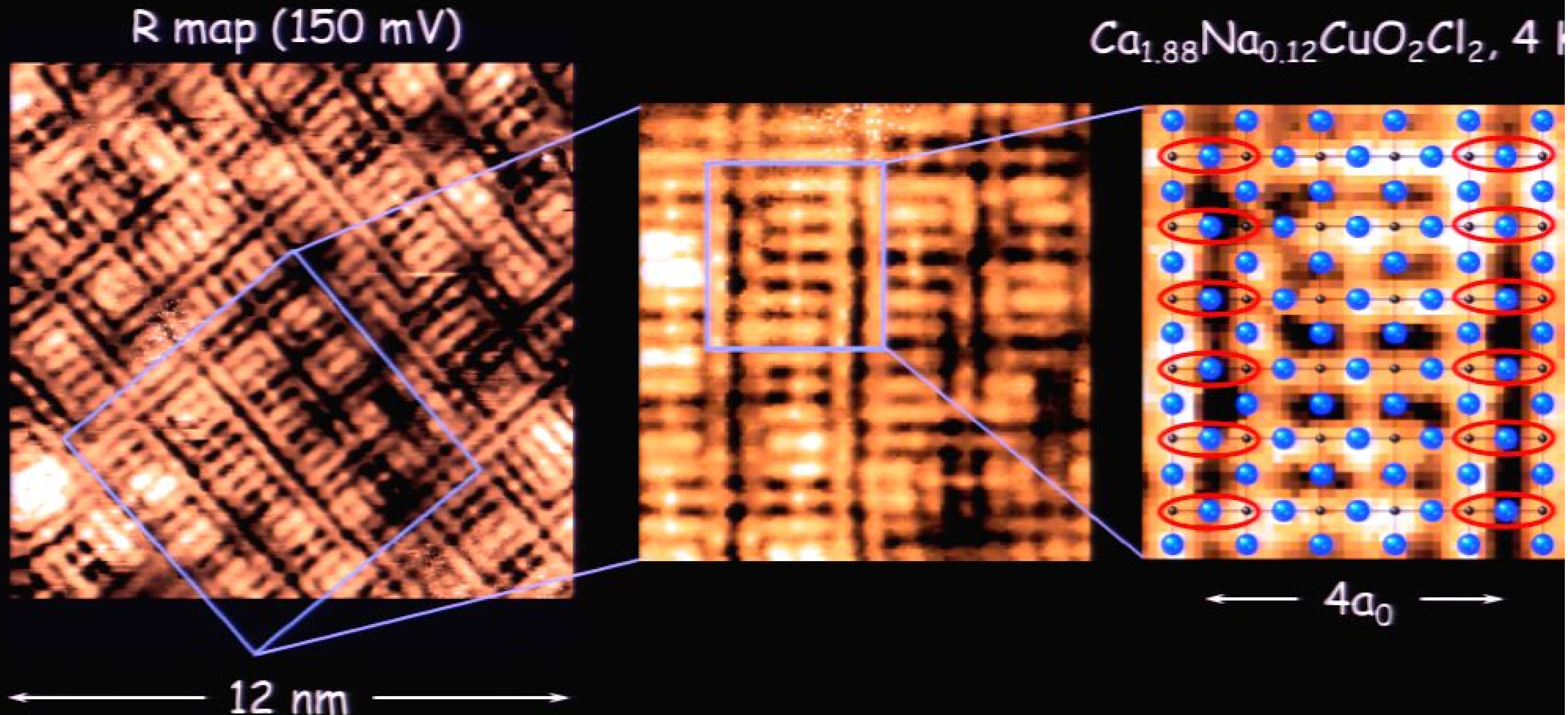

Evidence for a predicted valence bond supersolid

S. Sachdev and N. Read, *Int. J. Mod. Phys.* B **5**, 219 (1991).

M. Vojta and S. Sachdev, *Phys. Rev. Lett.* **83**, 3916 (1999).

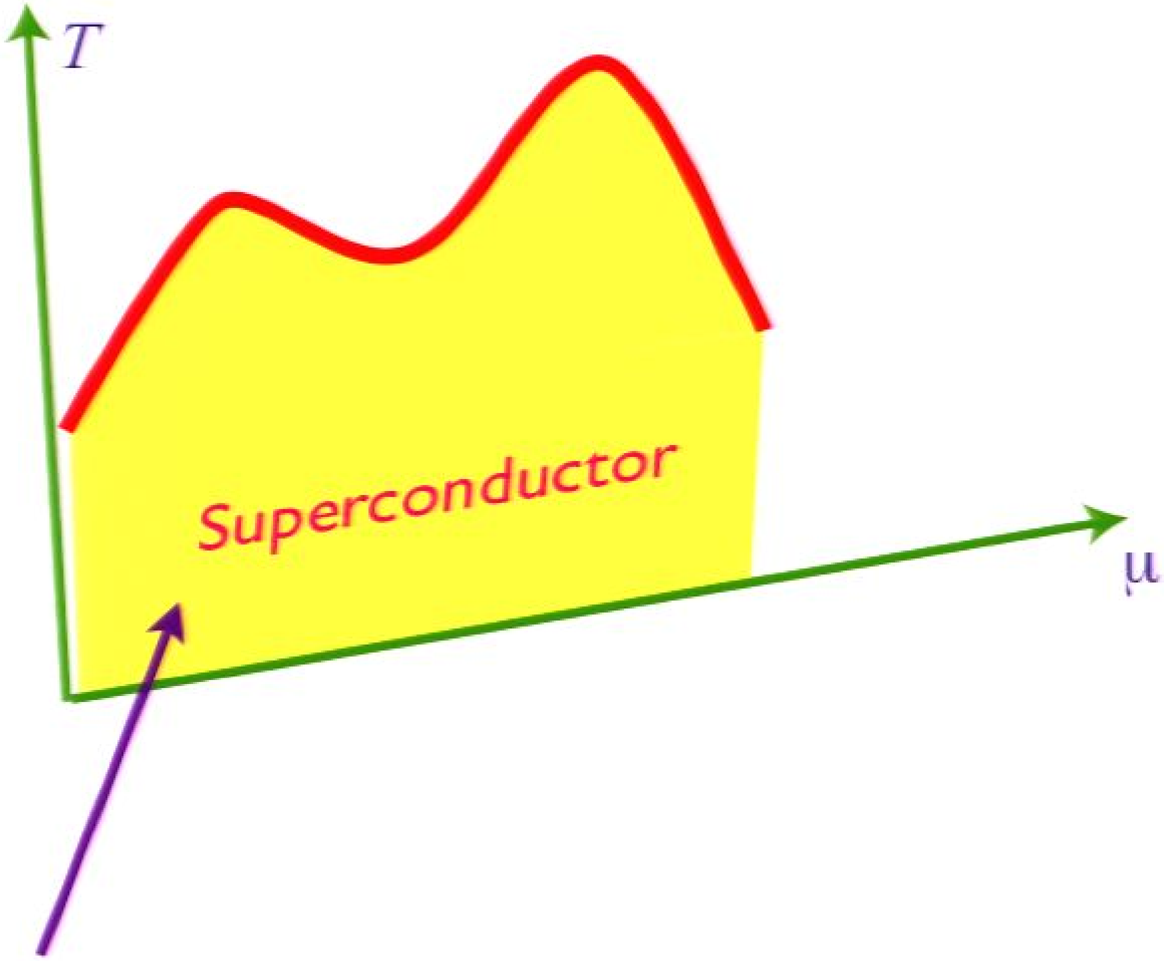

Scanning tunnelling microscopy

Use coupling *g* to induce a transition to a VBS insulator

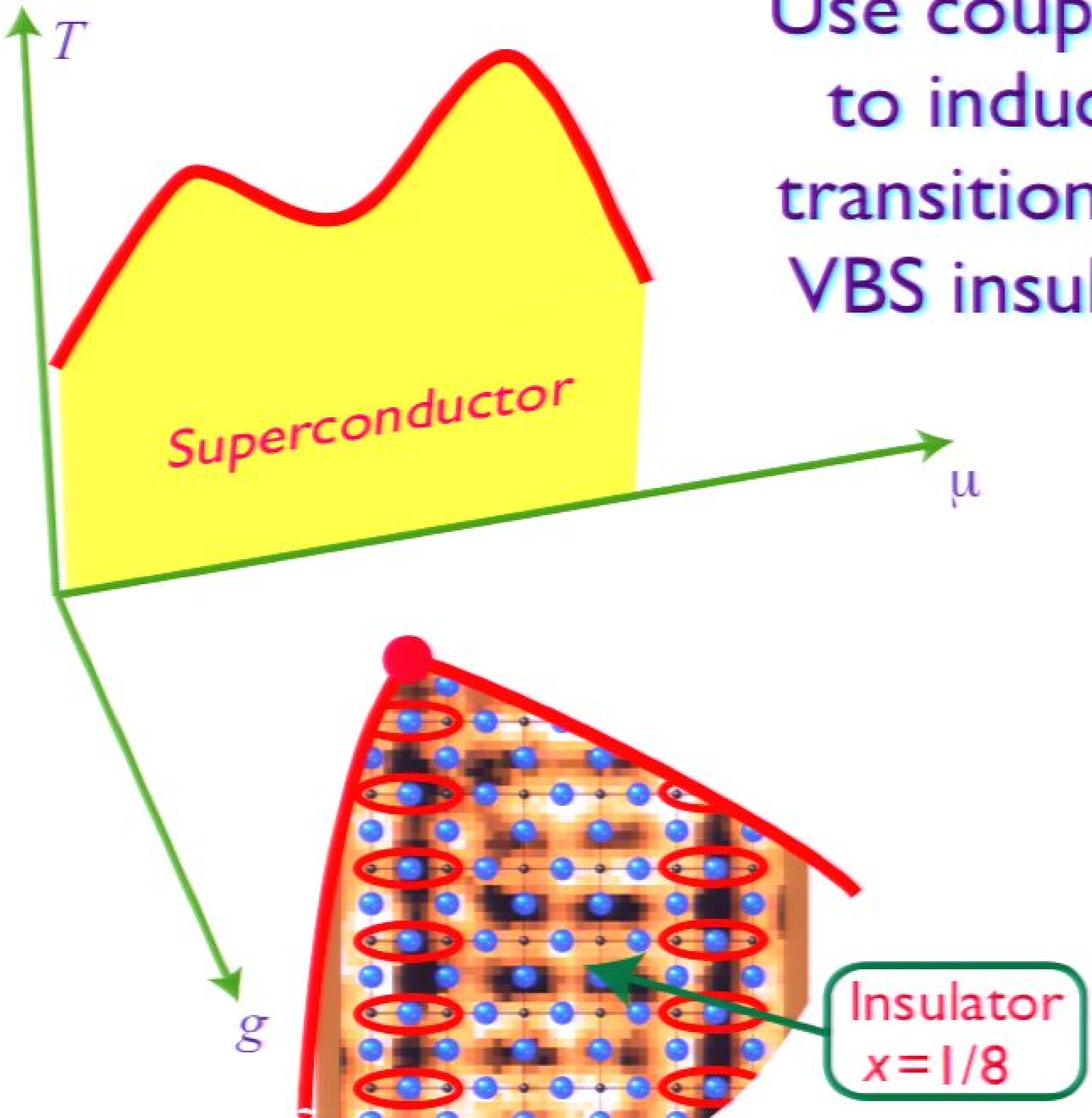

Use coupling g to induce a transition to a VBS insulator

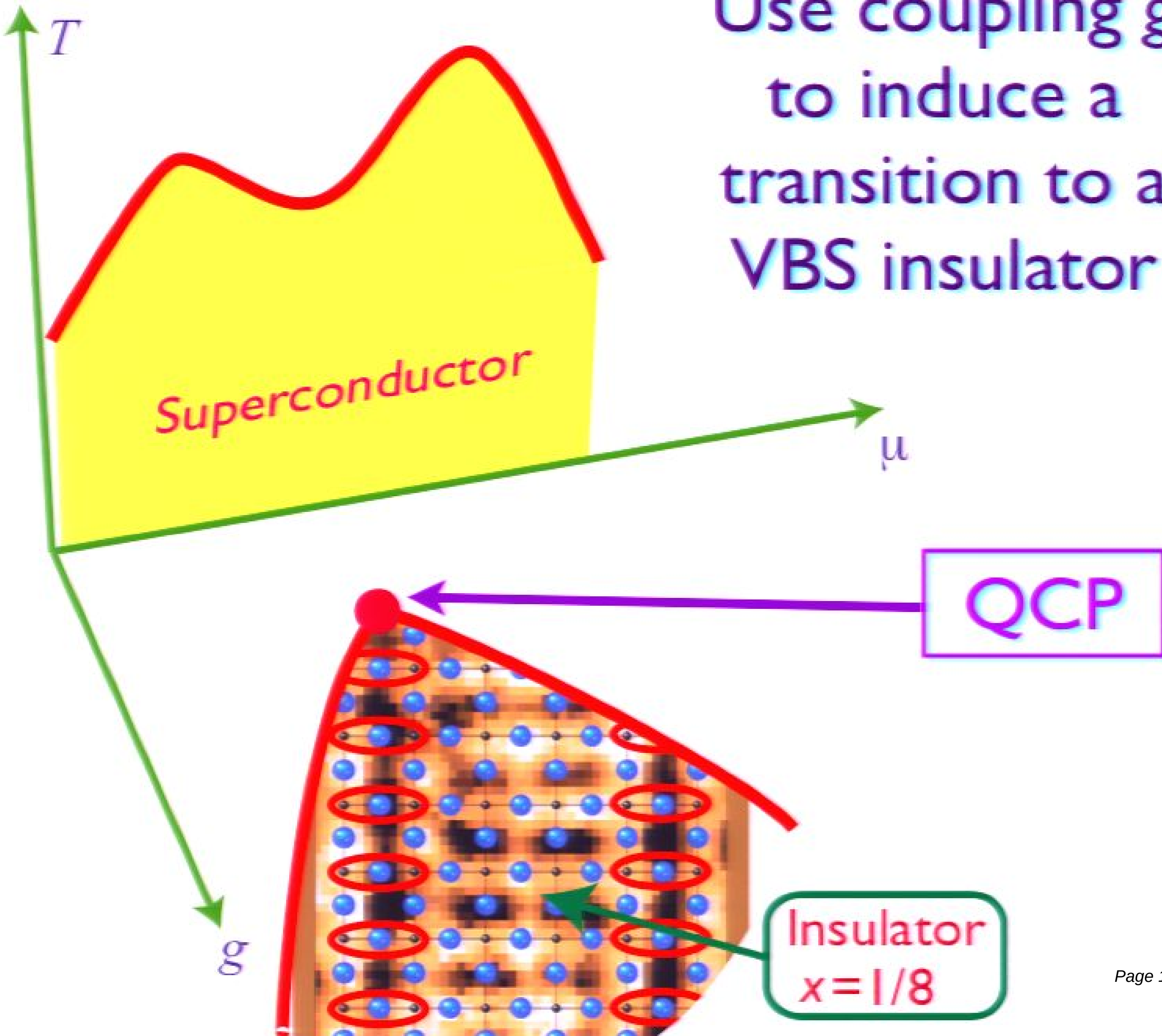

Proposed generalized phase diagram

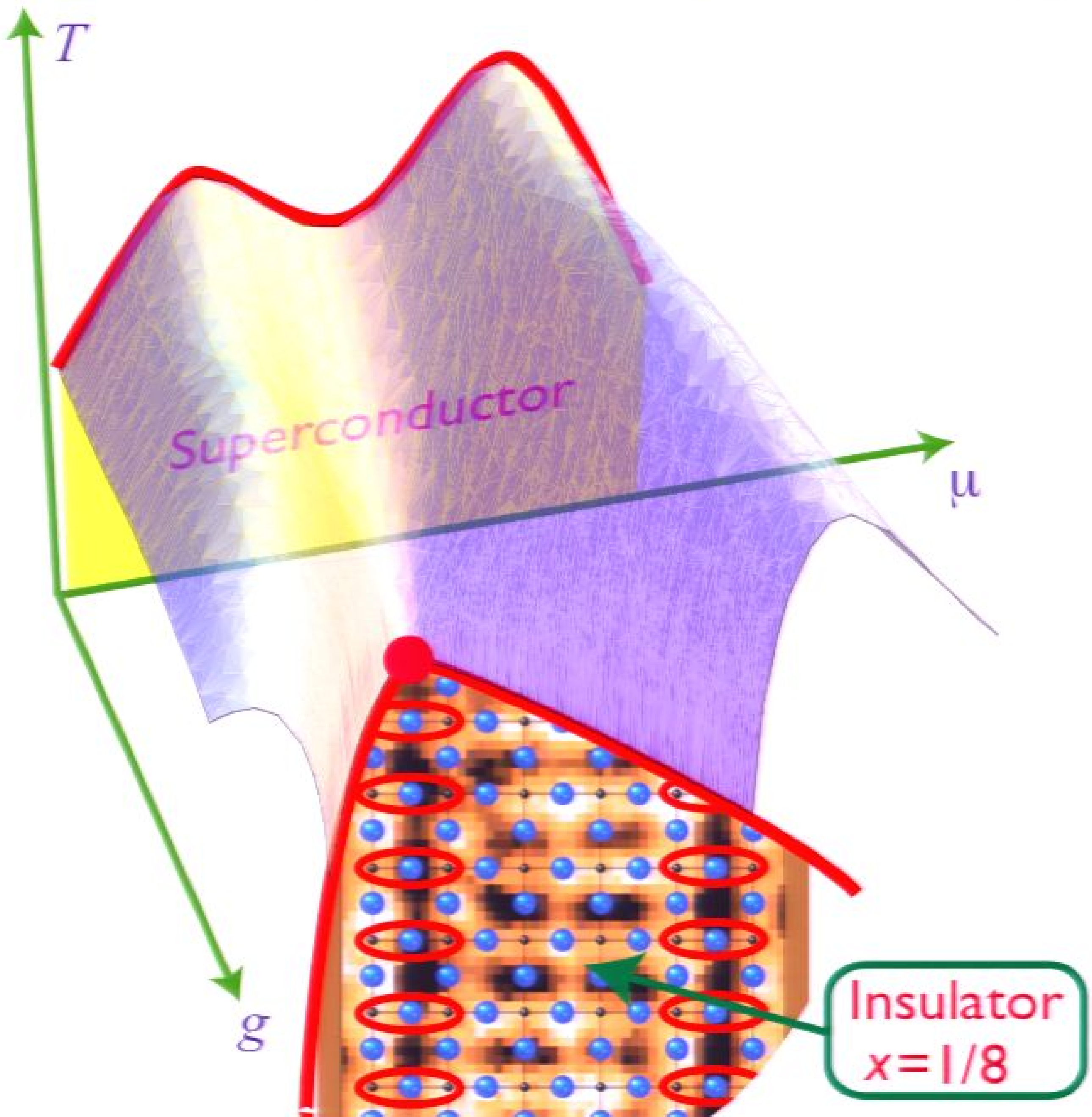

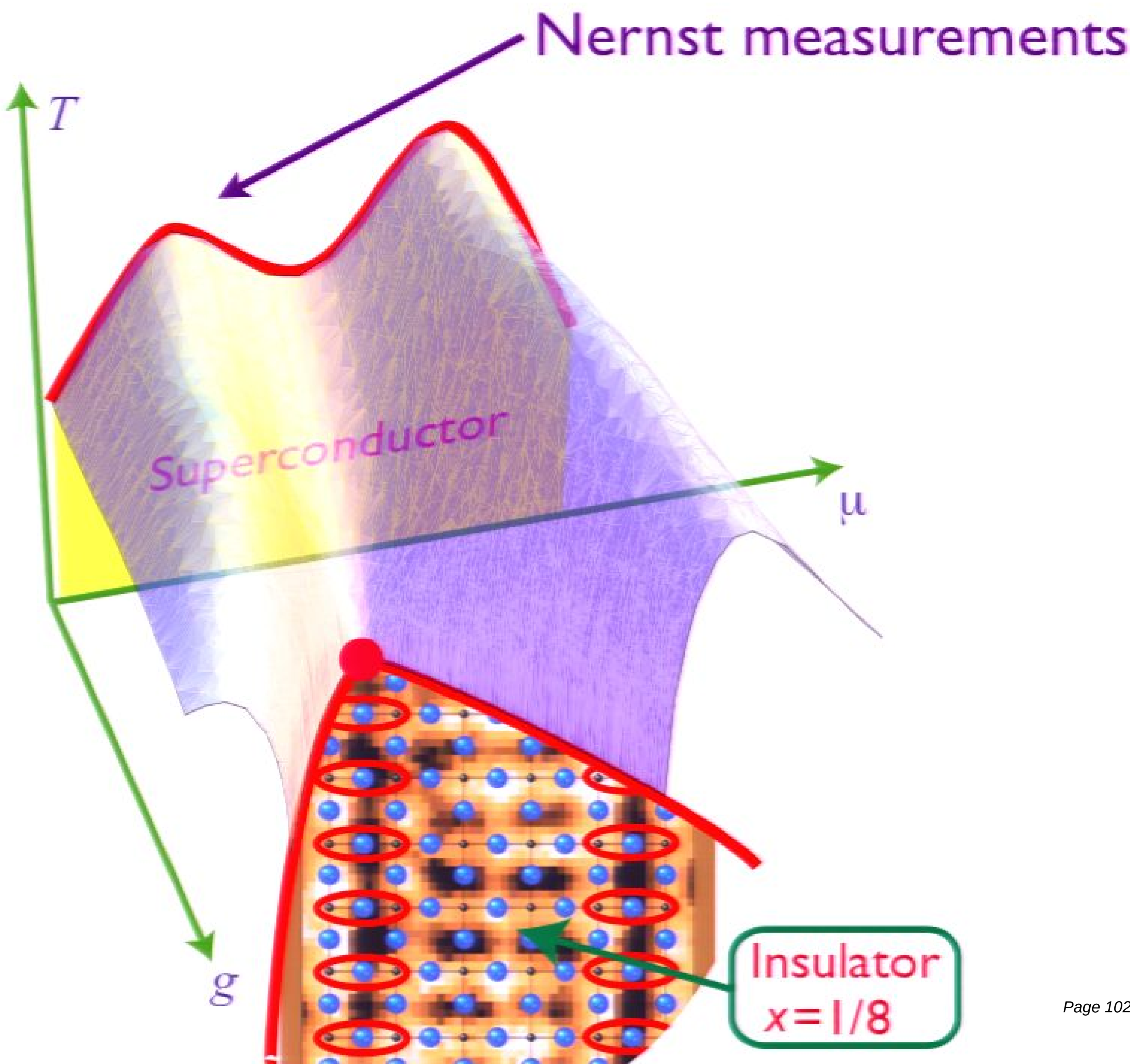
Nernst measurements
T
Superconductor
μ
g
Insulator
x=1/8

Nernst experiment

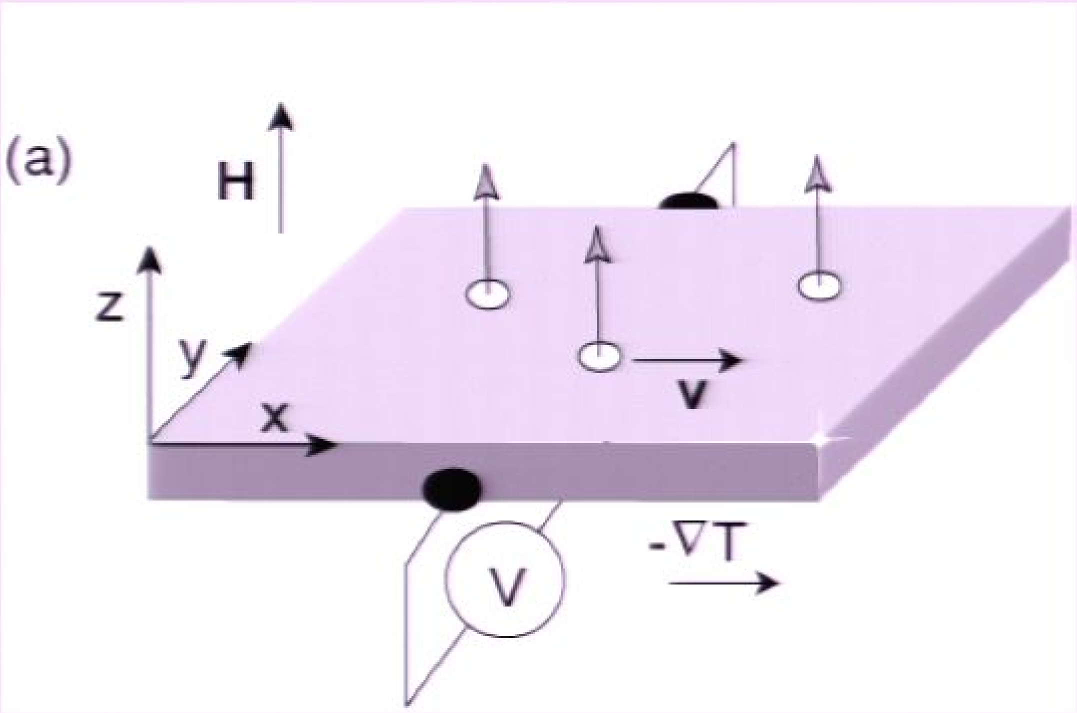

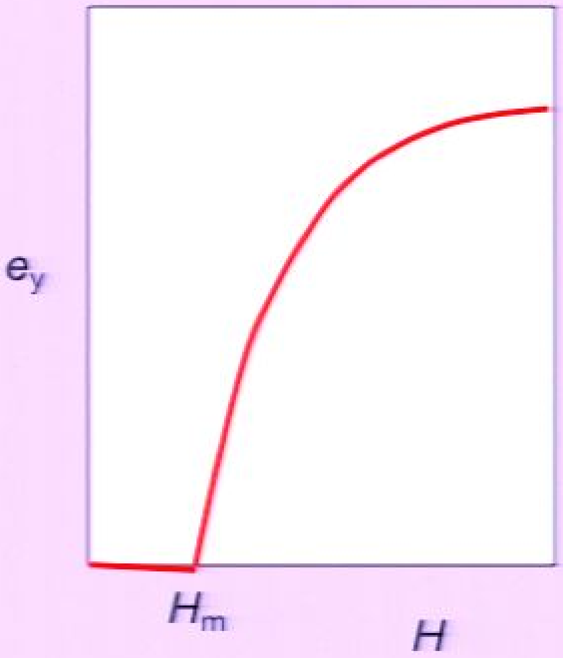

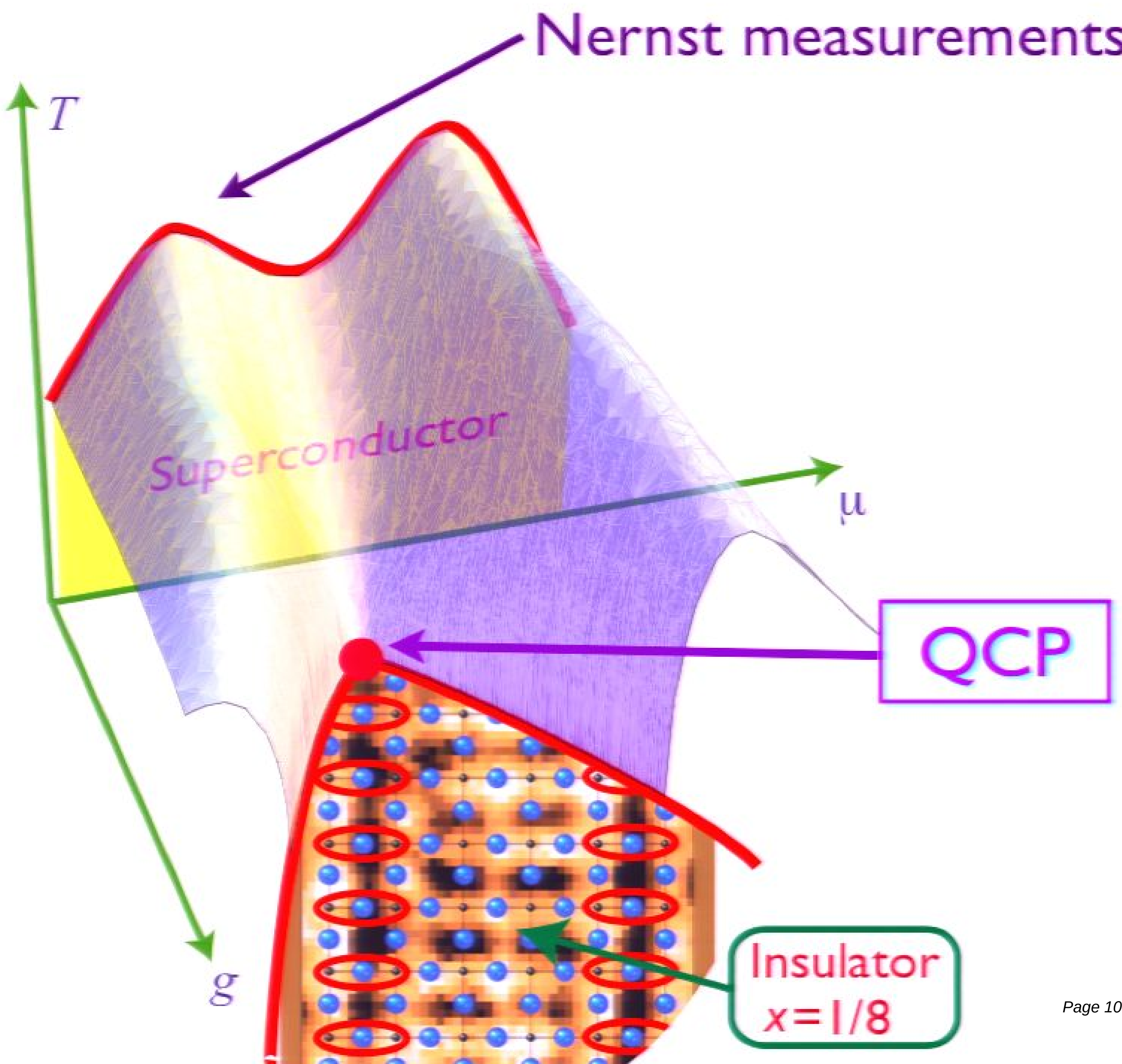
Nernst measurements
T
Superconductor
μ
QCP
g
Insulator
x=1/8

Non-zero temperature phase diagram

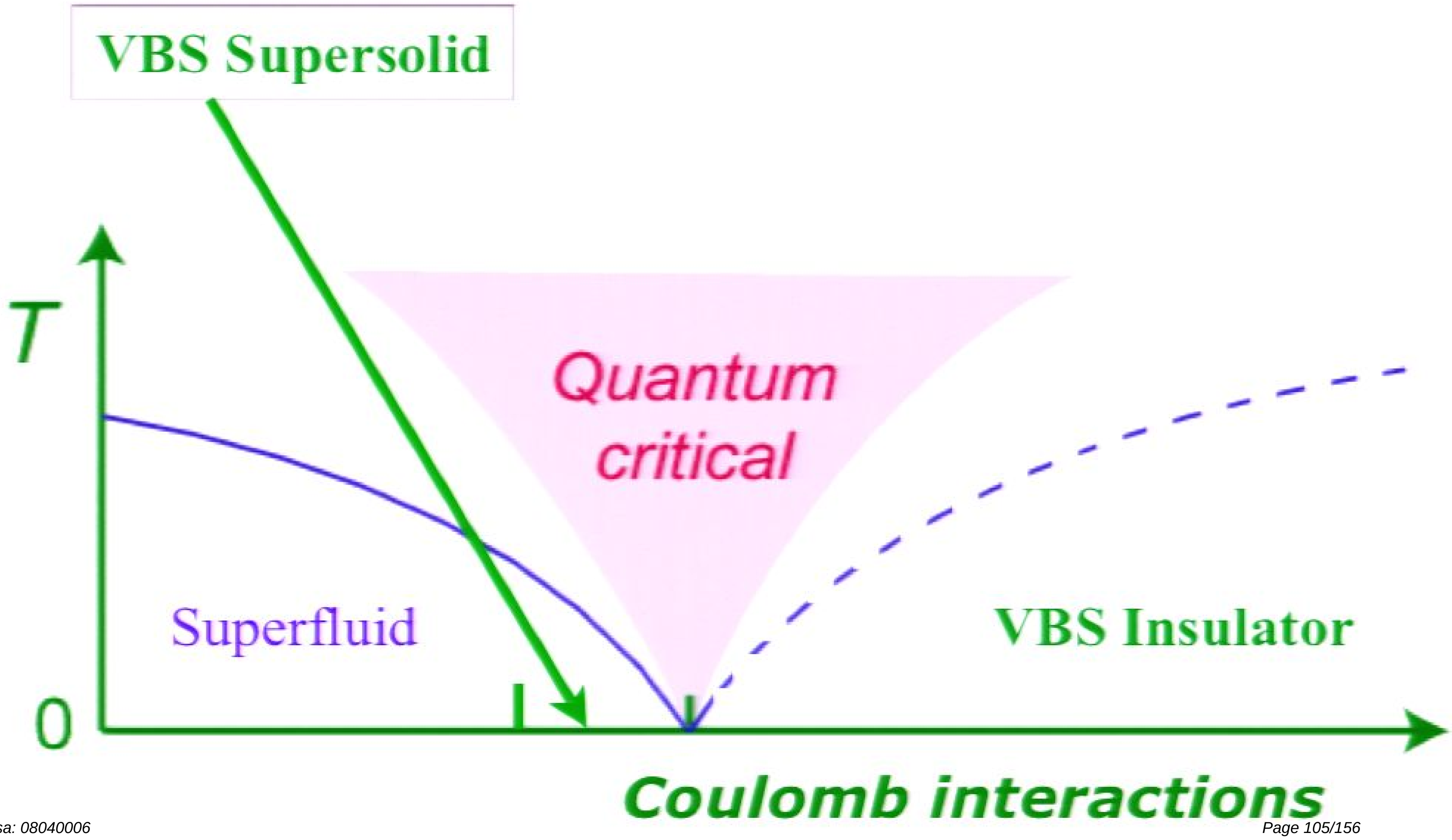

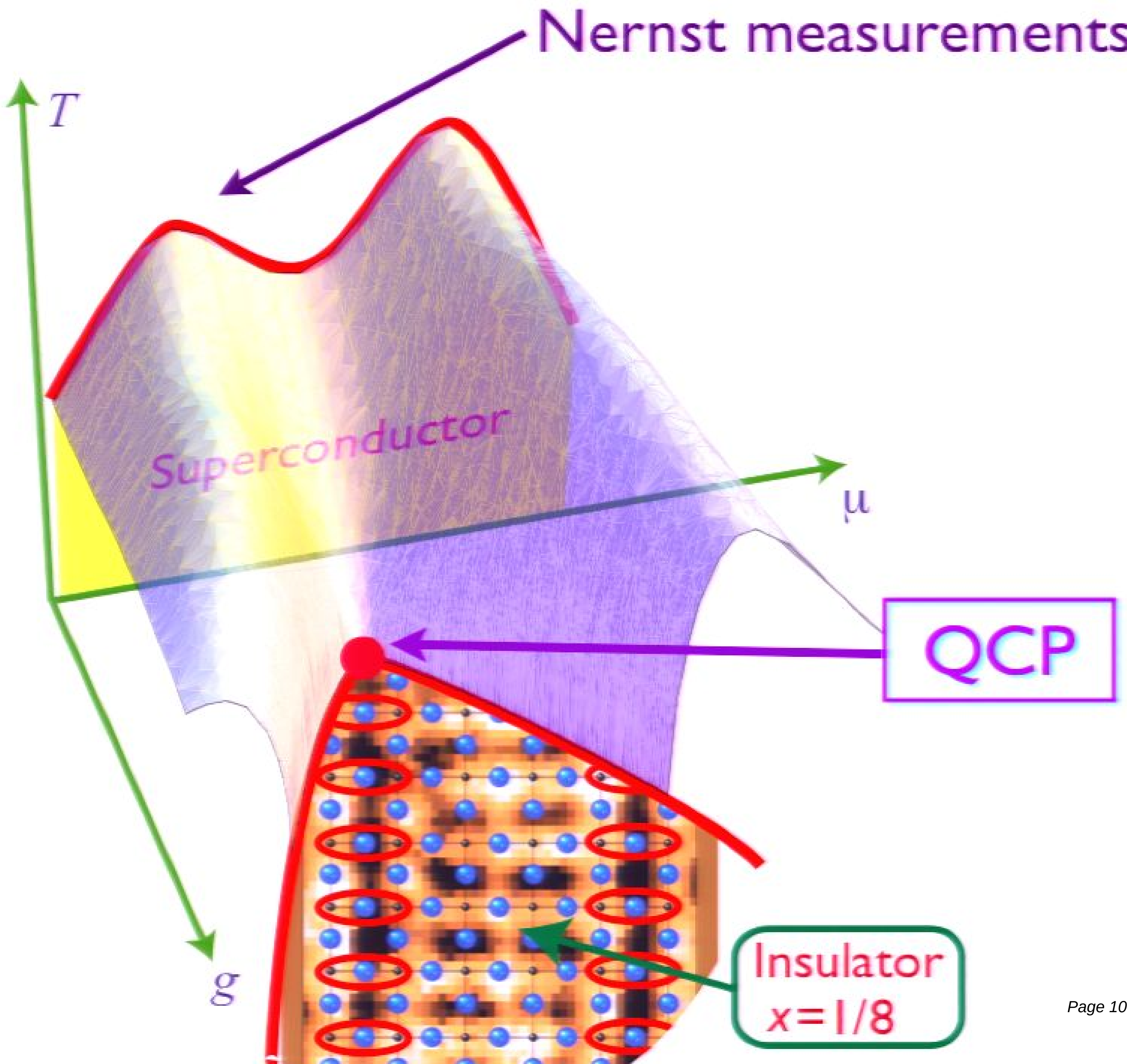
Nernst measurements
T
Superconductor
μ
QCP
g
Insulator
x=1/8

Non-zero temperature phase diagram

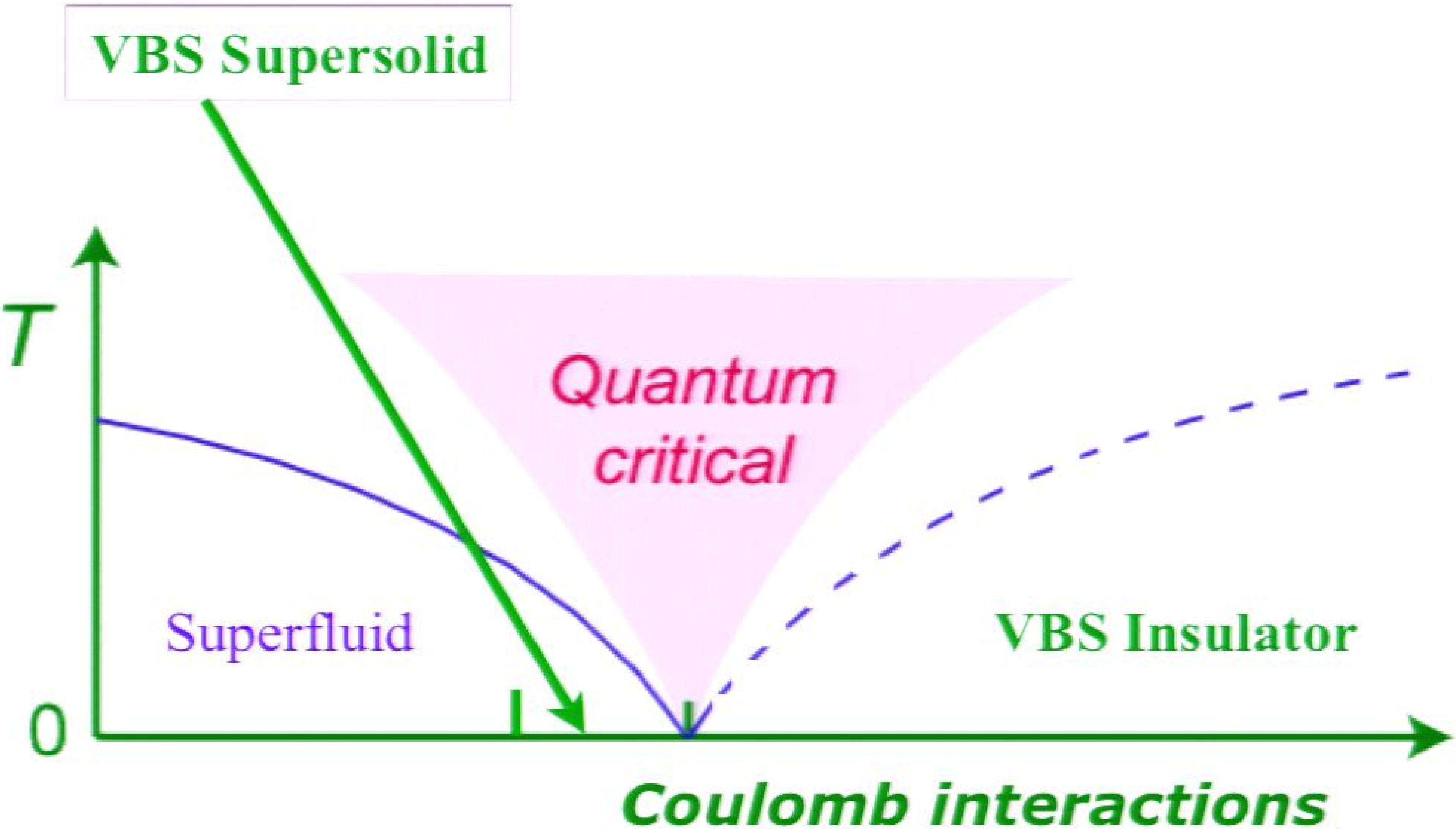

Non-zero temperature phase diagram

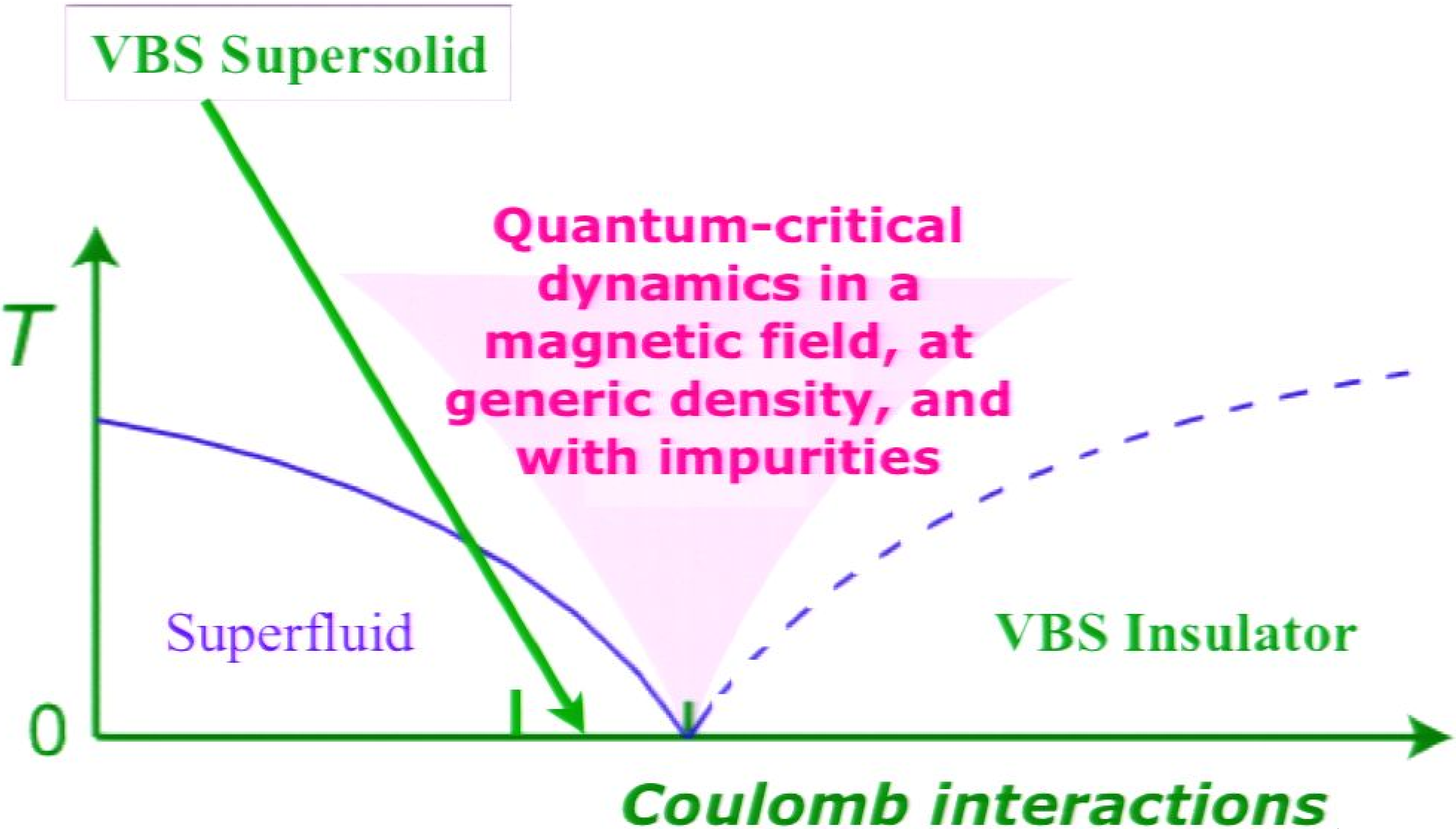

To the CFT of the quantum critical point, we add

- A chemical potential μ
- A magnetic field B

After the AdS/CFT mapping, we obtain the Einstein-Maxwell theory of a black hole with

- An electric charge
- A magnetic charge

S.A. Hartnoll, P.K. Kovtun, M. Müller, and S. Sachdev, Phys. Rev. B (2007)

To the CFT of the quantum critical point, we add

- A chemical potential μ
- A magnetic field B

After the AdS/CFT mapping, we obtain the Einstein-Maxwell theory of a black hole with

- An electric charge
- A magnetic charge

A precise correspondence is found between general hydrodynamics of vortices near quantum critical points and solvable models of black holes with electric and magnetic charges

S. A. Hartnoll, P.K. Kovtun, M. Müller, and S. Sachdev, Phys. Rev. B (2007)

In the hydrodynamic regime, $\hbar\omega \ll k_B T$, we can use classical principles involving relaxation to local equilibrium to understand these perturbations.
The variables entering the hydrodynamic theory are

- the external magnetic field $F^{\mu\nu}$,

$$F^{\mu\nu} = \begin{pmatrix} 0 & 0 & 0 \\ 0 & 0 & B \\ 0 & -B & 0 \end{pmatrix},$$

- $T^{\mu\nu}$, the stress energy tensor,
- J^{μ}, the current,
- ρ, the local number density,
- ε, the local energy density,
- P, the local pressure,
- u^{μ}, the local velocity, and
- σ_Q, a universal conductivity, which is the **single transport co-efficient**.

The dependence of ε, P, σ_Q on T and v follows from simple scaling arguments

Lorentz invariance and positivity of entropy production lead to the hydrodynamic equations of motion and constitutive relations:

S.A. Hartnoll, P.K. Kovtun, M. Müller, and S. Sachdey, *Phys. Rev.* B **76** 144502 (2007)

Lorentz invariance and positivity of entropy production lead to the hydrodynamic equations of motion and constitutive relations:

$$
\begin{aligned}
\partial_\mu J^\mu &= 0 \\
\partial_\mu T^{\mu\nu} &= F^{\mu\nu} J_\nu + \frac{1}{\tau_{\rm imp}} (\delta^\mu_\nu + u^\mu u_\nu) T^{\nu\gamma} u_\gamma \\
T^{\mu\nu} &= (\varepsilon + P) u^\mu u^\nu + P g^{\mu\nu} \\
J^\mu &= \rho u^\mu + \sigma_Q (g^{\mu\nu} + u^\mu u^\nu) \left[(-\partial_\nu \mu + F_{\nu\lambda} u^\lambda) + \mu \frac{\partial_\mu T}{T} \right]
\end{aligned}
$$

Momentum relaxation from impurities

S.A. Hartnoll, P.K. Kovtun, M. Müller, and S. Sachdev, *Phys. Rev.* B **76** 144502 (2007)

From these relations, we obtained results for the transport co-efficients expressed in terms of a "cyclotron" frequency and damping:

$$\omega_c = \frac{2eB\rho v^2}{c(\varepsilon + P)} \quad , \quad \gamma = \frac{B^2 v^2}{c^2(\varepsilon + P)}$$

Transverse thermoelectric co-efficient

$$\left(\frac{h}{2ek_B}\right)\alpha_{xy} = \Phi_s \overline{B}\,(k_B T)^2 \left(\frac{2\pi\tau_{\rm imp}}{\hbar}\right)^2 \frac{\overline{\rho}^2 + \Phi_\sigma \Phi_{\varepsilon+P}(k_B T)^3\,\hbar/2\pi\tau_{\rm imp}}{\Phi_{\varepsilon+P}^2 (k_B T)^6 + \overline{B}^2 \overline{\rho}^2 (2\pi\tau_{\rm imp}/\hbar)^2}$$

where

$$B = \overline{B}\phi_0/(\hbar v)^2 \quad ; \quad \rho = \overline{\rho}/(\hbar v)^2.$$

S.A. Hartnoll, P.K. Kovtun, M. Müller, and S. Sachdev, *Phys. Rev.* B **76** 144502 (2007)

Lorentz invariance and positivity of entropy production lead to the hydrodynamic equations of motion and constitutive relations:

$$
\begin{aligned}
\partial_\mu J^\mu &= 0 \\
\partial_\mu T^{\mu\nu} &= F^{\mu\nu} J_\nu + \frac{1}{\tau_{\text{imp}}} \left(\delta^\mu_\nu + u^\mu u_\nu\right) T^{\nu\gamma} u_\gamma \\
T^{\mu\nu} &= (\varepsilon + P) u^\mu u^\nu + P g^{\mu\nu} \\
J^\mu &= \rho u^\mu + \sigma_Q (g^{\mu\nu} + u^\mu u^\nu) \left[\left(-\partial_\nu \mu + F_{\nu\lambda} u^\lambda\right) + \mu \frac{\partial_\mu T}{T} \right]
\end{aligned}
$$

Momentum relaxation from impurities

S.A. Hartnoll, P.K. Kovtun, M. Müller, and S. Sachdev, *Phys. Rev.* B **76** 144502 (2007)

Lorentz invariance and positivity of entropy production lead to the hydrodynamic equations of motion and constitutive relations:

$$\begin{aligned} \partial_\mu J^\mu &= 0 \\ \partial_\mu T^{\mu\nu} &= F^{\mu\nu} J_\nu \\ T^{\mu\nu} &= (\varepsilon + P) u^\mu u^\nu + P g^{\mu\nu} \\ J^\mu &= \rho u^\mu + \sigma_Q (g^{\mu\nu} + u^\mu u^\nu) \left[(-\partial_\nu \mu + F_{\nu\lambda} u^\lambda) + \mu \frac{\partial_\mu T}{T} \right] \end{aligned}$$

Single dissipative term allowed by requirement of positive entropy production. There is only one independent transport co-efficient

S.A. Hartnoll, P.K. Kovtun, M. Müller, and S. Sachdev, *Phys. Rev.* B **76** 144502 (2007)

Lorentz invariance and positivity of entropy production lead to the hydrodynamic equations of motion and constitutive relations:

$$\begin{aligned} \partial_\mu J^\mu &= 0 \\ \partial_\mu T^{\mu\nu} &= F^{\mu\nu} J_\nu \\ T^{\mu\nu} &= (\varepsilon + P) u^\mu u^\nu + P g^{\mu\nu} \\ J^\mu &= \rho u^\mu \end{aligned}$$

Constitutive relations which follow from Lorentz transformation to moving frame

S.A. Hartnoll, P.K. Kovtun, M. Müller, and S. Sachdev, *Phys. Rev.* B **76** 144502 (2007)

Lorentz invariance and positivity of entropy production lead to the hydrodynamic equations of motion and constitutive relations:

S.A. Hartnoll, P.K. Kovtun, M. Müller, and S. Sachdev, *Phys. Rev.* B **76** 144502 (2007)

Lorentz invariance and positivity of entropy production lead to the hydrodynamic equations of motion and constitutive relations:

$$\begin{aligned} \partial_\mu J^\mu &= 0 \\ \partial_\mu T^{\mu\nu} &= F^{\mu\nu} J_\nu \end{aligned}$$

Conservation laws/equations of motion

S.A. Hartnoll, P.K. Kovtun, M. Müller, and S. Sachdev, *Phys. Rev.* B **76** 144502 (2007)

Lorentz invariance and positivity of entropy production lead to the hydrodynamic equations of motion and constitutive relations:

$$\begin{aligned} \partial_\mu J^\mu &= 0 \\ \partial_\mu T^{\mu\nu} &= F^{\mu\nu} J_\nu \\ T^{\mu\nu} &= (\varepsilon + P) u^\mu u^\nu + P g^{\mu\nu} \\ J^\mu &= \rho u^\mu \end{aligned}$$

Constitutive relations which follow from Lorentz transformation to moving frame

S.A. Hartnoll, P.K. Kovtun, M. Müller, and S. Sachdev, *Phys. Rev.* B **76** 144502 (2007)

Lorentz invariance and positivity of entropy production lead to the hydrodynamic equations of motion and constitutive relations:

$$
\begin{aligned}
\partial_\mu J^\mu &= 0 \\
\partial_\mu T^{\mu\nu} &= F^{\mu\nu} J_\nu \\
T^{\mu\nu} &= (\varepsilon + P) u^\mu u^\nu + P g^{\mu\nu} \\
J^\mu &= \rho u^\mu + \sigma_Q (g^{\mu\nu} + u^\mu u^\nu) \left[(-\partial_\nu \mu + F_{\nu\lambda} u^\lambda) + \mu \frac{\partial_\mu T}{T} \right]
\end{aligned}
$$

Single dissipative term allowed by requirement of positive entropy production. There is only one independent transport co-efficient

S.A. Hartnoll, P.K. Kovtun, M. Müller, and S. Sachdev, *Phys. Rev.* B **76** 144502 (2007)

Lorentz invariance and positivity of entropy production lead to the hydrodynamic equations of motion and constitutive relations:

$$\begin{aligned}
\partial_\mu J^\mu &= 0 \\
\partial_\mu T^{\mu\nu} &= F^{\mu\nu} J_\nu + \frac{1}{\tau_{\rm imp}} (\delta^\mu_\nu + u^\mu u_\nu) T^{\nu\gamma} u_\gamma \\
T^{\mu\nu} &= (\varepsilon + P) u^\mu u^\nu + P g^{\mu\nu} \\
J^\mu &= \rho u^\mu + \sigma_Q (g^{\mu\nu} + u^\mu u^\nu) \left[(-\partial_\nu \mu + F_{\nu\lambda} u^\lambda) + \mu \frac{\partial_\mu T}{T} \right]
\end{aligned}$$

Momentum relaxation from impurities

S.A. Hartnoll, P.K. Kovtun, M. Müller, and S. Sachdev, *Phys. Rev.* B **76** 144502 (2007)

From these relations, we obtained results for the transport co-efficients expressed in terms of a "cyclotron" frequency and damping:

$$\omega_c = \frac{2eB\rho v^2}{c(\varepsilon + P)} \quad , \quad \gamma = \frac{B^2 v^2}{c^2(\varepsilon + P)}$$

Transverse thermoelectric co-efficient

$$\left(\frac{h}{2ek_B}\right)\alpha_{xy} = \Phi_s \overline{B} (k_B T)^2 \left(\frac{2\pi\tau_{\rm imp}}{\hbar}\right)^2 \frac{\overline{\rho}^2 + \Phi_\sigma \Phi_{\varepsilon+P} (k_B T)^3 \hbar/2\pi\tau_{\rm imp}}{\Phi^2_{\varepsilon+P}(k_B T)^6 + \overline{B}^2 \overline{\rho}^2 (2\pi\tau_{\rm imp}/\hbar)^2}$$

where

$$B = \overline{B}\phi_0/(\hbar v)^2 \quad ; \quad \rho = \overline{\rho}/(\hbar v)^2.$$

S.A. Hartnoll, P.K. Kovtun, M. Müller, and S. Sachdev, *Phys. Rev.* B **76** 144502 (2007)

LSCO Experiments

Measurement of $\alpha_{xy} \approx \sigma_{xx} e_N$

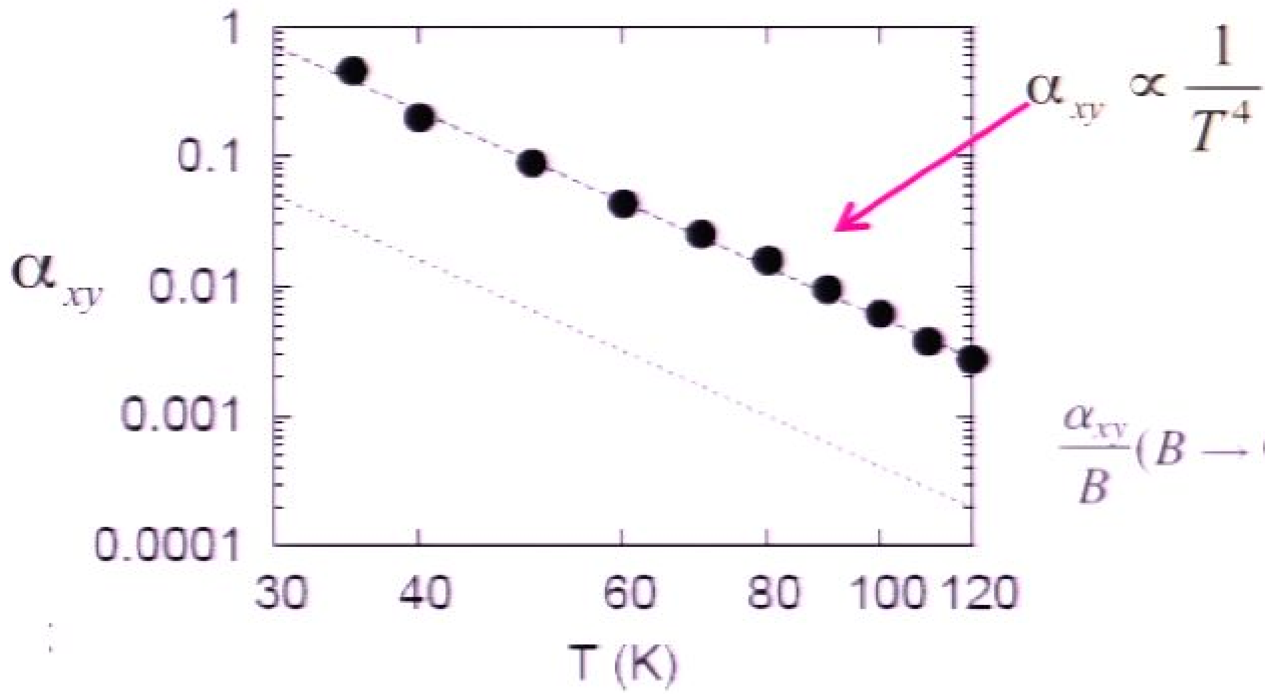

Y. Wang et al., Phys. Rev. B 73, 024510 (2006).

$$\alpha_{xy} \propto \frac{BT^2\left(\#\rho^2\tau_{imp} + \#T^3\right)}{T^6 + \#B^2\rho^2\tau_{imp}^2}$$

(T small)

$$\frac{\alpha_{xy}}{B}(B \to 0) \approx \left(\frac{2ek_B}{h\phi_0}\right)\frac{\Phi_s}{\Phi_{\varepsilon+P}^2}\left(\frac{2\pi\tau_{\rm imp}}{\hbar}\right)^2\frac{\rho^2(\hbar v)}{(k_BT)^4}$$

From these relations, we obtained results for the transport co-efficients expressed in terms of a "cyclotron" frequency and damping:

$$\omega_c = \frac{2eB\rho v^2}{c(\varepsilon + P)} \quad , \quad \gamma = \frac{B^2 v^2}{c^2(\varepsilon + P)}$$

Transverse thermoelectric co-efficient

$$\left(\frac{h}{2ek_B}\right)\alpha_{xy} = \Phi_s \overline{B}\,(k_B T)^2 \left(\frac{2\pi\tau_{\rm imp}}{\hbar}\right)^2 \frac{\overline{\rho}^2 + \Phi_\sigma \Phi_{\varepsilon+P}(k_B T)^3\,\hbar/2\pi\tau_{\rm imp}}{\Phi^2_{\varepsilon+P}(k_B T)^6 + \overline{B}^2\overline{\rho}^2(2\pi\tau_{\rm imp}/\hbar)^2}$$

where

$$B = \overline{B}\phi_0/(\hbar v)^2 \quad ; \quad \rho = \overline{\rho}/(\hbar v)^2.$$

S.A. Hartnoll, P.K. Kovtun, M. Müller, and S. Sachdev, *Phys. Rev.* B **76** 144502 (2007)

LSCO Experiments

Measurement of $\alpha_{xy} \approx \sigma_{xx} e_N$

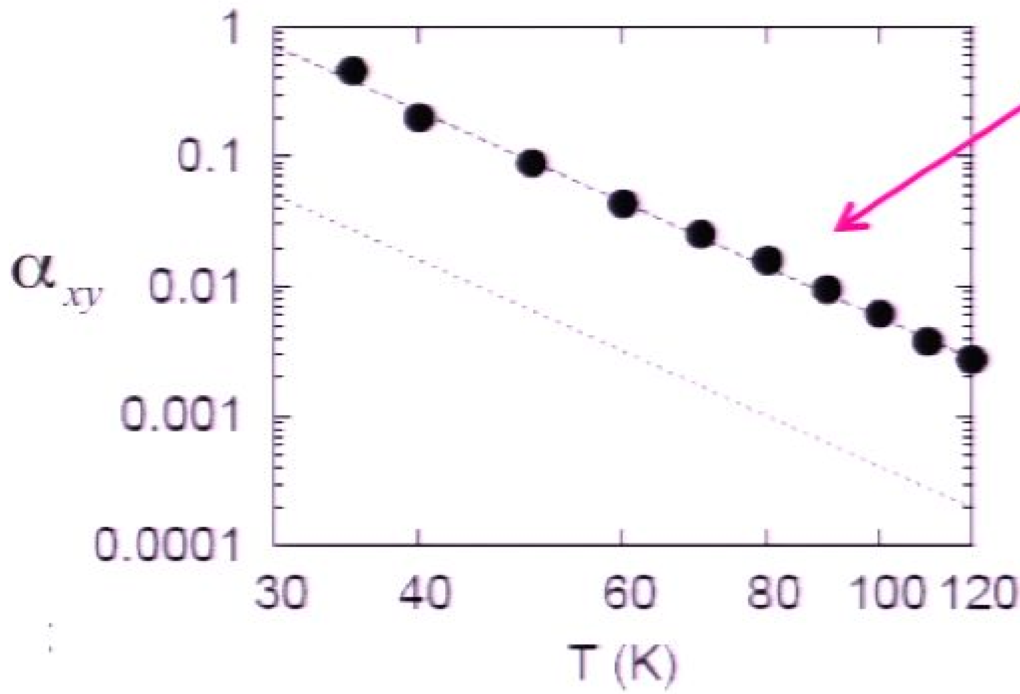

$$\alpha_{xy} \propto \frac{1}{T^4}$$

$$\alpha_{xy} \propto \frac{BT^2\left(\#\rho^2\tau_{imp} + \#T^3\right)}{T^6 + \#B^2\rho^2\tau_{imp}^2}$$

(T small)

$$\frac{\alpha_{xy}}{B}(B \to 0) \approx \left(\frac{2ek_B}{h\phi_0}\right)\frac{\Phi_s}{\Phi_{\varepsilon+P}^2}\left(\frac{2\pi\tau_{\text{imp}}}{\hbar}\right)^2 \frac{\rho^2(\hbar v)}{(k_B T)^4}$$

Y. Wang et al., Phys. Rev. B ***73****, 024510 (2006).*

LSCO Experiments

Measurement of $\alpha_{xy} \approx \sigma_{xx} e_N$

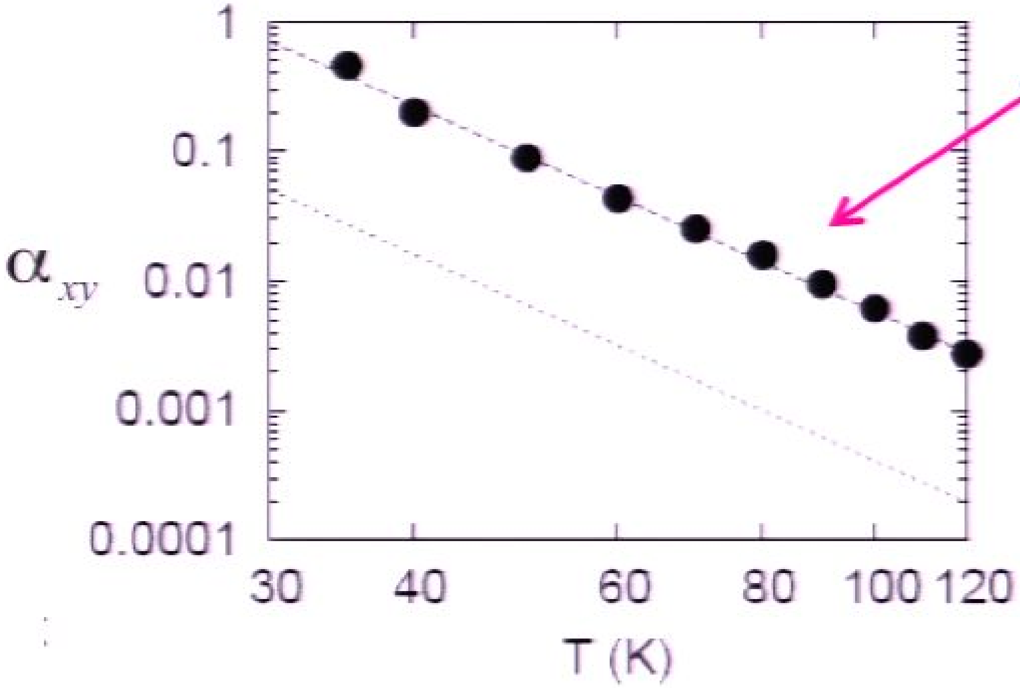

Y. Wang et al., Phys. Rev. B **73**, 024510 (2006).

$$\alpha_{xy} \propto \frac{1}{T^4}$$

$$\alpha_{xy} \propto \frac{BT^2\left(\#\rho^2\tau_{imp} + \#T^3\right)}{T^6 + \#B^2\rho^2\tau_{imp}^2}$$

(T small)

$$\frac{\alpha_{xy}}{B}(B \to 0) \approx \left(\frac{2ek_B}{h\phi_0}\right)\frac{\Phi_s}{\Phi^2_{\varepsilon+P}}\left(\frac{2\pi\tau_{\rm imp}}{\hbar}\right)^2\frac{\rho^2(\hbar v)}{(k_BT)^4}$$

$\hbar v \approx 47 \text{meV Å}$

$v \approx 2.5 \times 10^{-5} c$

$\tau_{imp} \approx 10^{-12}\text{s}$

LSCO Experiments

Measurement of $\alpha_{xy} \approx \sigma_{xx} e_N$

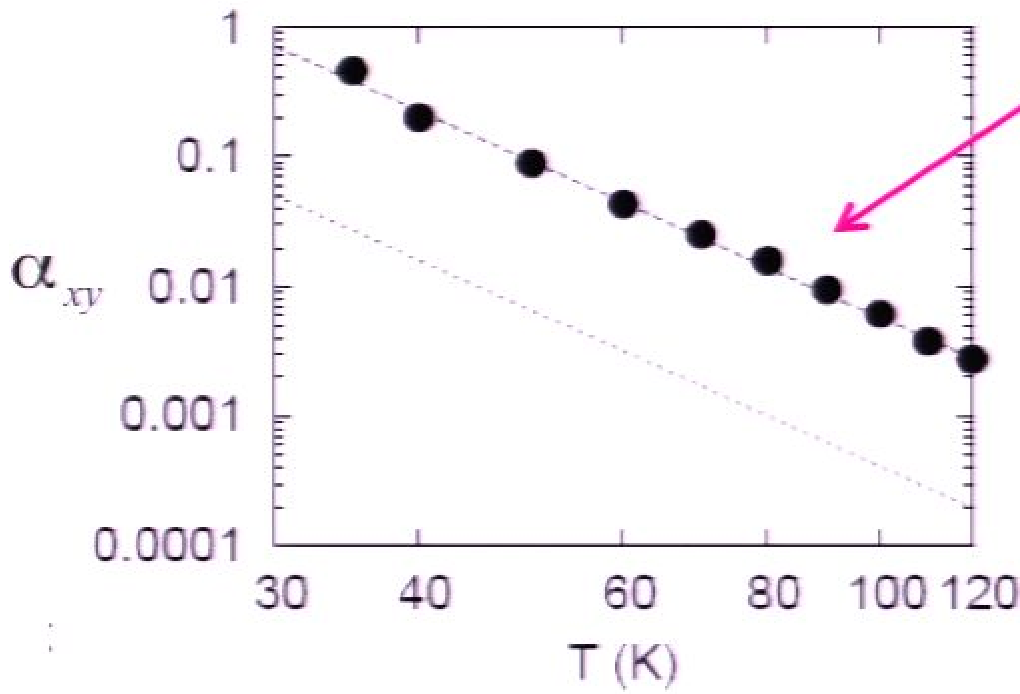

$\alpha_{xy} \propto \frac{1}{T^4}$

$$\alpha_{xy} \propto \frac{BT^2\left(\#\rho^2\tau_{imp} + \#T^3\right)}{T^6 + \#B^2\rho^2\tau_{imp}^2}$$

(T small)

$$\frac{\alpha_{xy}}{B}(B \to 0) \approx \left(\frac{2ek_B}{h\phi_0}\right)\frac{\Phi_s}{\Phi_{\varepsilon+P}^2}\left(\frac{2\pi\tau_{\text{imp}}}{\hbar}\right)^2\frac{\rho^2(\hbar v)}{(k_B T)^4}$$

$\hbar v \approx 47\,\text{meV}\,\mathring{A}$

$v \approx 2.5 \times 10^{-5}\, c$

$\tau_{imp} \approx 10^{-12}\,\text{s}$

Y. Wang et al., Phys. Rev. B ***73****, 024510 (2006).*

→ Prediction for ω_c:

$$\omega_c = 6.2\ \text{GHz}\frac{B}{1\ \text{T}}\left(\frac{35\ \text{K}}{T}\right)^3$$

- T-dependent cyclotron frequency!
- 0.035 times smaller than the cyclotron frequency of free electrons (at T=35 K)
- Only observable in ultra-pure samples where $\tau_{imp}^{-1} \leq \omega_c$

LSCO Experiments

B, T-dependence

Theory for $\alpha_{xy} \approx \sigma_{xx} N$

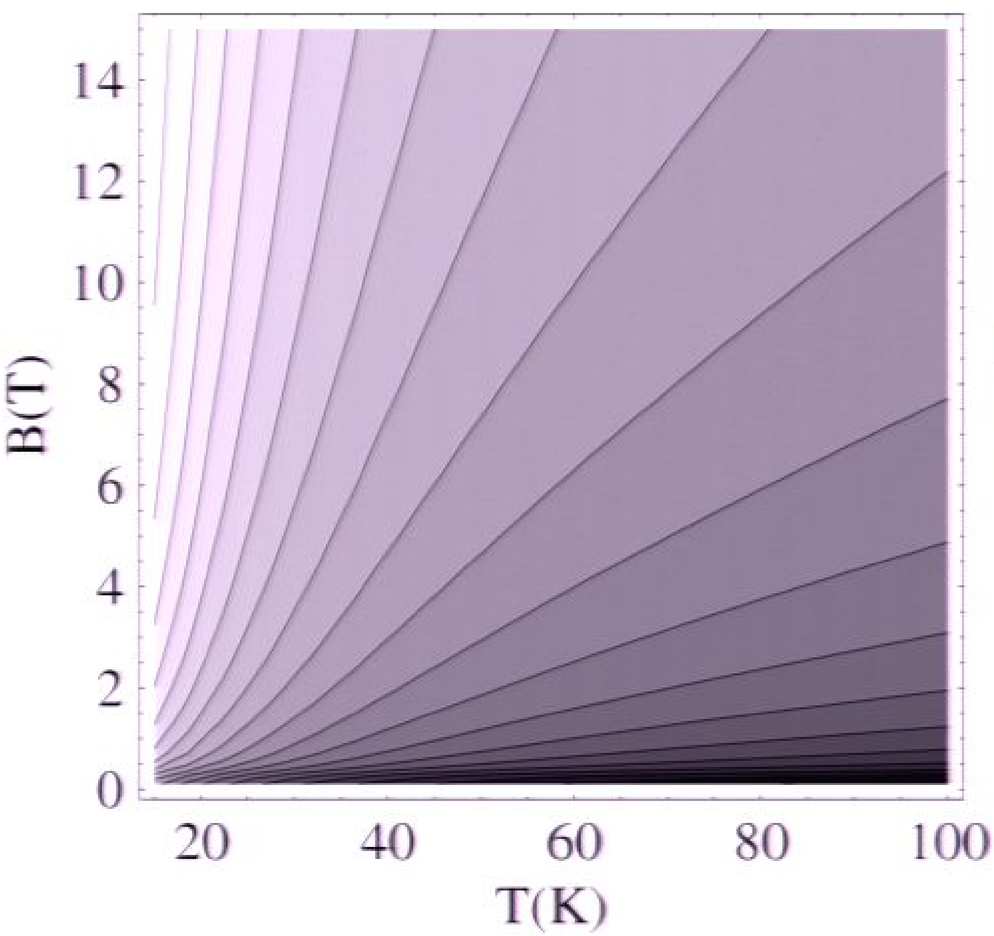

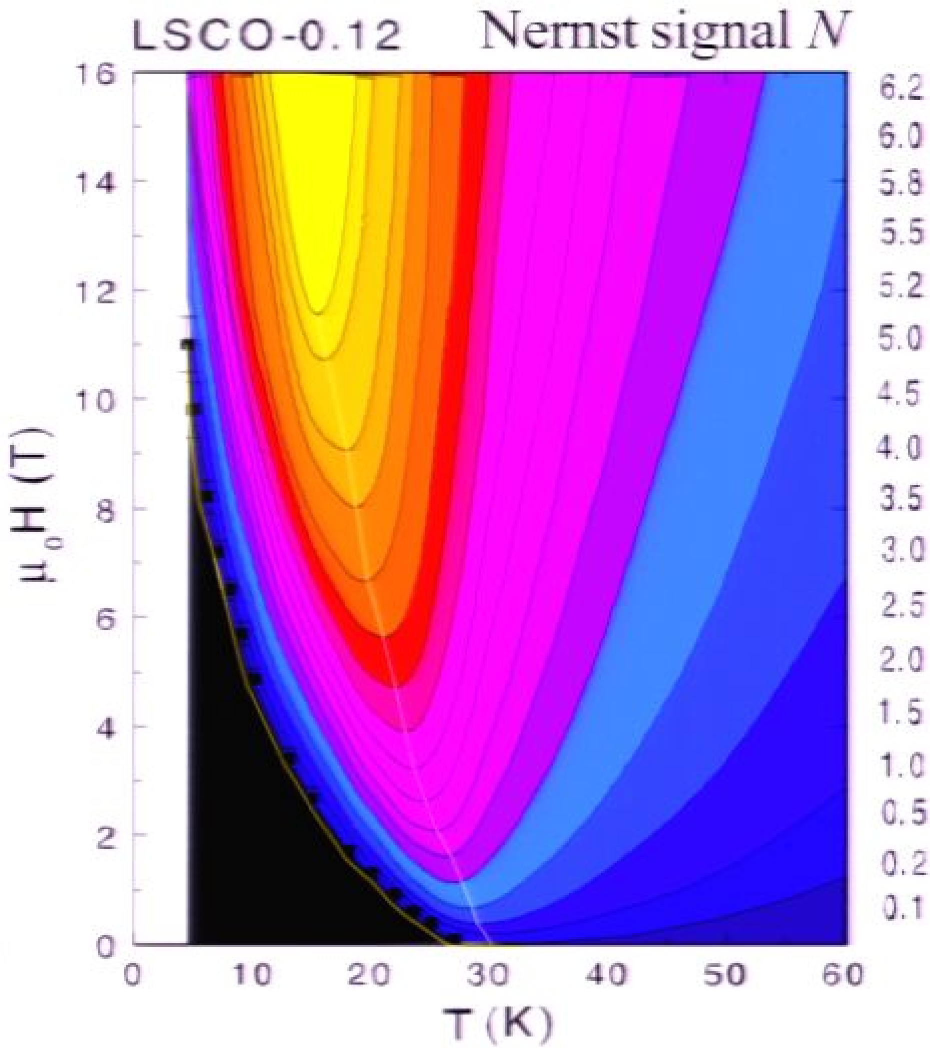

Y. Wang, L. Li, and N. P. Ong, Phys. Rev. B **73***, 024510 (2006).*

LSCO Experiments

Measurement of $\alpha_{xy} \approx \sigma_{xx} e_N$

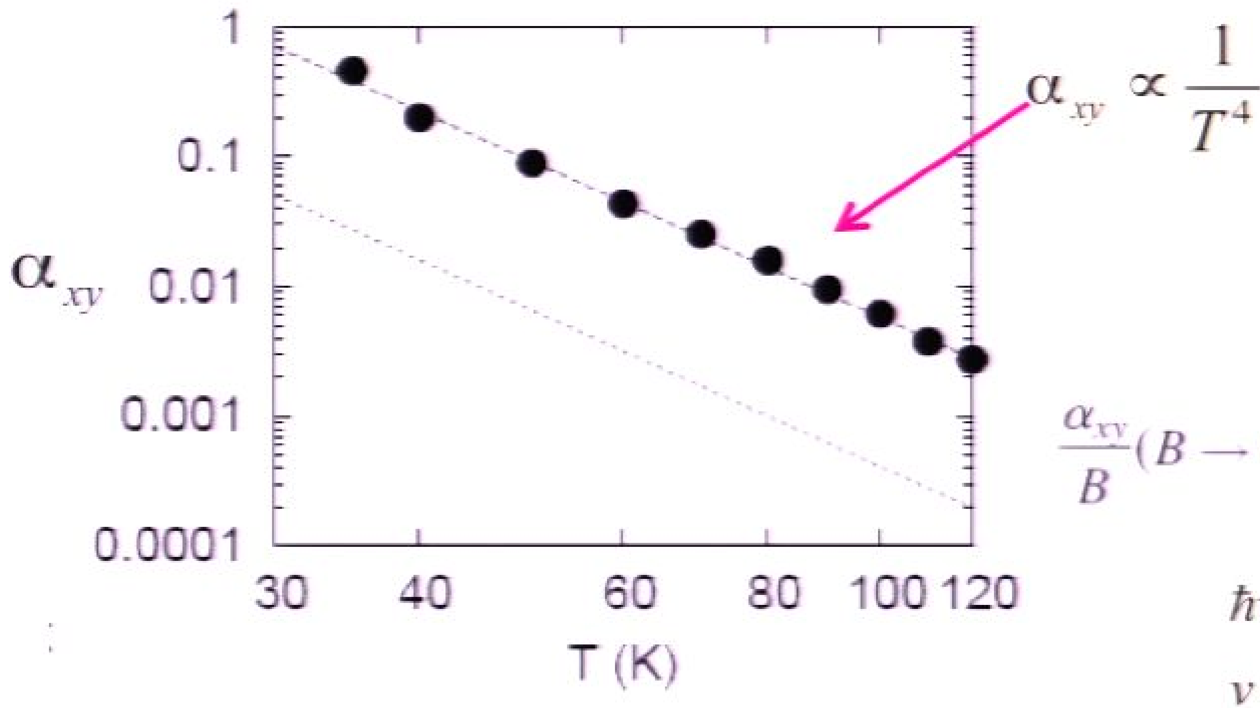

Y. Wang et al., Phys. Rev. B 73, 024510 (2006).

$$\alpha_{xy} \propto \frac{BT^2\left(\#\rho^2\tau_{imp} + \#T^3\right)}{T^6 + \#B^2\rho^2\tau_{imp}^2}$$

(T small)

$$\frac{\alpha_{xy}}{B}(B \to 0) \approx \left(\frac{2ek_B}{h\phi_0}\right)\frac{\Phi_s}{\Phi_{\varepsilon+P}^2}\left(\frac{2\pi\tau_{\rm imp}}{\hbar}\right)^2 \frac{\rho^2(\hbar v)}{(k_B T)^4}$$

$\hbar v \approx 47 \text{meV Å}$

$v \approx 2.5 \times 10^{-5} c$

$\tau_{imp} \approx 10^{-12} \text{s}$

→ Prediction for ω_c:

$$\omega_c = 6.2 \text{ GHz} \frac{B}{1 \text{ T}} \left(\frac{35 \text{ K}}{T}\right)^3$$

- T-dependent cyclotron frequency!
- 0.035 times smaller than the cyclotron frequency of free electrons (at T=35 K)
- Only observable in ultra-pure samples where $\tau_{imp}^{-1} \leq \omega_c$.

LSCO Experiments

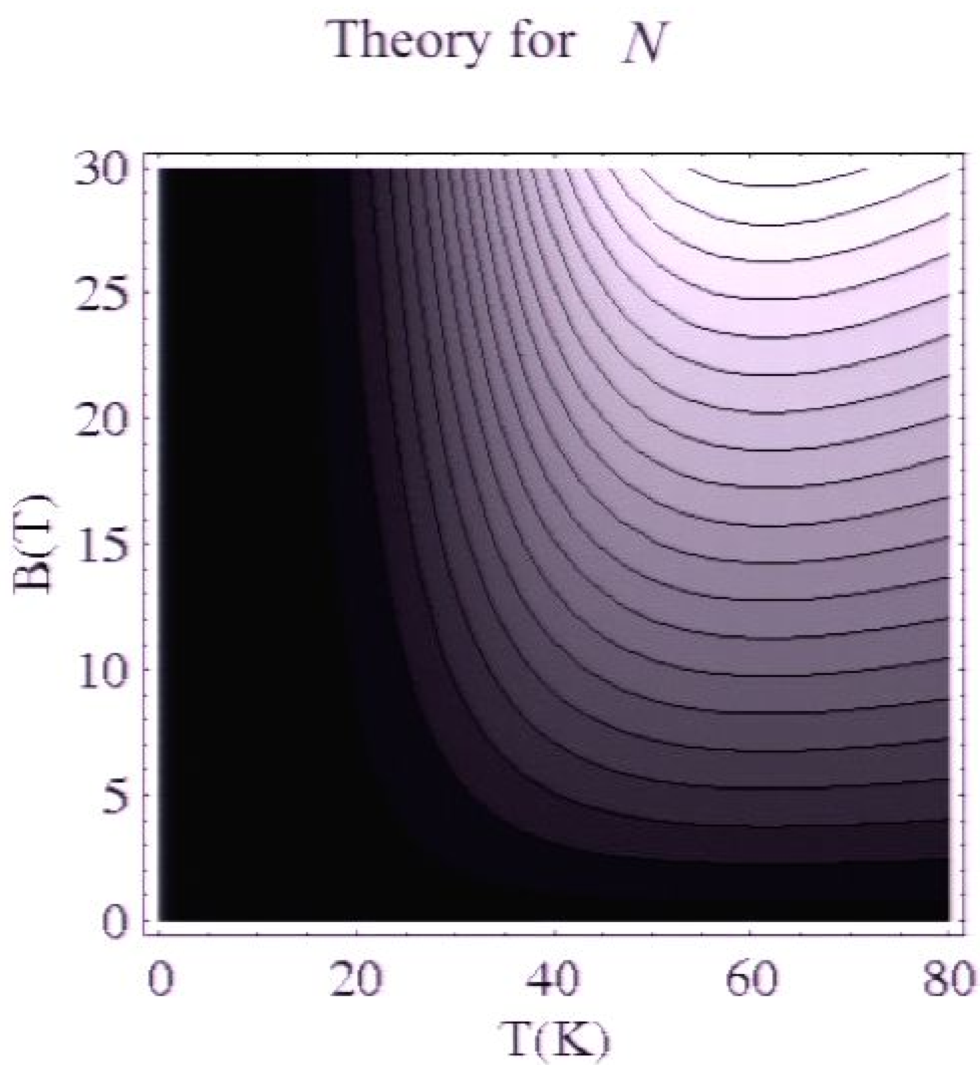

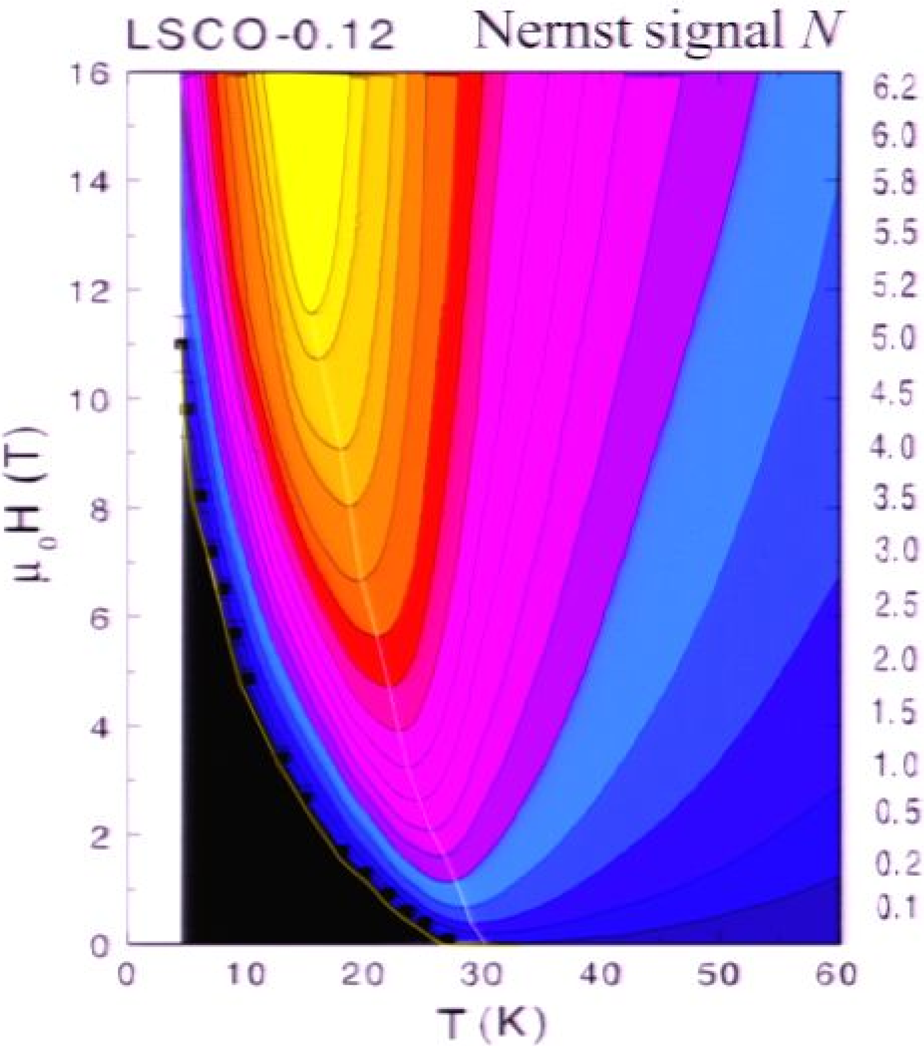

Y. Wang, L. Li, and N. P. Ong, Phys. Rev. B **73**, *024510 (2006).*

LSCO Experiments

Measurement of $\alpha_{xy} \approx \sigma_{xx} e_N$

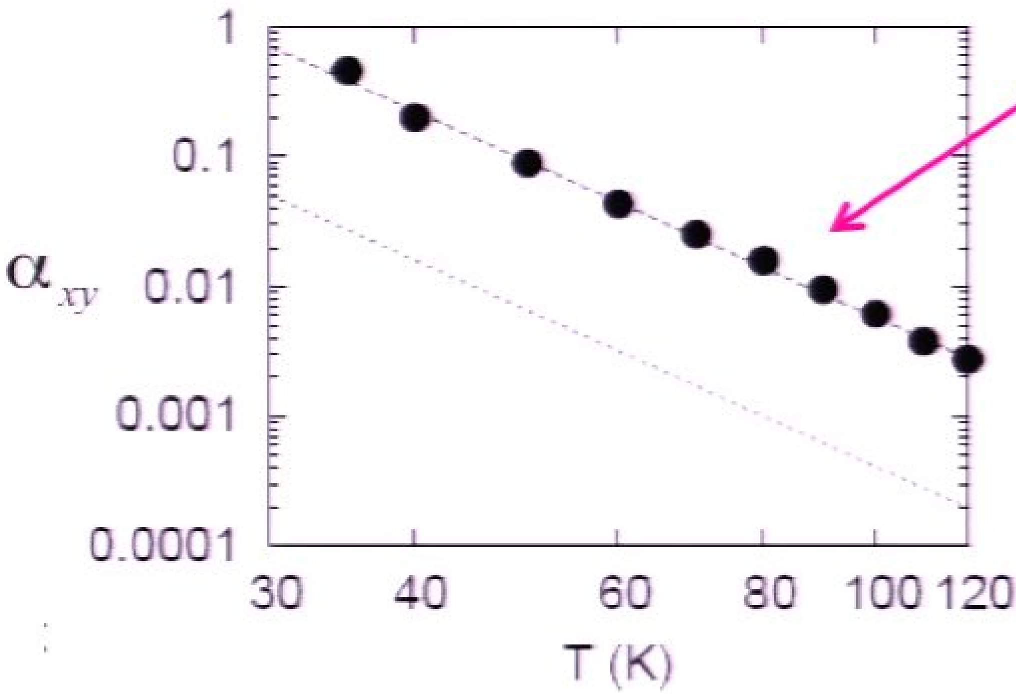

$\alpha_{xy} \propto \frac{1}{T^4}$

$$\alpha_{xy} \propto \frac{BT^2\left(\#\rho^2\tau_{imp} + \#T^3\right)}{T^6 + \#B^2\rho^2\tau_{imp}^2}$$

(T small)

$$\frac{\alpha_{xy}}{B}(B \to 0) \approx \left(\frac{2ek_B}{h\phi_0}\right)\frac{\Phi_s}{\Phi_{\varepsilon+P}^2}\left(\frac{2\pi\tau_{\rm imp}}{\hbar}\right)^2\frac{\rho^2(\hbar v)}{(k_BT)^4}$$

$\hbar v \approx 47\,\text{meV}\,\mathring{A}$

$v \approx 2.5 \times 10^{-5}\,c$

$\tau_{imp} \approx 10^{-12}\,\text{s}$

Y. Wang et al., Phys. Rev. B ***73****, 024510 (2006).*

→ Prediction for ω_c:

$$\omega_c = 6.2\ \text{GHz}\frac{B}{1\ \text{T}}\left(\frac{35\ \text{K}}{T}\right)^3$$

- T-dependent cyclotron frequency!
- 0.035 times smaller than the cyclotron frequency of free electrons (at T=35 K)
- Only observable in ultra-pure samples where $\tau_{imp}^{-1} \leq \omega_c$

LSCO Experiments

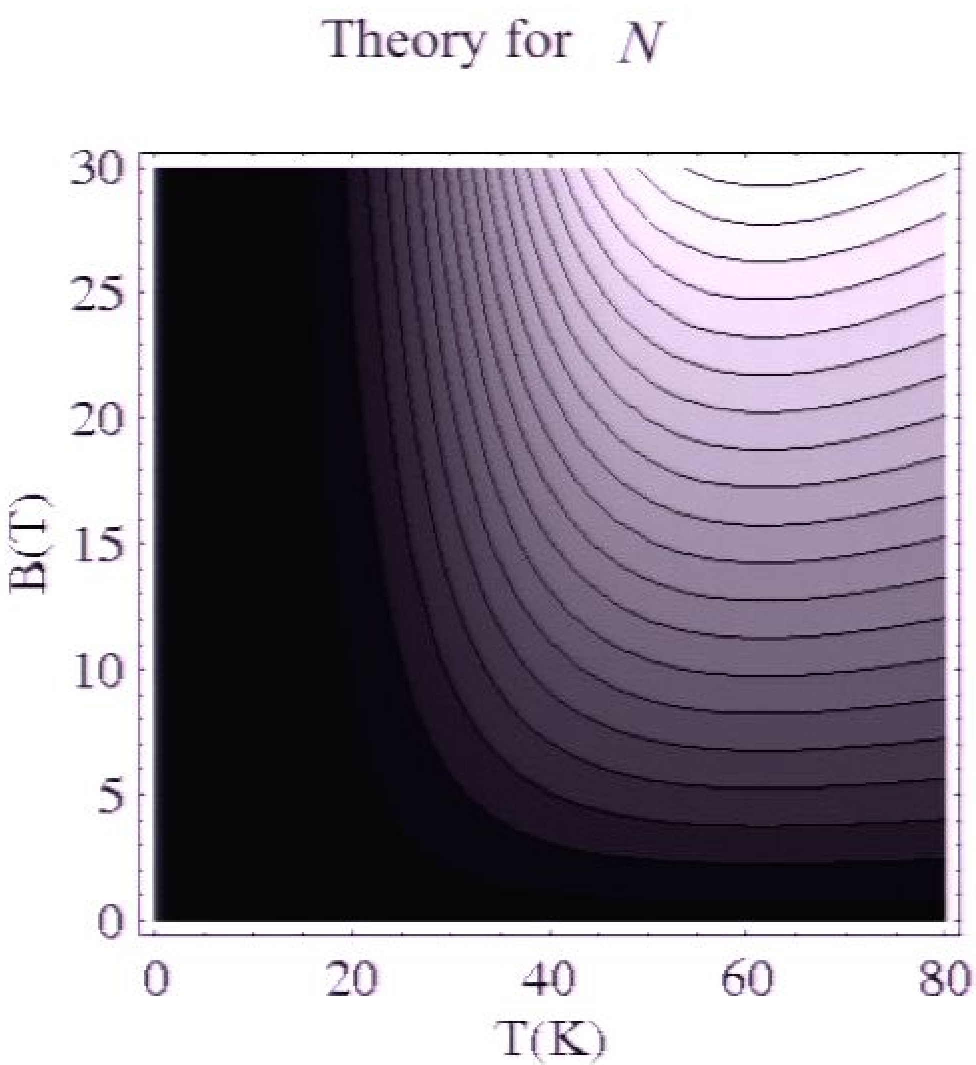

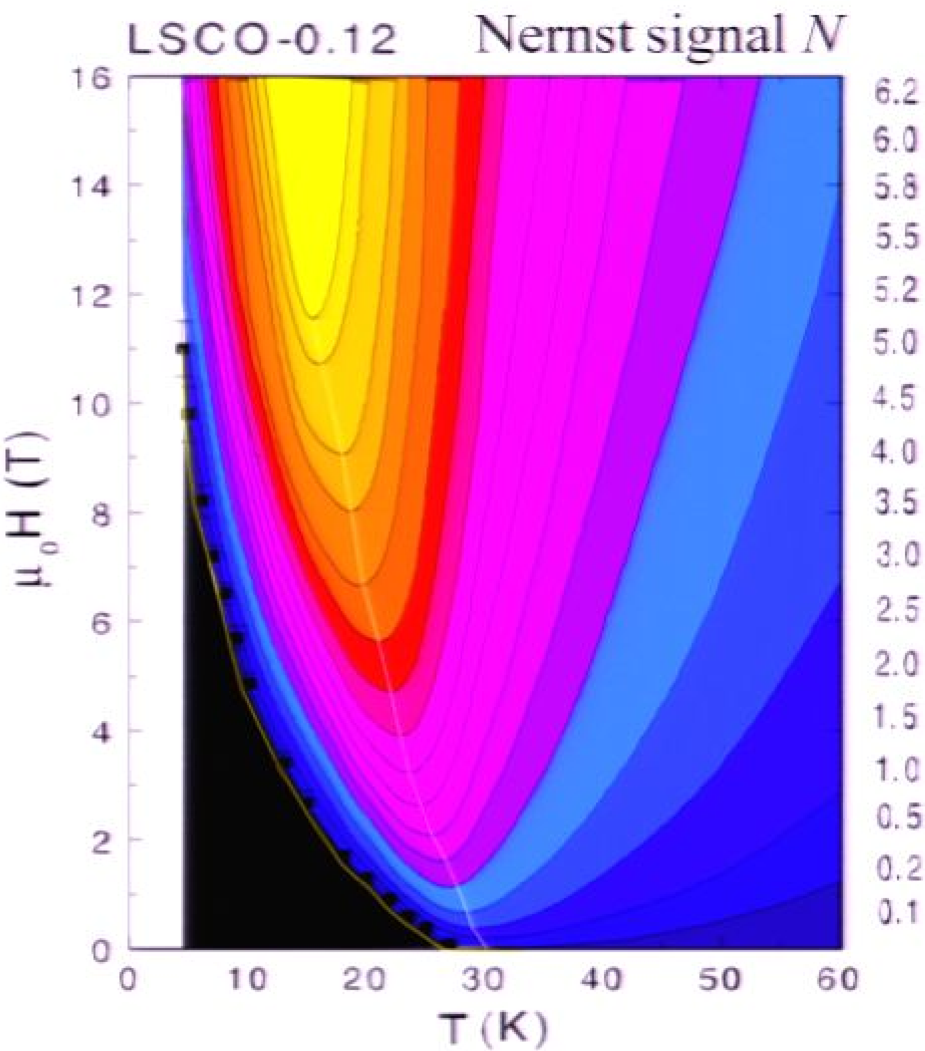

Y. Wang, L. Li, and N. P. Ong, Phys. Rev. B 73, 024510 (2006).

LSCO Experiments

Measurement of $\alpha_{xy} \approx \sigma_{xx} e_N$

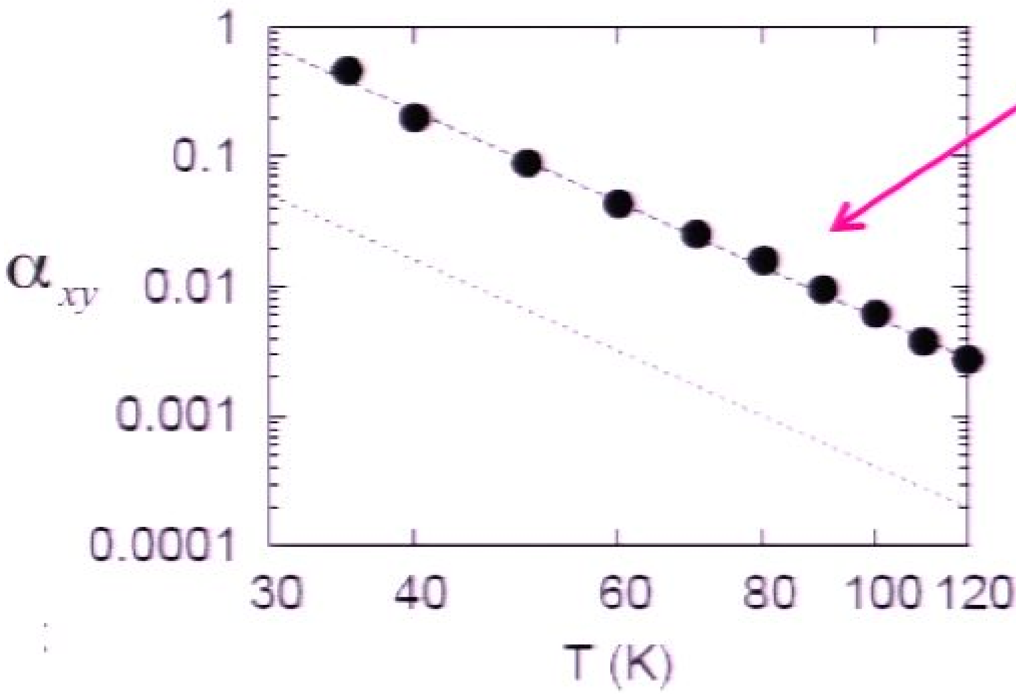

$\alpha_{xy} \propto \frac{1}{T^4}$

$$\alpha_{xy} \propto \frac{BT^2\left(\#\rho^2\tau_{imp} + \#T^3\right)}{T^6 + \#B^2\rho^2\tau_{imp}^2}$$

(T small)

$$\frac{\alpha_{xy}}{B}(B \to 0) \approx \left(\frac{2ek_B}{h\phi_0}\right)\frac{\Phi_s}{\Phi_{\varepsilon+P}^2}\left(\frac{2\pi\tau_{\rm imp}}{\hbar}\right)^2\frac{\rho^2(\hbar v)}{(k_B T)^4}$$

$\hbar v \approx 47\,\text{meV}\,\text{Å}$

$v \approx 2.5 \times 10^{-5} c$

$\tau_{imp} \approx 10^{-12}\,\text{s}$

Y. Wang et al., Phys. Rev. B ***73***, *024510 (2006).*

→ Prediction for ω_c:

$$\omega_c = 6.2\ \text{GHz}\frac{B}{1\ \text{T}}\left(\frac{35\ \text{K}}{T}\right)^3$$

- T-dependent cyclotron frequency!
- 0.035 times smaller than the cyclotron frequency of free electrons (at T=35 K)
- Only observable in ultra-pure samples where $\tau_{imp}^{-1} \le \omega_c$

LSCO Experiments

B, T-dependence

Theory for $\alpha_{xy} \approx \sigma_{xx} N$

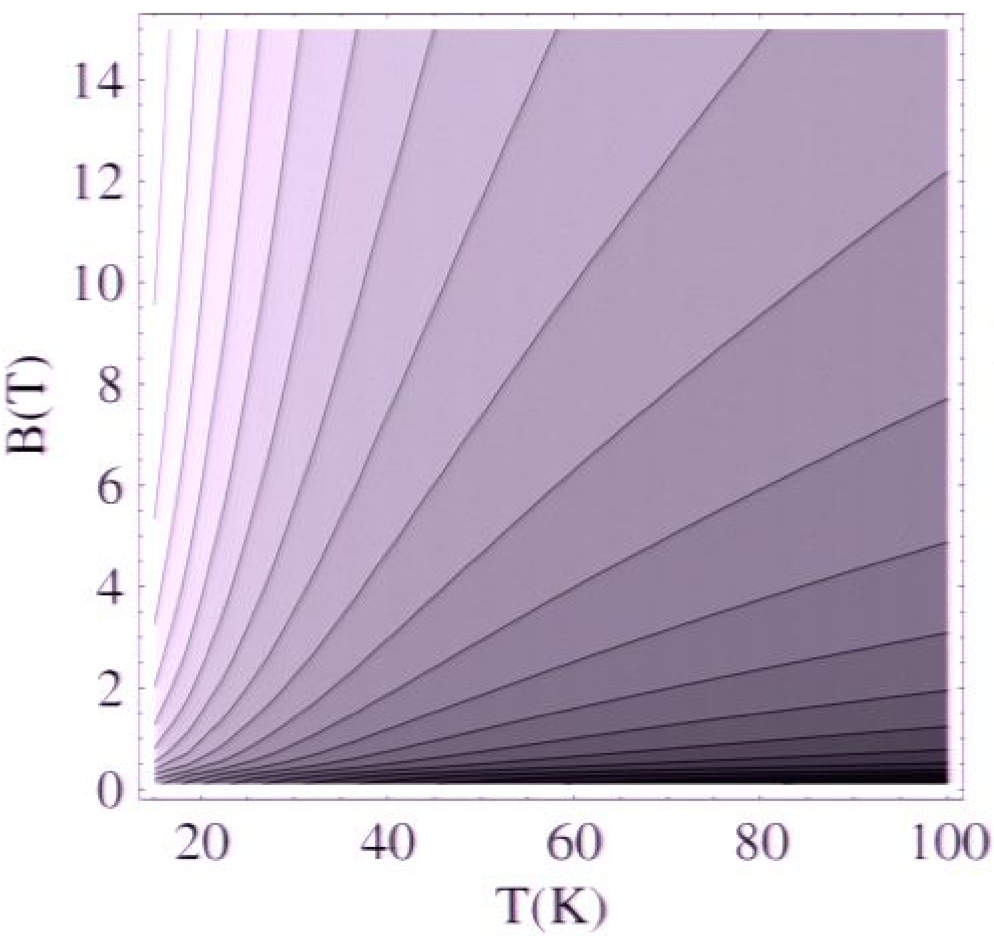

LSCO-0.12 Nernst signal N

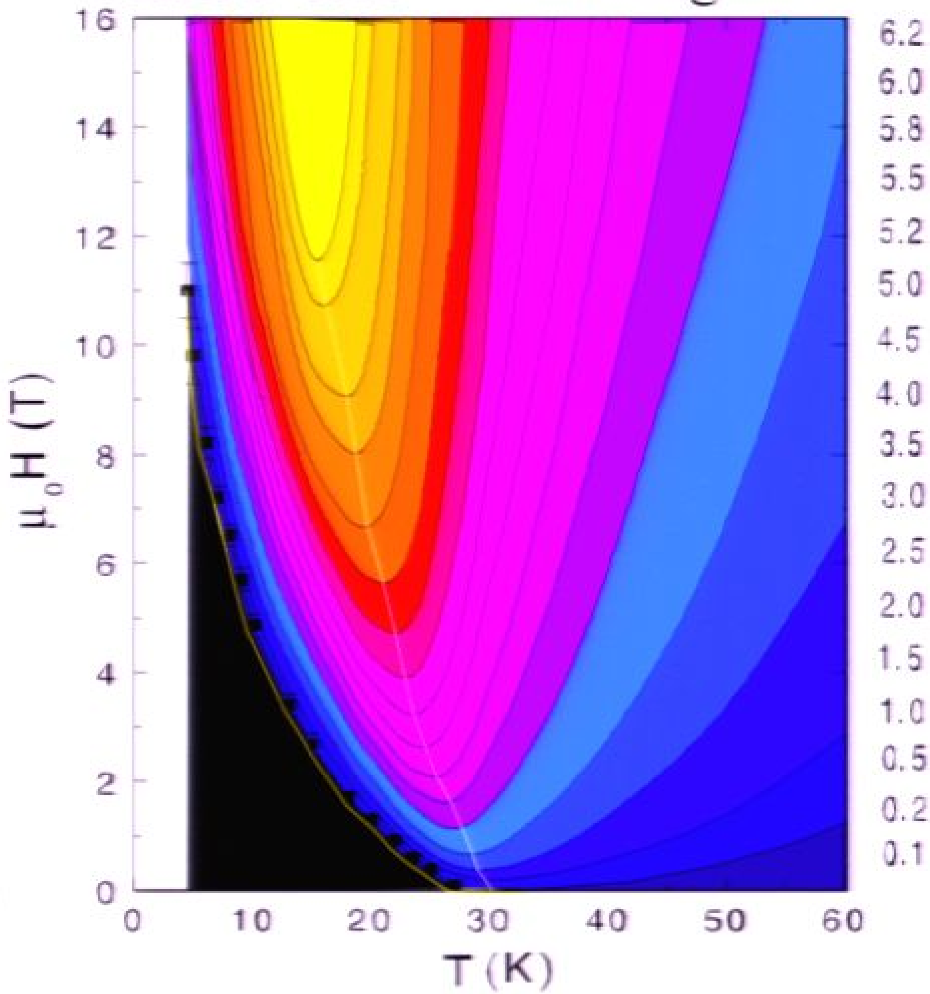

Y. Wang, L. Li, and N. P. Ong, Phys. Rev. B ***73****, 024510 (2006).*

LSCO Experiments

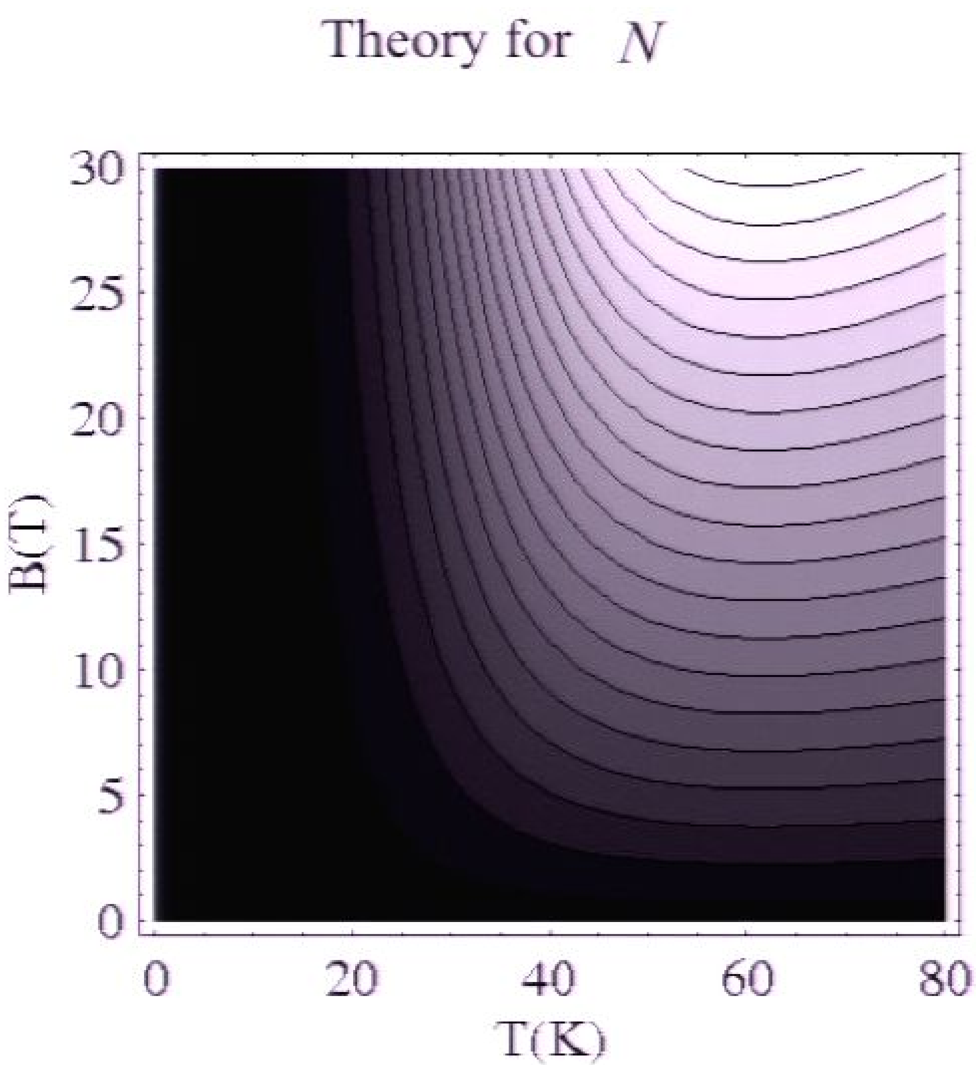

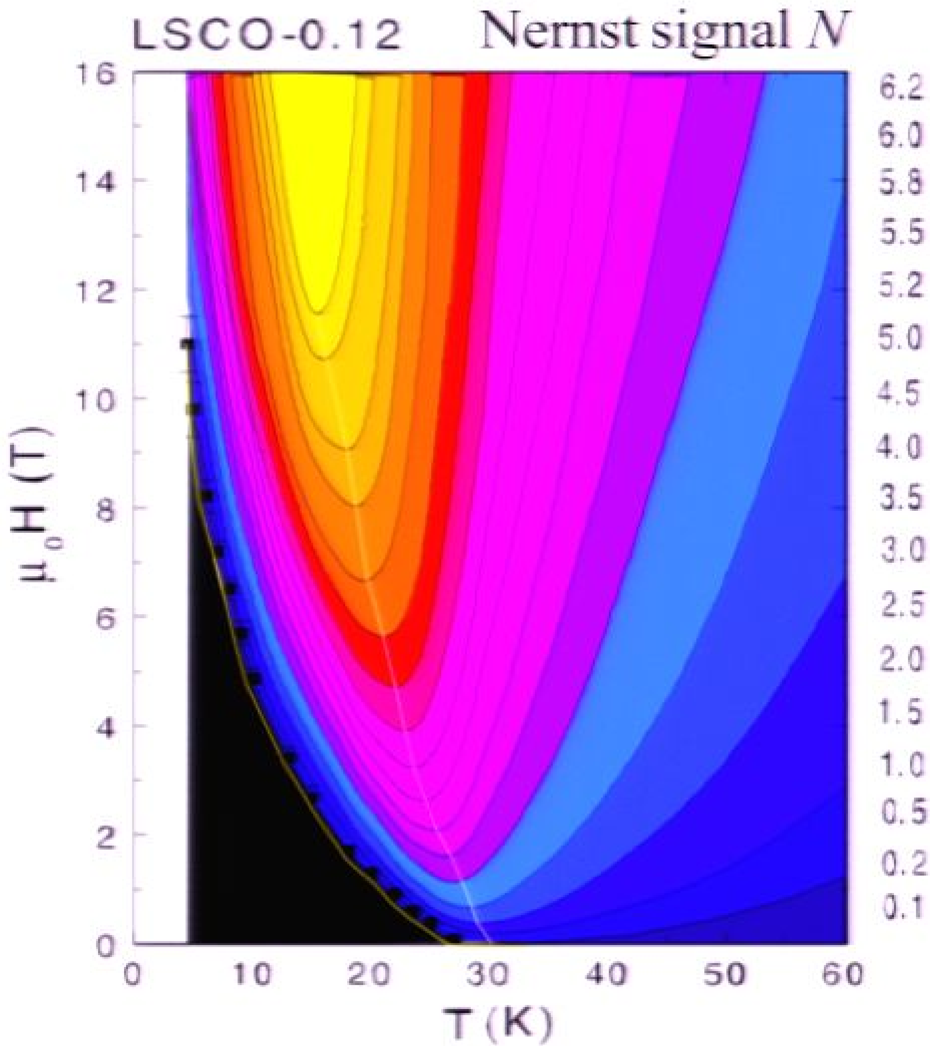

Y. Wang, L. Li, and N. P. Ong, Phys. Rev. B 73, 024510 (2006).

LSCO Experiments

B, T-dependence

Theory for $\alpha_{xy} \approx \sigma_{xx} N$

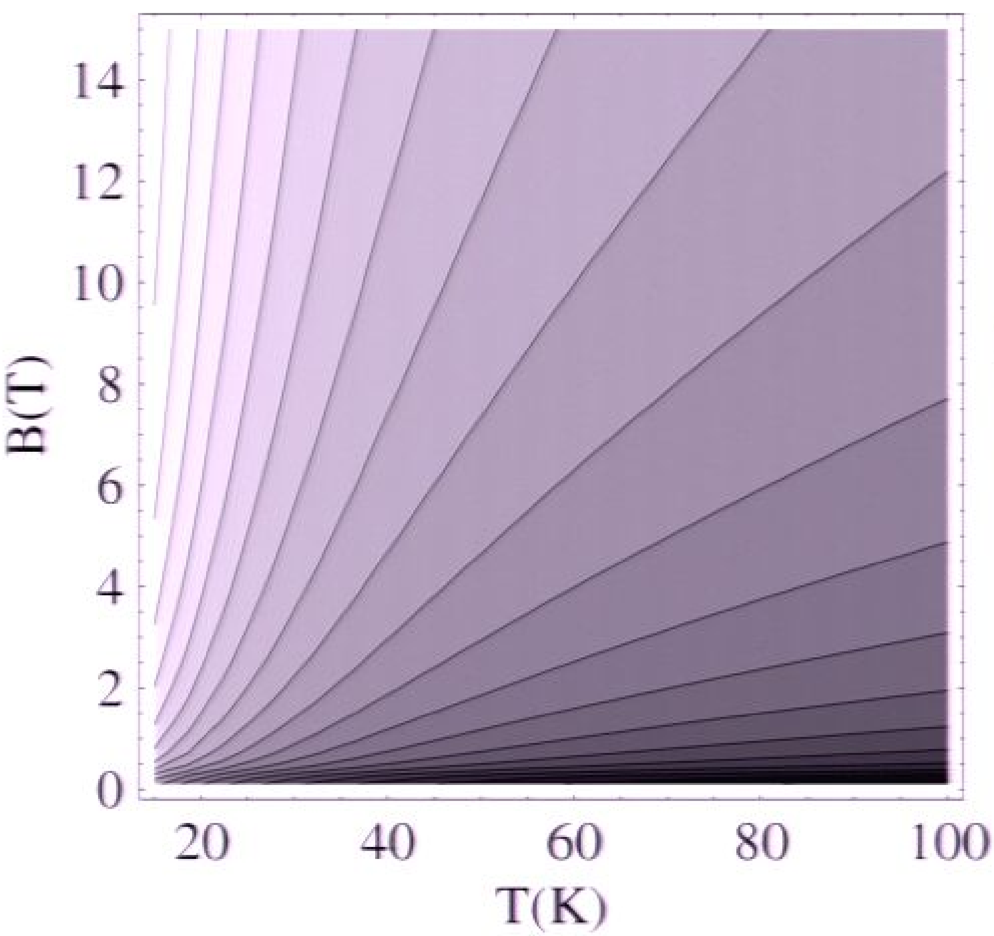

LSCO-0.12 Nernst signal N

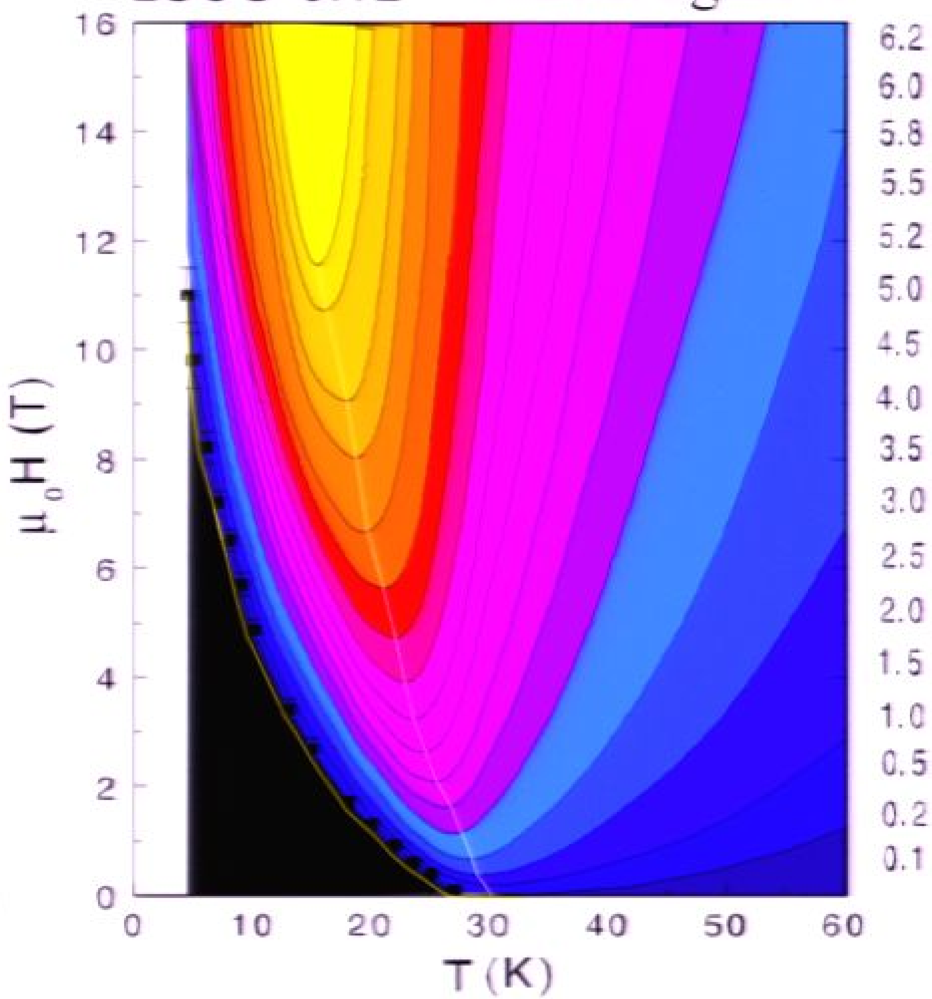

Y. Wang, L. Li, and N. P. Ong, Phys. Rev. B **73**, 024510 (2006).

LSCO Experiments

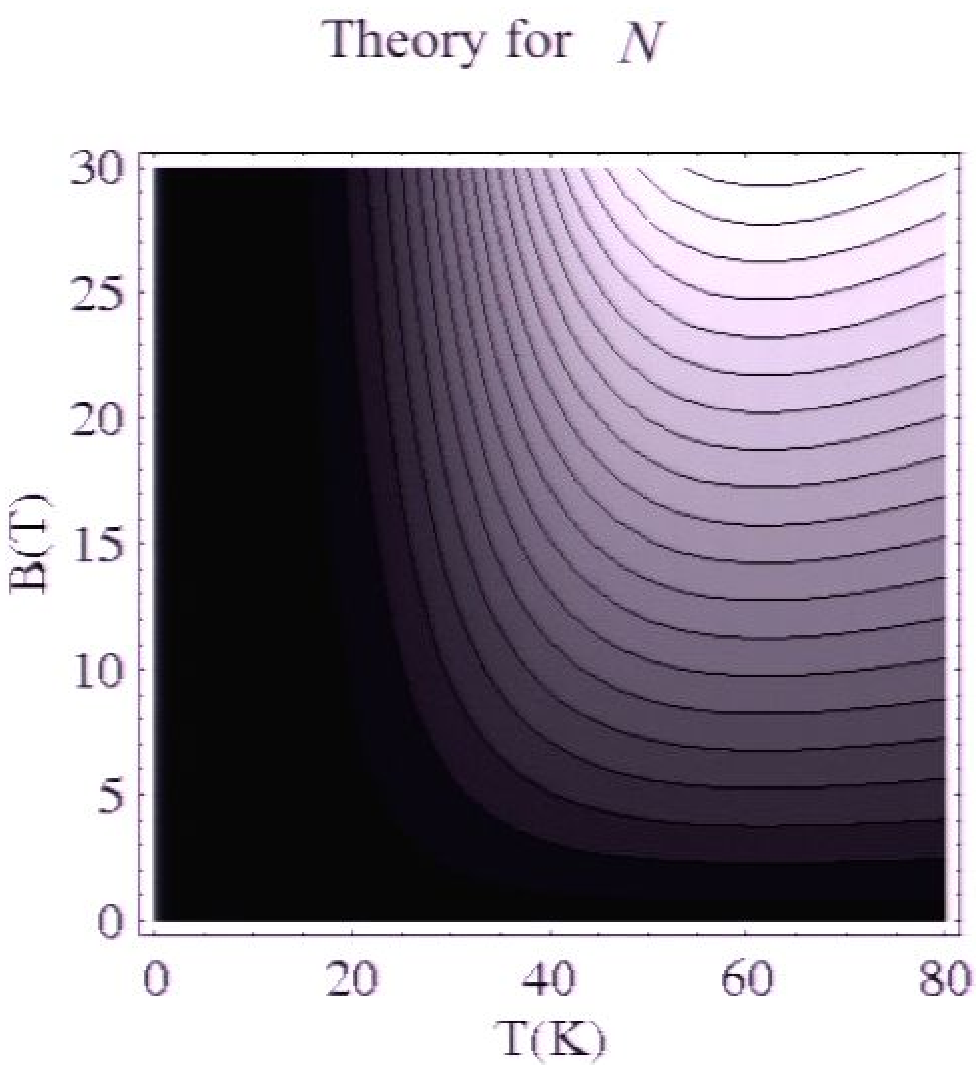

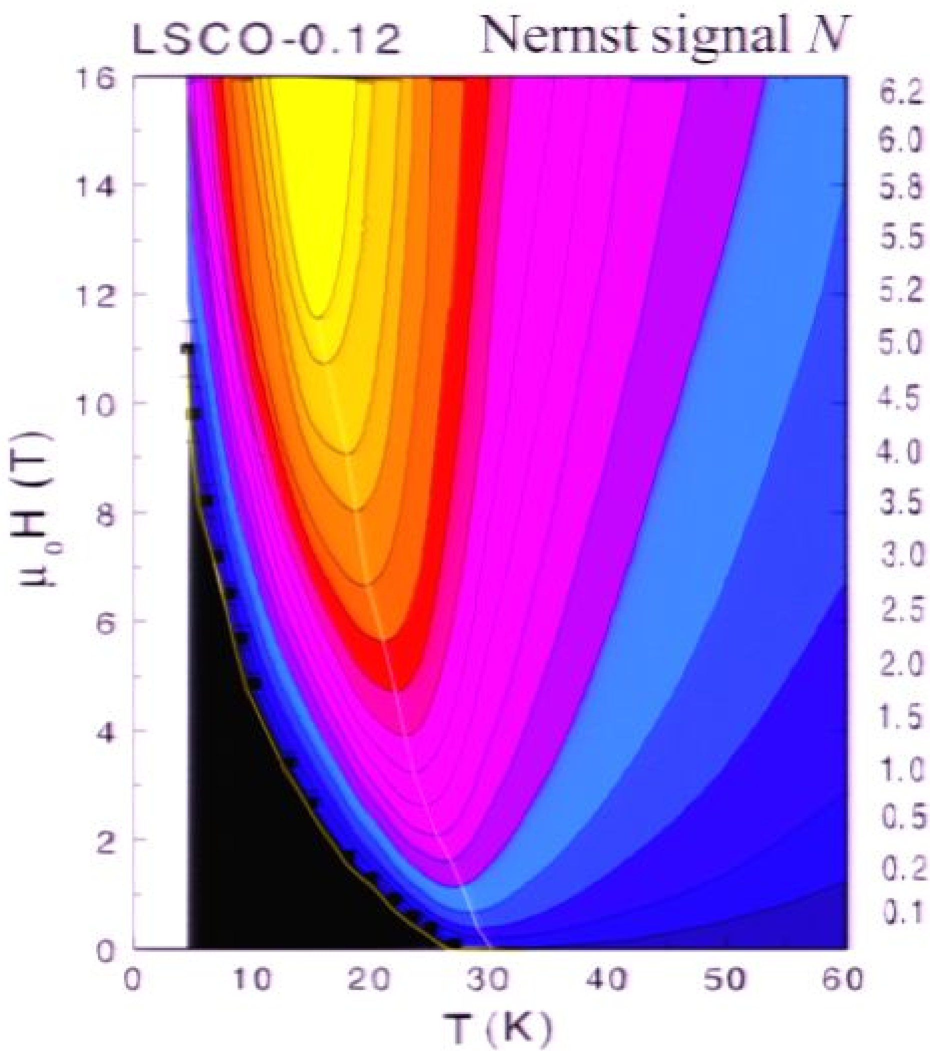

Y. Wang, L. Li, and N. P. Ong, Phys. Rev. B 73, 024510 (2006).

To the CFT of the quantum critical point, we add

- A chemical potential μ
- A magnetic field B

After the AdS/CFT mapping, we obtain the Einstein-Maxwell theory of a black hole with

- An electric charge
- A magnetic charge

A precise correspondence is found between general hydrodynamics of vortices near quantum critical points and solvable models of black holes with electric and magnetic charges

S.A. Hartnoll, P.K. Kovtun, M. Müller, and S. Sachdev, Phys. Rev. B (2007)

Outline

1. Entanglement of spins
   Experiments on antiferromagnetic insulators

2. Black Hole Thermodynamics
   Connections to quantum criticality

3. Nernst effect in the cuprate superconductors
   Quantum criticality and dyonic black holes

4. Quantum criticality in graphene
   Hydrodynamic cyclotron resonance and Nernst effect

Outline

1. Entanglement of spins
   Experiments on antiferromagnetic insulators

2. Black Hole Thermodynamics
   Connections to quantum criticality

3. Nernst effect in the cuprate superconductors
   Quantum criticality and dyonic black holes

4. Quantum criticality in graphene
   Hydrodynamic cyclotron resonance and Nernst effect

Graphene

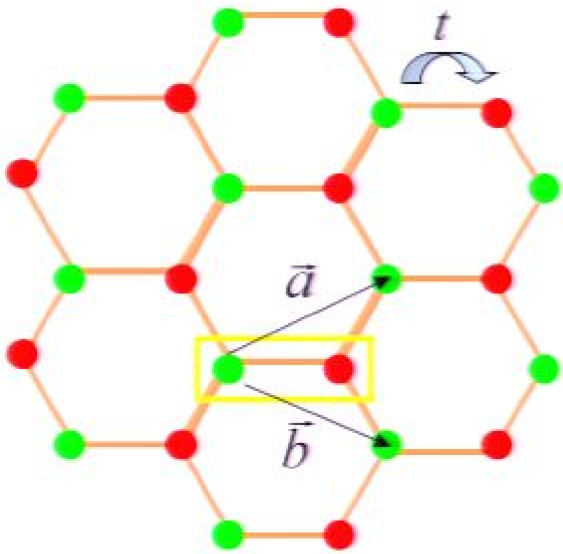

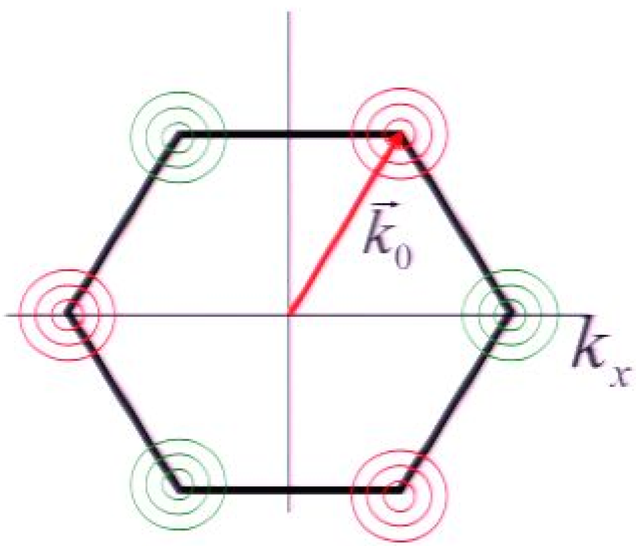

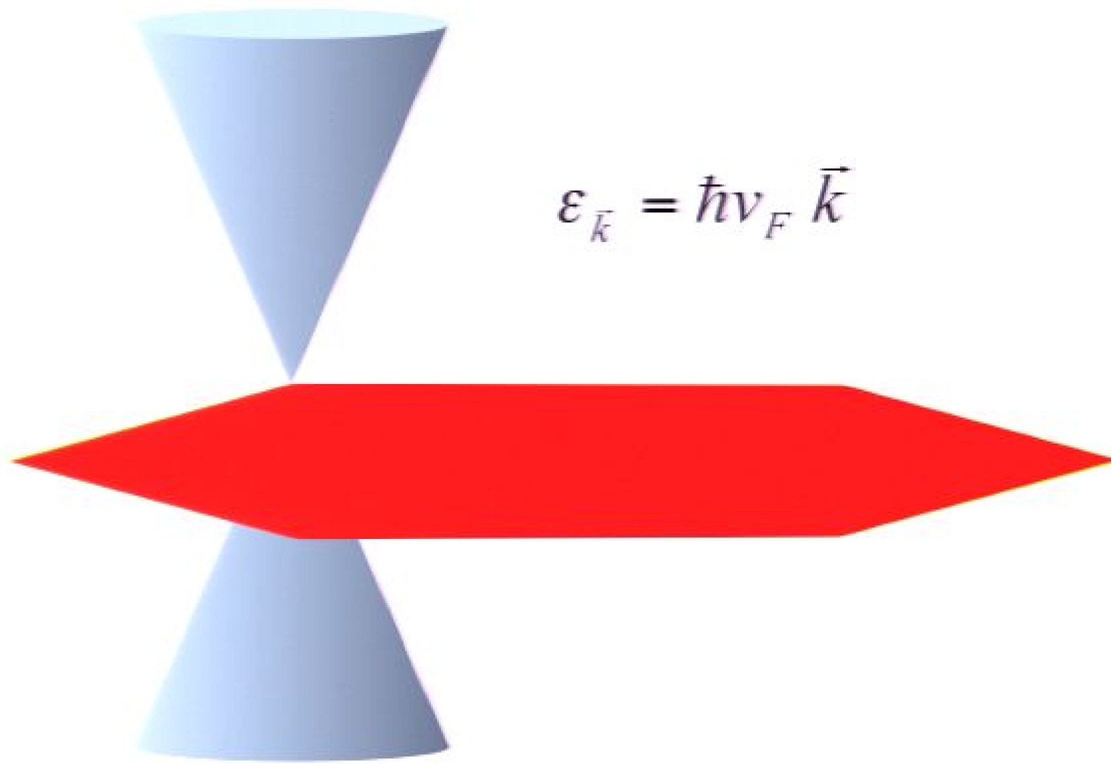

$$\varepsilon_{\vec{k}} = \hbar v_F \vec{k}$$

Graphene

Low energy theory has 4 two-component Dirac fermions, ψ_α, $\alpha = 1 \ldots 4$, interacting with a $1/r$ Coulomb interaction

$$\mathcal{S} = \int d^2 r d\tau \psi_\alpha^\dagger \left(\partial_\tau - i v_F \vec{\sigma} \cdot \vec{\nabla} \right) \psi_\alpha + \frac{e^2}{2} \int d^2 r d^2 r' d\tau \psi_\alpha^\dagger \psi_\alpha(r) \frac{1}{|r - r'|} \psi_\beta^\dagger \psi_\beta(r')$$

Dimensionless "fine-structure" constant $\lambda = e^2/(4\hbar v_F)$.
RG flow of α:

$$\frac{d\lambda}{d\ell} = -\lambda^2 + \ldots$$

Behavior is similar to a CFT3 with $\lambda \sim 1/\ln(\text{scale})$

Cyclotron resonance in graphene

M. Mueller, and S. Sachdev, arXiv:0801.2970.

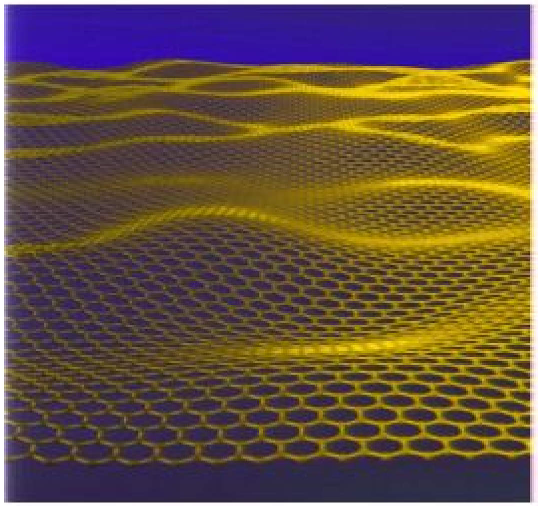

$$\omega = \pm\omega_c^{rel} - i\gamma - i/\tau$$

$$v = 1.1 \times 10^6\, m/s \approx c/300$$

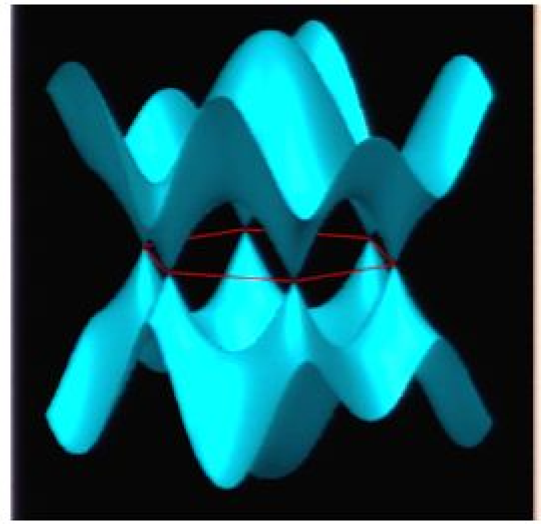

Conditions to observe resonance

- Negligible Landau quantization $E_{LL} = \hbar v\sqrt{\frac{2eB}{\hbar c}} << k_B T$
- Hydrodynamic, collison-dominated regime $\hbar\omega_c^{rel} << k_B T$
- Negligible broadening $\gamma, \tau^{-1} < \omega_c^{rel}$
- Relativistic, quantum critical regime $\rho \leq \rho_{th} = \frac{(k_B T)^2}{(\hbar v)^2}$

$T \approx 300\,\mathrm{K}$

$B \approx 0.1\,\mathrm{T}$

$\rho \approx 10^{11}\,\mathrm{cm}^{-2}$

$\omega_c \approx 10^{13}\,\mathrm{s}^{-1}$

THEORETICAL PHYSICS

A black hole full of answers

Jan Zaanen

A facet of string theory, the currently favoured route to a 'theory of everything', might help to explain some properties of exotic matter phases — such as some peculiarities of high-temperature superconductors.

NATURE|Vol 448|30 August 2007

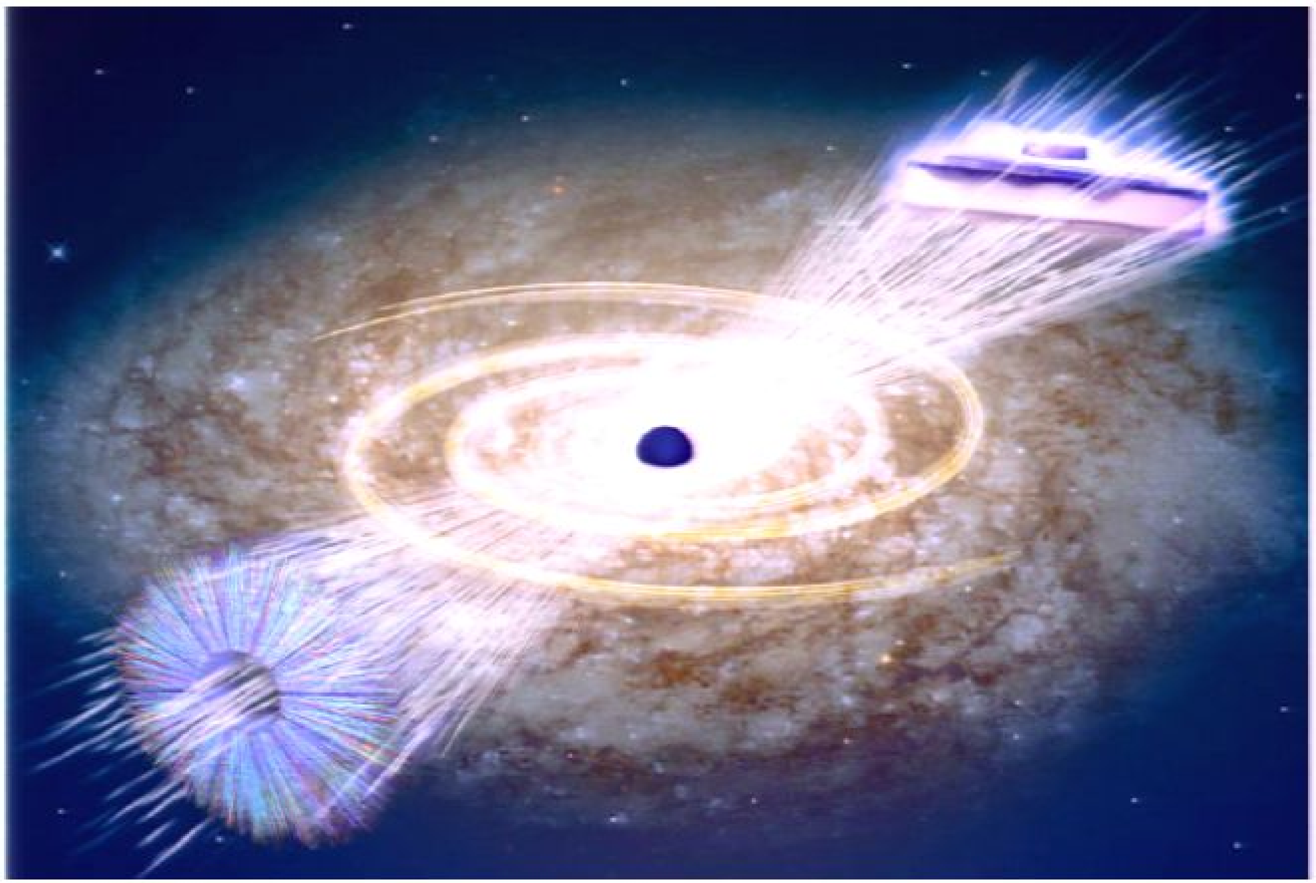

Conclusions

- Quantum phase transitions in antiferromagnets
- Exact solutions via black hole mapping have yielded first exact results for transport co-efficients in interacting many-body systems, and were valuable in determining general structure of hydrodynamics.
- Theory of VBS order and Nernst effect in curpates.
- Quantum-critical transport in graphene.

Remarkable power of Einstein's equation

In addition to describing gravitational phenomena
(black holes, gravitational waves, etc.)
it describes

- Renormalization group flow
- Hydrodynamics
- Quantum criticality
- Superconductivity of paired particles

S. Hartnoll, C. Herzog, G. Horowitz, arXiv:0803.3295

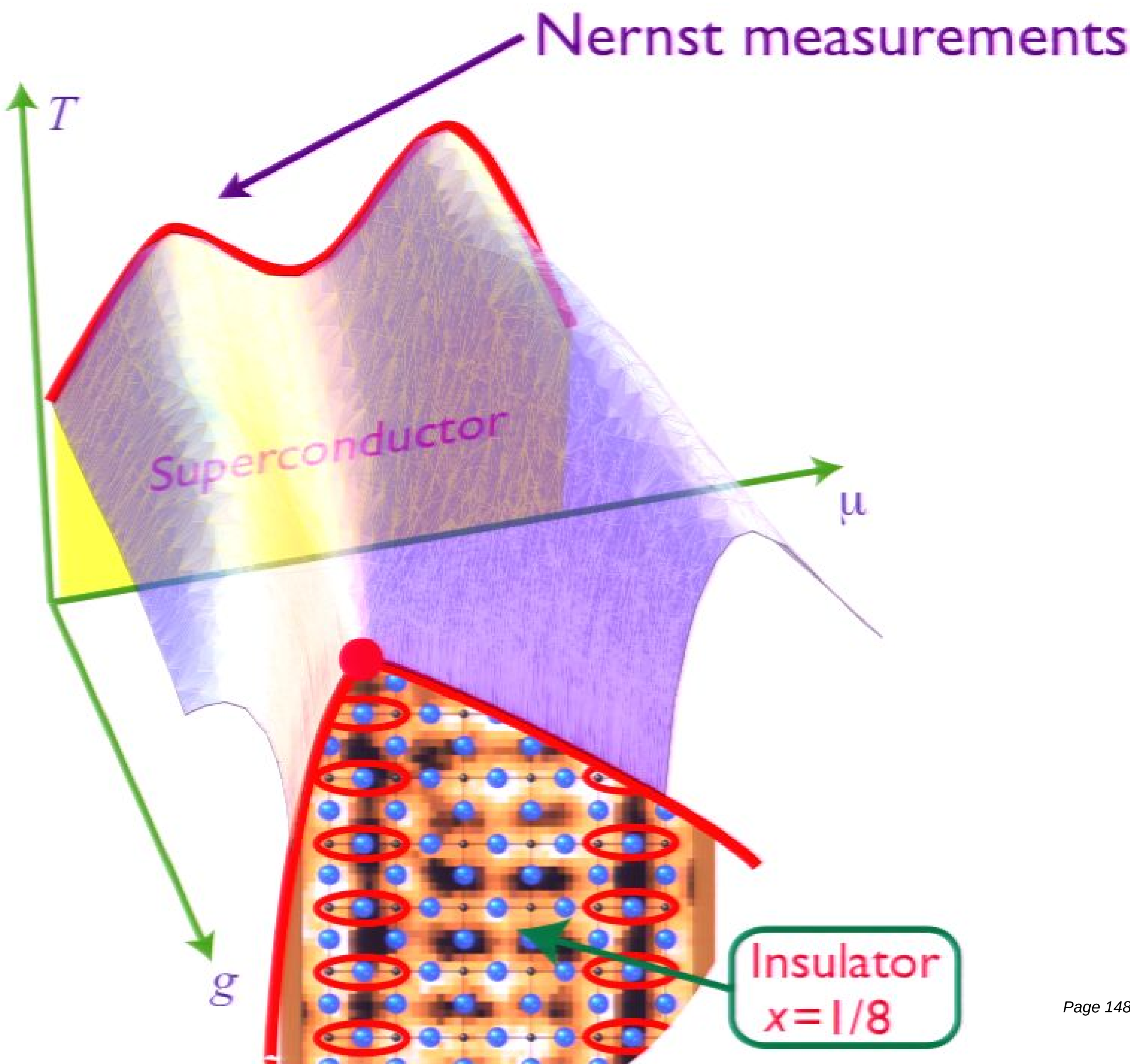

Nernst measurements
T
Superconductor
μ
g
Insulator
x=1/8

Non-zero temperature phase diagram

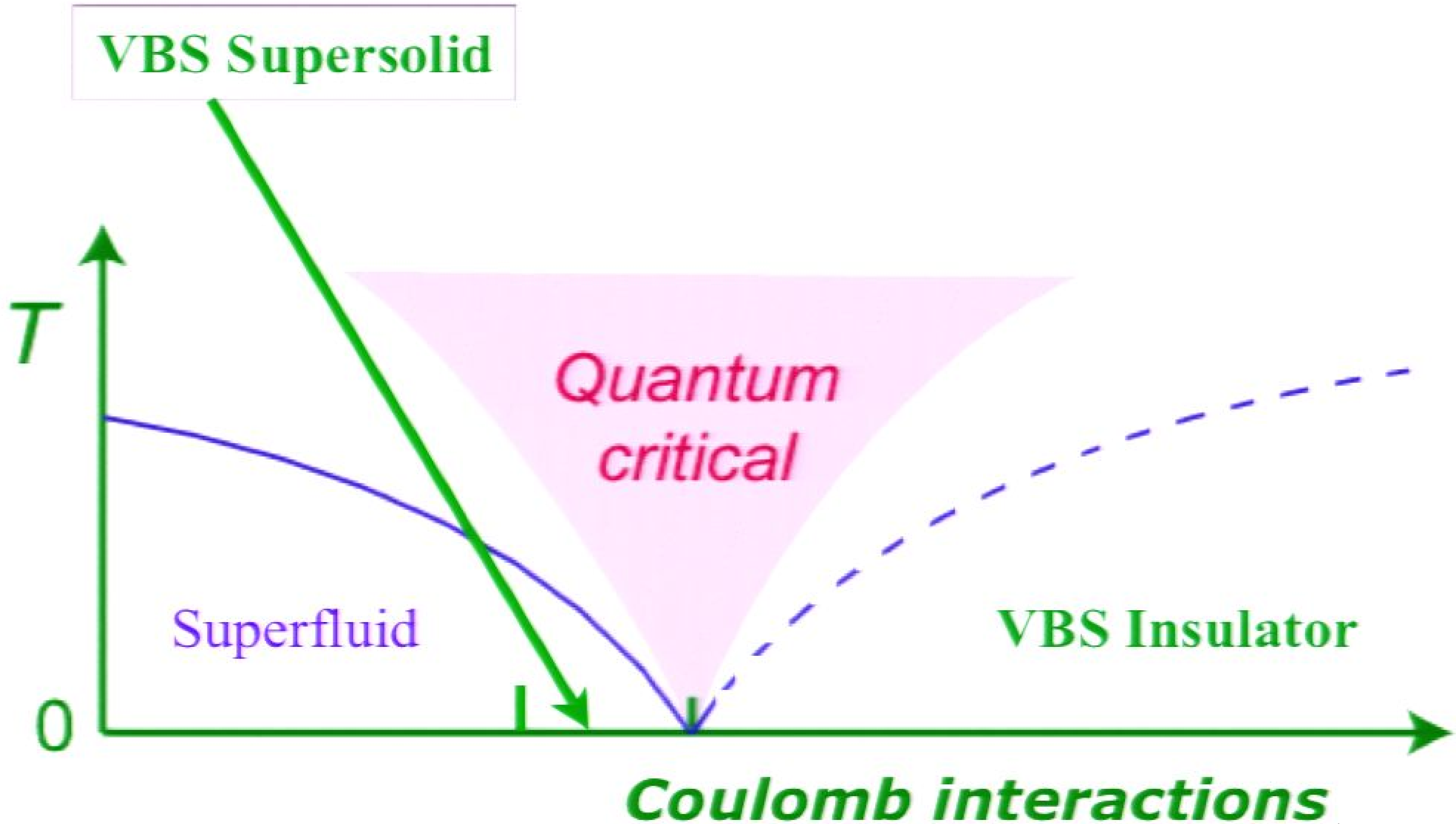

Conclusions

- Quantum phase transitions in antiferromagnets
- Exact solutions via black hole mapping have yielded first exact results for transport co-efficients in interacting many-body systems, and were valuable in determining general structure of hydrodynamics.
- Theory of VBS order and Nernst effect in curpates.
- Quantum-critical transport in graphene.

A black hole full of answers

Jan Zaanen

A facet of string theory, the currently favoured route to a 'theory of everything', might help to explain some properties of exotic matter phases — such as some peculiarities of high-temperature superconductors.

NATURE|Vol 448|30 August 2007

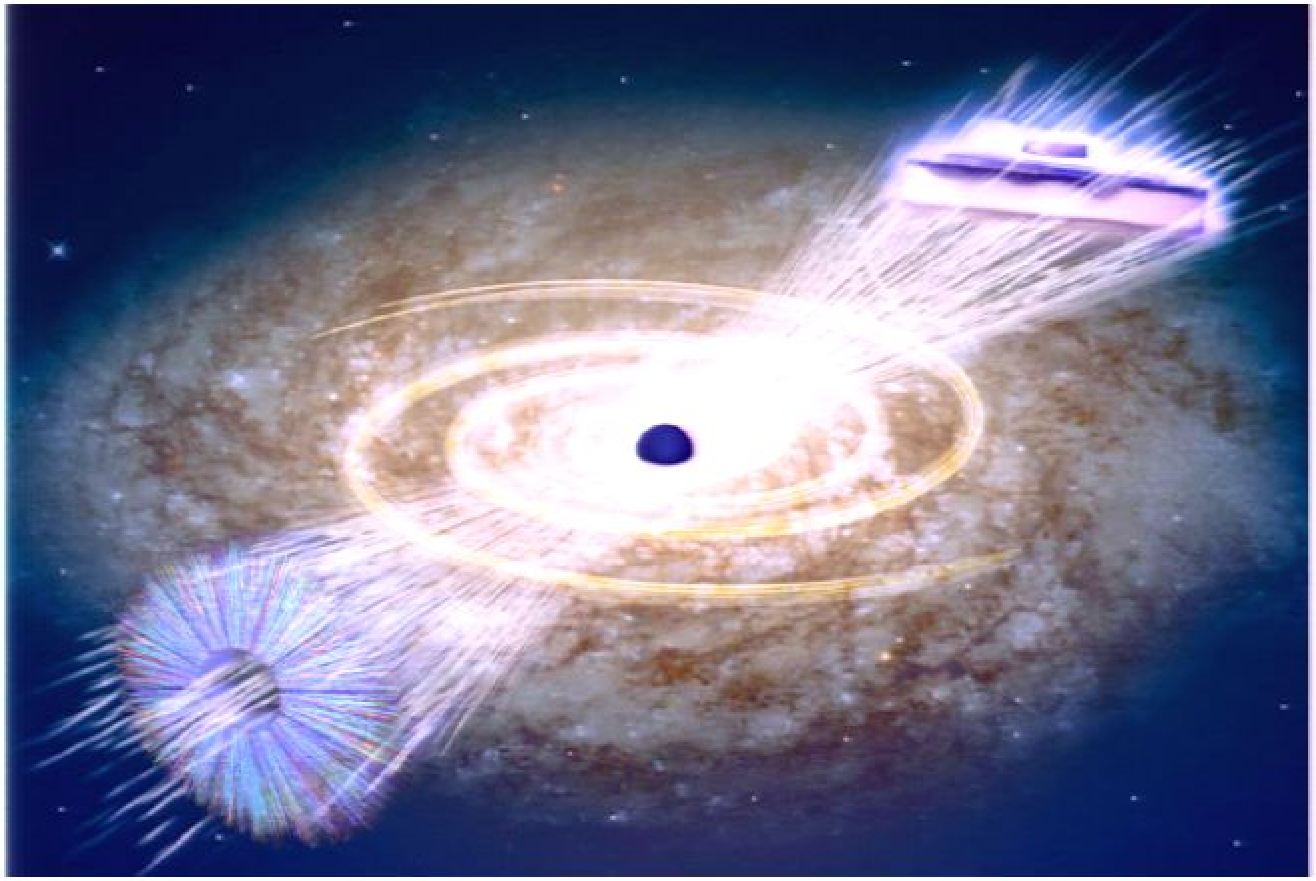

THEORETICAL PHYSICS

A black hole full of answers

Jan Zaanen

A facet of string theory, the currently favoured route to a 'theory of everything', might help to explain some properties of exotic matter phases — such as some peculiarities of high-temperature superconductors.

NATURE|Vol 448|30 August 2007

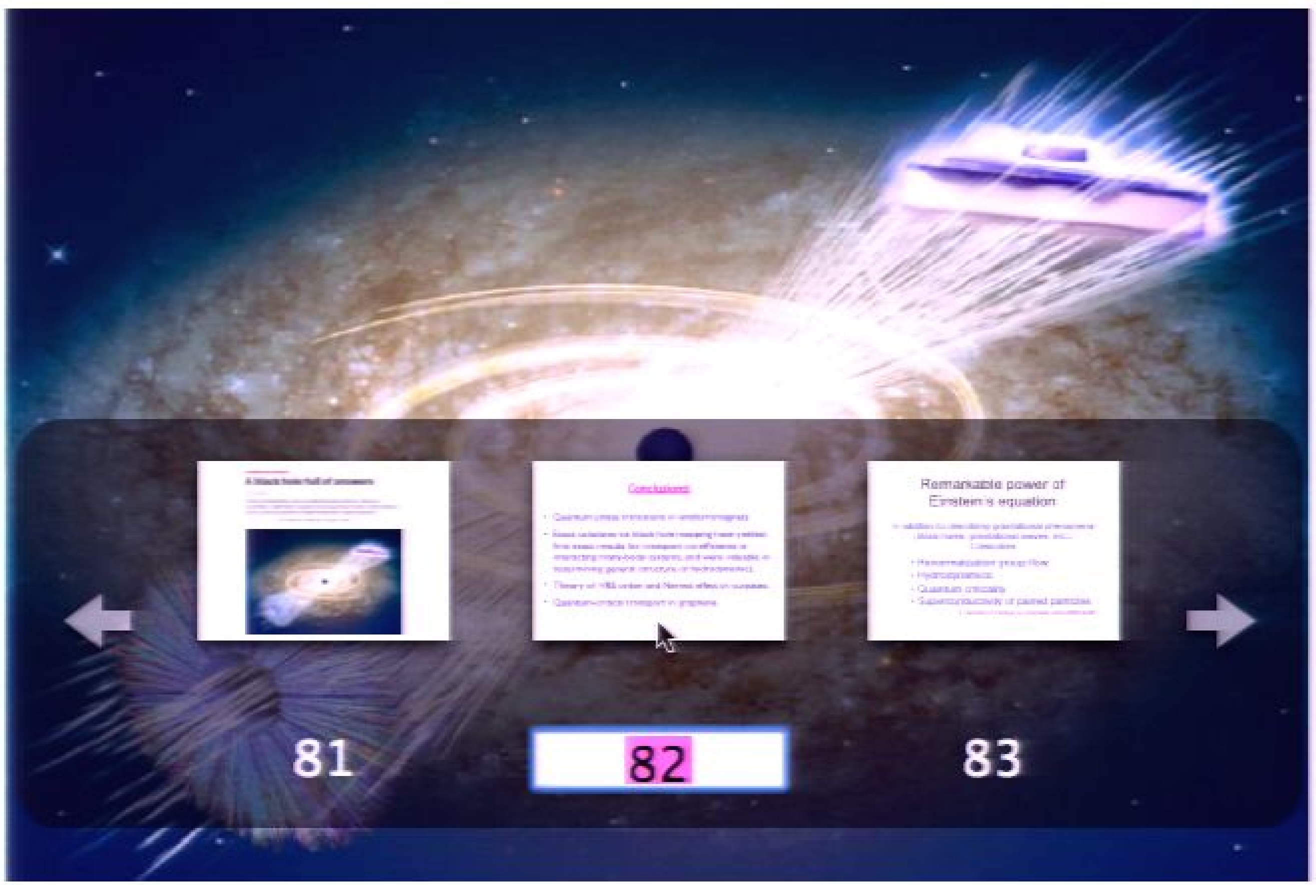

Quantum Entanglement

Hydrogen atom:

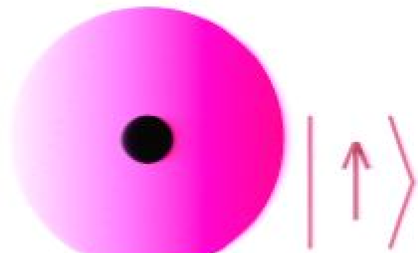

Hydrogen molecule:

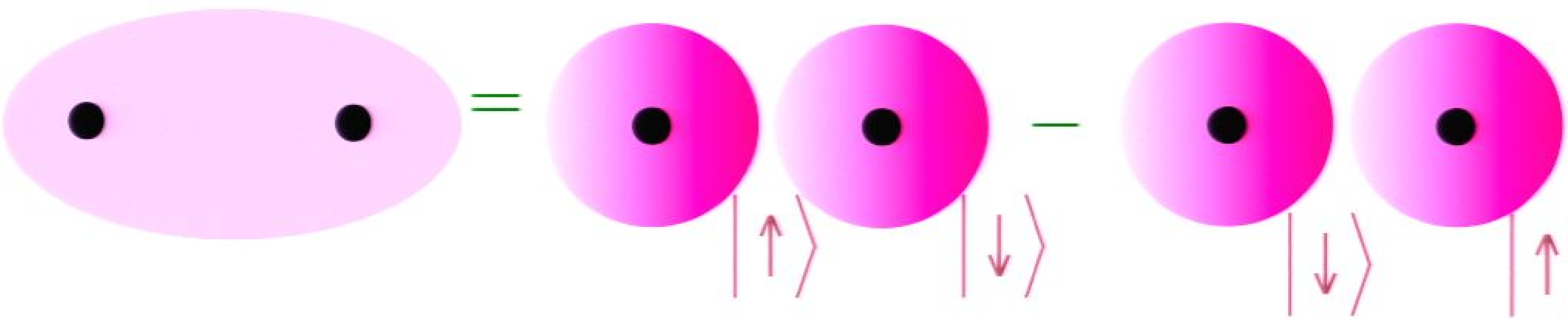

$$= \frac{1}{\sqrt{2}}\left(|\uparrow\downarrow\rangle - |\downarrow\uparrow\rangle\right)$$

Superposition of two electron states leads to non-local correlations between spins diagram as a function of the ratio of exchange interactions, λ

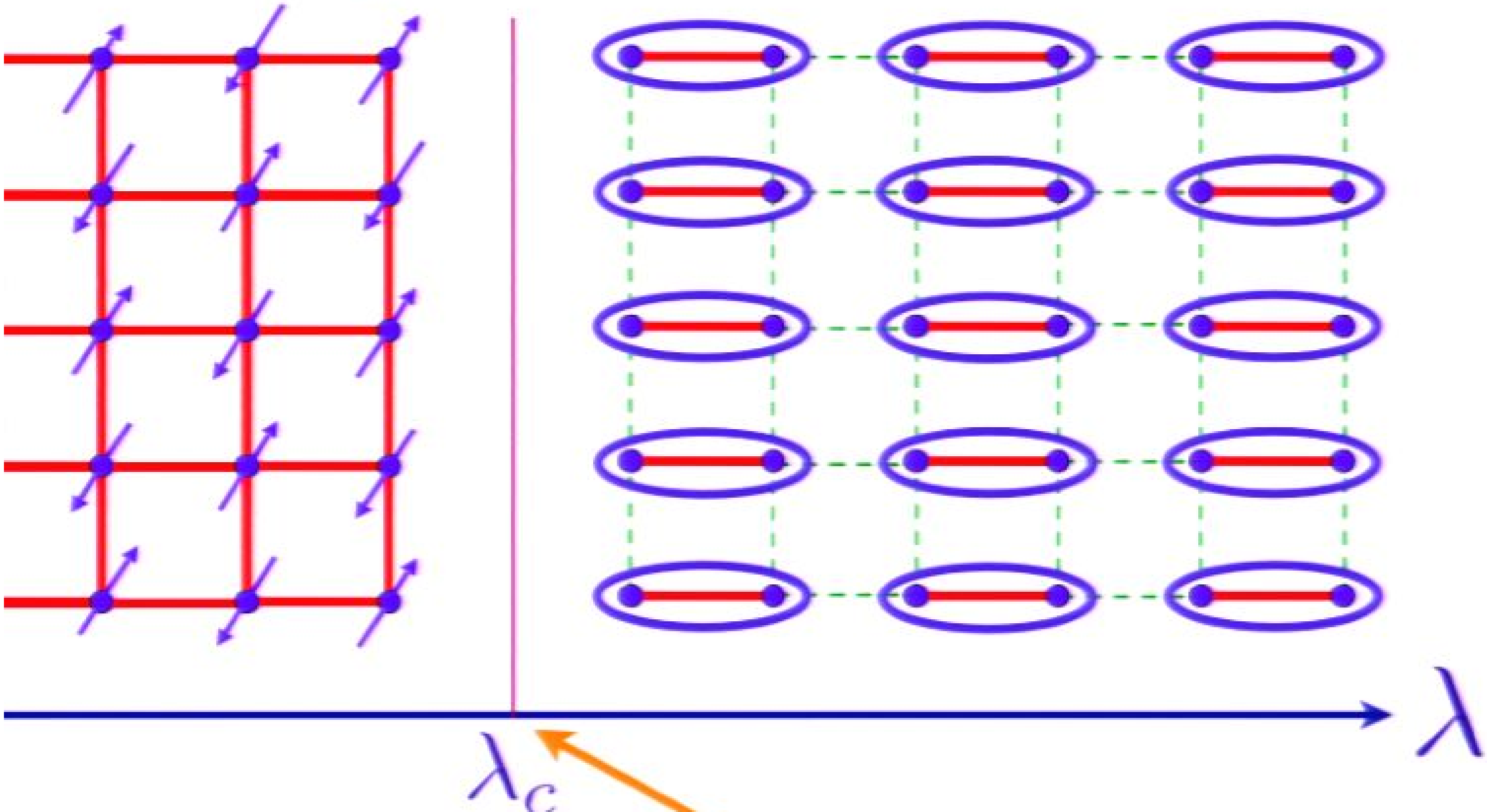

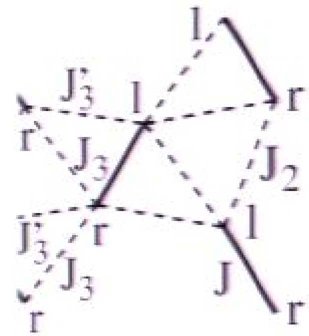

Quantum critical point with non-local entanglement in spin wavefunction

$TlCuCl_3$

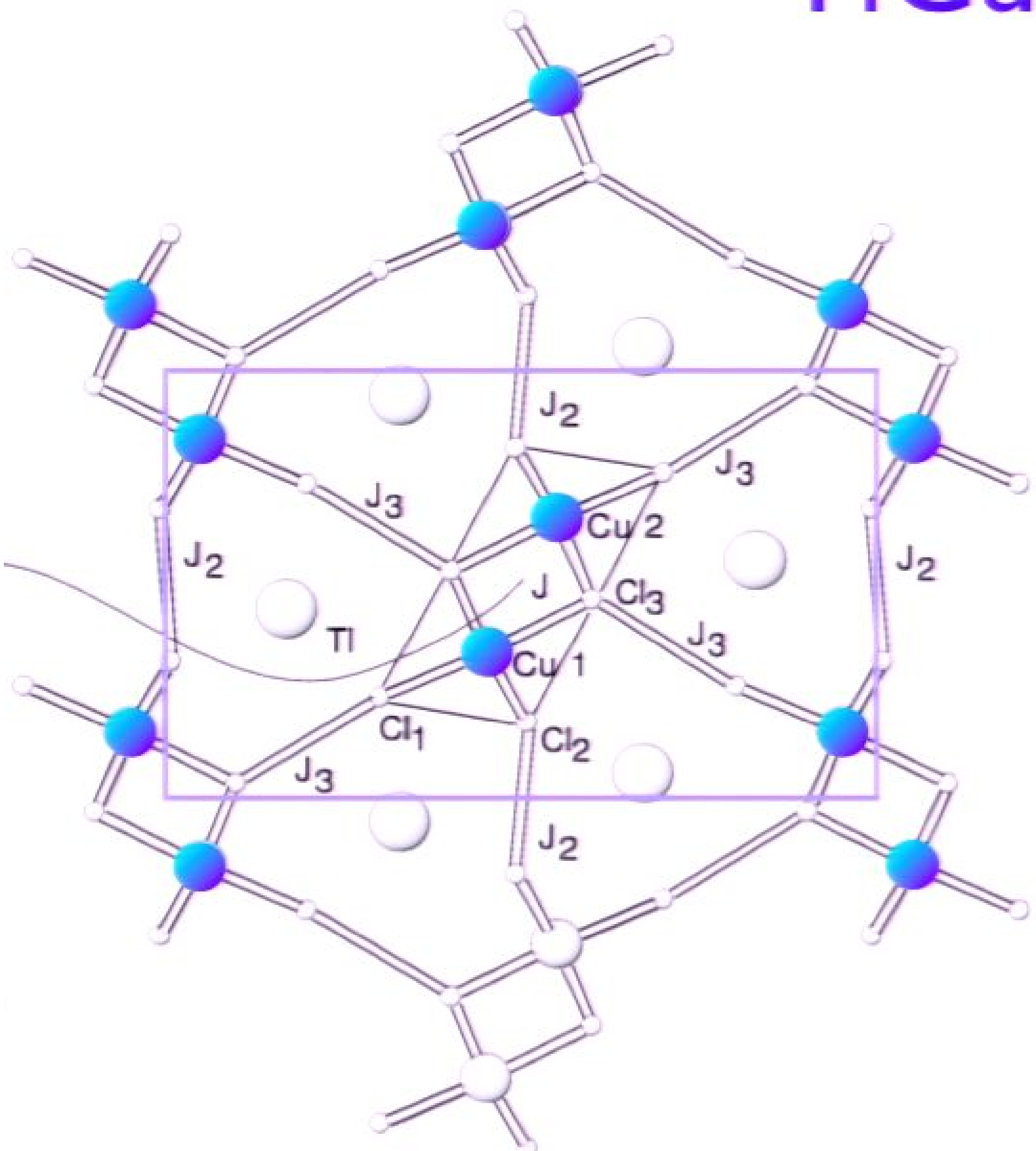
J2
J3
Cu 2
J2
J
Cl3
Tl
J3
Cu 1
Cl1
Cl2
J3
J2

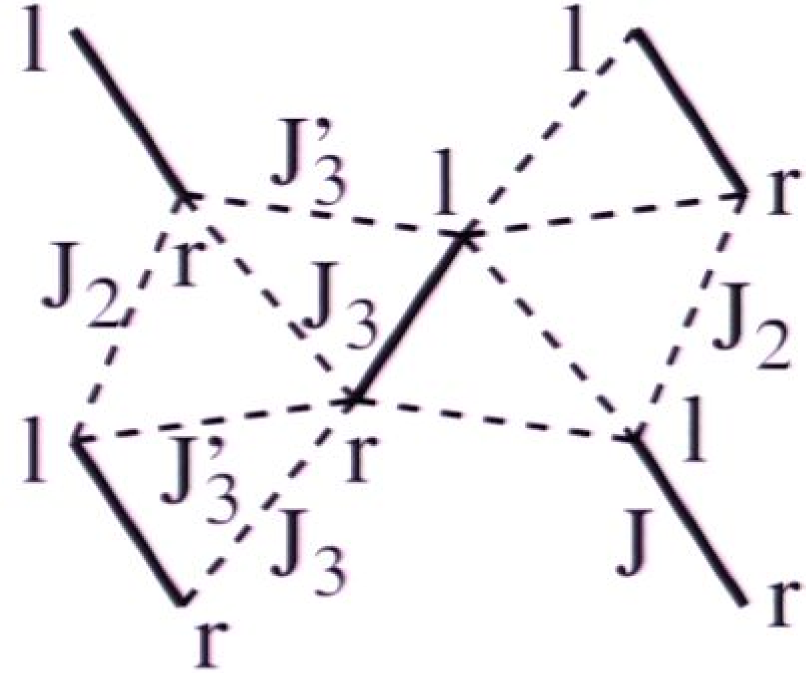
l
l
J'3
l
r
r
J2
J3
J2
l
l
r
J'3
J3
J
r
r

Quantum phase transition with full square lattice symmetry

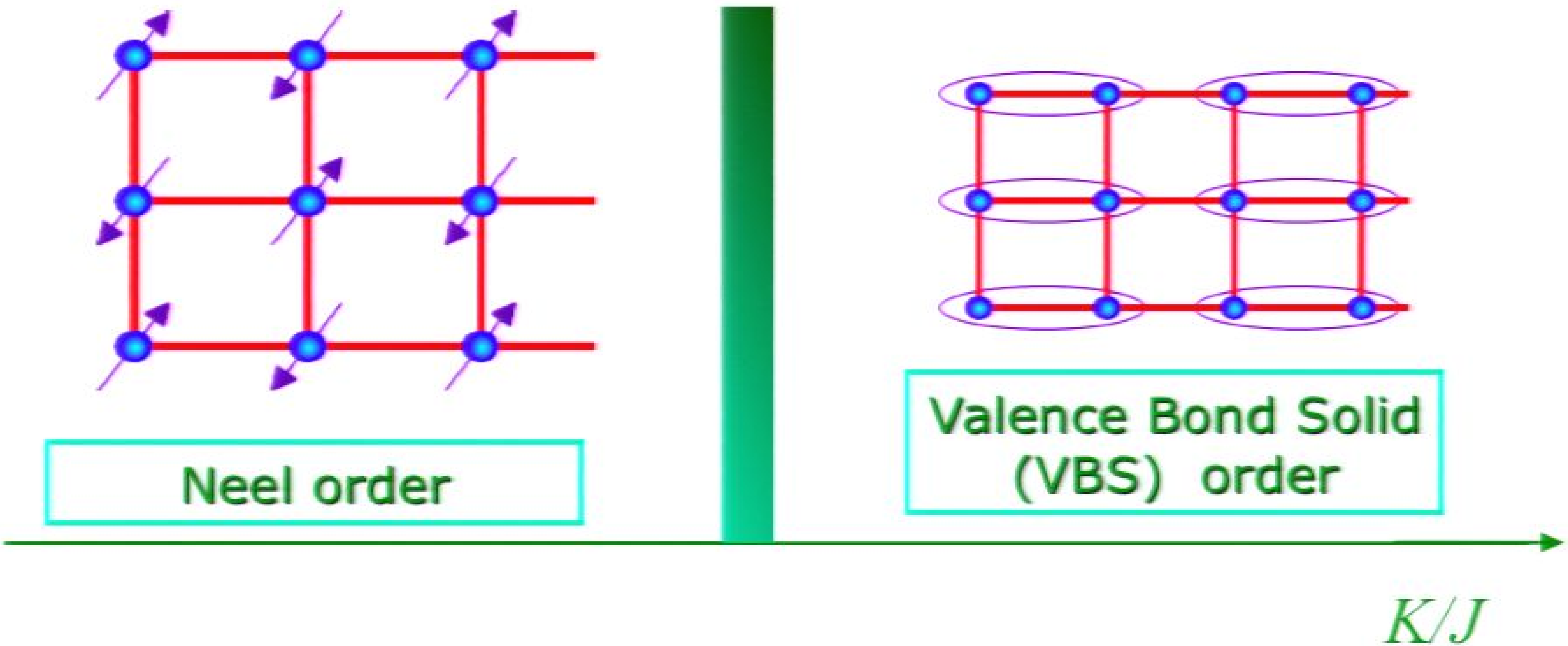

$$H = J \sum_{\langle ij \rangle} \vec{S}_i \cdot \vec{S}_j + K \sum_{\Box} \text{four spin exchange}$$

A. W. Sandvik, *Phys. Rev. Lett.* **98**, 227202 (2007)
N. Read and S. Sachdev, *Phys. Rev. Lett.* **62**, 1694 (1989)